INFORMATION TO USERS

This manuscript has been reproduced from the microfilm master. UMI films the text directly from the original or copy submitted. Thus, some thesis and dissertation copies are in typewriter face, while others may be from any type of computer printer.

The quality of this reproduction is dependent upon the quality of the copy submitted. Broken or indistinct print, colored or poor quality illustrations and photographs, print bleedthrough, substandard margins, and improper alignment can adversely affect reproduction.

In the unlikely event that the author did not send UMI a complete manuscript and there are missing pages, these will be noted. Also, if unauthorized copyright material had to be removed, a note will indicate the deletion.

Oversize materials (e.g., maps, drawings, charts) are reproduced by sectioning the original, beginning at the upper left-hand corner and continuing from left to right in equal sections with small overlaps. Each original is also photographed in one exposure and is included in reduced form at the back of the book.

Photographs included in the original manuscript have been reproduced xerographically in this copy. Higher quality 6" x 9" black and white photographic prints are available for any photographs or illustrations appearing in this copy for an additional charge. Contact UMI directly to order.

UMI

A Bell & Howell Information Company
300 North Zeeb Road, Ann Arbor MI 48106-1346 USA
313/761-4700 800/521-0600

SCREW CONFIGURATION EFFECTS DURING TWIN-SCREW EXTRUSION OF STARCHY AND PROTEINACEOUS MATERIALS

A

THESIS

Presented to the Faculty

of the University of Alaska Fairbanks

in Partial Fulfillment of the Requirements

for the Degree of

DOCTOR OF PHILOSOPHY

By

Akhilesh Gautam, M.S., B.Tech

Fairbanks, Alaska

May 1998

SCREW CONFIGURATION EFFECTS DURING TWIN-SCREW EXTRUSION OF STARCHY AND PROTEINACEOUS MATERIALS

By

Akhilesh Gautam

RECOMMENDED:

Dr. Conly L. Hansen

Dr. Debendra K. Das

Dr. Donald E. Kramer

Dr. John K. Kelley

Dr. Scott T. Smiley

Dr. Gour S. Choudhury (Committee Chair)

Director (FIPC)

APPROVED:

Dean (School of Fisheries and Ocean Sciences)

Dean (Graduate School)

Date

ABSTRACT

This study investigated the effects of screw configuration and feed composition during extrusion of starchy and proteinaceous materials. All experiments were carried out in a twin-screw extruder with a length/diameter ratio of 32:1. The screw speed, feed flow rate, and moisture content were 400 rpm, 12 kg/h, and 15%, respectively. Kneading block (KB) and reverse screw elements (RSE) were placed at different locations in the 200 mm experimental zone near the die, where the temperature was maintained at 150°C.

An on-line method for measurement of residence time distribution (RTD) in a food extruder was developed, tested, and validated. The technique was based on the electrical conductivity of the material in the die, which was altered by addition of an electrolyte tracer at the feed inlet. The change in current flow was measured as a proportional voltage response across a resistor. The on-line method correlated well with the established erythrosine dye method and precisely determined the effects of screw speed, feed flow rate, screw configuration on RTD.

The effects of type, length and position of mixing elements and spacing between two elements on energy inputs, RTD, molecular changes of starch, and macroscopic extrudate characteristics were compared. The results showed that the specific mechanical energy (SME), mean residence time, and extent of starch breakdown were higher for screw profiles with RSE than that with KB. These parameters also increased with longer

mixing elements, increased distance of the elements from the die, and with increased spacing between two elements. Specific thermal energy (STE) input showed opposite trend to that of SME. Die temperature was highest when the elements were placed at 0 mm from the die. Such a screw profile produced an extrudate with highest overall expansion and lowest apparent density. Radial expansion was highest with KB in the screw profile than with RSE. KB seemed to be the element of choice for maximizing radial expansion. Increasing mixing element length or spacing between two elements decreased product expansion. Hardness of the product decreased linearly with increasing radial expansion as shown by the breaking strength data.

Changing feed composition by adding arrowtooth flounder muscle decreased the SME input, increased STE and mean residence time. Hydrolysis changed the properties of arrowtooth flounder muscle so much that it enhanced the expansion characteristics of starch in rice flour and improved extrudate texture.

TABLE OF CONTENTS

LIST OF FIGURES

LIST OF TABLE

ACKNOWLEDGEMENTS

I sincerely wish to express my gratitude to my supervisor, Dr. Gour S. Choudhury. His guidance, encouragement, suggestions, and moral support have greatly contributed to the successful completion of my doctoral degree in Food Engineering. I would have asked nothing more from a major professor.

I would also like to thank the members of my advisory and examining committee, Dr. Conly L. Hansen, Professor of Food Engineering; Dr. Debendra K. Das, Professor of Mechanical Engineering; Dr. Donald E. Kramer, Professor of Seafood Technology; Dr. John J. Kelley, Professor of Marine Sciences and Dr. Scott T. Smiley, Associate Professor of Biology for their unflagging encouragement, full support, and for their valuable time and participation in this project.

Special thanks are due to my colleagues, Dr. Binoy Gogoi, Mr. David Wilson, Mr. Philip Tschersich and Dr. K.P Singh for their unselfish friendship, moral support and professional help on many occasions.

All the help from Laura Bender at the School of Fisheries and Ocean Sciences is greatly appreciated. I wish to express my modest and cordial thanks to the staff members of Bio Sciences and Rasmuson Library for their untiring assistance. Help from Mr. Jim Anderson, Ms. Carol Haas, and Ms. Karen Jensen is acknowledged.

The financial support from Sea Grant College Program, School of Fisheries and Ocean Sciences, and Graduate School, University of Alaska Fairbanks is acknowledged.

This work would have been difficult without their support. Many thanks are due to Dean Vera Alexander, Dean Joseph Kan, and Director Ron Dearborn.

Constant encouragement from my grandfather, parents, and brothers is highly appreciated. Finally, this work would have never been completed without the constant support and encouragement of my loving wife, Shalini and precious daughter, Rupali. Their patience and many sacrifices are deeply recognized.

CHAPTER 1

INTRODUCTION

Extrusion is defined as a process to form or shape by forcing through a specifically designed die. This mechanism has been known and used extensively since the late eighteenth century in the plastic and rubber industry (Harper, 1981; Yacu, 1995). The application of this technology revolutionized the food industry in the 1930's, when single-screw extruders were introduced for production of pasta products (Harper, 1981). One of the first food extruders used was a low shear, ram and piston type to stuff casings for manufacturing sausages. High shear, single-screw extruders for expanded products and breakfast cereals were commercially developed in the 1940's (Harper, 1981). Significant advancements in the design, shape and size of extruders to produce ready-to-eat breakfast cereals, dry expanded snack foods, and pet foods took place during 1950-1970 (Harper, 1981). Twin-screw extruders were introduced in the food industry in the 1970's, and their applications expanded in the 1980's (Harper, 1981; Yacu, 1995). Despite being more complex and costlier than their conventional single-screw counterparts, twin-screw extruders have found various applications in the food industry (Bhattacharya and Choudhury, 1994). Twin-screw extruders are suitable for processing both high and very low moisture feeds because of positive conveyance and better mixing efficiency (Choudhury *et al.*, 1997; Choudhury and Gautam, 1998a).

A myriad of fabricated, cooked, flavored and shaped products are

manufactured from starchy and proteinaceous ingredients using single- and twin-screw extruders. Extrusion processing is versatile and has several advantages over other thermal processing techniques (Harper, 1981). It offers better utilization of ingredients with no or very little waste and can handle a variety of raw ingredients under different process conditions. The process is energy efficient with low production cost.

1.1 OVERVIEW OF FOOD EXTRUSION

Food extrusion is a thermomechanical process in which starchy and/or proteinaceous materials are processed in a food extruder under a variety of process conditions, and finally forced through a specifically designed die opening at a predetermined rate (Harper, 1981; Gopalakrishna and Jularia, 1991). A food extruder has flighted screws that rotate in a tightly fitting stationary barrel and works as a scraped surface heat exchanger (Choudhury and Gogoi, 1995). There are two types of food extruders: single-screw and twin-screw. The latter has two screws lying side by side which are of equal length. Twin-screw extruders are further classified based on direction of rotation of the two screws (co- and counter-rotating) and extent of intermeshing (fully, partially, and non-intermeshing). The co-rotating fully intermeshing twin-screw extruders are most widely used in the food industry.

One of the major differences between the single- and twin-screw extruders is the dissimilarity in the transport of material. Frictional drag flow is the mechanism

for transport in a single-screw extruders, while positive displacement of material is the mechanism in the twin-screw extruder. The complex flow patterns in a twin-screw extruder result in better mixing and heat transfer. These are operational at very low moisture requiring no or minimum post extrusion drying (Harper, 1981; Dziezak, 1989). In addition, twin-screw extruders allow greater flexibility of operations to control product characteristics by monitoring a desired time, temperature, and shear history for the processed material because of an additional independent variable viz., screw configuration. Single- and twin-screw extruders are described in detail by Harper (1981) and Martelli (1983), respectively.

Extrusion processing is widely used in the food industry for production of a variety of fabricated, cooked and shaped products of varying texture (Hauck, 1980). While passing through the extruder, food materials are subjected to numerous unit operations such as feeding, conveyance, heat transfer, mixing, shearing, forming, texurizing, etc. Starch and proteins in the food undergo a number of physicochemical changes such as gelatinization, starch-lipid complexation, and protein denaturation during extrusion under relatively high shear, temperature and pressure. In addition, extrudate expands as it exits from the die during low moisture extrusion (Appendix 1). This expansion or puffing phenomenon also has considerable influence on the extrudate structure.

Extrudate characteristics depend on physicochemical changes occurring during extrusion (Fig. 1.1). The independent process variables such as temperature, screw

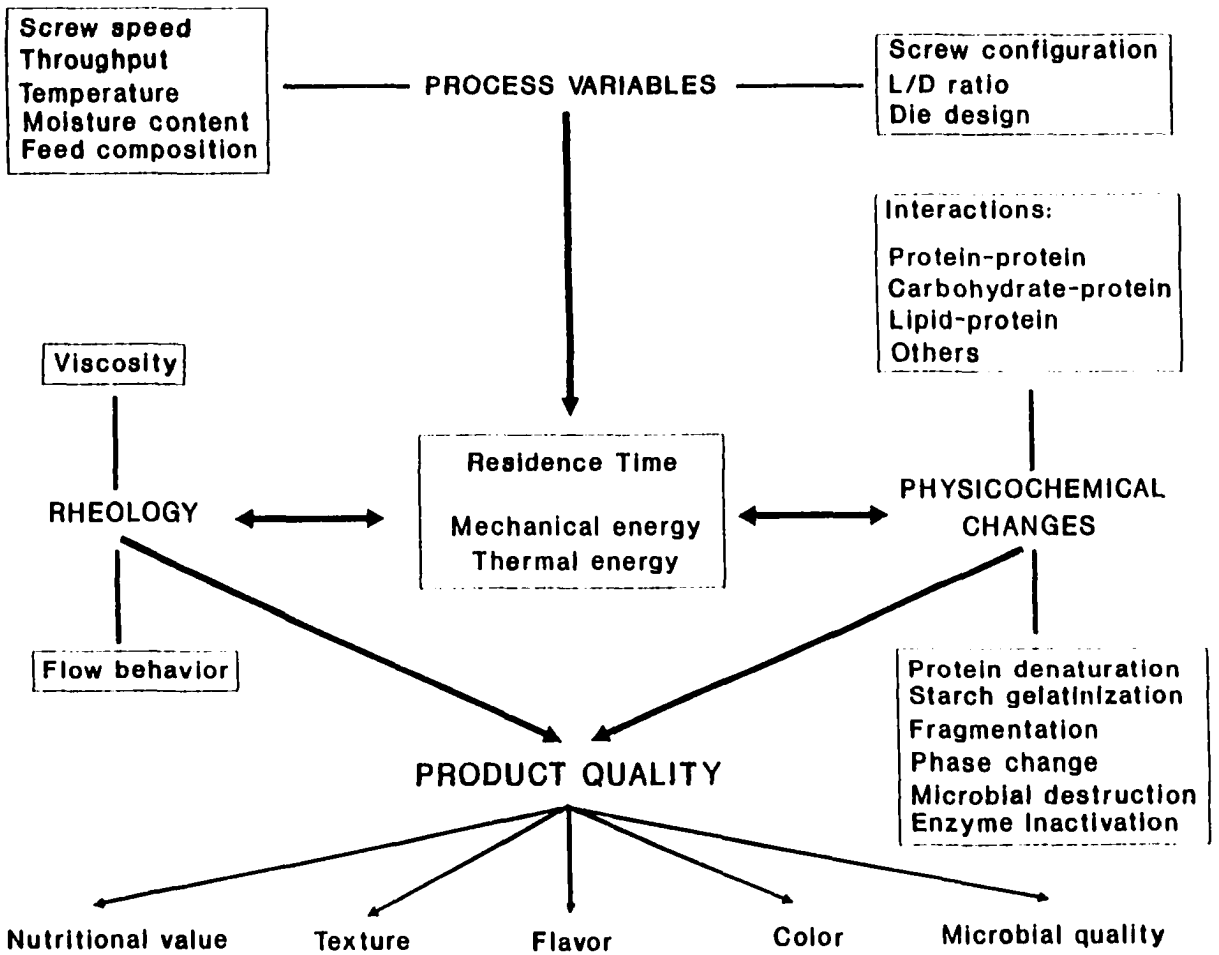

Figure 1.1 Schematic of extrusion processing illustrating the effects of process variables on product attributes (Adapted from Choudhury *et al.*, 1997).

speed and throughput along with screw configuration and die geometry result in mechanical and thermal energy input, and residence time (Choudhury *et al.*, 1997; Choudhury and Gautam, 1998a). These intermediate process parameters induce reactions that affect the product attributes.

Screw configuration is a dominant process variable that influences extent of mixing, residence time distribution and energy input during extrusion. Extruder screws can be built from different types of conveying and mixing elements (kneading and reverse screw elements). The kneading elements (KE) are mild flow restricting elements and individually have no conveying effect. However, they can be combined and oriented to cause static mixing and/or weak forward or backward conveying effect. The reverse screw elements (RSE) are characterized by a reverse flight pushing the material backward. The pitch, stagger angle, length, location, and spacing of screw element(s) define a screw profile and are important parameters during extrusion processing. This study was undertaken to investigate the effects of screw configuration on system parameters and extrudate characteristics during twin-screw extrusion of starchy and proteinaceous ingredients.

1.2 CHALLENGES FOR UTILIZATION OF ARROWTOOTH FLOUNDER

Arrowtooth flounder (*Atheresthes stomias*) is classified as a deep-water flatfish as it is found in water depths of 150-220 fathoms (Kramer *et al.*, 1995). It is the most abundant flatfish in the Gulf of Alaska but is currently not utilized (Witherell, 1995).

Total allowable catch in the Gulf of Alaska may be as high as 200,000 metric tons a year (Otto. 1996; Wilderbuer and Brown, 1994). Currently, arrowtooth flounder is not marketable due to the presence of proteolytic enzyme(s) in its muscle. The protease causes extensive degradation of muscle tissue at temperatures of 55-60°C (Wasson *et al.*, 1992a) and turns flesh to mush during normal cooking (Green and Babbitt, 1990).

Attempts have been made to produce surimi using sulphydryl blocking agents (Babbit, personal communications; Reppond and Babbitt, 1993; Wasson *et al.*, 1992b). However, the arrowtooth flounder surimi is only medium grade (Babbitt, personal communication; Cullenberg, 1995). Surimi technology using chemical additives, will utilize less than 20% of the harvested resource (Pedersen *et al.*, 1989; Lee, 1986). Furthermore, consumers do not like food products manufactured with additives. In order to satisfy consumer demand, food manufacturers are avoiding use of food additives.

Past efforts to utilize arrowtooth flounder have been to inactivate or remove muscle protease. In contrast, this study utilizes the endogenous protease(s) present in the arrowtooth flounder as a processing aid to hydrolyze myofibrillar proteins. The fish muscle was subjected to heat induced myofibrillar degradation and drying to produce autolyzed fish mince powder. Research on fish muscle extrusion carried out in our laboratory (Gogoi *et al.*, 1996 a and b; Gautam *et al.*, 1997; Choudhury *et al.*, 1998) indicated the possibility of developing extruded snack food from arrowtooth

flounder muscle. This study was undertaken to determine the extrusion process conditions for production of snack food from autolyzed arrowtooth flounder muscle. The data generated should be applicable to other fish species with similar enzyme(s).

1.3 OBJECTIVES

Type and extent of reactions occurring in food material during extrusion are dictated by independent process variables as they influence energy input and reaction time. Effects of temperature, screw speed and throughput on physicochemical changes and extrudate characteristics of starchy and proteinaceous materials have been extensively studied (Mercier and Feillet, 1975; Burgess and Stanley, 1976; Jeunink and Cheftal, 1979; Colonna *et al.*, 1983 and 1984; Bhattacharya *et al.*, 1986; Bhattacharya and Hanna, 1987; Sheard *et al.*, 1984; Hager, 1984; Gomez and Aguilera, 1984; Aguilera and Stanley, 1986; Rossi and Peri, 1986; Chinnaswamy and Hanna, 1990). A few isolated studies of screw configuration effects on extrudate characteristics and system parameters during extrusion are available (Olkku *et al.*, 1980; Colonna *et al.*, 1983 and 1984; Chang and Halek, 1991; Erdemir *et al.*, 1992). However, a systematic research is lacking.

Extrusion studies on blends of starchy and proteinaceous materials have shown that increasing the amount of proteins in the feed reduced product expansion with undesirable affect on product texture (Yu *et al.*, 1981; Mohamed, 1990, Areas, 1992; Gogoi *et al.*, 1996a and b; Gautam *et al.*, 1997; Choudhury *et al.*, 1998).. Such

undesirable effects of protein on extrudate expansion was minimized by manipulation of screw configuration (Gogoi *et al.*, 1996a and b; Gautam *et al.*, 1997; Choudhury *et al.*, 1998). Screw configuration was shown to play a key role affecting the intermediate process variables such as energy inputs and residence time distribution, which in turn influenced the product characteristics. It is needless to reiterate the importance of screw configuration during extrusion of starchy and proteinaceous materials. Thus this study aimed at detailed examination of screw configuration effects during extrusion.

Choudhury (1994) suggested that modification of protein structure can be used as a tool to improve product expansion. The present study also aimed at exploring this new avenue of modifying protein size and structure as a mechanism to alter extrudate characteristics. The overall objective of this study was to understand the screw configuration and feed composition effects during twin-screw extrusion of rice flour and autolysed fish proteins. The specific objectives were:

1) To design a system for on line measurement of residence time distribution.
2) To study the effects of screw configuration on energy inputs, system parameters, residence time distribution, starch breakdown and macroscopic extrudate properties.
3) To evaluate the effects of hydrolysis time and protein concentration on energy input, system parameters, residence time distribution, and macroscopic extrudate characteristics at the desired screw configuration.

CHAPTER 2

LITERATURE REVIEW

2.1 RESIDENCE TIME DISTRIBUTION

The rate and extent of any physical or chemical reaction are governed by time-temperature effects. Residence time in a food extruder is an important intermediate process variable (Fig. 1.1), which controls the extent of reactions that determine the extrudate characteristics. Residence time distribution (RTD) data is used for determining the extent of mixing (Wolf and White, 1976; Wolf *et al.*, 1986; Lin and Armstrong, 1990), scale-up, and for improving equipment design (Todd, 1975). The effects of independent process variables such as screw profile, throughput, screw speed, moisture content, and barrel temperature (Fig. 1.1) on mean residence time and residence time distribution in twin-screw extruders have been well documented (Olkku *et al.*, 1980; Kao and Allison, 1984; Altomare and Ghossi, 1986; Van Zuilichem *et al.*, 1988; Yeh *et al.*, 1992; Gogoi and Yam, 1994). These studies have shown that the mean residence time decreases with increasing feed flow rate and screw speed, and with decreasing feed moisture content. Screw configuration and feed flow rate have been shown to have the most effect on RTD.

Stimulus-response is a typical technique used to measure residence time in an extruder. The stimulus is provided by a tracer, usually a colored dye, and the response is measured as dye concentration in the extrudates either by absorption

spectrophotometry (Kao and Allison, 1984; Yeh *et al.*, 1992) or by reflectance colorimetry (Altomare and Ghossi, 1986; Gogoi and Yam, 1994). The tracers that have been used in the dye method are a yellow dye and carbon black (Kao and Allison, 1984), FD&C No. 40 red dye (Altomare and Ghossi, 1986; Gogoi and Yam, 1994), and erythrosine (Yeh *et al.*, 1992; Greghaigne *et al.*, 1983). These post-run methods measure the dye concentration in the extrudate after completing the extrusion experiment. Although the methods measure RTD accurately, considerable time is needed for sample preparation and determination of tracer concentration. Moreover, manual sample collection and preparation increase experimental error.

Attempts have been made to use radioactive, dielectric and optical properties of the tracer for on-line measurement of RTD in extruders. Radioactive tracers that have been used are $^{56}MnSO_4 \cdot H_2O$ (Olkku *et al.*, 1980), ^{64}Cu (Van Zuilichem *et al.*, 1988), and Indium-113m (Kiani *et al.*, 1996). The tracer activity in the die was measured either by a scintillation detector or a probe. Use of radioactive materials in a food extruder may not be practical or desirable. Golba (1980) used dielectric properties of carbon black for on-line measurement of RTD in a extruder. The test cell consisted of a specially designed parallel plate capacitor incorporated in a slit die. Application of this method is limited to a slit die. Optical property of the tracer was used by Chen *et al.* (1995) for on-line measurement of RTD. The problems with this method, as stated by the authors, were fluctuation and drift of the photomultiplier output signal and the non-uniformity of the tracer concentration in

the cross-section of the flow at the end of the screws. It is evident that no simple on-line method to measure residence time in a food extruder is available. Thus one of the objectives of this study was to develop, test, and validate a new on-line method for measurement of RTD in a twin-screw extruder.

2.2 EFFECT OF SCREW CONFIGURATION DURING EXTRUSION

The screw is the principal component of a food extruder. It accepts feed material at the inlet, conveys, mixes, and forces the material through the die restriction at the discharge (Harper, 1981). The extruder screws are divided into three zones depending on the function:

a) Feeding zone: Portion of the screws which accepts the feed material. Usually, in a single screw-extruder this portion is characterized by deep flights and in a twin-screw extruder, this zone is distinguished by a larger pitch of the element. The feed zone is typically 10-25% of the total length (Harper, 1981).

b) Compression zone: Sometimes referred as transition zone, this section is achieved by gradual decrease in the flight depth or pitch of the element in the direction of discharge. The feed is heated and worked into a continuous dough mass in this zone. The powdery, granular, or particulate state of feed is converted into an amorphous or plastic dough. This portion is the longest of the screws and is about half the length of the extruder (Harper, 1981).

c) Metering zone: The portion of the screw nearest to the exit of the extruder

which is characterized by very shallow flights or small pitch of the elements. Maximum shear rate and thus very high viscous dissipation of mechanical energy is observed in this zone.

Extruder screws transfer the motor power to the material through viscous heat dissipation. Twin-screw extruders use a segmented design which offers the process flexibility to alter the screw geometry, thereby influencing shear, mixing and residence time. Extruder screws can be built from different types of conveying and mixing elements (reverse screw and kneading elements). These elements differ in their mixing and conveying mechanism and capabilities.

Results from various studies on the effects of screw configuration are summarized in Tables 2.1, 2.2, and 2.3. These isolated studies investigated the effects of screw configuration on degree of fill (extent of filled volume with material), residence time distribution, specific mechanical energy input, and product transformation. Colonna *et al.* (1983) used a longitudinally-split barrel with RSE at the die end to study the internal modifications of maize starch during extrusion. They found that the degree of fill was higher close to RSE. Similar results were observed by Chang and Halek (1991) for KE. The restrictions provided by RSE and KE during twin-screw extrusion accounted for higher mixing and degree of fill which in turn affected the residence time of the material in the extruder.

Residence time distribution (RTD) in an extruder is a function of screw configuration. Meuser *et al.* (1987) showed that inclusion of two reverse pitch

Table 2.1 Twin-screw extrusion studies on screw configuration effects using reverse screw element (RSE).

EXTRUDER	RESULTS FROM INCLUSION OF RSE	REFERENCE
Creusot-Loire BC-45	Increased motor current and product with better solubility.	Olkku (1981).
Creusot-Loire BC-45	Greater severity of treatment.	Olkku *et al.* (1983).
Creusot-Loire BC-72	Distinct zones with higher degree of fill.	Colonna *et al.* (1983).
Continua-58	Starch gelatinization, and solubilization with enzyme.	Hakulin *et al.* (1983).
Continua-37	Longer mean residence time.	Meuser *et al.* (1987).
Clextral BC-45	Higher die temperature.	Della Valle *et al.* (1987).
Continua-58	Intensive extrusion condition to inactivate cereal enzymes.	Fretzdorff and Seiler (1987).
Clextral BC-45	A mathematical model relating feed rate and pressure drop in the RSE was developed.	Tayeb *et al.* (1988).
Clextral BC-45 and Clextral BC-72	RSE was shown to play a major role in energy transfer and transformation of wheat flour as measured by solubility.	Barres *et al.* (1990).
Continua-37	Specific mechanical energy (SME) values were high.	Erdemir *et al.* (1992).
Clextral BC-21	Manipulation of extrudate expansion.	Gogoi *et al.* (1996a).
Clextral BC-21	Higher energy input and better product expansion.	Gautam *et al.* (1997).
Clextral BC-21	Systematic increase in SME input and water solubilty index with increased distance from die.	Choudhury and Gautam (1998a).
Clextral BC-21	Residence time increased by almost two folds.	Choudhury and Gautam (1998b).

Table 2.2 Twin-screw extrusion studies on screw configuration effects using kneading elements (KE).

EXTRUDER	RESULTS FROM INCLUSION OF KE	REFERENCE
Baker Perkins M-P™	Increased mixing.	Todd and Irving (1969).
Continua-58	Liquefaction of wheat starch and saccharification by enzyme.	Hakulin *et al.* (1983).
Baker Perkins MPF-50	Destruction of starch granules and different dispersion rheology of extrudate during extrusion of cooked maize.	Brenner *et al.* (1986).
Continua-58	Mild extrusion condition to inactivate cereal enzymes.	Fretzdorff and Seiler (1987).
Werner & Pfleiderer ZSK-57	Severe screw configuration increased the average residence time and the residence time distribution spread.	Altomare and Ghossi (1986)
Baker-Perkins MPF-50D	SME input to product increased and melt viscosity decreased with the number of KE.	Kirby *et al.* (1988).
Werner & Pfleiderer ZSK-30	Increased degree of fill and higher viscous heat dissipation (4-6 times).	Chang and Halek. (1991).
Continua-37	SME decreased in the order of KE with reverse orientation, KE with forward orientation, and conveying screw.	Erdemir *et al.* (1992).
Clextral BC-21	Highest product expansion.	Gautam *et al.* (1997).
Clextral BC-21	Increased SME input and higher water solubity index.	Choudhury and Gautam (1998a).
Clextral BC-21	Increased protein content of extrudate without loss of product expansion.	Choudhury *et al.*(1998)

Table 2.3 Twin-screw extrusion studies on screw configuration effects using combination of kneading elements and reverse screw elements (KE+RSE).

EXTRUDER	RESULTS FROM INCLUSION OF KR	REFERENCE
Clextral BC-21	Location and spacing of KE+RSE affected energy inputs and extrudate characteristics.	Gogoi *et al.* (1996b).
Clextral BC-21	Most severe screw configuration which reduced the expansion of the product and produced highest SME input, and starch breakdown.	Gautam *et al.* (1997).
Clextral BC-21	Very severe screw configuration produced highest SME input, WSI and reduced product expansion.	Choudhury and Gautam (1998a).

elements increased the mean residence time in the extruder by 14 seconds under otherwise identical conditions. Altomare and Ghossi (1986) observed that the screw configuration was an important factor affecting the RTD. They compared two screw configurations, viz., moderate and severe. With severe screw configuration, both average residence time and RTD spread was higher than those with moderate screw configuration.

Screw configuration influences mechanical energy input to feed ingredients. Screw profile using low conveying elements (RSE and KE) showed greater specific mechanical energy (SME) input compared to the configurations with conveying elements alone. Replacing a conveying element with a RSE increased the motor current, which in turn increased the mechanical energy input (Olkku, 1981). Inclusion of RSE during extrusion of rye and barley resulted in greater severity of treatment (Olkku *et al.*, 1983). Kirby *et al.* (1988) showed that the SME input increased with increasing number (length) of KE. Barres *et al.* (1990) improved the theoretical approach developed by Tayeb *et al.* (1988) to correlate the specific energy to product transformation. RSE was shown to play a major role in transformation of wheat flour during extrusion as measured by its solubility. The level of transformation correlated well with energy input and thus verified the dominant role of SME on product transformation. The viscous heat dissipation occurring with KE in a co-rotating twin-screw extruder was studied by Chang and Halek (1991). In completely filled sections these elements were found to dissipate 4-6 times more

viscous heat than conveying elements. Erdemir *et al.* (1992) showed that the SME values were highest for configurations with RSE and decreased following the order: KE with reverse orientation, KE with forward orientation, and conveying screw. Studies in our laboratory have shown that product attributes can be manipulated by screw configuration (Gogoi *et al.* 1996a and b; Gautam *et al.* 1997; Choudhury *et al.*, 1998). Kneading elements were the mildest and a combination of kneading and reverse screw element was the most severe flow restricting element. Specific mechanical energy input and water solubility index increased in the order: KE, RSE, and KE+RSE combination.

Della Valle *et al.* (1987) studied the effect of RSE on temperature and pressure profiles during twin-screw extrusion and linked the increase in temperature with the position of RSE. Brenner *et al.* (1986) compared two screw configurations: one with conveying elements and the other having three sets of KE distributed along the length of the extruder. The dispersion rheology of extrudate obtained from these two configurations were different. Kirby *et al.* (1988) demonstrated that low conveying screw configurations (increase in number of KE) produced melts with lower viscosity.

Colonna *et al.* (1983) placed a RSE before the die and showed that the combined effects of shear, heat and pressure were mainly responsible for starch modifications. Wheat starch was gelatinized and melted with a heat stable α-amylase in a twin-screw extruder using a combination of RSE and KE (Hakulin *et al.*, 1983).

Starch granule structure was destroyed by using a screw configuration having KE (Brenner *et al.*, 1986). The study of Fretzdorff and Seiler (1987) used both RSE and KE for inactivation of enzymes in wheat, rye, oats and other milled products during twin-screw extrusion. The configuration with KE had a milder effect compared to that with RSE. Gautam *et al.* (1997) have shown that expansion ratio was maximum with kneading elements, and minimum for combination of kneading and reverse screw elements in the screw profile.

It is clear from these isolated studies that the screw configuration is a dominant variable that influences the intermediate process parameters such as extent of mixing, residence time distribution, and SME input during extrusion. These intermediate variables have profound effects on the overall extrudate properties as they influence the physicochemical changes during extrusion. In this study, effects of type, position, length of mixing elements (kneading blocks and reverse screw elements), and spacing between two elements on system parameters and extrudate characteristics were investigated.

2.3 FISH MUSCLE EXTRUSION

Research on extrusion processing of fish muscle started in the 1980's (Choudhury and Gogoi, 1995). The aim was to use underutilized species, by-catch fish, and muscle recovered from by-products of filleting, canning and surimi operations. Literature on extrusion of fish muscle is rather sparse (Choudhury and

Gogoi, 1995). Some studies have been reported on attempts to develop product categories such as expanded snacks, seafood analogues, marine beef, fish sticks, fish fingers, and aquaculture feed. Blends of various fish muscle from various species and starchy ingredients were extruded. Extrusion of fish muscle can be divided into three categories depending on the moisture content of the feed (Choudhury and Gogoi, 1995).

2.3.1 High moisture extrusion (moisture content more than 50%)

The impetus for increased interest in high moisture extrusion has come from recent developments and improvements in twin-screw extrusion technology. The high moisture extrusion studies have mainly focused on developing fibrous structure in the extrudate (Choudhury and Gogoi, 1995). Sardine and defatted soy flour were used to develop a multilayered extrudate (Kitagawa and Nishi, 1987). Kitabatake *et al.* (1988) attempted to produce a crab meat analogue from flying fish mince and salt. Aoki *et al.* (1989) investigated texturization of pollack surimi. Texturization of chum salmon have been investigated by Kitagawa and Nishi (1989) and Isobe *et al.* (1990). High-moisture extrusion of pink salmon mince was studied by Choudhury and Bhattacharya (1994) to determine the effects of soy flour (0-15%), rice flour (0-25%) and salt (0-5%), and temperature on extrudate characteristics. The feed composition, level of additives, and temperature of extrusion significantly influenced textural attributes of the extrudates. The high-temperature, short-time (HTST) capability of

a twin-screw extruder to inactivate protease in arrowtooth flounder was examined by Choudhury and Gogoi (1994). The results indicated that protease in arrowtooth muscle can be completely inhibited by a combination of temperature and residence time.

2.3.2 Intermediate moisture extrusion (moisture content between 35-50%)

Some studies on extrusion processing of blends of minced fish and starchy or proteinaceous ingredients having moisture content in the range of 35-50% have been carried out using single-screw extruders (Choudhury and Gogoi, 1995). Murray and Stanley (1980) studied co-extrusion of minced fish and soy proteins and concluded that co-extrudates with specific textural and nutritional characteristics can be prepared by controlling compositional and process variables. Shelf-stable, intermediate moisture fish products were prepared from a mixture of fermented mince, wheat flour, and starch using intermediate moisture technology and extrusion (Hilmarsdottir and Karmas, 1984; Karmas and Lauber, 1987; Bhattacharya *et al.* 1988, 1990).

2.3.3 Low-moisture extrusion (moisture content less than 35%)

Generally, dry, expanded snack food products have been produced using single- and twin-screw extruders from feeds with low moisture content (Table 2.4). Yu *et al.* (1981) studied extrusion of fish crackers from a mixture of ground tapioca

Table 2.4 Studies on low moisture extrusion (moisture content less than 35%).

EXTRUDER	FEED COMPOSITION	RESULTS	REFERENCE
Brabender (Model 20DN)	Fish (*Chirocentrus dorab*) mince and tapioca flour.	Product expansion upon frying depended on fish content.	Yu *et al.* (1981).
Werner & Pfleiderer, Continua 37/5.	Cod mince, potato flour, wheat flour, potato starch, waxy maize starch, and salt.	Expanded snacks, soup ingredients, and pasta with fish content up to 50%.	Kristensen *et al.* (1984).
Brabender Plasticorder, Model PL-V500.	Carp mince and rice flour.	Precooked blend with no detectable off flavor at room temperature for up to 6 months.	Maga and Reddy (1985).
Laboratory model extrusion cooker.	Deodorized croaker mince, wheat flour, refined oil, and salt.	Crispy, light colored product with negligible fish odor.	Venugopal (1987).
Haake Rheodrive, Model 3000, Mixer/Extruder.	Cod mince and rice flour.	Process conditions for puffed snack and meat extender.	Clayton and Miscourides, 1992.

Table 2.4 (Contd.)

EXTRUDER	FEED COMPOSITION	RESULTS	REFERENCE
Clextral BC-21	Pink salmon muscle powder and rice flour	Manipulation of energy inputs and product characteristics by feed composition and screw configuration with reverse screw elements.	Gogoi *et al.* (1996a).
Clextral BC-21	Pink salmon muscle powder and rice flour	Loss in expansion due to increased protein content was compensated by incorporation of combination of kneading and reverse screw elements.	Gogoi *et al.* (1996b).
Clextral BC-21	Pink salmon muscle powder and rice flour.	Most expanded product with incorporation of kneading element in the screw profile.	Gautam *et al.* (1997).
Clextral BC-21	Pink salmon muscle powder and rice flour.	Manipulation of extrudate characteristics with inclusion of kneading element in screw profile.	Choudhury *et al.* (1998).

flour and minced fish (*Chirocentrus esculentus*). The extruded products were compared with those prepared by traditional methods. The effects of feed composition and temperature were investigated. Die temperature and screw speed were maintained at 100°C and 120 rpm, respectively. The temperature of the second barrel section close to the die was varied from 60 to 140°C. Extrudate linear expansion was found to increase with temperature up to 100°C upon frying . Slightly reduced expansion was reported on further increase in temperature. Increasing fish content decreased the extrudate expansion. The extruded product was similar to those prepared by traditional methods and was organoleptically acceptable. Kristensen *et al.* (1984) attempted to produce snack food and noodles using cod mince and other ingredients such as potato starch, potato flour, crossbonded waxy maize starch, wheat flour, salt, calcium stearoyl-2- lactylate and dodecyl gallate. The throughput and screw speed were varied from 28 to 45 g/min and 40 to 75 rpm, respectively. The temperature of the die head and first two zones were maintained at 94°C, 70°C, and 120°C, respectively. The die opening was 0.7 mm high and 20 mm wide and screw compression ratio was 1:2. Extrudates with low fat fish (up to 50% of fish weight) did not develop objectionable flavor. However, the fish taste intensified during storage. Flavor of expanded products was stabilized by addition of crossbonded waxy maize starch. Maga and Reddy (1985) extruded blends of rice flour and carp mince (0-35%) in a Brabender Plasticorder equipped with a 3/1 screw, and a 0.5 cm die. Raw mince was used for 0-20% blends, and cooked mince for 25-35% blends. The latter was produced by baking at 120°C for 40 minutes, which was

necessary to reduce the mince moisture to 50%. Blends of rice flour, fish and water were mixed to adjust the moisture to 25% and extruded at a screw speed and barrel temperature of 150 rpm and 150°C, respectively. The extrudate obtained could be stored at room temperature for six months without development of off-odor. Snack food prepared from the extrudate containing up to 35% carp was found to be acceptable by a sensory panel. Extrusion of partially deodorized fish croaker meat was investigated by Venugopal (1987). Deodorization was accomplished by boiling the flesh in 0.3% orthophosphoric acid followed by dewatering in a screw press. Mixture of the pressed cake, wheat flour, salt, refined oil and water was extruded in a laboratory extruder at a barrel temperature of 150°C. The product could be stored without development of significant fish odor for two years. The study of Clayton and Miscourides (1992) examined extrusion of underutilized fish tissue for production of protein enriched expanded products, meat substitutes or extenders, and/or fish fillet analogues with a protein content of 50-90% (dry basis). The effects of feed composition and operating variables such as moisture content (25-65%, dry basis), protein content (10-90%), screw speed (40-120 rpm) and temperature (120-180°C) were evaluated. They concluded that shelf-stable, texturized food products with a range of rheological and nutritional properties can be prepared.

Several studies in our laboratory have focused on utilization of pink salmon (Gogoi *et al.* 1996a and b; Gautam *et al.* 1997; Choudhury *et al.*, 1998) using a twin-screw extruder. Three levels of fish proteins (0, 30 and 60%) with various screw

configurations were studied. Twelve screw profiles were built using kneading, reverse, and combination of kneading and reverse screw elements. It was shown that lowering of SME input due to addition of proteins and other product characteristics (expansion, shear stress, apparent density, and water solubility index) could be manipulated by incorporation of mixing elements in the screw profile.

It is evident that limited progress has been made to explore the effects of screw configuration on extrudate characteristics and system parameters. Studies in our laboratory suggest that the protein content of an expanded extrudate can be increased without compromising the desired product attributes by manipulation of screw configuration. Extrusion of enzyme modified protein may provide another approach for improving protein content and nutritional value of snack food (Choudhury, 1994).

CHAPTER 3

MATERIALS AND METHODS

3.1 OVERALL EXPERIMENTAL PLAN

In order to achieve the objectives of the study, the research was undertaken in three steps:

1. Residence time distribution (RTD) of the material in an extruder is one of the key intermediate process variable which affects physicochemical changes during extrusion. No simple technique was available to measure the RTD. The initial phase of the work was focused on development of an on-line method for RTD measurement.

2. The main focus of this study was to understand the effects of screw configuration on energy inputs, residence time, and extrudate characteristics. This phase was planned, based on the screw configuration studies carried out in our laboratory (Gogoi *et al.*, 1996 a, b; Gautam *et al.*, 1997; Choudhury *et al.*, 1998; Choudhury and Gautam, 1998a). The effect of kneading element (KE), reverse screw element (RSE), and combination (KE+RSE) on system parameters and extrudate characteristics were compared. The combination was found to be the most severe screw configuration generating a very high torque (SME input), which resulted in extensive breakdown of polysaccharides, and significant decrease in the radial expansion. In addition, extrudate expansion decreased considerably when mixing

elements were placed beyond 200 mm from the die. Therefore, in the present study, the KE+RSE combination was not considered and experimental zone was restricted to 200 mm from the die. The screw profile in this experimental zone was systematically altered by changing the type, position, length of mixing elements and spacing between two elements. Screw speed, feed flow rate, moisture content, and temperature profile were fixed based on the literature available for extruded rice products (Bhattacharya and Choudhury, 1994; Gogoi *et al.*, 1996a, b).

3. Feed composition effects on extrudate characteristics and system parameters were investigated in the last stage of this study.

3.2 MATERIALS

Rice flour and arrowtooth flounder muscle were the two main ingredients used in this study. Sodium nitrate ($NaNO_3$) was used as the tracer for on-line technique to measure RTD and erythrosine (red color dye) was used to validate the on-line method.

3.2.1 Rice flour

Rice flour, obtained from Pacific Grain Products, Inc. (Woodland, CA), was used as the main feed material for all the experiments. The composition and particle size distribution of rice flour are presented in Tables 3.1 and 3.2.

Table 3.1 Proximate composition of rice flour and arrowtooth flounder muscle.

Components	Composition (%)	
	Rice flour	Arrowtooth flounder muscle
Moisture	9.95	79.88
Protein	5.85[a]	15.77
Fat	0.56	3.50
Ash	0.47	0.85
Crude fiber	1.74	-
Carbohydrate	81.43[b]	-

[a]N*5.95

[b]Carbohydrate by difference

Table 3.2 Particle size distribution of rice flour

	US sieve number	%
Retained on	50	0.9
	80	16.1
	100	7.5
	140	19.0
	200	18.5
Passed through	200	38.0

3.2.2 Arrowtooth flounder muscle

Arrowtooth flounder was supplied by International Seafoods of Alaska, Inc. and processed as described by Choudhury and Gogoi (1996). Heading, gutting, and filleting were carried out using a Baader filleting machine (Model 175, Baader Food Processing Machinery, Baader North America Corporation, Fort Myers, FL). Fish fillets or headed and gutted fish were minced in a belt and drum mechanical deboner/mincer (Baader 697, Baader North America Corporation, Fort Myers, FL) and frozen in a Dole plate freezer (Dole Refrigeration Company, Lewisberg, TN) for 2 hr. The mince was stored at -40°C and used whenever needed. Moisture, protein, fat and ash of arrowtooth flounder mince were determined using standard AOAC (1984) methods. The proximate composition of arrowtooth flounder mince is presented in Table 3.1.

3.2.3 Tracer

The tracers, sodium nitrate ($NaNO_3$) and erythrosine dye, were purchased from Mallinckrodt Chemical Works (St. Louis, MO) and Sigma Chemicals (St. Louis, MO), respectively.

3.3 EQUIPMENT

3.3.1 Extruder

All the experiments were carried out using a co-rotating, intermeshing, self-wiping twin-screw extruder (Model BC 21, Clextral, Firminy Cedex, France). It was

equipped with modular barrels, each 100 mm long, and bored with two 25 mm diameter holes (Fig. 3.1). The twin-screws had segmental screw elements (Fig. 3.2), each 25 or 50 mm in length, so that kneading or reverse screw elements could be placed at a desired location along the length of a splined shaft. Thermal energy was provided by induction heaters mounted on 100 mm barrel sections. Length to diameter (L/D) ratio was 32:1 and a 5 mm diameter circular die was used. Material was fed into the extruder inlet port by a twin-screw (30 mm pitch) metering feeder, supplied by K-Tron Corporation (Pitman, NJ). Screw speed, material feed rate, barrel temperatures, %torque, die temperature, and power consumed by the induction heaters were monitored from a control panel.

3.4 ON-LINE MEASUREMENT OF RESIDENCE TIME DISTRIBUTION

An on-line system to measure the residence time distribution of the material in the twin-screw extruder was designed, fabricated and used in this study.

3.4.1 On-line measurement system

The technique investigated was based on the electrical conductivity of the material in the die. Figure 3.3 shows the schematics of the on-line system. A series circuit consisting of the die, a 10 ohm resistor, and a 15 V dc power supply (VWR Scientific, Seattle, WA) was used. A 5 mm diameter stainless steel circular die with two opposing electrodes was specifically designed and fabricated for this study (Fig. 3.4). The inside

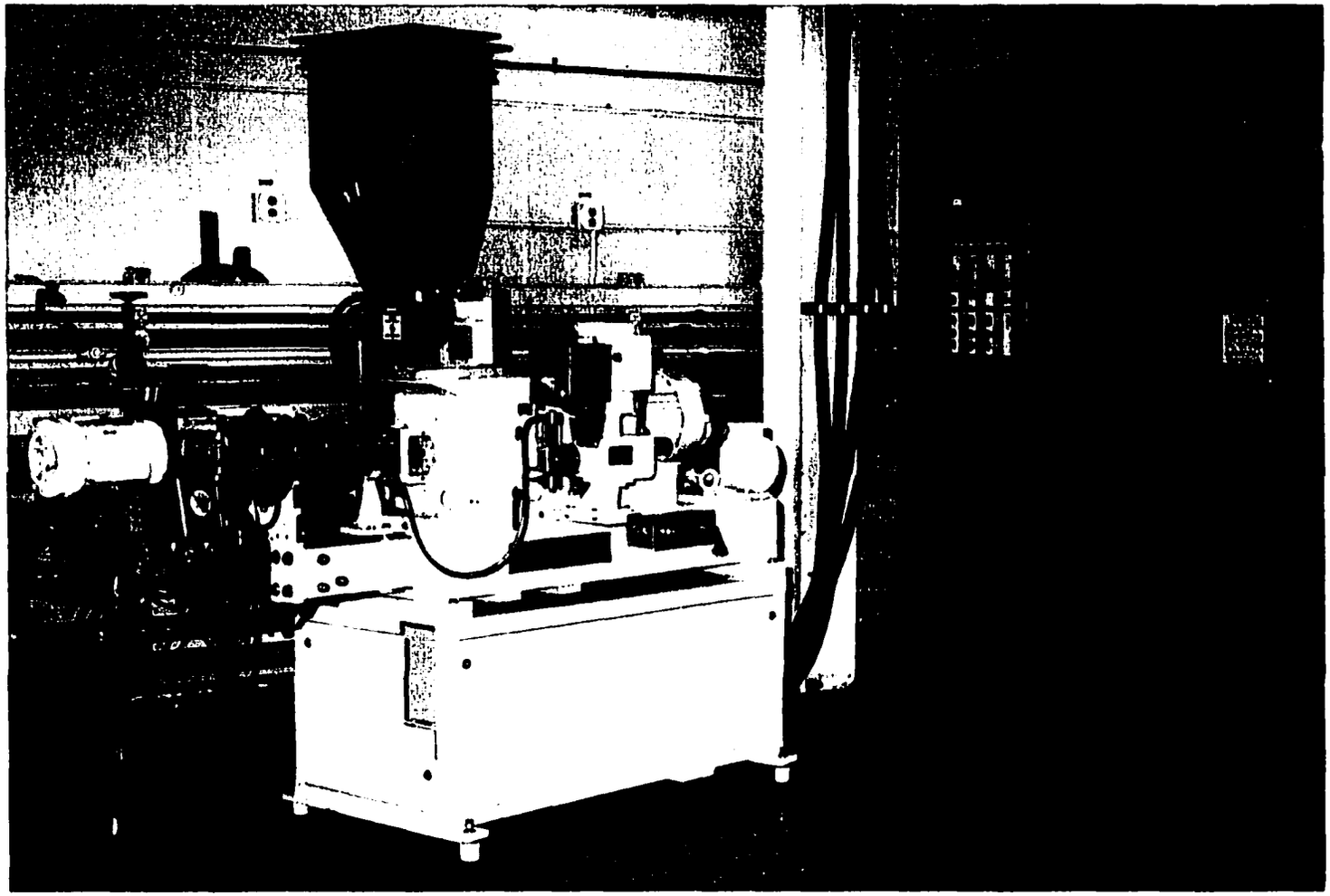

Figure 3.1 Clextral BC-21 twin-screw extruder

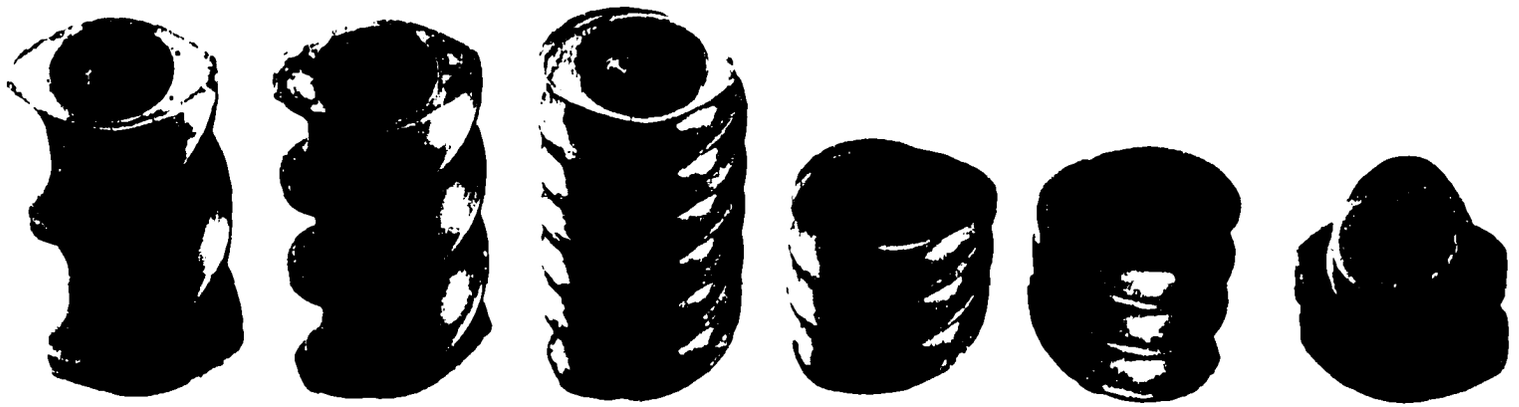

Figure 3.2 Examples of conveying (con) and mixing elements with different pitch (P) and length (L) in mm: 1 (con, P=50 & L=50), 2 (con, P=33.3 & L=50), 3 (con, P=16.6 & L=50), 4 (con, P=16.6 & L=25) 5 (RSE, P=16.6 & L=25), 6 (KB, Stagger angle=90°, L=20mm).

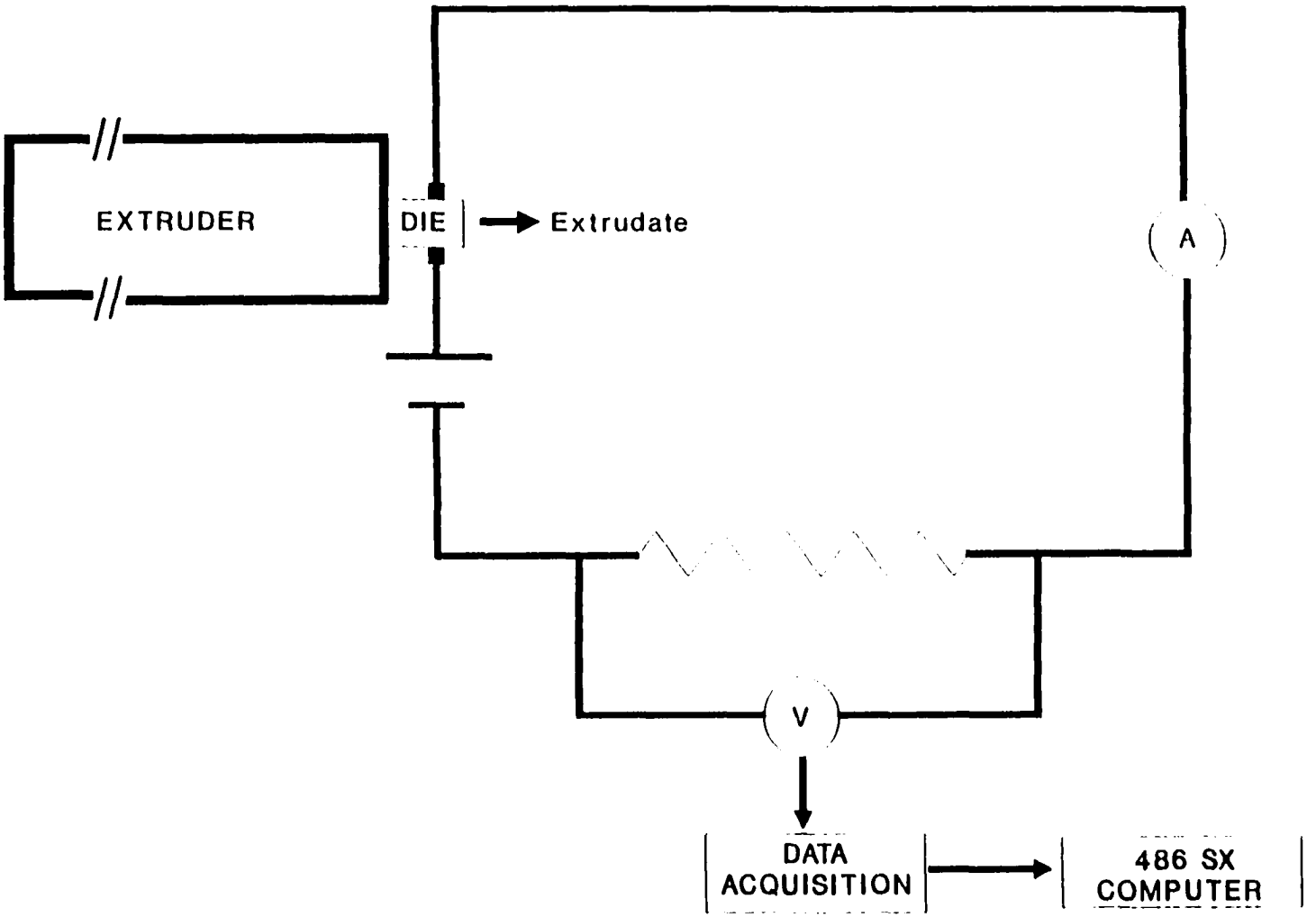

Figure 3.3 Schematic of the on-line system for RTD measurement.

Figure 3.4 Extruder die for on-line RTD measurement.

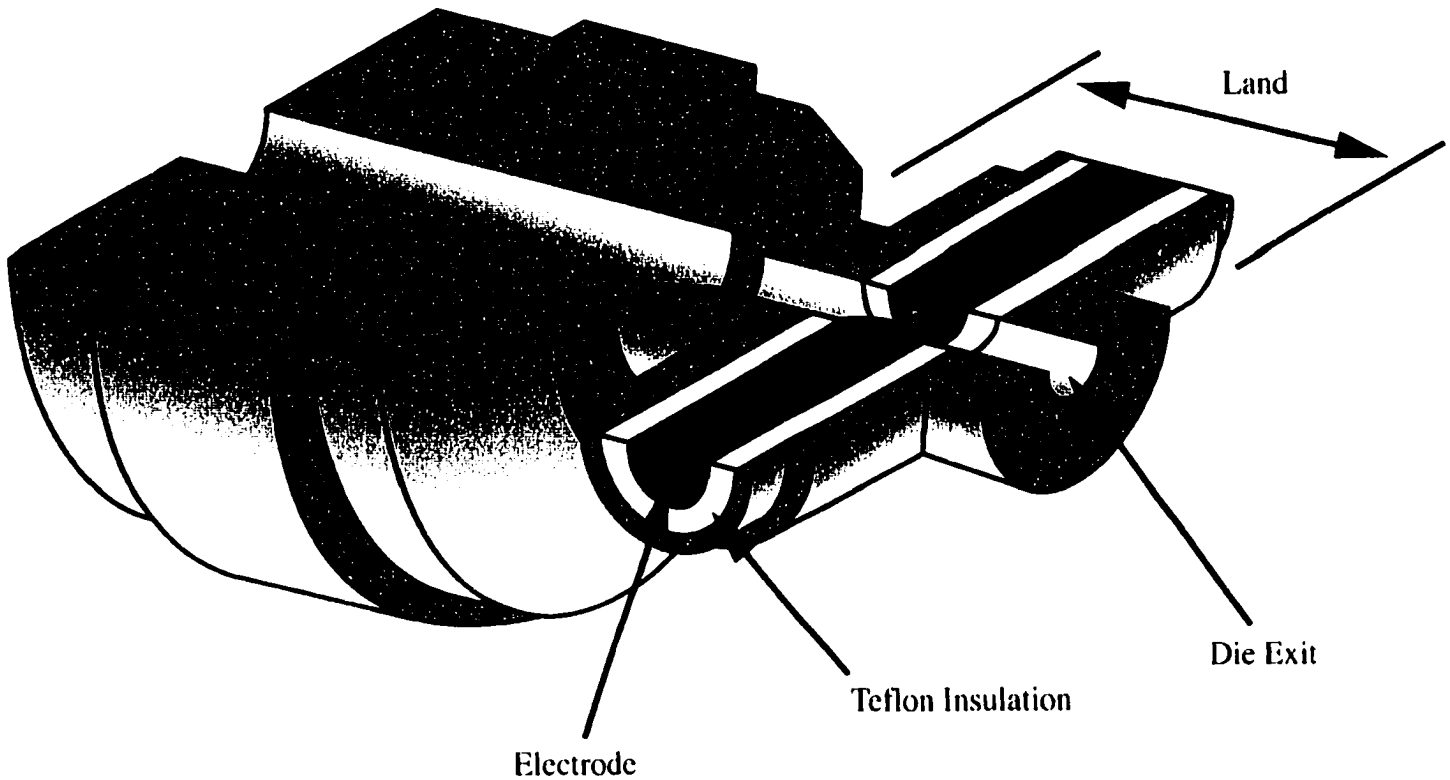

Figure 3.5 Longitudinal crossection of the die for RTD measurement.

of the die was insulated with high grade teflon. Material conductivity in the die was monitored as a proportional voltage response across the 10 ohm resistor using a Fluke multimeter (VWR Scientific, Seattle, WA) and recorded by a data logger (Model 21X, Campbell Scientific, Logan, UT) connected to a 486 SX computer. The monitoring and recording systems were equipped with a timer.

3.4.2 Preparation of tracer mixes

Rice flour, air dried in a convection oven at 105°C, was mixed with tracers for addition at the feed inlet. For use in the on-line method, a calculated amount of saturated $NaNO_3$ solution was added to dry rice flour to adjust the moisture content of the mix to 20% (w/w). The tracer mix for the post-run method was prepared by mixing erythrosine dye with dry rice flour in the ratio 20:80 and adjusting the moisture content to 20% (w/w) by water addition. In each method, 2.5 g of the tracer mix was used for measurement of RTD.

3.4.3 Determination of RTD by the on-line method

A conveying screw configuration (Configuration 1 in Table 3.3) was used during RTD measurement. The barrel temperature profile used is shown in Fig. 3.6. The feed flow rate and screw speed were 12 kg/h and 400 rpm, respectively. At steady state extrusion condition, indicated by steady temperature and torque, the on-line system was switched on to obtain the baseline voltage. The sodium nitrate tracer mix (2.5 g) was

Table 3.3 Screw configurations showing location of conveying and reverse screw element(s) during RTD experiments.

Screw configuration#	Profile of conveying elements and reverse screw element(s) (pitch/length/number)							
1	50/50/3	33.3/50/4	25/50/3	25/25/3	16.6/50/2	16.6/25/5		
2	50/50/3	33.3/50/4	25/50/3	25/25/3	16.6/50/1	16.6/25/4	[a]LH16.6/25/1	16.6/50/1

[a]LH = Left handed screw, reverse screw element (25 mm long)

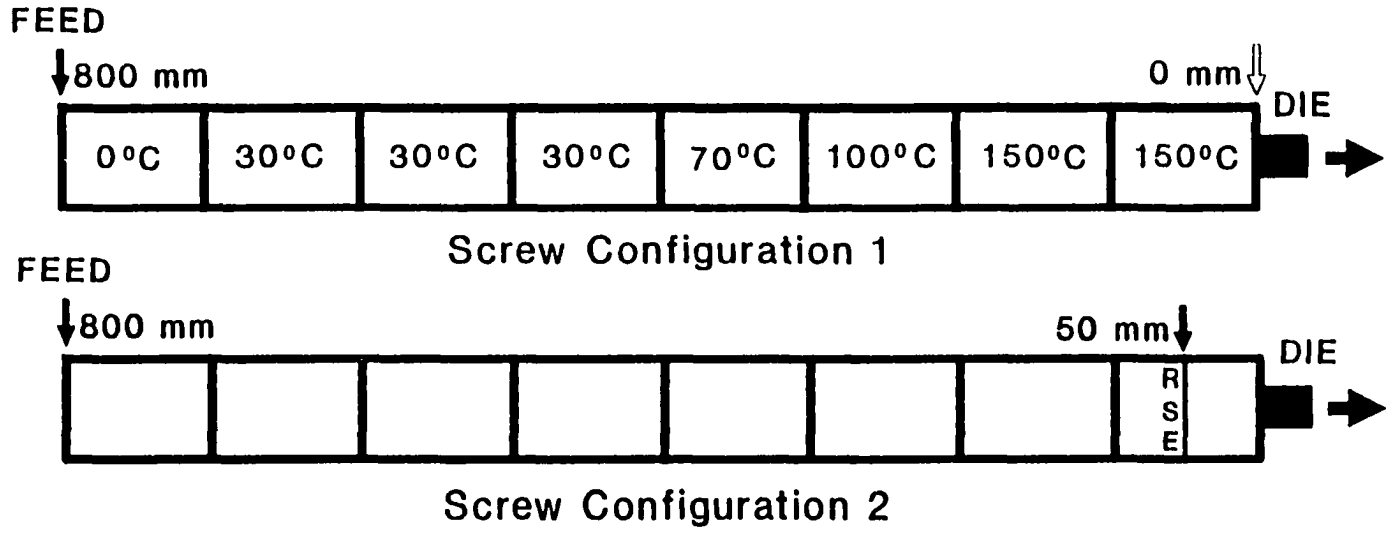

Figure 3.6 Extruder layout showing temperature profile and location of reverse screw element (RSE) for on-line RTD measurement.

then introduced as a pulse into the feed inlet using an extended funnel. Change in material conductivity in the die was continuously recorded as a proportional voltage drop across the 10 ohm resistor. The data was transferred and saved on the hard drive of the computer after the voltage across the resistor returned to the baseline. Reported results are average of two replicate extrusion runs.

The E(t), F(t) functions, mean residence time (t_{mean}), and normalized functions were calculated using the following equations (Levenspiel, 1972):

$$E(t) = \frac{c_i}{\int_0^\infty c_i\, dt} \approx \frac{c_i}{\sum_0^\infty c_i\, \Delta t_i} \qquad (1)$$

$$F(t) = \int_0^t E(t)\, dt \cong \frac{\sum_0^t c_i\, \Delta t_i}{\sum_0^\infty c_i\, \Delta t_i} \qquad (2)$$

where c_i is the tracer concentration in the sample at time t_i, and Δt_i is time interval between successive samplings.

$$t_{mean} = \int_0^t t_i\, E(t)\, dt \cong \frac{\sum_0^\infty t_i\, c_i\, \Delta t_i}{\sum_0^\infty c_i\, \Delta t_i} \qquad (3)$$

The normalized functions are given by:

$$F(\theta) = F(t) \quad (4)$$

$$\theta = \frac{t}{t_{mean}} \quad (5)$$

3.4.4 Validation of the on-line method

A post-run method using erythrosine dye was used to validate the on-line technique. The extrusion conditions (screw configuration, feed rate, screw speed and temperature profile) were the same as those used during RTD measurement by the on-line method. Axial velocity of the extrudate was measured after attaining steady state extrusion condition. Erythrosine tracer mix (2.5 g) was then introduced as a pulse into the feed inlet using an extended funnel. Simultaneously, a timer was started and a continuous rope of extrudate was collected on a conveyor belt until the red die was no longer visible. Sections of extrudate corresponding to every instantaneous second were cut. These sections were dried overnight at 20±1°C and comminuted. Color was extracted by stirring 0.5 g of ground extrudates in 50 mL of 1 M potassium hydroxide at room temperature for 45 min (Bounie, 1988). The resultant solution was centrifuged at 12,000 g for 15 minutes in a refrigerated centrifuge (Sorvall RC5C, DuPont Instruments, Newton, CT) at 4°C. Optical density of the supernatant was measured in a Spectronic-21 (VWR Scientific, Seattle, WA) at 531 nm. Duplicate samples were used for each extrusion run. The data from the post-run method was used to calculate the E(t)

function and mean residence time (t_{mean}) as described above, and compared with those determined by the on-line method.

3.4.5 Sensitivity of the on-line method

The sensitivity of the on-line method was evaluated by determining its capability to determine the effects of extrusion process variables on residence time distribution. The process variables studied were two screw configurations (Table 3.3), two feed flow rates (8 and 12 kg/h), and two screw speeds (300 and 400 rpm). Screw configuration 1 consisted of conveying screw elements only, and the second configuration had a 25 mm long reverse screw element (16.6 mm pitch) at 50 mm from the die end (Fig. 3.6). The K-Tron feeder was calibrated to determine the set point of the rotary switch to obtain feed flow rates of 8 and 12 kg/h. Moisture content of the feed was 15% (w/w), and was achieved by adjusting the flow rate on a piston pump (Clextral Inc., Firminy Cedex, France). Barrel temperatures in the eight sections from feed to die end were as shown in Figure 3.6. When extrusion operations were under steady state conditions, indicated by steady temperature and torque, RTD was determined by the on-line method.

3.5. SCREW CONFIGURATION STUDY

The screw configuration study was carried out to determine the effects of composite screws, built from different types of conveying and mixing elements (kneading and reverse screw), on extrudate characteristics and system parameters.

3.5.1 Extrusion condition

The extruder was divided into two zones: experimental and non-experimental zones. The length and pitch of conveying screw elements were kept constant in the 600 mm long non-experimental zone. The screw profile in this section from feed end was:

50/50/3 33.5/50/4 25/50/3 25/25/3 16.6/25/1

The numbers in each of the five sets represent: pitch(mm)/length (mm)/number of elements.

A total of twenty nine screw configurations were studied (Table 3.4 a and b and Fig. 3.7). Configuration 1 had no mixing elements and is referred to as "conveying screw configuration". Remaining twenty eight screw configurations were built by placing either one (25 mm) or two (50 mm) kneading block(s) or reverse screw element(s) at different locations in the 200 mm experimental zone. A set of five kneading elements (KEs), each 5 mm long was used as a kneading block. The KEs were oriented at 77 and 103° with each other to minimize the conveying capability in either forward or backward direction. Position effects of mixing element(s) were evaluated by placing both 25 and 50 mm long mixing elements at 0, 50, 100, and 150 mm from the die (configurations 2 to 9 and 16 to 23). Length and 0 mm spacing effects of mixing elements were studied by placing two (each 25 mm long) mixing elements at 0, 50, 100, and 150 mm from the die (configurations 6 to 9 and 20-23). Another twelve screw profiles were developed by creating 25, 75, and 125 mm spacing between two (each 25 mm long) mixing elements (configurations 10-15 and 24-29).

Table 3.4a Screw configurations in the experimental zone (600-800 mm) showing location of conveying elements and kneading block(s).

Screw config. #	Location of KB from the die (mm)	Parameters evaluated	Profile of conveying elements and kneading block(s) (pitch/length/number or KB/length/number)				
1	-	-	16.6/50/2	16.6/25/4			
2	0	Position	16.6/50/2	16.6/25/3	*KB/25/1		
3	50		16.6/50/2	16.6/25/1	KB/25/1	16.6/25/2	
4	100		16.6/25/3	KB/25/1	16.6/50/2		
5	150		16.6/25/1	KB/25/1	16.6/25/2	16.6/50/2	
6	0 & 25	Length/ Spacing	16.6/50/2	16.6/25/2	KB/25/2		
7	50 & 75		16.6/50/2	KB/25/2	16.6/25/2		
8	100 & 125		16.6/25/2	KB/25/2	16.6/50/2		
9	150 & 175		KB/25/2	16.6/25/2	16.6/50/2		
10	0 & 50	Spacing	16.6/50/2	16.6/25/1	KB/25/1	16.6/25/1	KB/25/1
11	50 & 100		16.6/25/3	KB/25/1	16.6/25/1	KB/25/1	16.6/25/2
12	100 & 150		16.6/25/1	KB/25/1	16.6/25/1	KB/25/1	16.6/50/2
13	0 & 100		16.6/50/1	16.6/25/1	KB/25/1	16.6/25/3	KB/25/1
14	50 & 150		16.6/25/1	KB/25/1	16.6/25/3	KB/25/1	16.6/50/1
15	0 & 150		16.6/25/1	KB/25/1	16.6/50/1	16.6/25/3	KB/25/1

* KB = Kneading Block (25 mm long)
= KE/77/1/5 KE/103/1/5 KE/77/1/5 KE/103/1/5 KE/77/1/5 (KE/Stagger angle (°)/No. of KE/length)

Table 3.4b Screw configurations in the experimental zone (600-800 mm) showing location of conveying and reverse screw element(s).

Screw config. #	Location of RSE from the die (mm)	Parameters evaluated	Profile of conveying and reverse screw element(s) (pitch/length/number)				
16	-	-	16.6/50/2	16.6/25/4			
17	0	Position	16.6/50/2	16.6/25/3	[b]LH16.6/25/1		
18	50		16.6/50/2	16.6/25/1	LH16.6/25/1	16.6/25/2	
19	100		16.6/25/3	LH16.6/25/1	16.6/50/2		
20	150		16.6/25/1	LH16.6/25/1	16.6/25/2	16.6/50/2	
21	0 & 25	Length/ Spacing	16.6/50/2	16.6/25/2	LH16.6/25/2		
22	50 & 75		16.6/50/2	LH16.6/25/2	16.6/25/2		
23	100 & 125		16.6/25/2	LH16.6/25/2	16.6/50/2		
24	150 & 175		LH16.6/25/2	16.6/25/2	16.6/50/2		
25	0 & 50	Spacing	16.6/50/2	16.6/25/1	LH16.6/25/1	16.6/25/1	LH16.6/25/1
26	50 & 100		16.6/25/3	LH16.6/25/1	16.6/25/1	LH16.6/25/1	16.6/25/2
27	100 & 150		16.6/25/1	LH16.6/25/1	16.6/25/1	LH16.6/25/1	16.6/50/2
28	0 & 100		16.6/50/1	16.6/25/1	LH16.6/25/1	16.6/25/3	LH16.6/25/1
29	50 & 150		16.6/25/1	LH16.6/25/1	16.6/25/3	LH16.6/25/1	16.6/50/1
30	0 & 150		16.6/25/1	LH16.6/25/1	16.6/50/1	16.6/25/3	LH16.6/25/1

[b] LH = Left Hand screw, 25 mm long reverse screw element

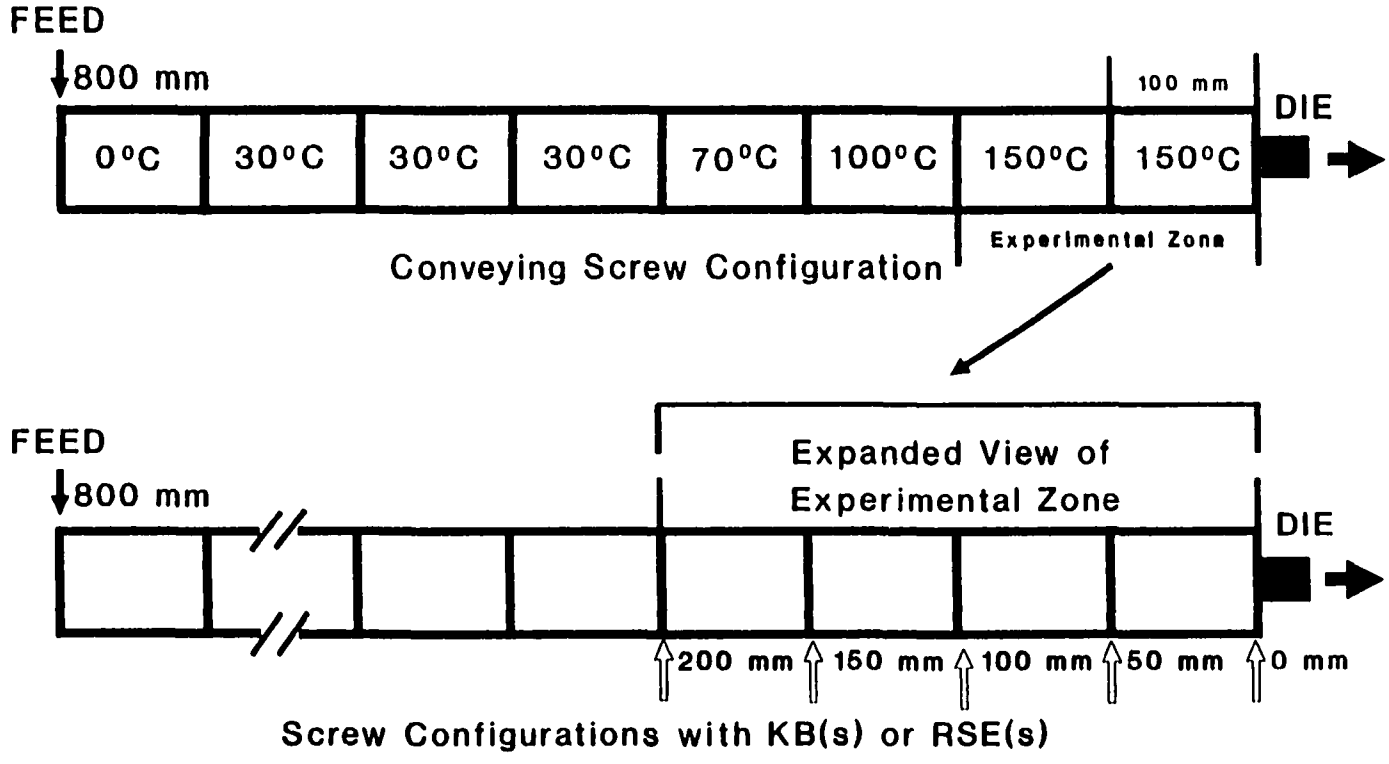

Figure 3.7 Extruder layout for screw configuration study showing temperature profile and location of kneading block(s) or reverse screw element(s) in the experimental zone.

The K-Tron feeder was calibrated to determine the set point of the rotary feeder switch for rice flour to obtain a flow rate of 12 kg/h for all the experimental runs. Screw speed and moisture content were fixed at 400 RPM and 15%, respectively. Temperature profile in the eight barrel sections from feed to die end were set at 0, 30, 30, 30, 70, 100, 150, and 150°C for all the experiments. When extrusion operations were under steady state conditions, indicated by steady state temperature and torque, samples were collected and dried overnight under ambient conditions for analysis of extrudate characteristics. All results are average of at least two extrusion runs.

3.5.2 Response Variables

Response variables used to evaluate the effects of screw configuration and feed composition were:

3.5.2.1 Energy input

i) Specific Mechanical Energy (SME)

SME was calculated using the equation:

$$SME = \frac{n\ (actual)}{n\ (rated)} * \frac{\%\tau}{100} * \frac{P\ (rated)}{\dot{m}} \qquad (6)$$

where, n = screw speed (rpm)

τ = net torque, defined as the measured torque less the lost frictional torque due to bearings and gear drive assembly

P = motor power (kJ/s)

$\dot{m}$ = feed rate (kg/s)

ii) Specific Thermal Energy (STE)

STE was calculated using the equation:

$$STE = \frac{k * 0.125}{t * \dot{m}} \quad (7)$$

where, k = power meter reading (kW.s)

t = time (s)

$\dot{m}$ = feed rate (kg/s)

0.125 = power meter constant

iii) Total Specific Energy

Total specific energy was calculated by adding specific mechanical and thermal energies.

3.5.2.2 System parameters

Die temperature, %torque, and power meter readings were read directly from the control panel.

3.5.2.3 Process energy demand

The energy demand of the process was calculated using the *law of conservation of energy*, which states that all energy entering a process is equal to that leaving the process plus the energy left in the process (Geankoplis, 1983). In extrusion processing there was no energy accumulation. Therefore, at steady state

$$\textit{Energy input} = \textit{Energy output} \tag{8}$$

i) Energy input

Energy input to the process was in two forms:

a) Mechanical Energy (ME): ME was calculated by multiplying the SME obtained from eq. 6 by mass flow rate.

b) Thermal Energy (TE): TE was determined by multiplying the STE obtained from eq. 7 by mass flow rate.

ii) Energy output

Energy output from the process consisted of the following:

a) Energy content of the material ($\dot{q}_{ex}$) just before the die exit, calculated as:

$$\dot{q}_{ex} = \dot{m}_{ex} * C_{p_{ex}} * (T_2 - T_1) \tag{9}$$

where, $\dot{m}_{ex}$ = mass flow rate of material (kg/s)

Cp_{ex} = specific heat of material (J/kg.K), determined using the

predictive model of Heldman and Singh (1981)

T_2 = material temperature at the die (K)

T_1 = material temperature at the feed inlet (K)

Predictive model of Heldman and Singh (1981) for the specific heat of food given by:

$$C_p = 1.424X_c + 1.549X_p + 1.675X_f + 0.837X_a + 4.18X_w \quad (10)$$

where, the subscripts represents various components of rice flour:

c = carbohydrate, p = proteins, f = fat, a = ash, and w = water.

b) Energy gained by the cooling water ($\dot{q}_w$), given by the equation:

$$\dot{q}_w = \dot{m}_w * (H_2 - H_1) \quad (11)$$

where, $\dot{m}_w$ = mass flow rate of cooling water (kg/s)

H_2 = specific enthalpy of water at the extruder exit (kJ/kg)

H_1 = specific enthalpy of water at the extruder inlet (kJ/kg)

c) Energy loss due to natural convection. The convective heat loss ($\dot{Q}_{total}$) was the sum of losses from each extruder component ($\dot{q}_{(loss)_i}$) calculated using the following equation:

$$\dot{q}_{(loss)_i} = h_i * A_i * (T_{2i} - T_1) \quad (12)$$

where, h_i = heat transfer coefficient ($W/m^2.K$) of the extruder component i.

A_i = heat exchange area (m^2) of the extruder component i.

T_{2i} = temperature (K) at the surface of component i

T_1 = room temperature (K)

The average natural convection heat-transfer coefficient (h_i) for extruder components was determined using the following general equation (Geankoplis, 1983):

$$N_{Nus} = \frac{(hL)}{K} = a\,(N_{Gr}N_{Pr})^m = a\left(\frac{L^3\rho^2 g\beta\Delta T}{\mu^2} * \frac{C_p\mu}{k}\right)^m \qquad (13)$$

where, N_{Nus} is the Nusselt number, h is the convective heat transfer coefficient ($W/m^2.K$), L is the characteristic geometric parameter (m), k is the thermal conductivity (W/m.K) of air, N_{Gr} is the Grashof number, N_{Pr} is the Prandtl number, a and m are constants that depend on the product of N_{Gr} and N_{Pr}, ρ is the density (kg/m^3) of air, g is the acceleration due to gravity (m^2/s), β is the volumetric coefficient of expansion (1/K) of air, ΔT is the positive temperature difference between the surface temperature of the extruder component and film temperature (K), μ is the viscosity (Pa.s), and C_p is the specific heat (J/kg.K) of air.

The values of the physical properties of air were determined at the film temperature (T_{film}) given by the equation (Geankoplis, 1983):

$$T_{film} = \frac{(T_{surface} + T_{room})}{2} \quad (14)$$

The extruder was divided into eight sections. Each section comprised of three components: a heater, a barrel, and a clamp. All extruder components were modeled as horizontal cylinders. Surface temperatures and heat exchange areas of components in contact with the room air were measured. A fortran program was written to calculate convective heat transfer coefficient for individual components (h_i), heat loss from each component ($\dot{q}_{(loss)_i}$), and total heat loss due to natural convection from the extruder surfaces ($\dot{Q}_{total}$).

3.5.2.4 Residence time distribution and mixing index

Residence time distribution was determined using the on-line system as described in section 3.4.4. The E(t), F(t) functions, mean residence time (t_{mean}), and normalized functions were calculated using equations 1, 2, 3, 4 and 5.

Peclet number, reciprocal of dispersion number (D/uL, where D is the diffusivity in m^2/s, u is the velocity in m/s, and L is length in m of vessel), was used to measure the extent of mixing (Levenspiel, 1972). When D/uL approaches zero, the dispersion is negligible and hence the flow is plug. As D/uL approaches infinity, there exists significant dispersion and hence the flow is mixed. In an extruder, the value of D/uL can be calculated from the mean residence time and normalized variance (σ_θ^2) of the curve, given by:

$$\sigma_\theta^2 = \frac{\sigma^2}{t_{mean}^2} = 2\frac{D}{uL} - 2\left(\frac{D}{uL}\right)^2 \left(1 - e^{-uL/D}\right) \quad (15)$$

Variance (σ^2), of the E(t) curve was determined using the equation:

$$\sigma^2 = \frac{\sum_0^\infty t_i^2 \, c_i \, \Delta t_i}{\sum_0^\infty c_i \, \Delta t_i} - t_{mean}^2 \quad (16)$$

A fortran program was written to calculate dispersion number (D/uL) by an iterative approach and using eq. 15. Peclet number (uL/D), reciprocal of dispersion number, was also calculated using the same program.

3.5.2.5 Determination of molecular changes of starch polymers during extrusion.

i) Starch breakdown by Gel Permeation Chromatography (GPC)

The combination of shear, temperature, and pressure during extrusion leads to fragmentation of starch. Molecular breakdown of starch polymers in the extrudate was determined by GPC. The principle of GPC is described in detail by Scopes (1994).

Ground extrudate samples (10 mg) were suspended in 3 mL of 100% dimethyl sulfoxide (DMSO) and stirred for 72 h at room temperature (19±1°C). The tubes were centrifuged at 10,000 x g for 30 minutes to recover the DMSO soluble starch.

Supernatants were diluted with distilled water to 50% DMSO and centrifuged again at 10,000 x g for 30 minutes. Aliquotes of 1.5 mL were chromatographed on a 2.5 cm diameter and 45 cm long column packed with Sephacryl S-1000 (Pharmacia Biotech, Uppsala, Sweden). The column was eluted with 50% DMSO at a flow rate of 80-85 mL/h. Fractions of 7.1 mL were collected in a fraction collector and assayed with phenol sulfuric acid (Dubois et al., 1956). Two mL of eluted sample was pipetted into a colorimetric tube, and 0.05 mL of 80% phenol was added, followed by rapid addition of 5 mL concentrated sulphuric acid. The solution was allowed to stand for 10 min, then shaken and placed in a water bath at 30°C for 20 min. The absorbance of the characteristic yellow-orange color was measured at 490 nm. Blanks were prepared by substituting distilled water for eluted sample. The amount of carbohydrate was determined using a standard curve.

ii) Starch gelatinization by Differential Scanning Calorimetry (DSC)

Starch gelatinization is the main reaction that occurs during low-moisture twin-screw extrusion of starchy ingredients. Degree of starch gelatinization was evaluated from DSC endotherms.

Unextruded rice flour and extrudates with different screw configurations were analyzed with a Perkin-Elmer DSC 7 differential scanning calorimeter (Perkin Elmer, Wilton, CT). Sample (10-20 μg) at 60% moisture were encapsulated in the stainless steel sample holders that can withstand high pressures. The DSC was purged with ultra high

pure nitrogen gas at 30 psig. The heating rate and scan range were 10°C/min and 40-115°C, respectively.

3.5.2.7 Macroscopic characteristics of the extrudates

The macroscopic attributes of the extrudates determined were apparent, solid and bulk densities; porosity; radial, axial, and overall expansion; and textural attributes.

i) Densities

The apparent density (ρ_{app}) was estimated by determining the mass and apparent volume of individual dry, cylindrical extruded rods. Apparent volume was calculated as the product of length and cross-section area of the extruded rods.

True powder density (ρ_{true}) and porosity (ϵ) of the extrudates were determined by using Quantachrome multipycnometer (Chang, 1988). The multipycnometer is a single station manually operated pycnometer designed to measure true volume of various quantities of solid materials. The technique employs Archimedes principle of fluid displacement to determine the volume. The displaced fluid is a gas which can penetrate the finest pores. For this reason, helium was used because its small atomic dimension assures penetration into crevices and pores approaching one Angstron (10^{-10}m). Figure 3.8 is a flow diagram of the multipycnometer (Quantachrome Corp., 1995).

The multipycnometer determines the true density of solid or powder samples by measuring the pressure difference when a known quantity of helium under pressure is allowed to flow from a precisely known reference volume (V_R) into a sample cell

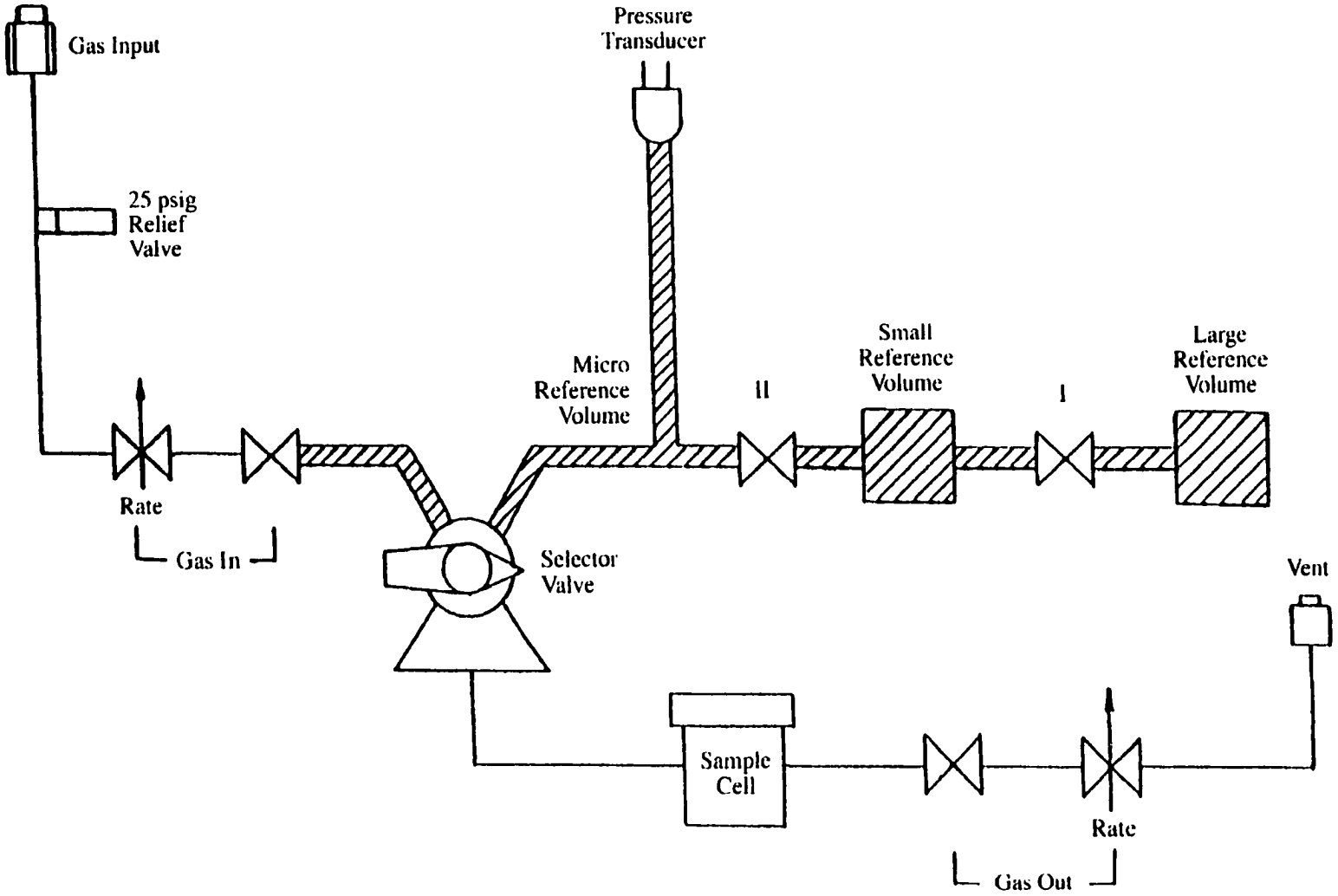

Figure 3.7 Schematic of multipycnometer (Quatachrome Corp., 1995).

containing the sample. The shaded area in Figure 3.7 represents the known reference volume V_R. After the system is purged with helium the selector valve is turned to "CELL", the "GAS OUT" toggle valve opened and the "GAS IN" toggle valve closed. The system is now at ambient pressure P_a and the state of the sample cell with sample is defined by:

$$P_a(V_c - V_p) = n_a RT_a \tag{17}$$

where n_a is the number of moles of gas occupying the cell volume (V_c) including the powder volume (V_p), and R is the gas constant and T_a is the ambient temperature.

When the reference volume is pressurized to approximately 17 psig, the state of the reference volume (V_R) can be expressed as

$$P_1 V_R = n_1 RT_a \tag{18}$$

where P_1 represents a pressure above ambient and n_1 is the total number of moles of gas in the reference volume (V_R). When the selector valve is turned to connect the sample cell, the pressure will fall to a lower pressure P_2, given by

$$P_2(V_C - V_P + V_R) = n_a RT_a + n_1 RT_a \tag{19}$$

Substituting equations (17) and (18) into (19), and simplifying, gives

$$V_C - V_P = \frac{P_1 - P_2}{P_2 - P_a} * V_R \tag{20}$$

Since P_a is made to read zero on the digital meter, i.e., all pressure measurements

are relative to P_a, equation 20 becomes

$$V_C - V_P = \frac{P_1 - P_2}{P_2} * V_R \tag{21}$$

or

$$V_P = V_C - V_R[\frac{P_1}{P_2} - 1] \tag{22}$$

Equation (22) is the working equation employed in the multipycnometer. True volume of a known mass of sample was determined to calculate true density.

ii) Porosity

Porosity of the sample was calculated as

$$porosity(\epsilon) = \frac{apparent\ volume\ of\ ex - true\ volume\ of\ ex}{apparent\ volume\ of\ ex} \tag{23}$$

where, ex is the extrudate.

iii) Expansion ratios

The radial expansion ratio was measured as the ratio of the cross-section area of the extruded rods (A_{ex}) to that of the die (A_{die}) (Bhattacharya and Choudhury, 1994):

$$(ER)_{radial} = \frac{A_{ex}}{A_{die}} = \frac{(D_{ex})^2}{(D_{die})^2} \tag{24}$$

where, D_{ex} is the diameter of the extruded product, and D_{die} is the diameter of the die measured by a digital vernier caliper (Mitutoyo Corp., Japan)

The overall expansion ratio was determined as a ratio of the apparent specific volume (v_{app}) to the true specific volume (v_{true}) of the extrudates:

$$(ER)_{overall} = \frac{v_{app}}{v_{true}} \tag{25}$$

The true volume was calculated by Quantachrome multipycnometer

Axial expansion of the extrudate was calculated from overall and radial expansion ratios using the equation:

$$(ER)_{Axial} = \frac{(ER)_{overall}}{(ER)_{radial}} \tag{26}$$

iv) Breaking strength

The force required to cut the product into two pieces was an indicator of its hardness. It was determined as the maximum force offered by the sample during cutting in an Instron Universal Testing machine (Model No. 1000) with a Warner-Bratzler shear attachment. The stainless steel shear blade was 1.22 mm thick with a shear angle of 60°. Instron was operated at a cross-head speed of 500 mm/min; the full load scale was 100 N. Single extruded cylindrical rods were placed in the Warner-Bratzler cell and cut into two pieces by the shear blade. Breaking strength was determined by dividing the maximum force to cut the product into two pieces by cross sectional area of the product

(Chinnaswamy and Hanna, 1988).

3.6 LOW-MOISTURE EXTRUSION OF ARROWTOOTH FLOUNDER MUSCLE

Blends of rice flour, unhydrolysed, and hydrolysed arrowtooth flounder muscle were extruded at the desired screw configuration.

3.6.1 Preparation of arrowtooth flounder muscle for extrusion

Frozen arrowtooth mince was thawed in a walk-in cooler (4°C) overnight. This mince was used to produce unhydrolysed and hydrolysed fish muscle powder as described below.

3.6.1.1 Unhydrolysed fish muscle

The thawed mince was mixed with 1.5% rice flour to increase viscosity, and stirred for 30 min in a Food Double Mixer (Leland, Detroit, MI). The protease(s) in the mince was inactivated by an extrusion process developed by Choudhury and Gogoi (1996). A conveying screw profile (Table 3.4a and Fig. 3.7) was used for this experiment. The barrel temperatures in the two sections closest to the die were maintained to ensure a material temperature of 105°C in the die. The rest of the barrel sections were kept at constant temperature of 20°C by circulating cold water through the jacketed barrels. The material flow rate and screw speed were 18 kg/h and 400 rpm,

respectively. The extrudate obtained was collected and immediately placed in a cold room (4°C).

3.6.1.2 Hydrolysed fish muscle

Wilson and Choudhury (1998) developed a continuous stir tank reactor (CSTR) for hydrolysis of arrowtooth flounder muscle. A typical hydrolysis curve from their work is shown in Figure 3.8. They used a 500 mL jacketed reactor to hydrolyse small amounts of fish muscle. Reaction rate was high during the initial phase of hydrolysis (Fig. 3.9). Hydrolysis conditions developed by Wilson and Choudhury (1998) were duplicated for large scale production of autolysed powder from arrowtooth flounder muscle.

Hydrolysis of arrowtooth flounder muscle was carried out in a jacketed kettle (Groen/Dover Ind. Co., Jackson, Mississippi). Water was added to the thawed mince in 4:1 ratio (mince:water). Steam was injected in the jacket to heat the mixture of mince and water, which was continuously stirred by a wooden paddle. When the material temperature reached about 50°C, steam supply was shut down and a stop clock was started. Hydrolysis for 5, 10, and 15 minutes were carried out in the kettle by continuously stirring the mixture and monitoring the temperature by a temperature probe. After the desired time, steam was again injected in the jacket to raise the material temperature above 80°C. Continuously stirred material was kept at this temperature for 8-10 minutes to inactivate the enzyme. Steam supply was shut down and hydrolysed material was collected and immediately transferred to the cold room.

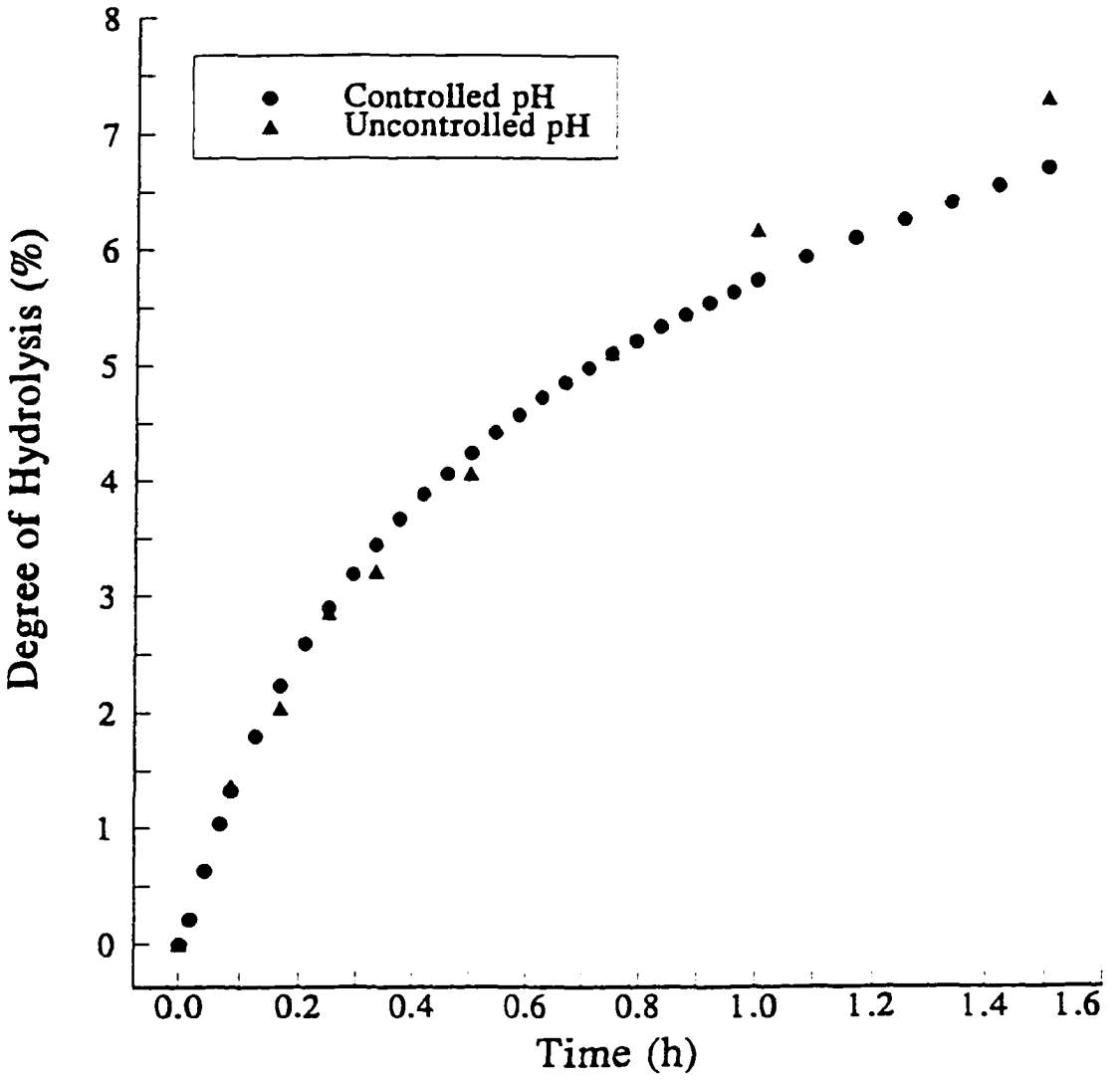

Figure 3.9 Kinetics of arrowtooth flounder muscle autolysis (Wilson and Choudhury, 1998) at 53°C. Controlled pH run was carried out at a pH 6.8.

The extent of protein hydrolysis was determined by sodium dodecylsulfate polyacrylamide gel electrophoresis (SDS-PAGE). The acrylamide concentration in the stacking and resolving gels were 4 and 12%, respectively. A Bio-Rad Protean II xi electrophoresis cell (Bio-Rad, Richmond, CA) with 16 x 20 cm plates was used. Samples were heated with loading buffer (1:10) at 95°C for 5 minutes, 20μL loaded per lane and run at 75 mA constant current for 2 gels with a Bio-Rad model 1000/500 power supply. Full fraction protein solubility and denaturing was ensured using a buffer containing 2 M thiourea, 8 M urea, 5% ß-mercaptoethanol, and 2% SDS. The buffer system of Yates and Greaser (1983) was used. Gels were held at a constant temperature of 10°C using a Brinkmann Lauda model RM-6 (Brinkmann Instrument, Westbury, NY) water circulator during each run. Gels were stained in 49.9% H_2O, 40% MeOH, 10% acetic acid, and 0.1% Bio-Rad Coomassie Brilliant Blue R-250 for 75 minutes and destained in 50% H_2O, 40% MeOH, and 10% acetic acid overnight using a Bio Rad Gel Destainer unit.

3.6.1.3 Drying of unhydrolysed and hydrolysed arrowtooth flounder muscle

A tray dryer (model CHU-150E, Enviro-pak, Clackamas, OR) was used to dry both unhydrolysed and hydrolysed Arrowtooth flounder muscle. The hydrolysed muscle (3-3.5 kg) was thinly spread on trays and kept in the dryer initially at 50°C for three hours. Temperature of the drier was increased to 65°C and the material was then dried for twenty hours.

3.6.1.4 Grinding and sieving of unhydrolysed and hydrolysed arrowtooth flounder solids

The moisture content of the dried solids was 5%. A Urschel Comitrol (model 1700, Urschel Laboratories Inc., IN) was used to grind the solids. Material passing through a 24 mesh size sieve was collected, packed in double polyethylene bags (Portco Packaging, Vancouver) and stored at 4°C.

3.6.3 Extrusion of unhydrolysed and hydrolysed arrowtooth flounder solids

A full factorial experimental design was used to evaluate the effects of hydrolysis time and fish solids content. Four hydrolysis time (0, 5, 10, and 15 minutes) were evaluated. Rice flour and its blends with fish solids (rice solids to fish solids ratio of 95/5, 90/10, and 85/15) for each hydrolysis time were prepared by blending rice flour and dried fish muscle in a Stock Mixer (Model A-200-11A) for 20 minutes. Concentration of fish proteins in each of the blends were:

Fish solids (%)	5	10	15
Fish proteins (%)	3.92	7.84	11.76

Screw configuration with a 25 mm long kneading block at 175 mm from the die was used (Fig. 3.10). The screw profile in the experimental zone (600-800 mm) showing location of conveying elements and 25 mm long KB was:

KB/25/1 16.6/25/3 16.6/50/2

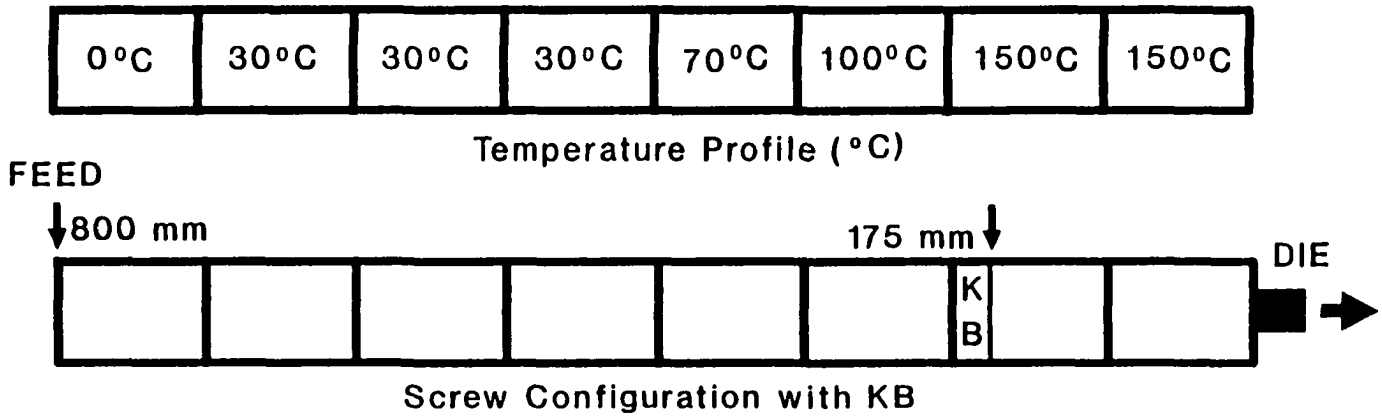

Figure 3.10 Extruder layout showing temperature profile and location of kneading block (KB) during extrusion of arrowtooth flounder muscle and rice flour blends.

Feed flow rate, screw speed, and moisture content were kept constant at 12 kg/h, 400 RPM, and 15%, respectively. The temperature profile in the eight barrel sections was fixed at 0, 30, 30, 30, 70, 100, 150, and 150°C. When extrusion operations were under steady state conditions, indicated by steady state temperature and torque, samples were collected and dried overnight under ambient conditions for analysis of extrudate characteristics. All results are average of two replicate runs.

Energy input, die temperature, residence time distribution, and macroscopic properties of the extrudates were evaluated as discussed in section 3.5.2.

3.7 STATISTICAL ANALYSIS

Descriptive statistics, coefficient of variation, t-test, analysis of variance (ANOVA) and comparison of means were performed. Descriptive statistics and coefficient of variation were calculated using the Axum graphics and data analysis software (Trimetrix, 1992). ANOVA and comparison of means were performed on all the response variables by a statistical analysis software (SAS Institute, Inc., 1996).

CHAPTER 4

RESULTS AND DISCUSSIONS

4.1 ON-LINE MEASUREMENT OF RESIDENCE TIME DISTRIBUTION (RTD)

An on-line technique was developed to measure the residence time distribution in the twin-screw extruder, one of the response variables used in this study.

4.1.1 Determination of RTD by the on-line method

A typical on-line voltage response across the 10 ohm resistor after addition of a sodium nitrate tracer mix is shown in Fig. 4.1. This response was obtained using a conveying screw configuration at a feed rate of 12 kg/h and a screw speed of 400 rpm. At steady state extrusion condition, the base line voltage due to current flow through rice flour was 13.61 ± 0.22 mV. After 11 s, the voltage rose rapidly as a result of increased current flow in the die due to the presence of the $NaNO_3$ tracer. The peak voltage of 26.78 mV was attained 18 s after addition of tracer, and it returned to the base line value after 75 s. Similar voltage response was obtained with all extrusion runs and the data were processed to validate the method and to determine its sensitivity.

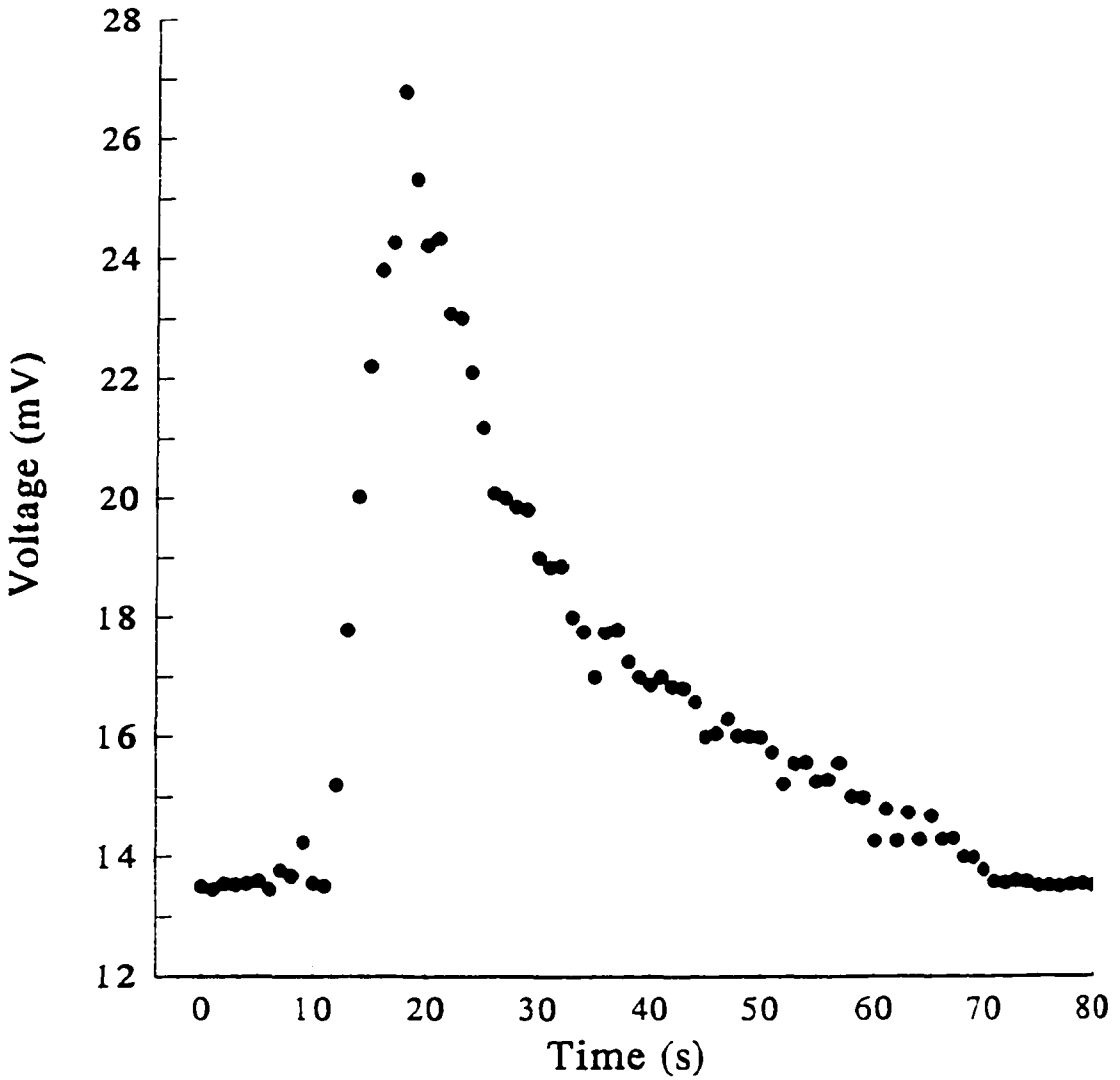

Figure 4.1 Voltage response across the resistor during on-line RTD measurement.

4.1.2 Validation of the on-line method

Figure 4.2. shows E(t), the age distribution curve, against time, for both on-line and post-run methods. The on-line method followed the same trend as that of the post-run method. The RTDs measured by the two methods superimposed on each other. The coefficient of variation (CV) during RTD measurement by the on-line method ranged between 0-5.5%, having 1 point with CV above 5% (Fig. 4.3a). The CV for the post-run method was somewhat higher (0-7%), having 11 points with CV at or above 5% (Fig. 4.3b). The new method had less experimental error because of on-line response measurement requiring less material handling. The mean residence times of rice flour obtained by the on-line and post-run methods were 29.84 and 29.53 s, respectively (Table 4.1). The total residence time was the same (75 s) as measured by on-line and post-run methods. The calculated t-values (Table 4.1) were much smaller than the tabulated t-value (3.078) at $p \leq 0.1$ indicating that the mean and total residence times obtained by the on-line and post-run methods were essentially the same.

4.1.3 Sensitivity of the on-line method

The sensitivity of the on-line method, indicated by its capability to determine the effects of three important extrusion process variables (feed rate, screw speed and screw configuration) on RTD is shown in Figure 4.4. The influence of screw speed on RTD was weaker compared to that of feed flow rate and screw configuration.

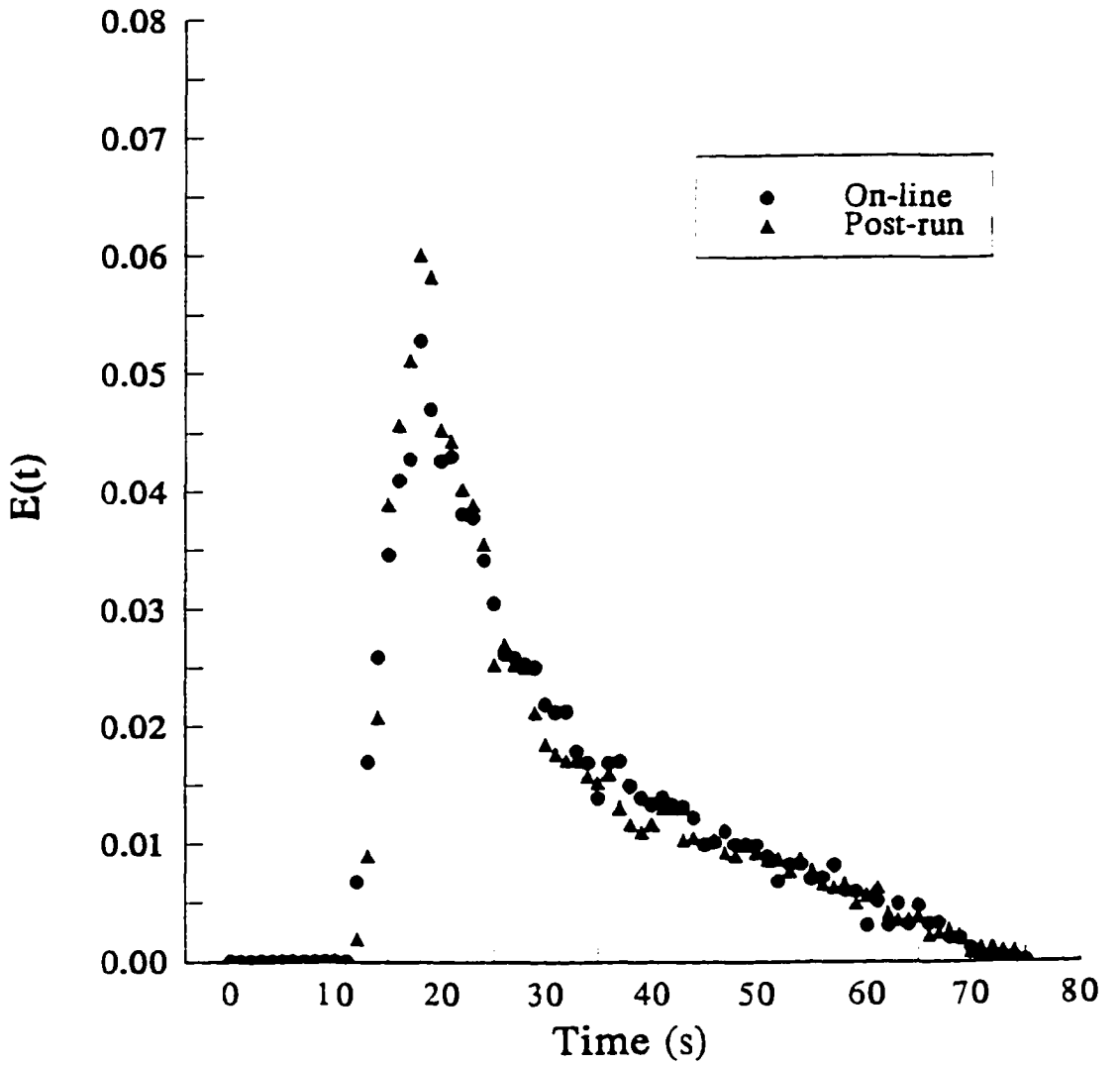

Figure 4.2 Age distribution curves obtained by the on-line and post-run techniques.

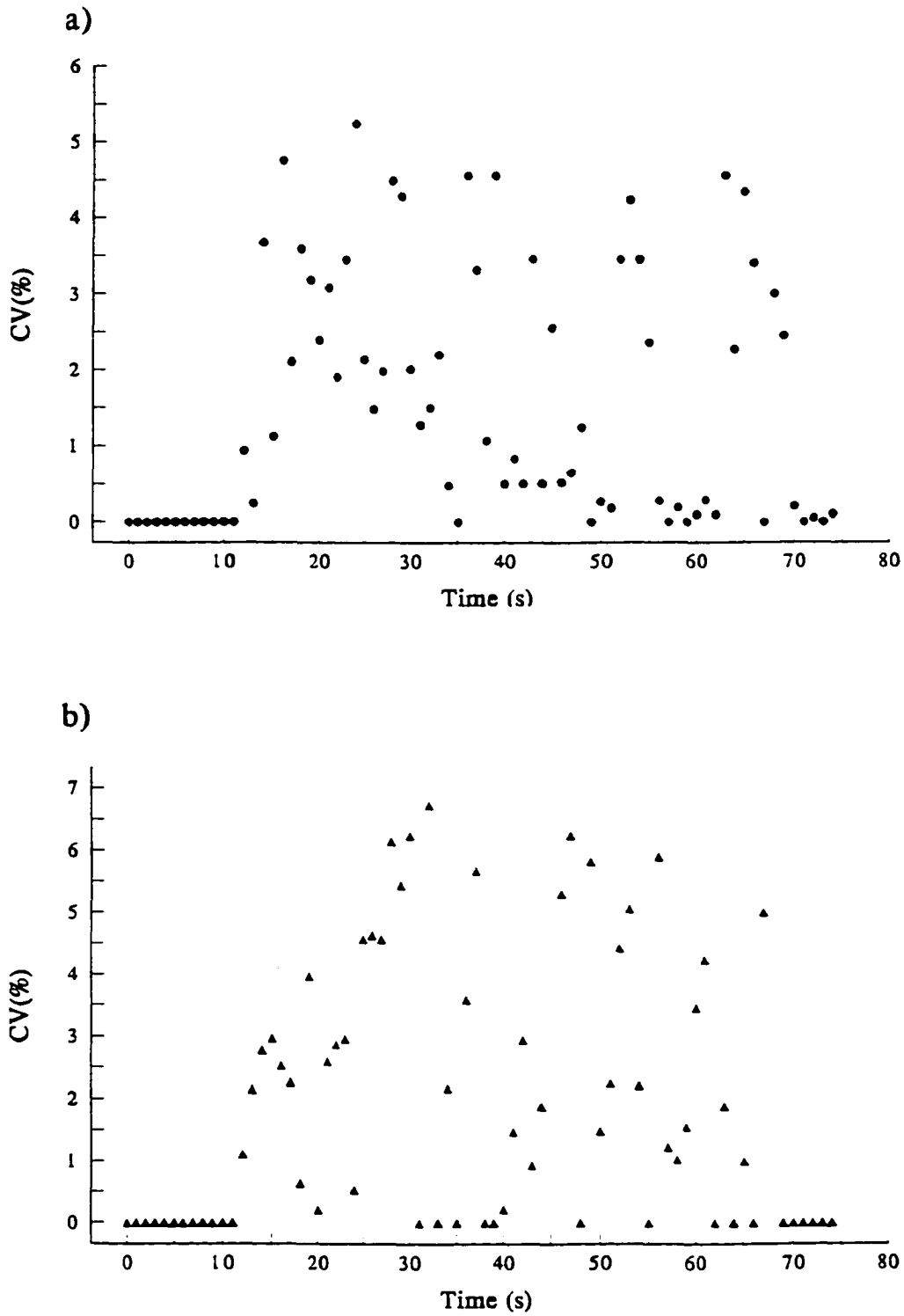

Figure 4.3 Coefficient of variation for (a) on-line and (b) post-run methods.

Table 4.1 Mean and total residence times determined by the on-line and post-run methods using a conveying screw configuration and under same experimental conditions.

Residence time (s)	Method		t value
	On-line	Post-run	
t_{mean}	29.84 ± 0.40	29.53 ± 0.45	0.73
t_{total}	75 ± 0.00	75 ± 1.41	0.00

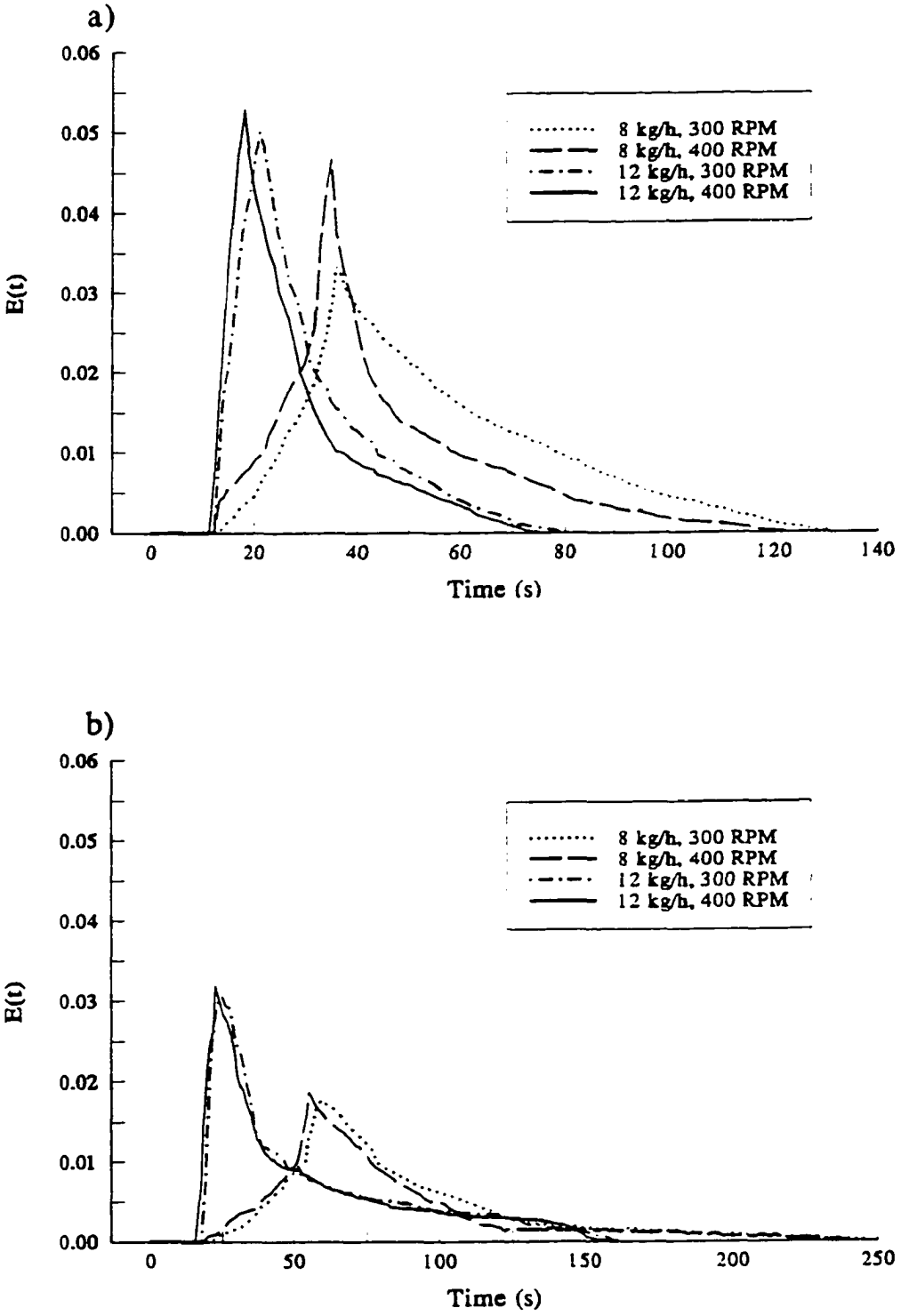

Figure 4.4 Age distribution curves measured by the on-line technique for (a) conveying screw profile and (b) screw profile with a reverse screw element at 50 mm from the die.

The effects of the three variables on mean and total residence times as determined by the on-line method are summarized in Table 4.2.

An increase in screw speed from 300 to 400 rpm did not change the RTD spread and had little effect on the shape of the RTD (Figs. 4.4 a and b). However, the on-line method was able to measure the effects of screw speed on total and mean residence times. The total residence time was reduced by 8 and 4 s when screw speed was increased from 300 to 400 rpm at a feed rate of 8 and 12 kg/h, respectively using a conveying screw configuration. Similar reduction in total residence time was observed with configuration 2 (Table 4.2 and Fig. 4.4). However, the effect on mean residence time was small in the screw speed range (300-400 rpm) studied. The reduction in mean residence time was between 1.03-2.51 s when screw speed was changed from 300 to 400 rpm at two feed flow rates and with two screw configurations (Table 4.2, Fig. 4.4). This weak effect of screw speed on mean residence time in the range of 300-400 rpm was observed by other investigators. Altomare and Ghossi (1986) reported a reduction of mean residence time between 1.9-2.6 s when screw speed was increased from 317 to 400 rpm during extrusion of rice flour (20-25% moisture content) in a Werner and Pfleiderer ZSK-57 twin-screw extruder at two feed flow rates of 121.4 and 174.1 kg/h. The average residence time was reduced by 3.1 s during extrusion of styrene-based copolymer in a Werner and Pfleiderer ZSK-30 twin-screw extruder when screw speed was increased from 300 to 400 rpm at a feed rate of 13.6 kg/h (Kao and Allison, 1984). The striking effect of feed flow rate on RTD, as measured by the on-line method, is

Table 4.2 Effects of extrusion process parameters on mean and total residence time measured by the on-line method.

Process Parameters			Residence Time	
Screw Configuration	Feed Rate (kg/h)	Screw Speed (rpm)	t_{mean} (s)	t_{total} (s)
Config. 1 (All conveying elements)	8	300	45.58 ± 0.85	130.00 ± 0.00
		400	44.55 ± 0.75	122.00 ± 1.41
	12	300	31.50 ± 0.51	79.00 ± 1.41
		400	29.84 ± 0.40	75.00 ± 0.00
Config. 2 (RSE at 50 mm from die end)	8	300	86.78 ± 1.27	247.00 ± 0.00
		400	84.27 ± 1.02	240.00 ± 2.83
	12	300	57.23 ± 0.59	163.00 ± 1.41
		400	54.78 ± 1.15	159.00 ± 2.83

shown in Fig.4.4. Higher and narrower peaks were observed with high feed flow rate (12 kg/h) compared to those at low feed flow rate (8 kg/h). A large tail was observed at low feed flow rate extending beyond 120 s for config. 1 and 240 s for config. 2. Vergnes *et al.* (1992) reported similar effects of feed flow rate on RTD. The on-line method measured large changes in total and mean residence times due to changes in feed flow rate. Increasing feed flow rate from 8 to 12 kg/h caused drastic reduction (30-39%) in total and mean residence times (Fig. 4.4, and Table 4.2). Kao and Allison (1984) reported 35% decrease in average residence time when feed flow rate was increased from 4.54 to 13.6 kg/h during extrusion of styrene-based copolymer in a Werner and Pfleiderer ZSK-30 twin-screw extruder.

Screw configuration has the most prominent effect on RTD and the data obtained by the on-line method reflect such strong effect (Figs. 4.4 and 4.5). Incorporation of a reverse screw element in the screw profile strikingly reduced the peak height and increased the RTD spread. The presence of RSE almost doubled the total and mean residence times. A similar strong effect of screw profile on RTD was reported by Altomare and Ghossi (1986) and Vergnes *et al.* (1992).

The cumulative RTD curves plotted as functions of the dimensionless time (θ) are shown in Figure 4.5 (a and b). The shape of the F distribution, obtained by the on-line method, is similar to that observed by Altomare and Ghossi (1986) for rice flour and by Kao and Allison (1984) for styrene-based copolymer.

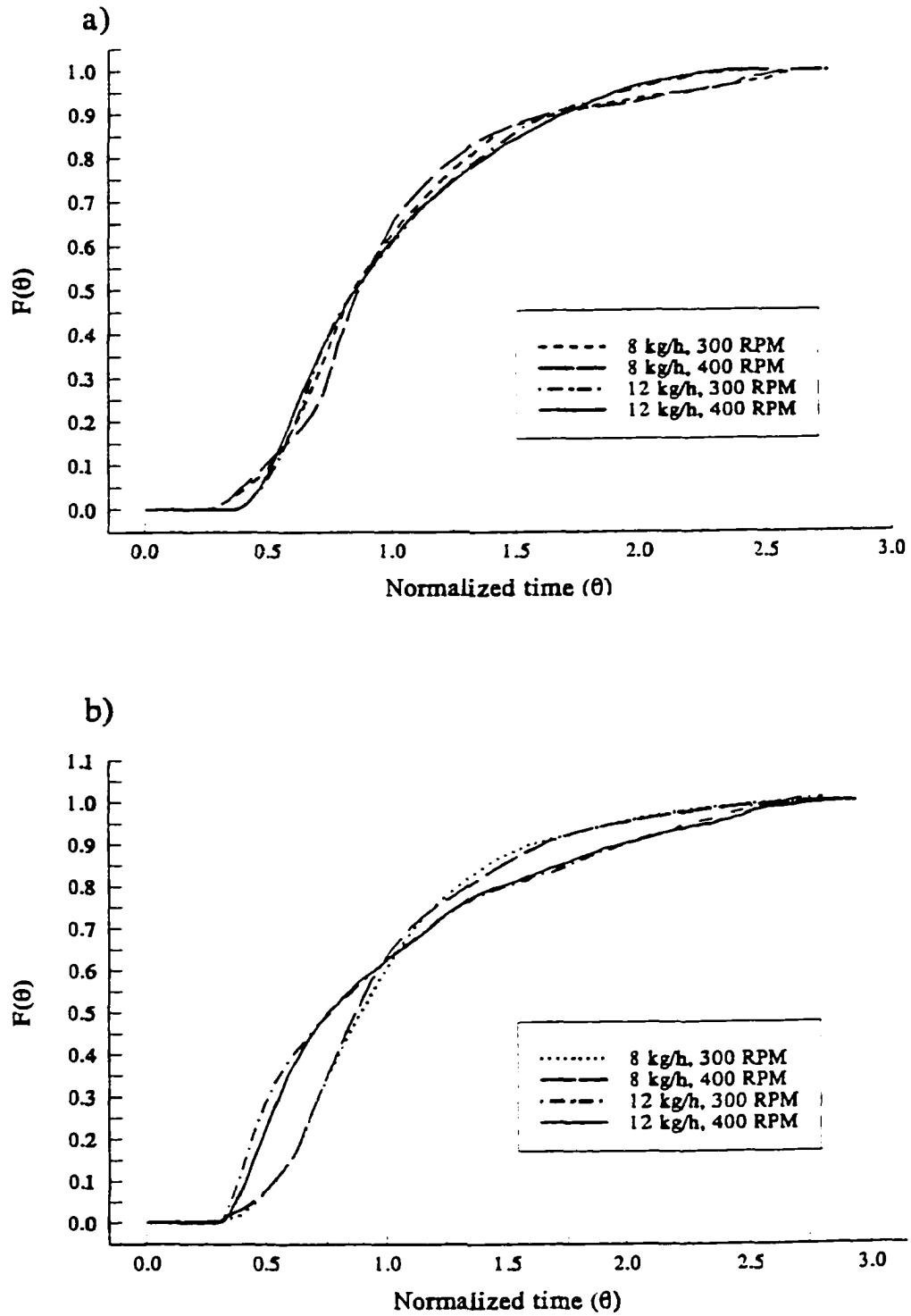

Figure 4.5 Cumulative age distribution curves obtained using the on-line technique for (a) conveying screw profile and (b) screw profile with a reverse screw element at 50 mm from the die.

4.2 SCREW CONFIGURATION STUDIES

Twin-screw extruders use segmented design which offers flexibility to alter the screw configuration, an important process variable during extrusion processing. Macroscopic extrudate characteristics can be manipulated by changing the screw configuration, as it influences energy input, residence time, and mixing, which in turn affects the rate and extent of physicochemical changes.

4.2.1 Effect of screw configuration on energy consumption, and system parameters

The extruder is a dynamic reactor. Changes in food material during extrusion are affected by both shear and thermal energy inputs. Material is heated by two forms of energy inputs in an extruder:

- viscous dissipation of mechanical energy.
- thermal energy transferred through the externally heated barrel walls.

4.2.1.1 Specific Mechanical Energy (SME)

Type, length, and position of mixing elements and their interactions affected the SME input significantly (Table 4.3). Conveying screw configuration (with no mixing elements) had the lowest SME input (47.8 kJ/kg). Incorporation of mixing elements (KB and RSE) increased the SME systematically (Fig. 4.6). For any position and length, SME input was lower with KB in the screw profile than with RSE.

Table 4.3 Analysis of variance data for energy input during extrusion of rice flour.

Source	DF	Mean Sum of Squares (MSS) and F-values for Energy Input (kJ/s)					
		Specific Mechanical Energy		Specific Thermal Energy		Total Energy	
		MSS	F	MSS	F	MSS	F
Type (Typ)	1	12836.03	2339.27**	132772.66	2404.91**	63042.01	1538.22**
Length (Len)	1	3852.23	702.04**	50851.65	921.08**	26710.95	651.75**
Position (Pos)	3	4176.43	761.12**	21180.33	383.64**	6641.17	162.04**
Typ x Len	3	1.85	0.34	1912.29	34.64**	1795.26	43.80**
Typ x Pos	3	88.48	16.12**	918.65	16.64**	957.88	23.37**
Len x Pos	3	15.61	2.85*	827.82	14.99**	925.14	22.57**
Typ x Len x Pos	1	126.68	23.09**	896.19	16.23**	436.96	10.66**
Error	16	5.49	-	55.21	-	40.98	-

**Highly significant at $p \leq 0.005$

*Significant at $p \leq 0.05$

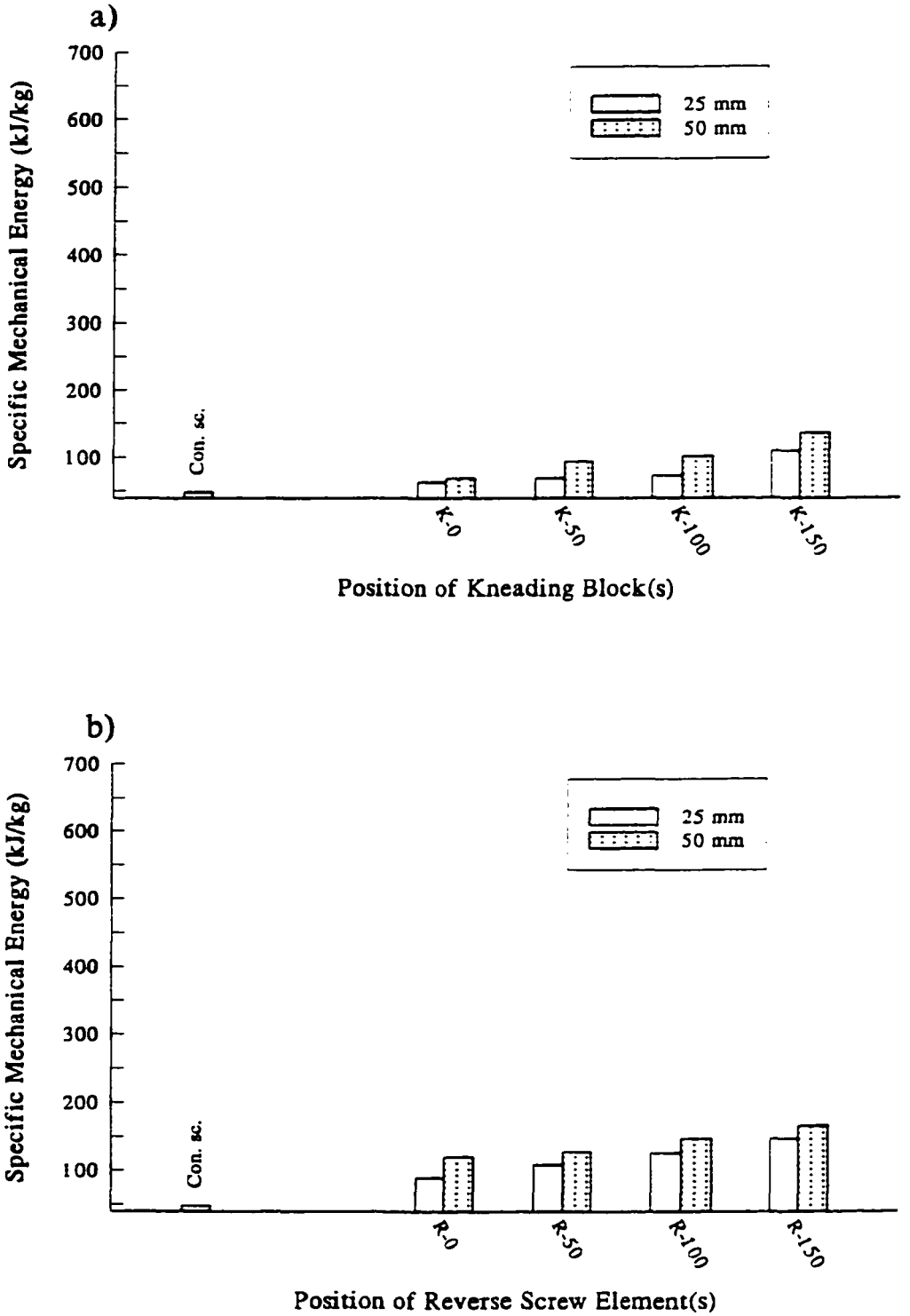

Figure 4.6 Position and length effects of (a) kneading block and (b) reverse screw element on specific mechanical energy during extrusion of rice flour.

For example, A shorter (25 mm) KB at 150 mm from the die generated 108 kJ/kg of SME input. By replacing KB at the same position by a RSE of similar length produced a higher SME input (145 kJ/kg).

A higher SME input was observed when the mixing element length was increased, irrespective of the type and position of the element (Fig. 4.6). SME input increased from 145 kJ/kg to 166 kJ/kg when 25 mm long RSE at 150 mm from the die was replaced by a 50 mm long RSE. A systematic increase in specific mechanical energy input was observed as the mixing elements (KB or RSE of any length) were moved farther away from the die (Fig 4.6 a and b). SME input increased from 63 to 108 kJ/kg when a 25 mm long KB was moved from 0 to 150 mm from the die.

The power transmitted by the drive motor to the screws can be expressed as (Martelli, 1983):

$$Z = f\left(\frac{Q^2\,\mu}{K_f},\ \bar{\mu},\ N,\ n^2\right) \qquad (27)$$

where, Q = output (m^3/s)

μ = melt viscosity in the die (Pa.s)

$\bar{\mu}$ = average viscosity in the filled channels (Pa.s)

N = number of filled flights

n = screw speed (1/s)

K_f = conductivity of the die (m^3)

In the present study, Q, n and K_f were constant. Therefore, equation 27 reduces to:

$$Z = f(\mu, \bar{\mu}, N) \quad (28)$$

Equation 28 suggests that the viscosity of material inside the extruder and number of filled flights (degree of fill) were the two main factors affecting the SME input. Process variables, other than screw configuration, influencing the degree of fill and viscosity were unchanged during this study. Mixing elements are flow restricting elements and vary in their ability to increase the degree of fill. RSE is a stronger flow restricting element compared to KB (Choudhury and Gautam, 1998a). For a particular position in the screw profile, severity of screw configuration due to incorporation of mixing elements was higher with RSE than with KB. More severe the screw configuration, the greater was the degree of fill (Yam *et al.*, 1994; Choudhury and Gautam, 1998a). In this study five kneading elements were oriented in a fashion to have minimum conveying effect in either forward or backward direction. A lower degree of fill is required to generate enough pressure to convey material in the forward direction with KBs than with RSEs. The filled length, and therefore, the power/SME input to the material was higher for RSE compared to that for KB (Fig. 4.6 a and b). Our data agreed with the findings of Kirby *et al.* (1988), Chang and Halek (1991), and Yam *et al.* (1994) who observed high degree of fill with increasing SME input.

A higher degree of fill is required to develop enough pressure for the flow of material across a longer element. Since degree of fill and SME input are directly proportional (eq. 28), thus a higher SME is observed with longer mixing element.

Similar effect of increasing element length on SME input was reported by Erdemir *et al.* (1992) during twin-screw extrusion of rice flour.

SME input also depends on material rheology. Higher SME is required for flow of more viscous material across a mixing element. Temperature affects viscosity. Rice flour in the extruder was subjected to increasingly higher temperature as it was conveyed from feed to die end, and therefore, the viscosity decreased as the material moved toward the die. Consequently, the SME input increased gradually as the mixing element, irrespective of type, was moved farther away from the die because it encountered melt with increasing viscosity or rice flour in a powdery state. Therefore, SME input increased with increasing distance of the mixing elements from the die (Fig. 4.6).

The spacing effect of mixing elements on SME input is compared in Fig. 4.7 (a and b). Addition of another mixing element resulted in higher SME input because of increased filled volume. Increased spacing between two elements, created by placing one element at 0, 50, or 100 mm from the die and then moving the second element towards the feed end, resulted in higher SME input. Similar increasing trend was observed when the two elements with constant spacing were moved farther away from the die (Fig. 4.7). This was because of high material viscosity in the region where rice flour encountered the first flow restricting element. In general, SME input was higher for RSE than with KB.

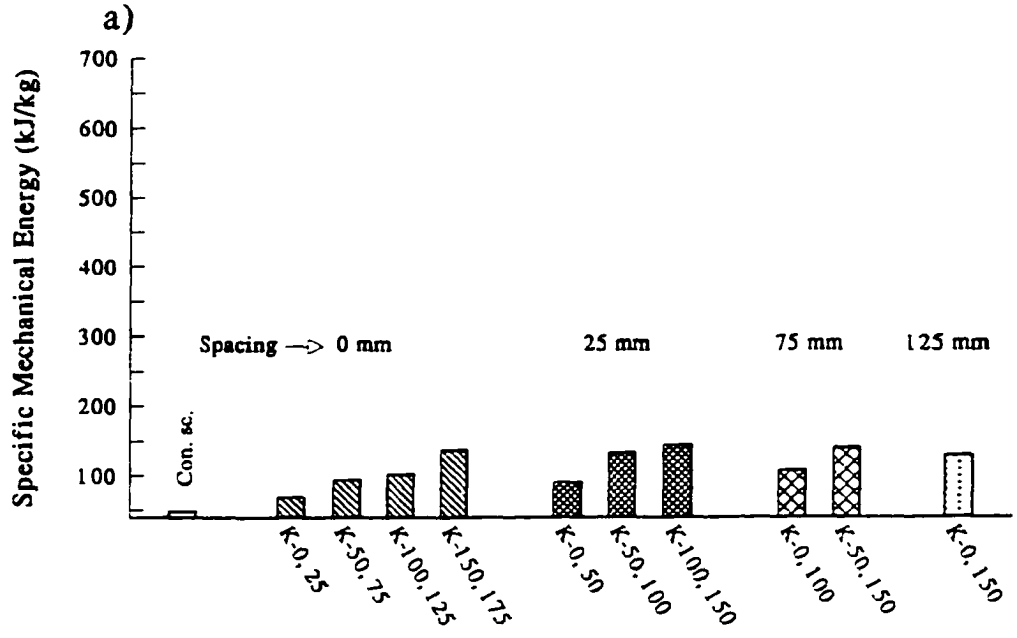

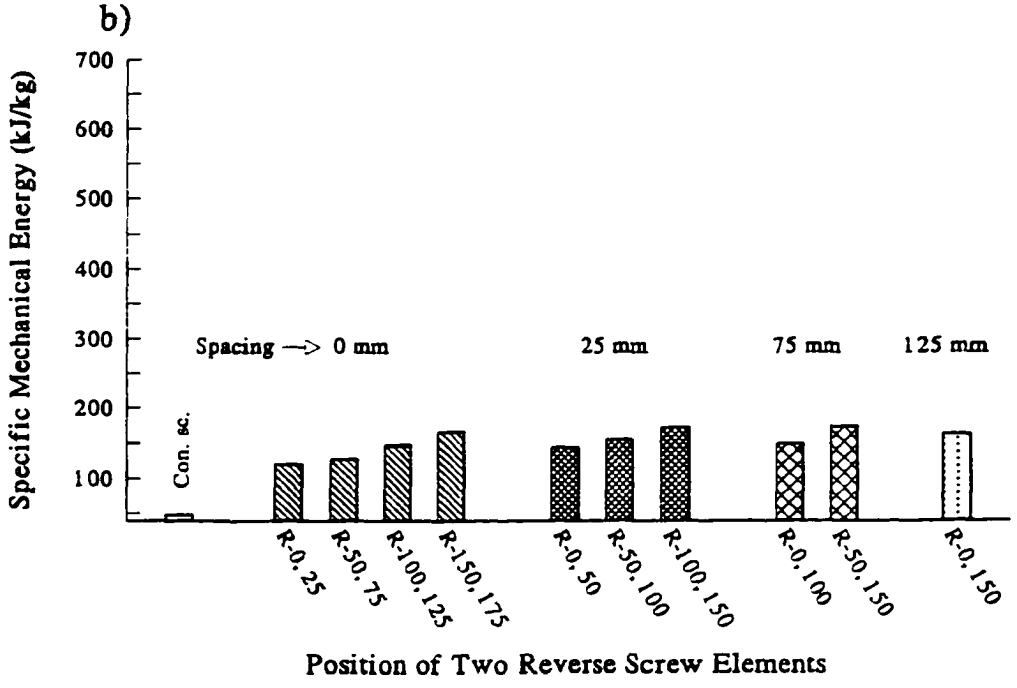

Figure 4.7 Position and spacing effects of (a) two kneading block(s) and (b) two reverse screw elements on specific mechanical energy during extrusion of rice flour.

4.2.1.2 Specific Thermal Energy (STE)

Effect of screw configuration on specific thermal energy was exactly opposite to that of SME. A very high specific thermal energy input (465 kJ/kg) was observed with conveying screw configuration. Inclusion of mixing elements in the screw profile lowered the STE input (Fig. 4.8 a and b). STE was higher with KBs than with RSEs. For example, a 50 mm long KB at 150 mm from the die had a specific thermal energy input of 365 kJ/kg. This value decreased to 263 kJ/kg when KB was replaced by a RSE of same length and at the same position. The effect of type, length and position of elements on STE was significant (Table 4.3). Specific thermal energy input decreased with increasing length of the mixing element. It also decreased systematically as the mixing elements were moved farther away from the die, irrespective of type and length of the element (Fig. 4.8 a and b).

Material temperature increases due to viscous heat dissipation with configurations producing high SME input. Hence, the electrical heaters mounted on the extruder drew less current indicating low thermal energy input to maintain constant barrel temperature profile. Similarly, with configurations producing less SME input there is a high demand for thermal energy to raise the material temperature to the set barrel temperature. Hence, the heaters drew more current producing high thermal energy input. Spacing effects of mixing elements is depicted in Figure 4.9. With these screw configurations, SME input was among the highest and therefore thermal energy input was lowest.

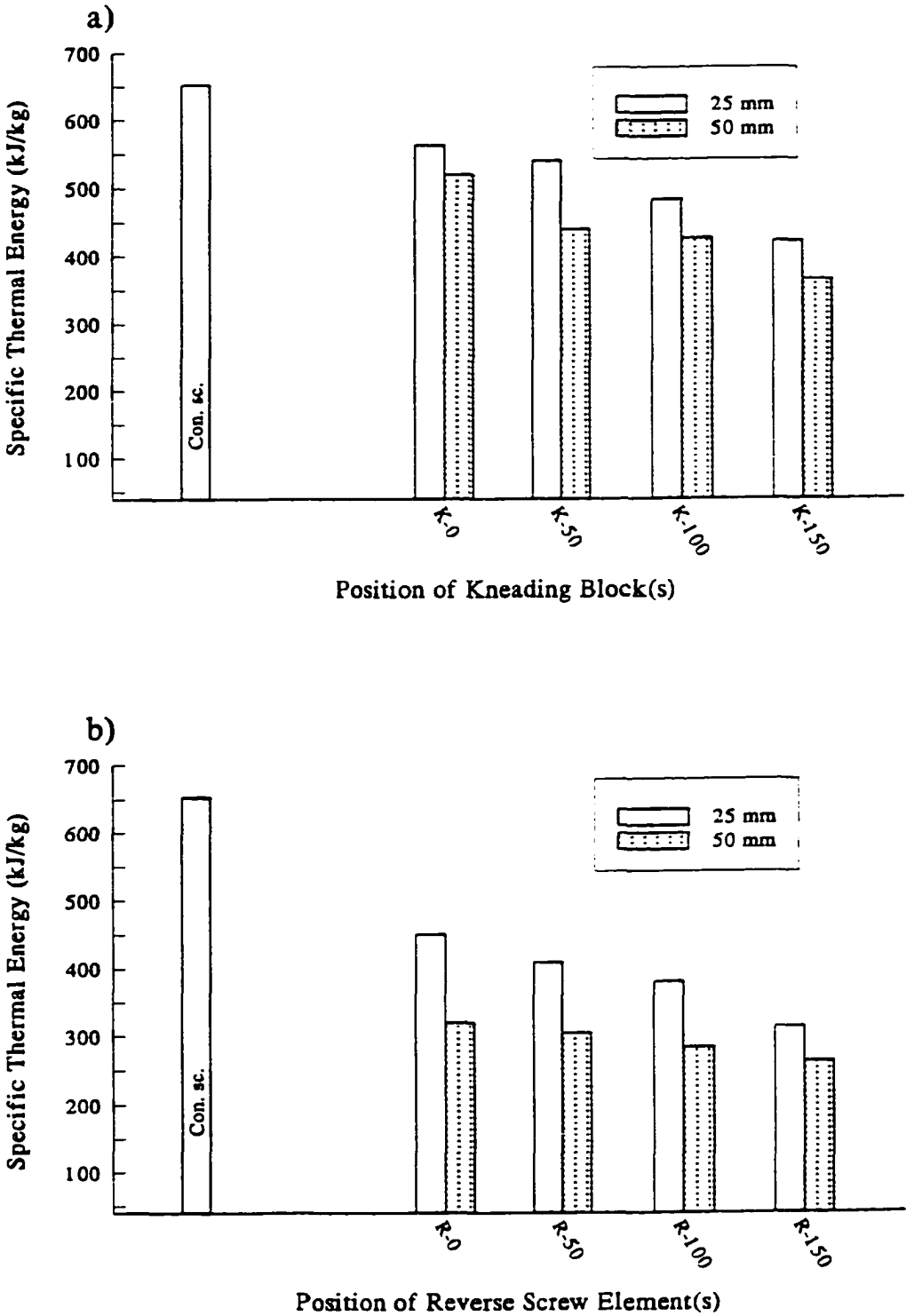

Figure 4.8 Position and length effects of (a) kneading block and (b) reverse screw element on specific thermal energy during extrusion of rice flour.

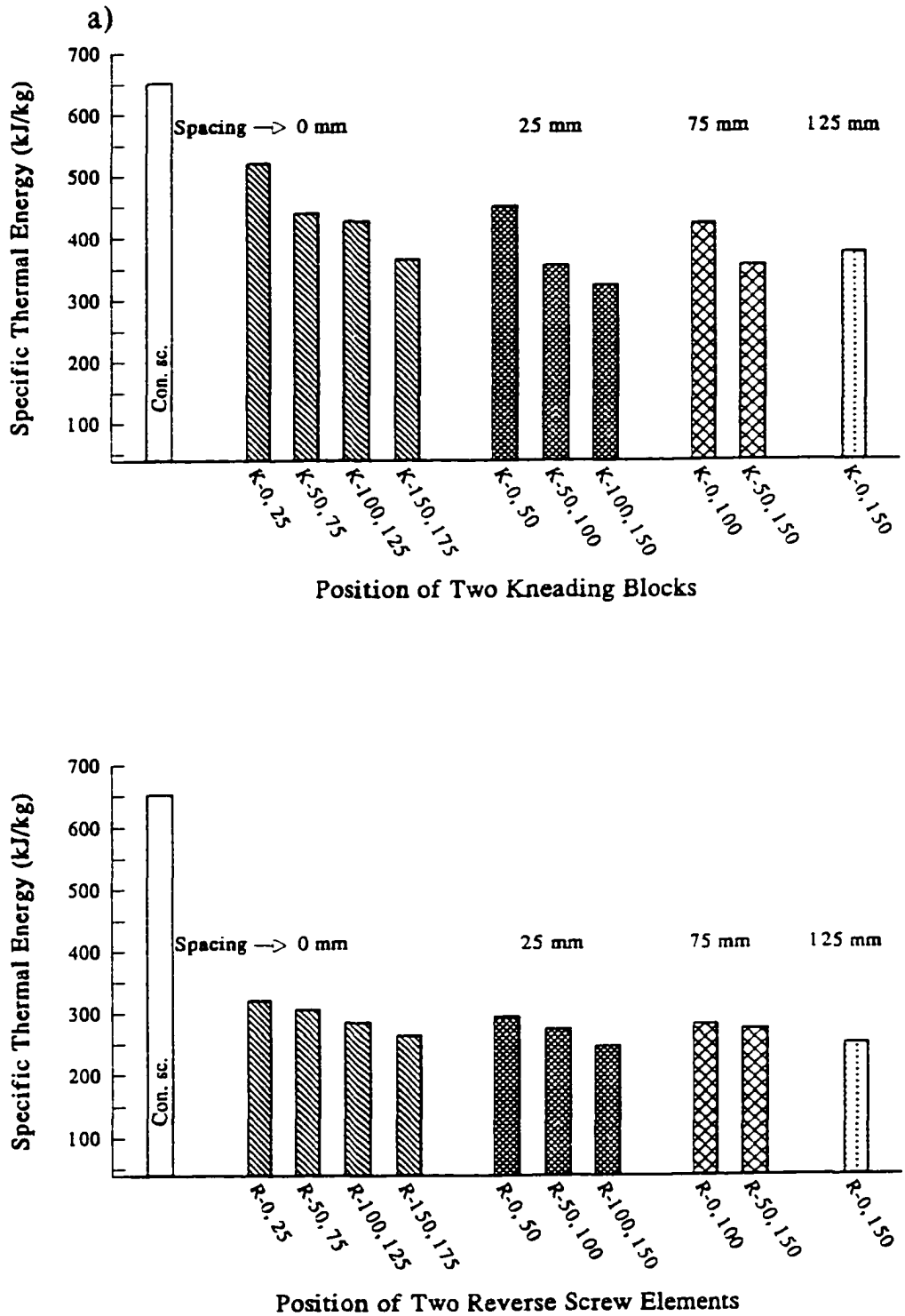

Figure 4.9 Position and spacing effects of (a) two kneading block(s) and (b) two reverse screw elements on specific thermal energy during extrusion of rice flour.

4.2.1.3 Total Energy input

The effects of type, length, and position of elements, and their interactions on the total energy input was significant (Table 4.3) and exhibited a similar trend as that of specific thermal energy (Figs. 4.10 and 4.11). It decreased when the mixing elements were moved farther away from the die. Total specific energy was low for longer mixing elements, and the value was always higher for kneading blocks. Increased spacing between the two mixing elements at different position decreased the total energy input (Fig. 4.11). Similar, decreasing trend was observed when the two elements with constant spacing were moved farther away from the die.

With all the screw configurations, the magnitude of the STE input was 1.5-14 times higher than the corresponding SME input. Hence, on addition the STE input dominated and the total specific energy followed the trend of specific thermal energy.

Figure 4.12 (a and b) show linear relationships between specific energies (SME, STE, and total specific energy) and the distance of the element from the die. SME input increased for 25 and 50 mm long mixing elements (KB and RSE) with larger distance of the element from the die ($R > 0.88$ and $F > 6.00$). STE decreased for the two lengths of mixing elements with distance (R values > 0.97 and $F > 29.00$). Total specific energy also decreased with increasing distance of mixing elements from the die ($R > 0.93$ and $F > 13.00$).

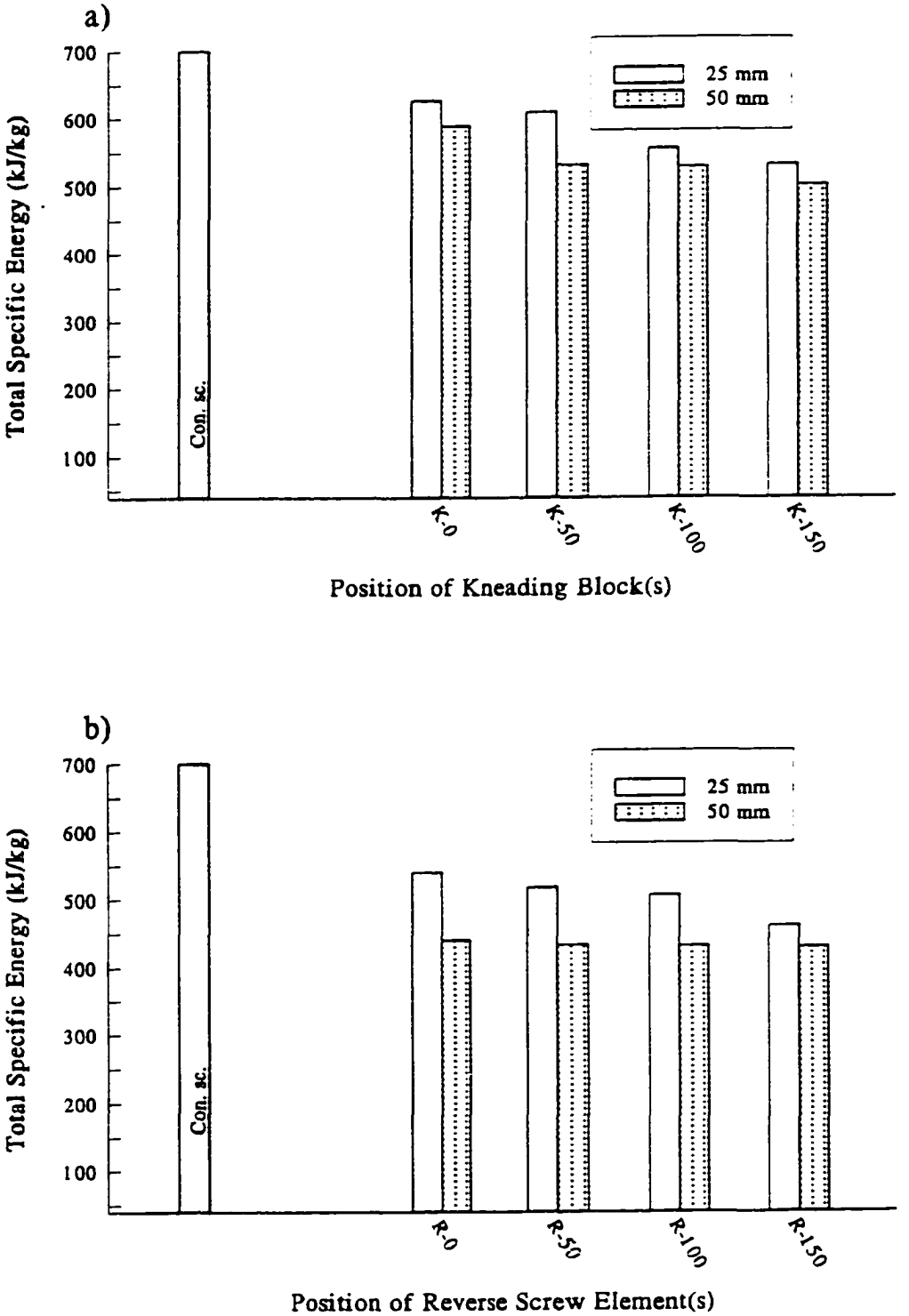

Figure 4.10 Position and length effects of (a) kneading block and (b) reverse screw element on total specific energy during extrusion of rice flour.

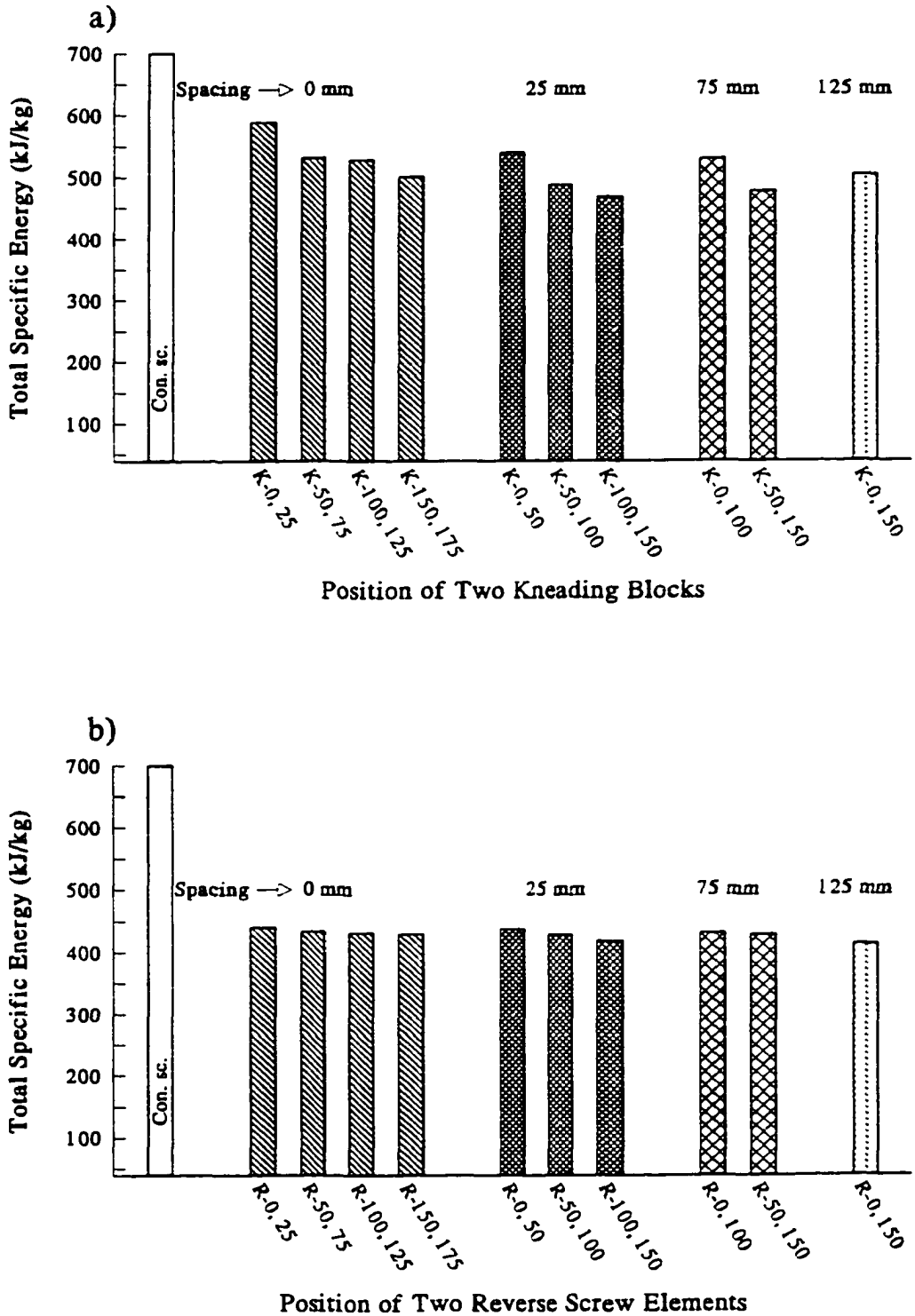

Figure 4.11 Position and spacing effects of (a) two kneading block(s) and (b) two reverse screw elements on total specific energy during extrusion of rice flour.

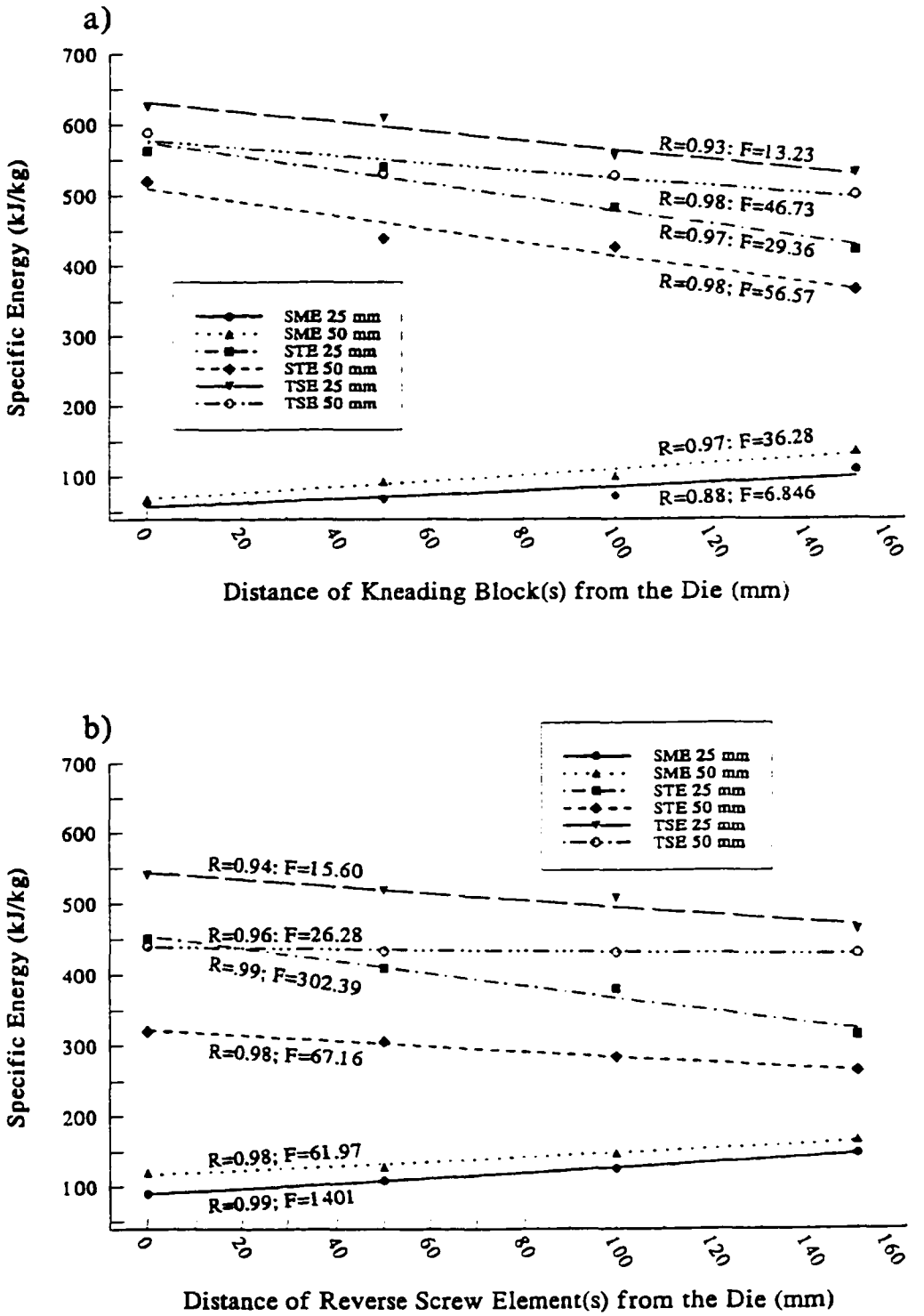

Figure 4.12 Effect of distance of mixing elements from the die on specific mechanical (SME), specific thermal (STE), and total specific energy (TSE).

4.2.1.4 Total Energy Output

Energy output consisted of:

- energy gained by the cooling water
- energy gained by the material (extrudate)
- energy lost to the surroundings due to natural convection from the extruder surface.

Table 4.4 (a and b) shows the measured energy input, calculated energy output, and the % error on the energy balance. The % error between measured energy input and calculated energy output varied between 0.3 and 13.6%. The thermal energy input and output by cooling water were maximum with conveying screw configuration. Generally, energy lost to cooling water decreased with low thermal energy input (Table 4.4 a and b). A straight line with a slope of 0.94 ($\approx$ 1), which passed through the origin was obtained (Fig. 4.13) when energy input and output for all screw configurations were plotted (R = 0.97 and F = 407.22).

4.2.1.5 System parameters

System parameters such as die temperature, % torque, and power meter readings were recorded from the control panel. The % torque and power meter readings were used to calculate the specific mechanical and thermal energies.

The effect of screw configuration on material temperature in the die is shown in Table 4.5. The die temperature is minimum (133°C) with no mixing element(s) in the

Table 4.4a. Energy balance on the extruder with kneading block (KB) as the mixing element in the screw profile. Energy output associated with the extrudate includes phase change and gelatinization of starch in rice flour.

Location of KB(s) from the Die (mm)	Measured Energy Input (kW)			Calculated Energy Output (kW)				% Error (Energy balance)
	Mechanical Energy	Thermal Energy	Total	Cooling Water	Extrudate	Natural Convection	Total	
None	0.159	2.175	2.334	1.490	0.705	0.059	2.254	3.4
0	0.210	1.876	2.086	1.057	0.771	0.083	1.911	8.4
50	0.230	1.800	2.030	1.066	0.743	0.071	1.880	7.3
100	0.242	1.607	1.849	0.858	0.733	0.072	1.663	10.1
150	0.362	1.406	1.768	0.832	0.730	0.075	1.637	7.4
0, 25	0.230	1.731	1.961	1.013	0.790	0.071	1.874	4.4
50, 75	0.305	1.464	1.769	0.866	0.755	0.072	1.693	4.3
100, 125	0.337	1.422	1.759	0.866	0.749	0.082	1.697	3.5
150, 175	0.451	1.216	1.667	0.814	0.743	0.070	1.627	2.4
0, 50	0.299	1.500	1.799	0.833	0.787	0.066	1.686	6.3
50, 100	0.439	1.184	1.623	0.658	0.728	0.063	1.449	10.8
100, 150	0.477	1.080	1.557	0.658	0.724	0.068	1.450	6.9
0, 100	0.356	1.406	1.763	0.866	0.740	0.074	1.680	4.7
50, 150	0.464	1.125	1.589	0.658	0.724	0.065	1.447	8.9
0, 150	0.426	1.250	1.676	0.866	0.731	0.074	1.671	0.4

Table 4.4b. Energy balance on the extruder with reverse screw element (RSE) being the mixing element in screw profile. Energy output associated with the extrudate includes phase change and gelatinization of starch in rice flour.

Location of RSE(s) from the Die (mm)	Measured Energy Input (kW)			Calculated Energy Output (kW)				% Error (Energy Balance)
	Mechanical Energy	Thermal Energy	Total	Cooling Water	Extrudate	Natural Convection	Total	
None	0.159	2.175	2.334	1.490	0.705	0.059	2.254	3.4
0	0.299	1.500	1.799	0.849	0.824	0.066	1.739	3.3
50	0.362	1.364	1.726	0.868	0.743	0.058	1.669	3.4
100	0.420	1.268	1.688	0.868	0.727	0.074	1.669	1.1
150	0.490	1.047	1.537	0.641	0.721	0.064	1.426	7.2
0, 25	0.400	1.067	1.467	0.416	0.830	0.069	1.315	10.3
50, 75	0.426	1.018	1.444	0.608	0.755	0.070	1.433	0.8
100, 125	0.490	0.947	1.437	0.608	0.746	0.074	1.428	0.7
150, 175	0.553	0.877	1.430	0.608	0.746	0.073	1.427	0.3
0, 50	0.458	0.978	1.436	0.426	0.799	0.072	1.297	9.7
50, 100	0.515	0.911	1.426	0.442	0.724	0.066	1.232	13.6
100, 150	0.572	0.820	1.392	0.416	0.724	0.068	1.208	13.3
0, 100	0.464	0.938	1.402	0.434	0.743	0.069	1.246	11.1
50, 150	0.579	0.844	1.423	0.442	0.721	0.068	1.231	13.5
0, 150	0.540	0.834	1.374	0.434	0.740	0.070	1.244	9.5

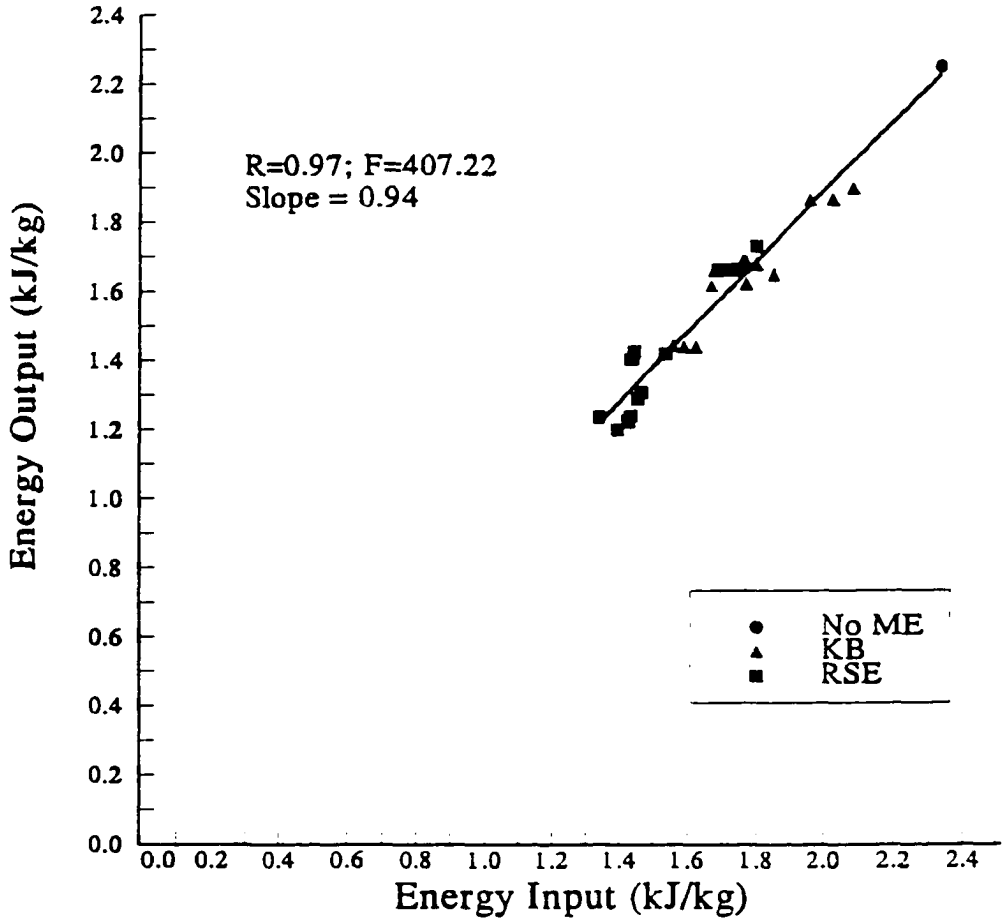

Figure 4.13 Energy balance on the extruder for all the screw configurations during extrusion of rice flour (No ME: No mixing element in the screw profile; KB: kneading block; RSE: reverse screw element).

Table 4.5 Effect of screw configuration with kneading block (KB) and reverse screw element (RSE) on die temperature during extrusion of rice flour.

Location of KB(s) or RSE(s) from the Die (mm)	Parameters Evaluated	Die Temperature (°C) in Presence of	
		KB(s)	RSE(s)
None	-	133.0 ± 0.00	133.0 ± 0.00
0	Position	139.5 ± 0.71	150.0 ± 0.00
50		137.0 ± 0.00	139.0 ± 0.71
100		135.5 ± 0.71	136.5 ± 0.71
150		135.0 ± 0.00	135.5 ± 0.71
0 & 25	Length/ Spacing	144.5 ± 0.71	152.0 ± 0.00
50 & 75		140.0 ± 0.00	140.0 ± 0.00
100 & 125		139.0 ± 0.00	139.5 ± 0.71
150 & 175		138.0 ± 0.00	138.5 ± 0.71
0 & 50	Spacing	143.0 ± 0.00	147.0 ± 1.41
50 & 100		134.5 ± 0.71	135.0 ± 0.00
100 & 150		134.0 ± 0.00	134.0 ± 0.00
0 & 100		136.5 ± 0.71	138.0 ± 0.00
50 & 150		134.0 ± 0.00	134.5 ± 0.71
0 & 150		135.0 ± 0.00	137.5 ± 0.71

screw profile and maximum (152°C) when a 50 mm long reverse screw element was placed at the die. Element type, length, and position affected the material temperature significantly (Table 4.6). The temperature was higher due to the presence of RSE than KB(s) at all positions and for both lengths. It was 150°C when a 25 mm long RSE was positioned at the die, and decreased to 139.5°C when a KB of similar length replaced RSE at same position. A longer mixing element always yielded a higher temperature. For example, temperature increased from 150 to 152°C by incorporation of a longer RSE at the die. Die temperature decreased systematically as the element was moved farther away from the die. When a 25 mm long KB was moved from 0 to 150 mm from the die, the temperature decreased from 139.5 to 135°C. Our results agreed with the findings of Della Valle *et al.* (1987) who showed an increase in the material temperature by incorporation of a RSE near the die. Due to high shear dissipation in starch melt there was a considerable increase in material temperature as the product passed through the RSE. Flow restricting RSEs are characterized by a reverse flight pushing the material backwards. During extrusion, material built up just before the RSE to generate enough pressure for flow of material across the element. Friction between material and barrel wall led to the viscous dissipation of mechanical energy to the material, which resulted in higher material temperature at the die.

In this study, the barrel temperature profile were set as shown in Figure 3.7. At steady state condition, the barrel temperatures were maintained at the specified levels by control panel. RSEs were more flow restricting than KBs (section 4.2.1.1). Thus,

Table 4.6 Analysis of variance data for die temperature during extrusion of rice flour.

Source	DF	Mean Sum of Squares (MSS) and F-values for Die Temperature (°C)	
		MSS	F
Type (Typ)	1	78.13	312.50**
Length (Len)	1	84.50	338.00**
Position (Pos)	3	152.58	610.33**
Typ x Len	3	6.13	24.50**
Typ x Pos	3	36.38	145.50**
Len x Pos	3	1.25	5.00*
Typ x Len x Pos	1	1.38	5.50*
Error	16	0.25	-

**Highly significant at $p \leq 0.005$

*Significant at $p \leq 0.05$

viscous heat dissipation due to friction between material and barrel wall was higher in case of RSEs than KBs, and as a result, higher die temperature was observed with RSEs. When a particular element was moved farther away from the die, a decrease in the die temperature was observed. For example, die temperature decreased from 139.5°C to 135°C when a 25 mm long KB was moved by a distance of 150 mm from the die. Energy gained by the material at 150 mm from the die was lost to cooling water because sufficient area and time were available for heat exchange. However, when a mixing element was placed at the die, material exited instantaneously after crossing the element. Increased energy input due to the presence of a mixing element at the die was reflected by a rise in the material temperature, and the time and heat exchange area were too short for water to cool the material. Thus, there was a systematic decrease in the die temperature as the element was moved farther away from the die. A longer element gave rise to a large build up of material (higher degree of fill) than a shorter element, and therefore resulted in a higher viscous heat dissipation as reflected by die temperature data (Table 4.5).

4.2.3 Effect of screw configuration on mean residence time and mixing

Residence time, apart from energy input, is an important variable affecting the rate and extent of reactions in an extruder. The type, length and position of the elements affected the mean residence time significantly (Table 4.7). The mean residence time with conveying screw configuration (no mixing elements) was 29.84 s. It increased to 41.70s

Table 4.7 Analysis of variance data for mean residence time and Peclet number during extrusion of rice flour.

Source	DF	Mean Sum of Squares (MSS) and F-values for t_{mean} (s) and Mixing Index			
		Mean Residence Time		Peclet Number	
		MSS	F	MSS	F
Type (Typ)	1	1397.49	2636.56**	5.68013513	145.29**
Length (Len)	1	2224.61	4197.06**	4.42233800	113.12**
Position (Pos)	3	40.84	77.05**	0.08839383	2.26
Typ x Len	3	18.34	34.61**	2.86681512	73.33**
Typ x Pos	3	5.92	11.17*	0.06097046	1.56
Pos x Len	3	10.73	20.25**	0.06853133	1.75
Typ x Len x Pos	1	6.38	12.05**	0.13708379	3.51
Error	16	0.53	-	0.03909506	-

**Highly significant at $p \leq 0.005$

*Significant at $p \leq 0.05$

when a 25 mm long KB was placed at the die (Table 4.8). The average residence time further increased to 48.71 s when KB was replaced by a RSE of similar length at the same position. Longer mixing element increased the mean residence time considerably. Our results are in agreement with Altomare & Ghossi (1986), Meuser *et al.* (1987), Kirby *et al.* (1988), and Vergnes *et al.* (1992) who showed that incorporation of mixing elements increased the residence time of the material. However, these investigators did not evaluate the systematic effect of type, length, and position of mixing elements on RTD. Altomare and Ghossi reported mean residence times of 21.9 and 33.4 s for moderate and severe screw configurations, respectively. Meuser *et al.* (1987) have shown that inclusion of two RSEs in the screw profile increased the residence time by two folds. Kirby *et al.* (1988) studied the effect of inclusion of kneading elements on residence time distribution and product characteristics. Screws of low conveying efficiencies gave rise to a longer residence time in the extruder. Vergnes *et al.* (1992) showed that by increasing the length of RSE from 50 to 100 mm in a Clextral BC-45 twin screw extruder, the mean residence time increased by a factor of 2 to 4 at different feed rates.

In this study, the mean residence time also increased as the mixing elements were moved farther away from the die (Table 4.8). The age distribution curves, E(t), obtained for various screw configurations are shown in Figures 4.14 and 4.15. A higher and narrower peak was obtained with a conveying screw configuration. Incorporation of both KB and RSE lowered the height and increased the spread of the curves (Fig. 4.14).

Table 4.8 Effect of screw configuration with kneading block (KB) and reverse screw element (RSE) on mean residence time (t_{mean}) during extrusion of rice flour.

Location of KB(s) or RSE(s) from the Die (mm)	Parameters Evaluated	t_{mean} (s) in Presence of	
		KB(s)	RSE(s)
None	-	29.84 ± 0.40	29.84 ± 0.40
0	Position	41.70 ± 2.12	48.71 ± 0.37
50		43.59 ± 0.27	54.80 ± 1.14
100		44.52 ± 0.72	58.79 ± 0.43
150		45.71 ± 0.15	60.06 ± 0.47
0 & 25	Length/ Spacing	57.63 ± 0.50	72.75 ± 0.40
50 & 75		58.74 ± 0.55	72.78 ± 0.42
100 & 125		59.16 ± 0.65	74.44 ± 0.33
150 & 175		60.64 ± 0.26	75.13 ± 0.21
0 & 50	Spacing	57.97 ± 0.11	74.06 ± 0.45
50 & 100		59.80 ± 0.46	74.34 ± 0.45
100 & 150		64.04 ± 0.57	77.58 ± 0.21
0 & 100		59.92 ± 0.40	74.87 ± 0.26
50 & 150		62.38 ± 0.37	77.05 ± 0.42
0 & 150		61.11 ± 0.54	75.64 ± 0.29

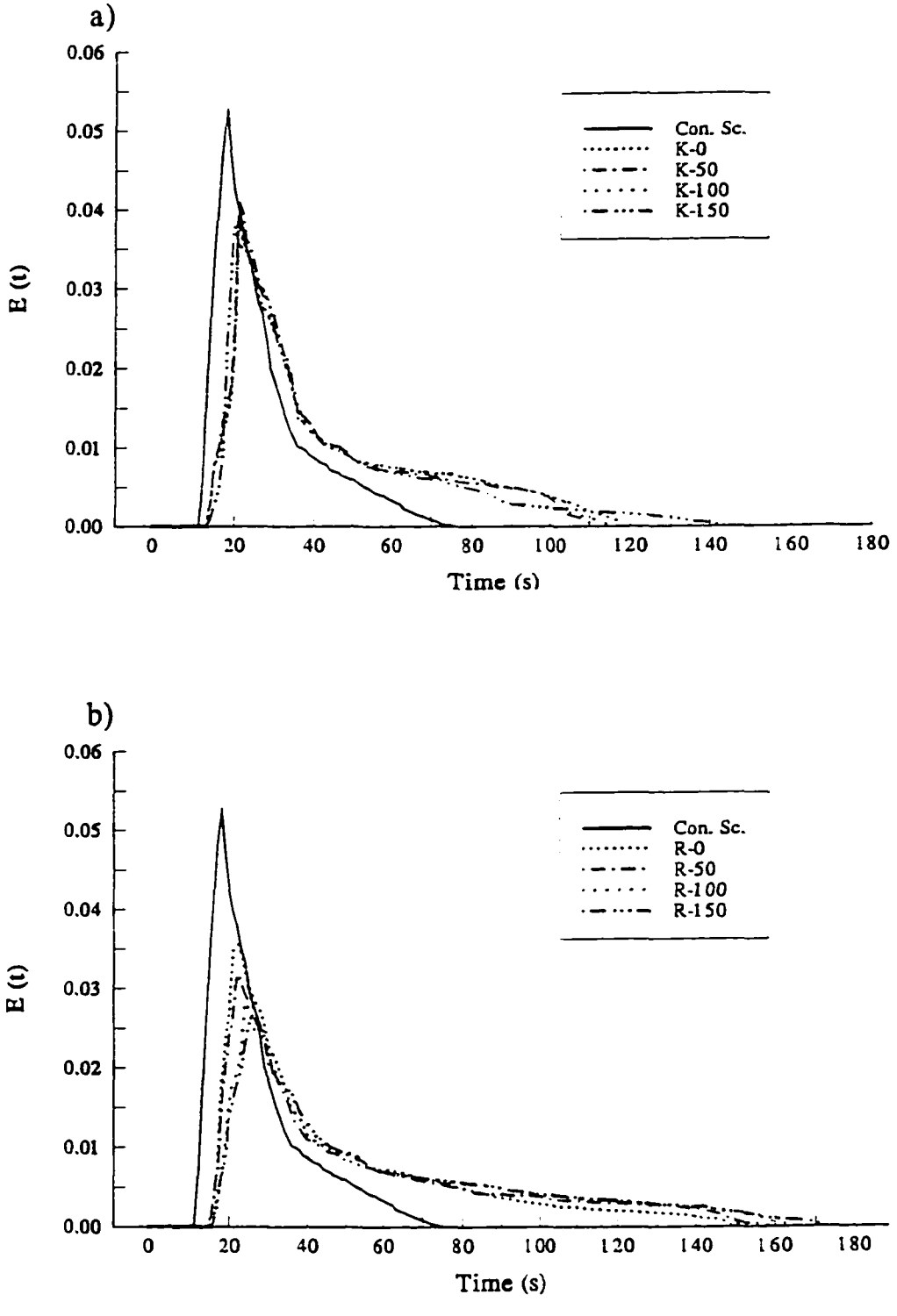

Figure 4.14 Position effect of (a) kneading block and (b) reverse screw element on residence time distribution curve, E(t), during extrusion of rice flour.

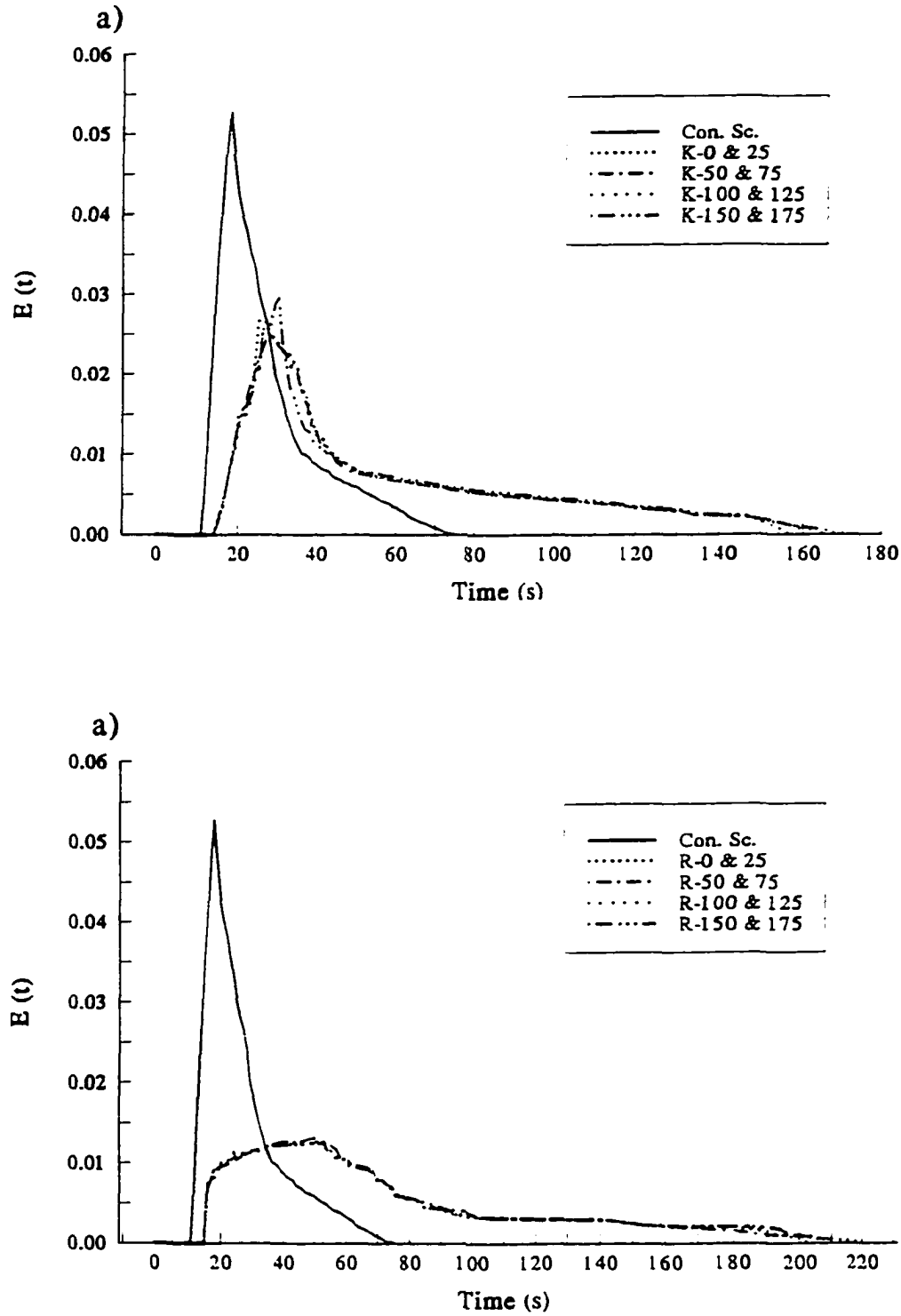

Figure 4.15 Length effect of (a) kneading blocks and (b) reverse screw elements on residence time distribution curve, E(t), during extrusion of rice flour.

However, RSE had a stronger effect on the spread. The peak height reduced from 0.054 to 0.04 with KB in the screw profile, and to 0.035 with RSE. The tails of the curves extended up to 145 s with KB and up to 170 s with RSE.

Although the position of mixing elements had a little effect on RTD, the length of elements changed the shape of RTD drastically (Fig. 4.15). Again, KB had a milder effect than RSE. With KB in the screw profile, the peak height was reduced below 0.03. However, with RSE, the residence time distribution broadened without a sharp peak. The tails extended up to 220 s. Vergnes *et al.* (1992) also showed the change of a sharp peak into a broad and flat plateau due to increased length of RSE. Similar lowering of peak and broadening of RTD spread due to incorporation of flow restricting elements at a certain position in the screw profile have been reported by several other investigators (Olkku *et al.*, 1980; Altomare & Ghossi, 1986; Meuser *et al.* 1987; and Vergnes *et al.* 1992). All these studies were carried out comparing two or three screw configurations, which were built by incorporation of mixing elements at one position in the screw profile. Olkku *et al.* (1980) reported remarkable broadening of RTD due to inclusion of one reverse screw element.

Mean residence time increased as the spacing between the two mixing elements became larger (Table 4.8), and by moving two elements (with constant spacing) farther away from the die. Figure 4.16 depicts the spacing effect on the shapes of E(t) curves, which are similar to the length effect (Fig. 4.15). The shapes are similar because in both the cases the total length of element was 50 mm.

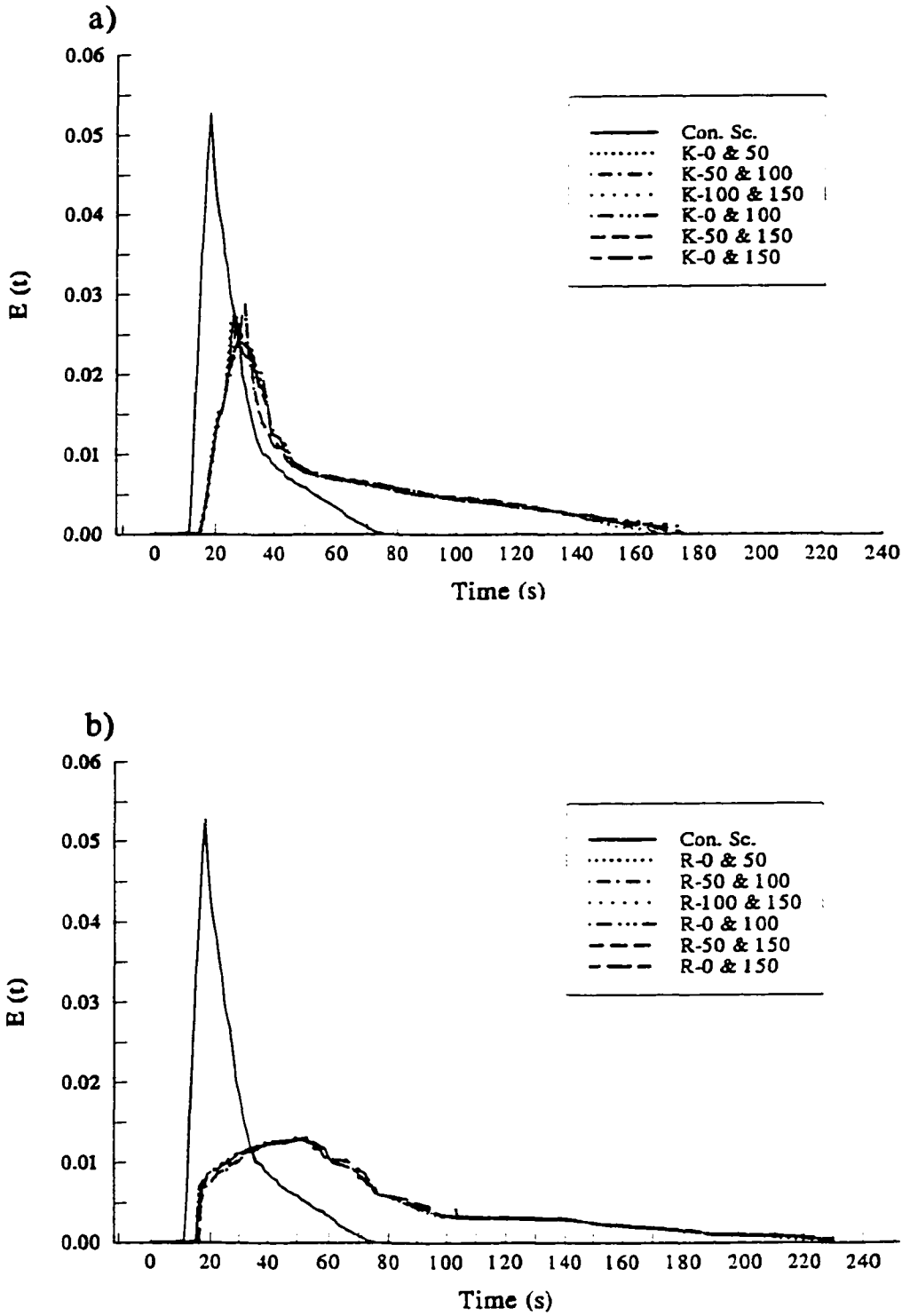

Figure 4.16 Spacing effect of (a) kneading blocks and (b) reverse screw elements on residence time distribution curve, E(t), during extrusion of rice flour.

Mean residence time in any reaction vessel is be given by a simple equation:

$$t_{mean} = \frac{Volume}{Volumetric\ flow\ rate} \quad (29)$$

The SME data showed that the RSEs were more flow restricting than KBs. A higher degree of fill was observed by inclusion of RSE, with longer elements, and by increased spacing between two elements. In this study, volumetric flow rate was constant because of the fixed mass flow rate. Incorporation of mixing elements caused large filled volume (degree of fill) and thus increased mean residence time was observed. A good correlation (R = 0.85 and F = 67.17) was found between the SME input and mean residence time (Fig. 4.17). As the SME input due to incorporation of mixing elements increased, higher mean residence time was observed.

The Peclet number, an indication of mixing in the extruder was calculated from the spread of age distribution curves (Table 4.9). Lower Peclet number indicates more mixing. Element type, length, and their interaction affected the mixing index significantly (Table 4.8). RSEs produced more mixing than KBs. RSEs are more flow restricting elements than KBs and push the material in the backward direction, resulting in better mixing. Mixing was also improved by increasing element length and spacing.

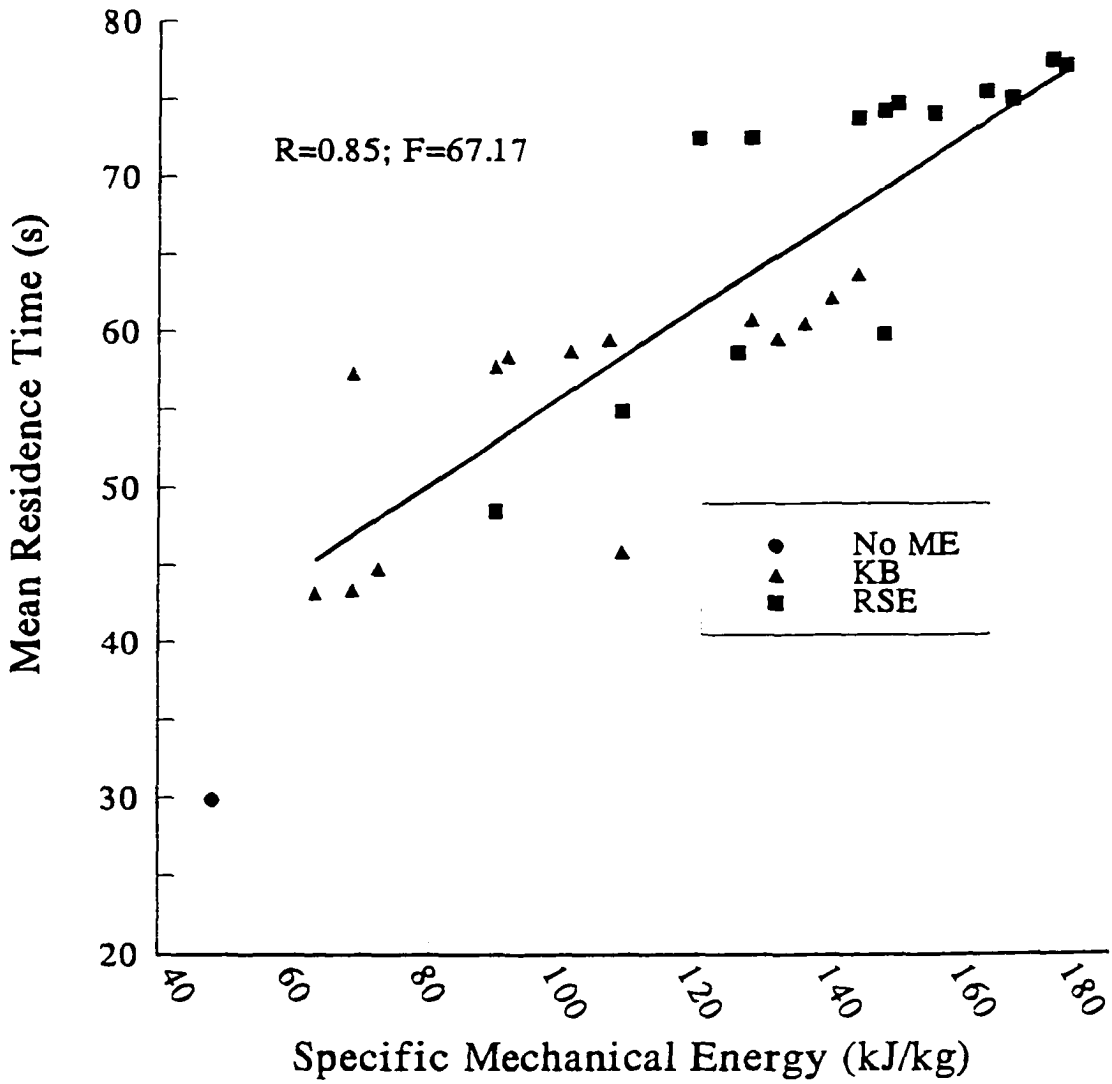

Figure 4.17 Relationship between mean residence time and specific mechanical energy during extrusion of rice flour. (No ME: No mixing element in the screw profile; KB: kneading block; RSE: reverse screw element).

Table 4.9 Effect of screw configuration with kneading block (KB) and reverse screw element (RSE) on Peclet number (mixing index) during extrusion of rice flour.

Location of KB(s) or RSE(s) from the Die (mm)	Parameters Evaluated	Peclet Number in Presence of	
		KB(s)	RSE(s)
None	-	8.71 ± 0.064	8.71 ± 0.0064
0	Position	5.48 ± 0.0424	3.80 ± 0.0354
50		5.59 ± 0.0354	3.92 ± 0.0283
100		5.56 ± 0.0071	4.00 ± 0.0495
150		5.31 ± 0.7707	4.00 ± 0.0382
0 & 25	Length/ Spacing	4.00 ± 0.0707	3.86 ± 0.0170
50 & 75		3.96 ± 0.0354	3.90 ± 0.0396
100 & 125		3.99 ± 0.0354	3.62 ± 0.0226
150 & 175		4.03 ± 0.0035	3.66 ± 0.0064
0 & 50	Spacing	4.06 ± 0.0141	3.96 ± 0.0474
50 & 100		4.01 ± 0.1061	3.78 ± 0.0566
100 & 150		3.94 ± 0.0212	3.74 ± 0.0071
0 & 100		3.94 ± 0.0424	3.65 ± 0.0283
50 & 150		4.05 ± 0.0495	3.78 ± 0.0566
0 & 150		3.89 ± 0.0636	3.72 ± 0.0495

Wolf and White (1976) proposed mixing models for two ideal systems: perfectly mixed and plug flow (Appendix A.1). However, the conditions in the extruder are neither that of perfect mixing nor plug flow (Altomare and Ghossi, 1986; Yeh *et al.*, 1992). To compare our experimental results with the two ideal flow models, the cumulative RTD curves, F(t), were plotted as functions of the dimensionless time (θ) (Fig. 4.18, 4.19, and 4.20). The shape of the F(t) distribution, obtained with mixing elements in the screw profile was similar to that observed by Altomare and Ghossi (1986) for moderate and severe screw configurations. Twin-screw extruders show a normalized delay time of approximately 0.48 (Altomare and Ghossi, 1986). We obtained a value of 0.46 with the conveying screw profile. Incorporation of mixing elements reduced the normalized delay time (Fig. 4.18) and increased the normalized time (θ), indicating that the flow behavior shifted towards perfectly mixed type. This finding is also supported by decreased Peclet number due to incorporation of mixing elements (Table 4.9), indicating better mixing. The normalized delay time was about 0.35 and 0.32 for screw profiles with KB and RSE, respectively. Increased length of KB and RSE further reduced the normalized delay time to 0.30 and 0.26, respectively. The Peclet number also decreased by incorporation of longer mixing elements in the screw profile. The F(t) curves for screw profiles with mixing elements intersected the conveying screw curve and shifted towards perfectly mixed type (Fig. 4.18, 4.19 and 4.20).

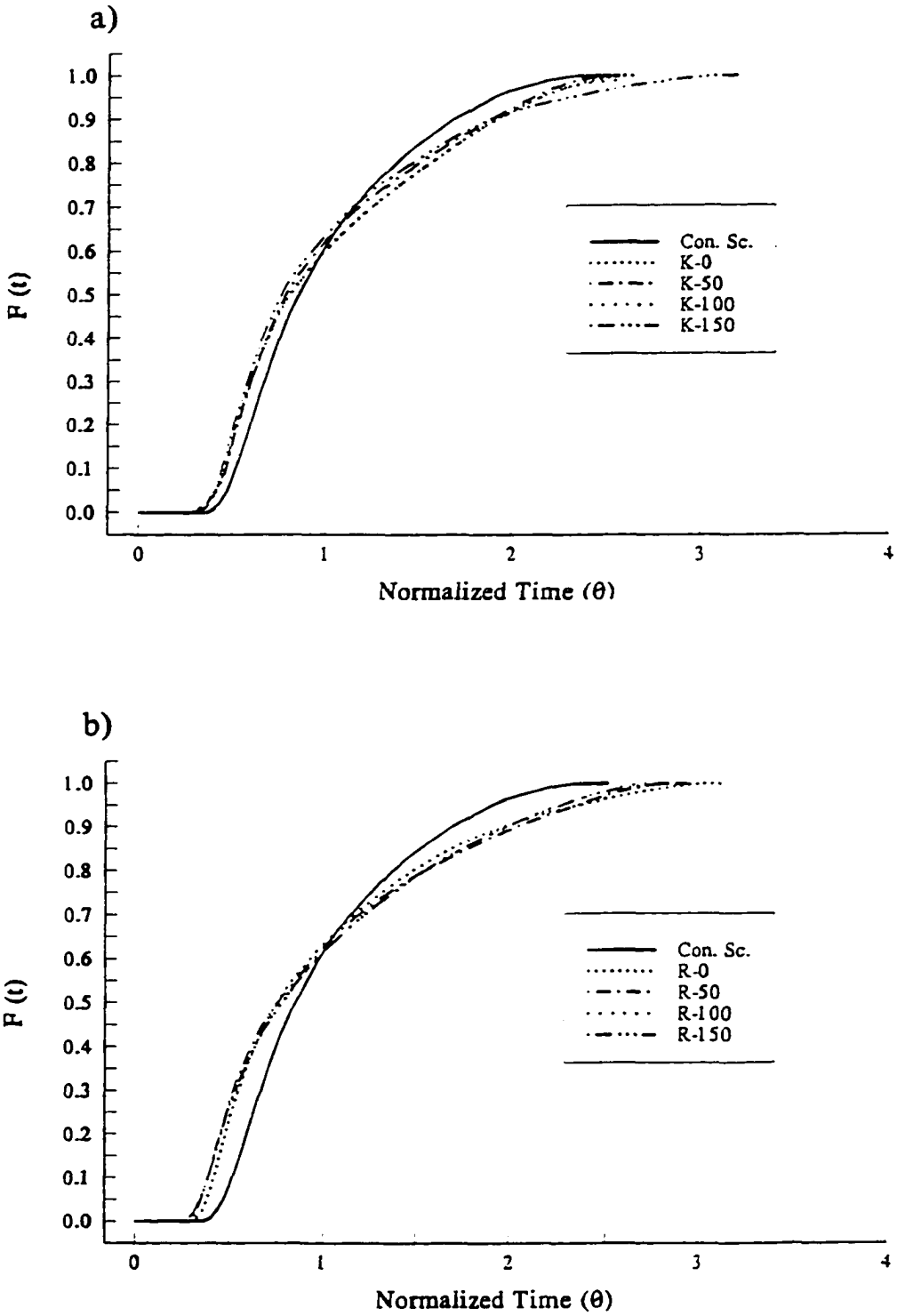

Figure 4.18 Position effect of (a) kneading block and (b) reverse screw element on cumulative residence time distribution curve, F(t), during extrusion of rice flour.

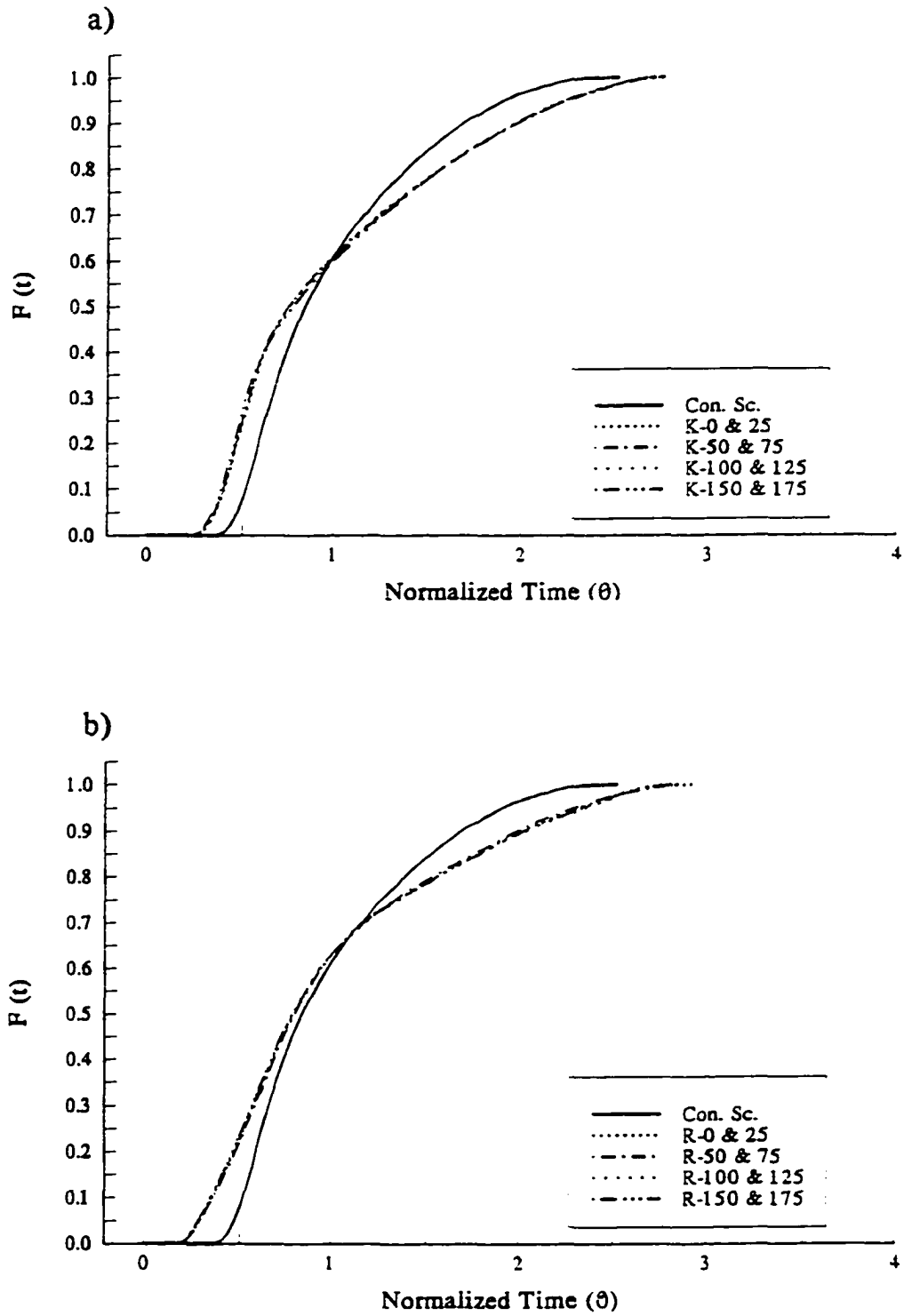

Figure 4.19 Length effect of (a) kneading blocks and (b) reverse screw elements on cumulative residence time distribution curve, F(t), during extrusion of rice flour.

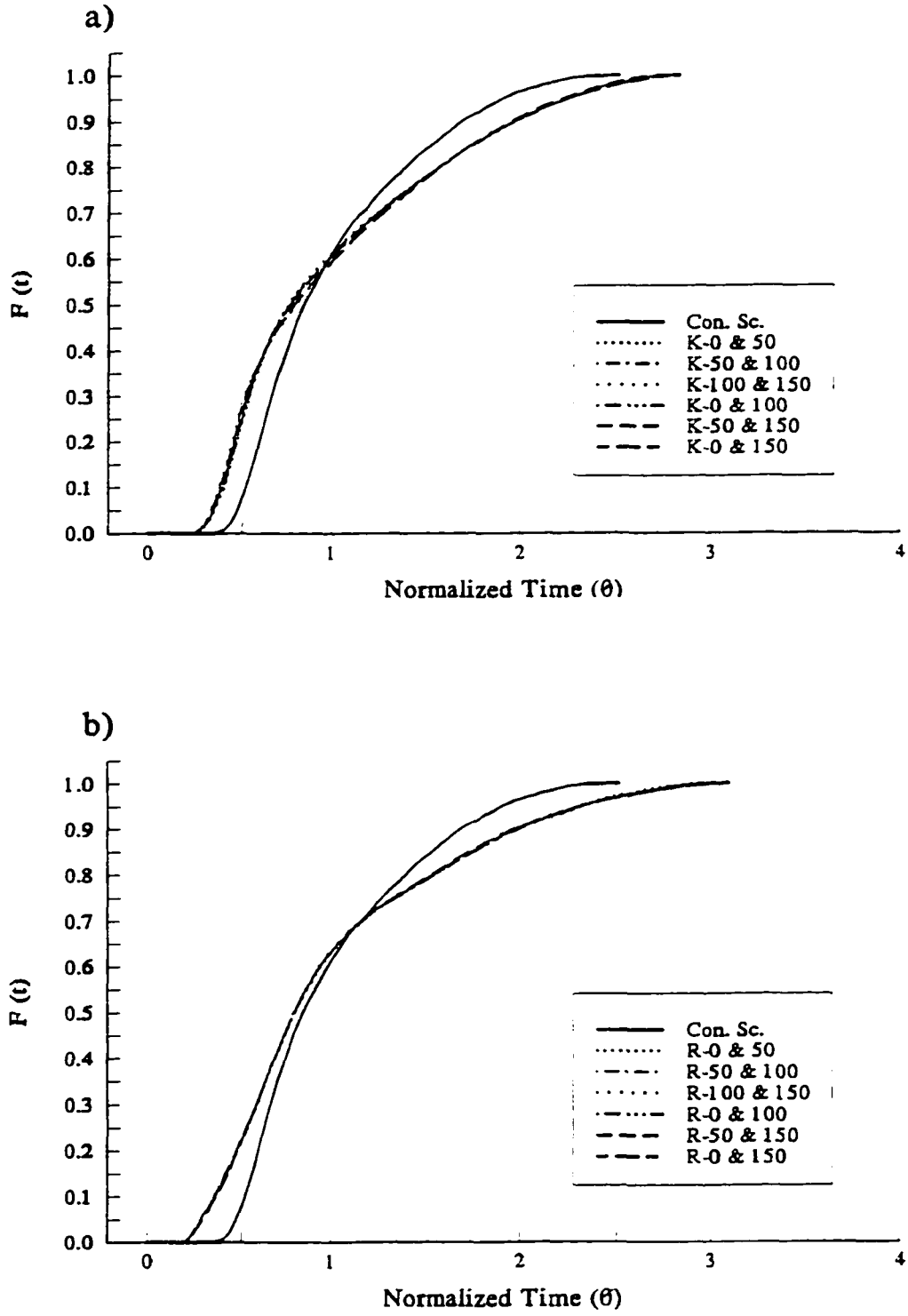

Figure 4.20 Spacing effect of (a) kneading blocks and (b) reverse screw elements on cumulative residence time distribution curve, F(t), during extrusion of rice flour.

4.2.4 Effect of screw configuration on molecular break down and changes of starch

The major constituent of rice flour is carbohydrate (Table 3.1). Starch is a polysaccharide which consists of linked glucose molecules in the form of:

- branched fraction, amylopectin
- linear portion, amylose.

Amylopectin has a molecular weight of 10^8, and amylose is only 250,000 daltons (Juliano, 1994; Yacu, 1995). Native starch granules are insoluble in water, and its mixtures with water has negligible viscosity. It has crystalline and amorphous regions, the former shows birefringence (Maltese cross) when viewed under polarized light (Kainuma, 1982; Juliano, 1994; Yacu, 1995). When starch is heated in excess water (moisture content > 60%), gelatinization takes place. The starch granules swells, with a loss of birefringence and melting of the crystalline region (Juliano, 1994; Yacu, 1995). Changes in starch structure and size during extrusion depend on independent process variables, such as moisture content, screw speed, feed flow rate, feed composition, and screw configuration (Fig. 1.1). Extruding with limited moisture, leads to fragmentation of starch as reported by various investigators. Indirect measurement of starch fragmentation include decreased viscosity (Owusu-Ansah *et al.*, 1983; Diosady *et al.*, 1985), decreased water adsorption index (Mercier and Feillet, 1975; Owusu-Ansah *et al.*, 1983), increased amylase susceptibility (Gomez and Aguilera, 1984), and increased water solubility index (Kirby *et al.*, 1988; Barres *et al.*,1990; Meuser *et al.*, 1991; Choudhury and Gautam, 1998a). Direct measurements documenting starch fragmentation in wheat

and corn starch by gel permeation chromatography have been reported by Colonna *et al.* (1984), Davidson *et al.* (1984), Chinnaswamy and Hanna (1990), and Wen *et al.* (1990).

4.2.4.1 Starch breakdown/fragmentation

Elution profile of three standard polymers with average molecular weight of two million, five hundred thousand, and seventy thousand daltons is shown in Fig. 4.21. Three peaks (one for each standard) were observed at 80, 100, and 125 mL. The lowest molecular weight standard eluted at a higher elution volume. Incorporation of mixing elements increased the breakdown of starch polymers. Carbohydrate profile for unextruded rice flour gave one peak, which eluted at 65 mL. Extrusion with a screw profile having conveying and mixing elements shifted this peak to the right, indicating reduction of molecular weight with breakdown of high molecular weight polysaccharides (Figs. 4.22 and 4.23). The extent of breakdown was reflected by the shift of elution profiles. A higher shift towards the right suggested a larger extent of breakdown, and vice versa. The magnitude of breakdown due to screw configuration had a similar trend as that of SME input. In general, lower SME input was observed with KB than with RSE (Fig. 4.6). Similarly, lesser extent of breakdown was observed with KB than with RSE (Figs. 4.22 and 4.23). For example, the peak with 25 mm long KB was observed at 75 mL, which shifted to 80-100 mL with inclusion of a RSE of similar length and at same position (Fig. 4.22). This was expected because of higher SME input due to greater restriction to material flow resulting in breakdown of polymers to smaller

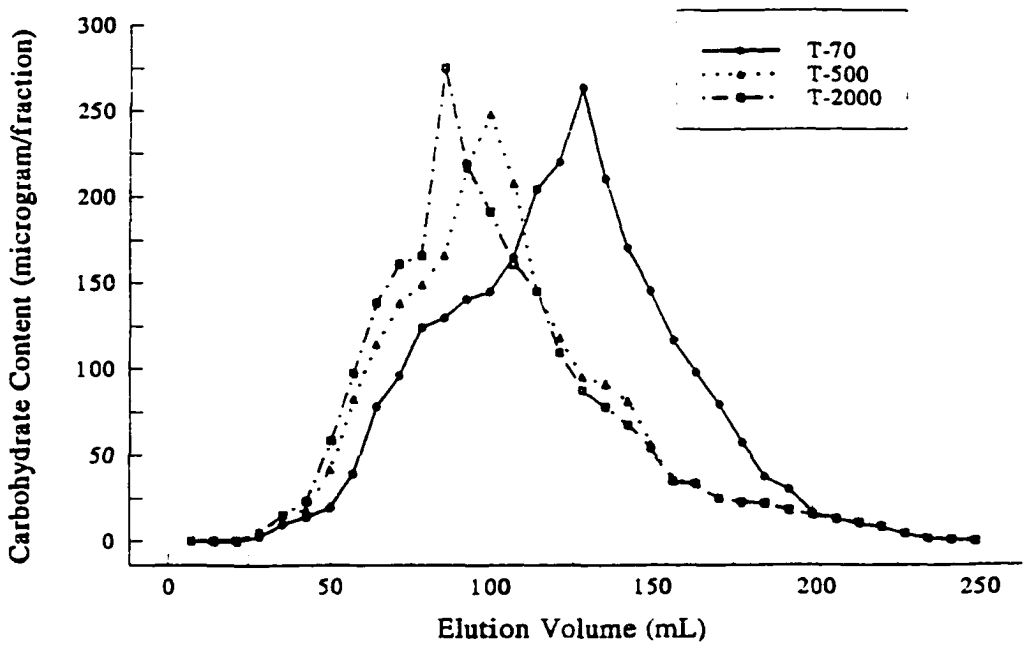

Figure 4.21 Elution profile of molecular weight standards. (T-70: 70,000 daltons; T-500: 500,000 daltons; T-2000: 2 million daltons average molecular weights).

molecules (Choudhury and Gautam, 1998a). An increase in shear energy input as well as residence time, by incorporation of mixing elements, can cause both depolymerization and degradation. Increased length of mixing elements produced a higher extent of breakdown (Fig. 4.24). Incorporation of 50 mm long KB and RSE shifted the peak to 75-80 mL, and to 80-100 mL, respectively (Fig. 4.23). A second peak at 155 mL was observed with a 50 mm long RSE placed at 100 or 150 mm from the die (Fig. 4.23 b). When the elements were moved farther away from the die, an increase in both SME input (Fig. 4.6) and starch breakdown was observed (Figs. 4.22 and 4.23). Our data agreed with the finding of several investigators who have shown that high shear can cause fragmentation products from starch (Gomez and Aguilera, 1983; Davidson *et al.*, 1984; Chinnaswamy and Hanna, 1990). Dextrinization (fragmentation of starch to very small molecular weight compounds called dextrins) was reported to be the predominant mechanism of starch degradation during low-moisture and high shear extrusion (Gomez and Aguilera, 1983). Starch fractions of wheat (Davidson *et al.*, 1984) and corn (Chinnaswamy and Hanna, 1990) undergo certain degree of fragmentation during extrusion. The characteristic pattern observed in these studies was decrease in high molecular weight material and a corresponding increase in low molecular weight polysaccharides. Work of Wen *et al.* (1990) showed two peaks of native corn meal in the chromatogram: Peak I for amylopectin and peak II for amylose. Extrusion under 15 process conditions resulted in reduction of amylopectin and was accompanied by peak

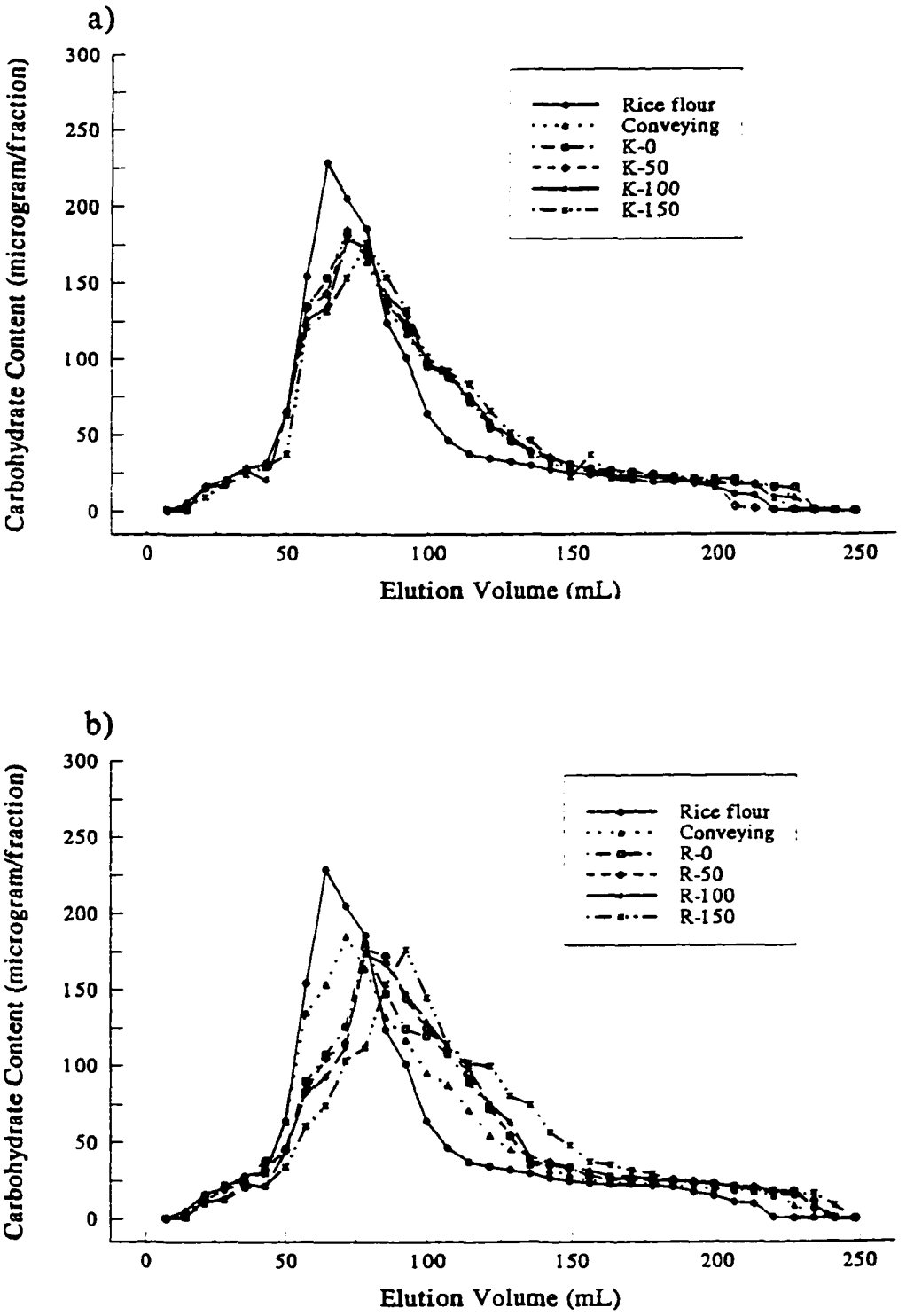

Figure 4.22 Position effect of (a) kneading block and (b) reverse screw element on starch breakdown during extrusion of rice flour.

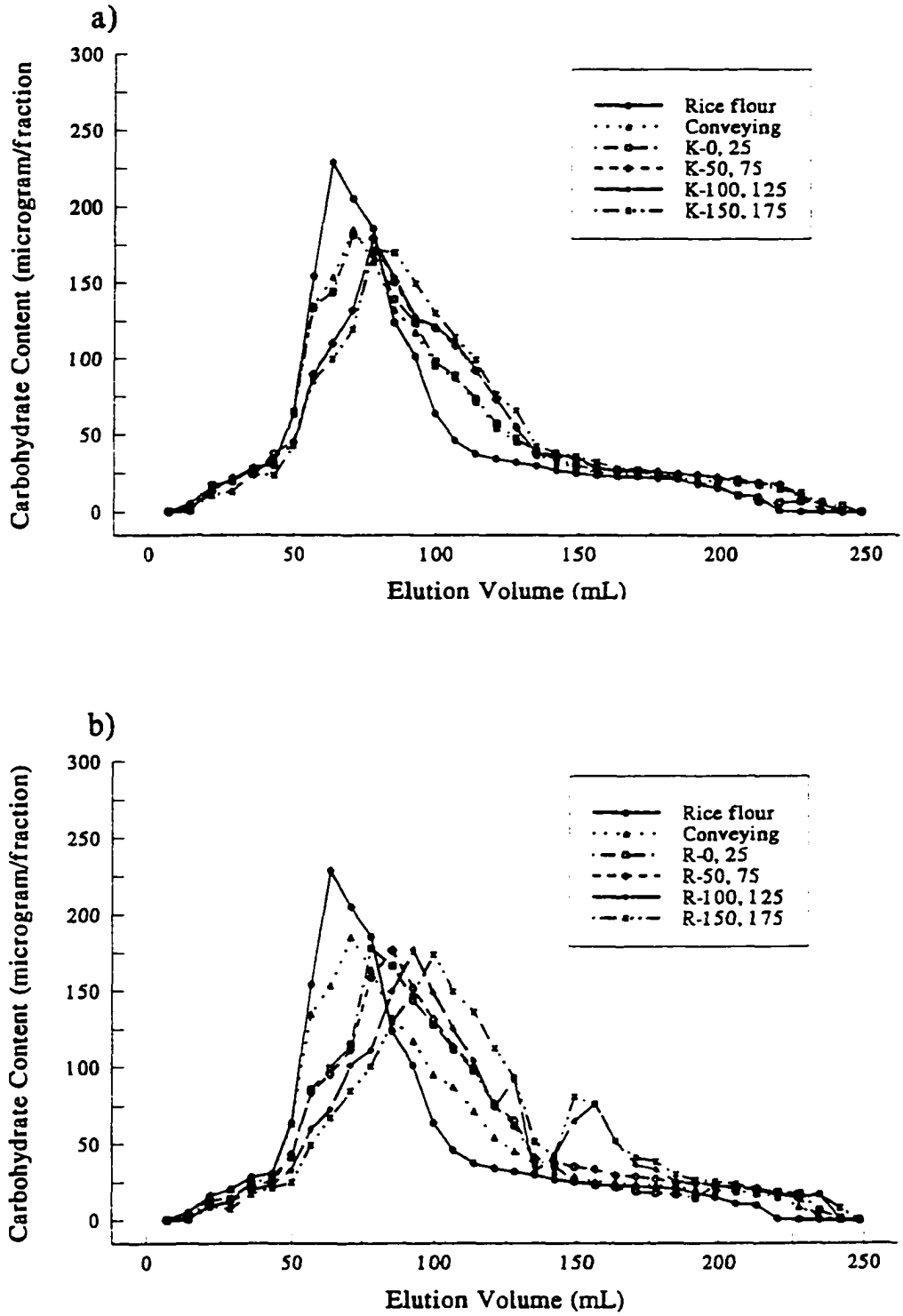

Figure 4.23 Length effect of (a) kneading blocks and (b) reverse screw elements on starch breakdown during extrusion of rice flour.

broadening and extensive tailing. Davidson *et al.* (1984) also showed the molecular size reduction of the amylopectin fraction. Water solubility index (WSI) is a good measure of macromolecular degradation during extrusion. Choudhury and Gautam (1998a) have shown that extent of shear breakdown of starch depends on severity of processing, which increased with increasing SME input. WSI increased with increasing severity of screw configuration, and the trend was generally consistent with the observations of Kirby *et al.*, (1988), Barres *et al.*, (1990), and Meuser *et al.*, (1991).

The spacing effect on the starch breakdown is shown in Figure 4.24. A very severe screw configuration with two RSE spaced by 25 or 75 mm produced maximum breakdown of high molecular weight fractions as shown by shifts of the elution profile to the right and subsequent appearance of a second peak after 150 mL of elution volume (Fig. 4.24 b). When the SME input was greater than 145 kJ/kg extensive breakdown of high molecular weight compounds was observed. Such severe processing might have produced dextrinized starches as have been observed by Gomez and Aguilera (1983, 1984), Colonna *et al.* (1984), and Davidson *et al.* (1984).

4.2.4.2 Starch gelatinization

Gelatinization of rice starch and flour has been studied by various investigators using Differential Scanning Calorimeter (Biliaderis *et al.*, 1986a and b; Normand and Marshall, 1989; Park and Hyun, 1989; Huang *et al.*, 1994). These studies showed that varying the water content of the starch or flour significantly affected the gelatinization

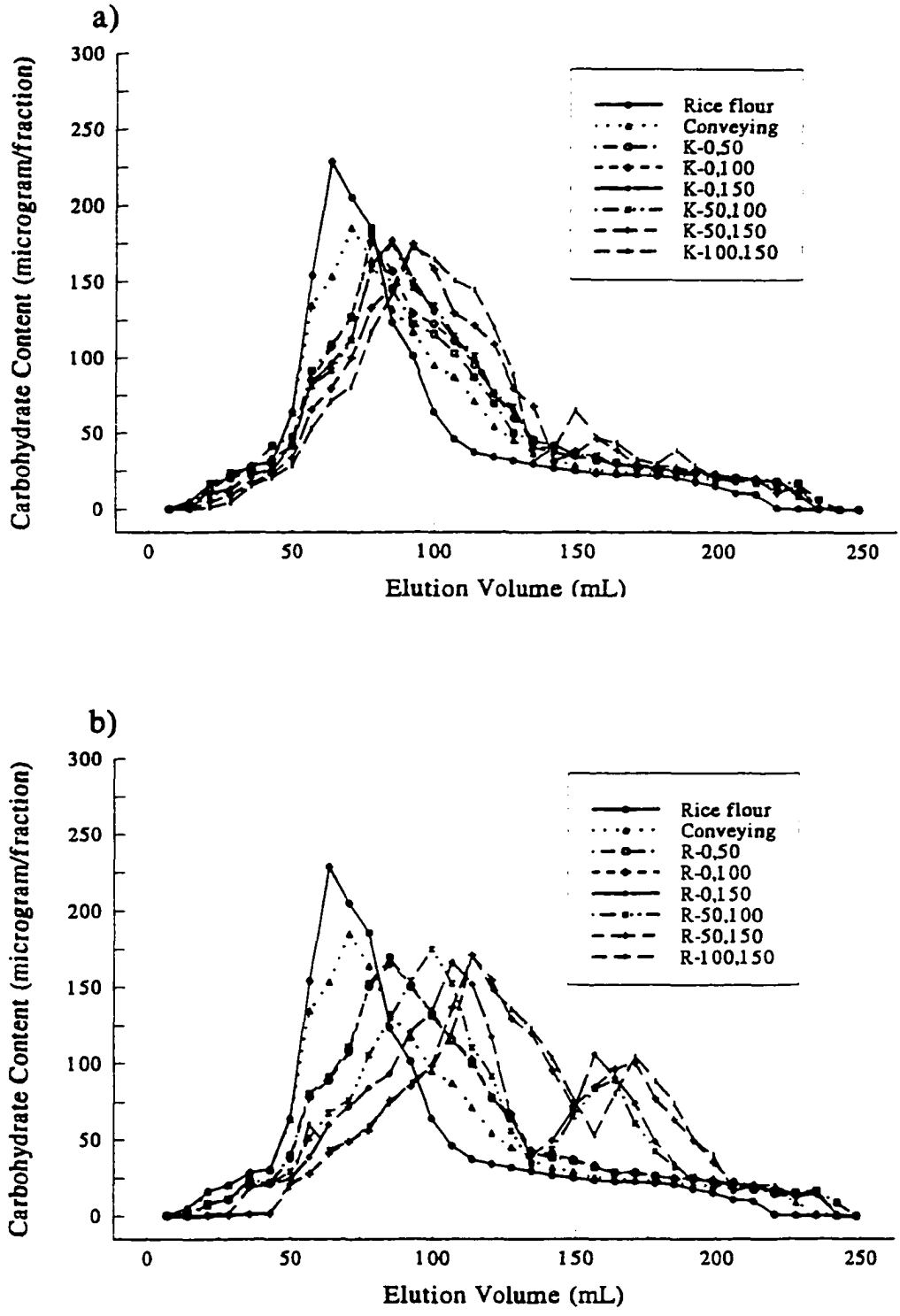

Figure 4.24 Spacing effect of (a) kneading blocks and (b) reverse screw elements on starch breakdown during extrusion of rice flour.

temperature. The onset temperature (gelatinization initiation) increased with decreasing moisture content in all the studies.

The endotherms obtained from DSC are shown in Fig. 4.25. The onset gelatinization, peak, and conclusion temperature for unextruded rice flour were 63.80, 70, and 78°C, respectively. The enthalpy change during gelatinization of rice flour was 2.837 J/g. Our results correlated very well with those of Park and Hyun (1989) who studied the thermal transition of two varieties of rice starch: *Japonica* and *Indica*. The onset, peak, and conclusion temperatures reported were 65-70°C, 78-81, and 87-91°C. The change in enthalpy varied from 3.51 to 2.76 J/g.

Biliaderis *et al.* (1986a) have shown that the peak gelatinization temperature for 75% rice starch (approximate composition of carbohydrate in this study) was about 120°C. The die temperature with the least severe screw configuration (conveying screw) was 133°C (Table 4.5), much higher than the peak gelatinization temperature. Our results show that the extrudate obtained even by the least severe screw configuration were completely gelatinized (Fig. 4.25). The sharp peak indicating the absorbance of energy during gelatinization was missing in the extrudates produced with and without any mixing elements in the screw profile. Therefore, starch in the extrudates obtained with different screw configurations was completely gelatinized.

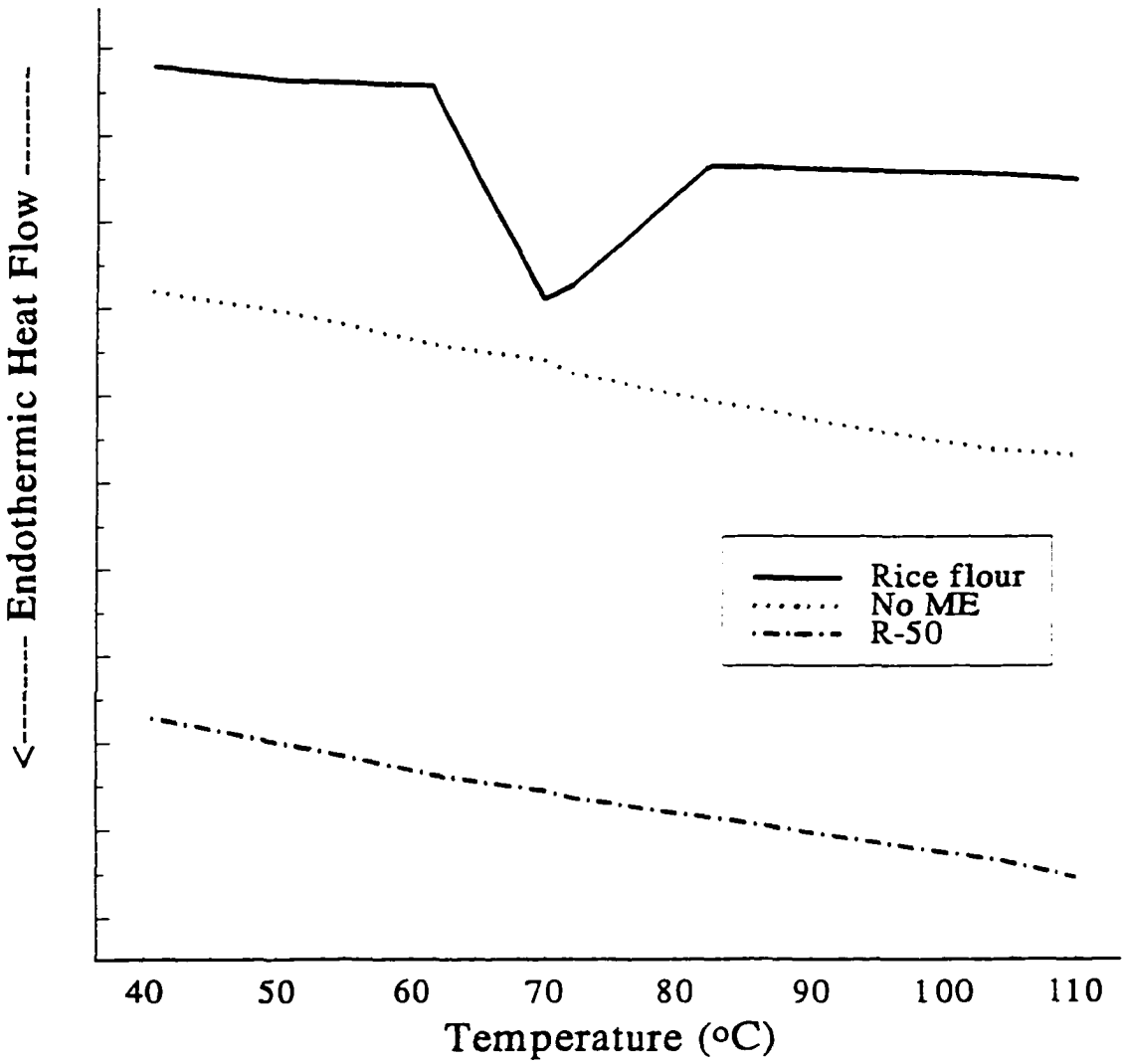

Figure 4.25 Differential scanning calorimetric thermal curves for rice flour and extrudates. No ME: no mixing element in the screw profile, and R-50: a screw profile with reverse screw element at 50 mm from the die.

4.2.5 Effect of screw configuration on macroscopic properties of the extrudates

The reactions taking place in the extruder are influenced by various independent process variables (Fig. 1.1), screw configuration being one of the important variables. This key parameter influences the energy inputs and residence time of the material inside the extruder. Magnitude of specific mechanical and thermal energy input to starchy and proteinaceous materials for different residence times in the extruder leads to various changes in the properties of the extrudates.

4.2.5.1 Densities

In food extrusion, starchy and proteinaceous materials are converted into a melt, which is forced through a die. The pressure drop across the die causes flashing of water as steam, resulting in an expanded matrix. The apparent density of an expanded product is always lower than that of the feed material.

Apparent density (AD): Type, length, and position, of elements affected the AD significantly. However, the interaction affects were not significant (Table 4.10). Extrudate from the conveying screw configuration had the highest apparent density (538 kg/m^3). Incorporation of mixing elements lowered the AD considerably (Fig. 4.26 a and b). Extrudates obtained with screw profiles having KB had a higher AD than that from screw profiles with RSE. Apparent density decreased with longer element, independent of position and type of element. For example, extrudate obtained with a 25 mm KB at 0 mm from the die had an AD of 242.89 kg/m^3. This value reduced to 187.73 kg/m^3

Table 4.10 Analysis of variance data for density of rice flour extrudates.

Source	DF	Mean Sum of Squares (MSS) and F-values for Density (kg/m^3)			
		Apparent Density		True Density	
		MSS	F	MSS	F
Type (Typ)	1	8225.19	26.32**	3937.75	3.06
Length (Len)	1	16916.23	54.14**	235.53	0.18
Position (Pos)	3	7096.57	22.71**	2220.19	1.73
Typ x Len	3	227.10	0.73	1279.78	0.99
Typ x Pos	3	836.97	2.68	92.09	0.07
Pos x Len	3	920.41	2.95	1162.57	090
Typ x Len x Pos	1	17.16	0.05	1255.37	0.98
Error	16	312.46	-	1286.78	-

**Highly significant at $p \leq 0.005$

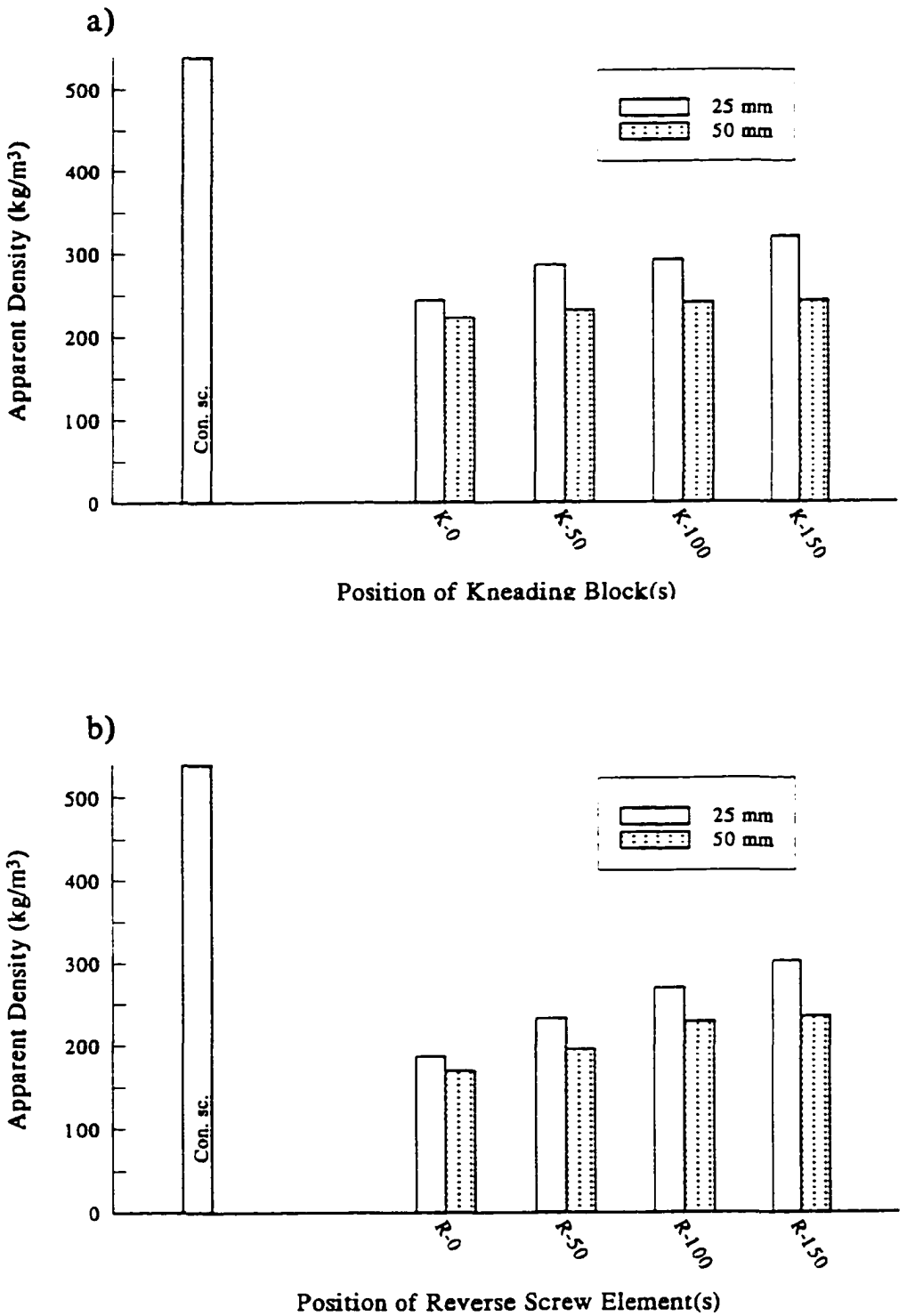

Figure 4.26 Position and length effects of (a) kneading block and (b) reverse screw element on apparent density during extrusion of rice flour.

when the KB was replaced by a RSE of similar length at the same position. But, a 50 mm long KB at the die produced an extrudate with an AD of 221.52 kg/m^3. AD increased systematically when the mixing elements were moved farther away from the die, irrespective of element type and length (Fig. 4.26). Larger spacing between the two elements also increased the apparent density (Fig. 4.27). Similarly, AD increased as the two elements (with constant spacing) were moved farther away from the die (Fig. 4.27).

According to Yacu (1995), higher die temperature caused more flashing at the die, which resulted in higher overall expansion and reduced density. We also observed that AD was lower when die temperature was higher. A negative correlation between die temperature and apparent density (R = 0.86 and F = 73.27) was found (Fig.4.28). Our results are in agreement with Bhattacharya and Hanna (1987), Grenus *et al.* (1992), and Bhattacharya and Choudhury (1994) who have shown that with a higher die temperature, apparent density of the product decreased.

True density: The effect of type, length and position of the element on the true density was not significant as illustrated in Table 4.10. True density of the material is not affected by the screw configuration (Table 4.11). The values were similar to those obtained with unextruded rice flour.

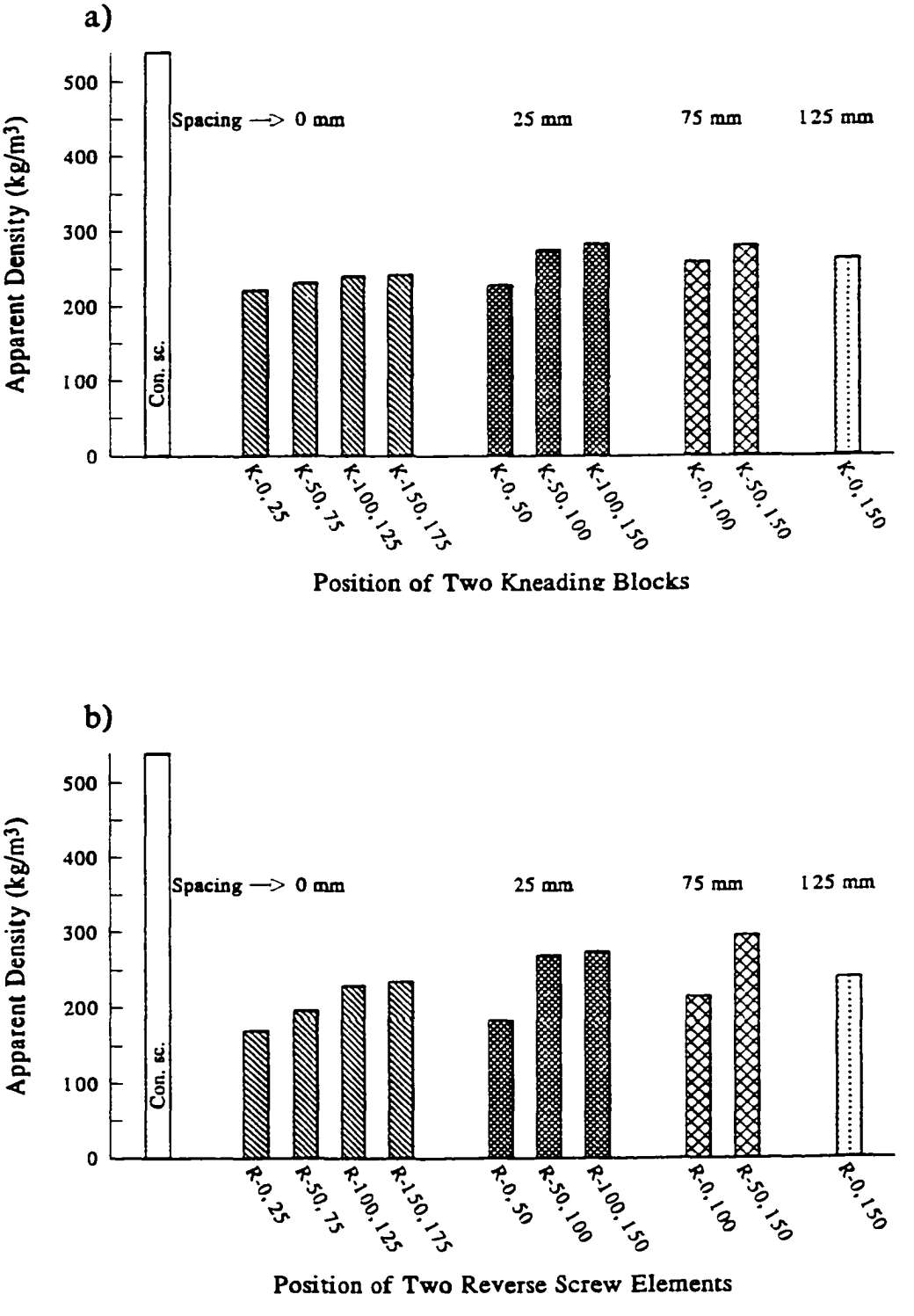

Figure 4.27 Position and spacing effects of (a) two kneading blocks and (b) two reverse screw elements on apparent density during extrusion of rice flour.

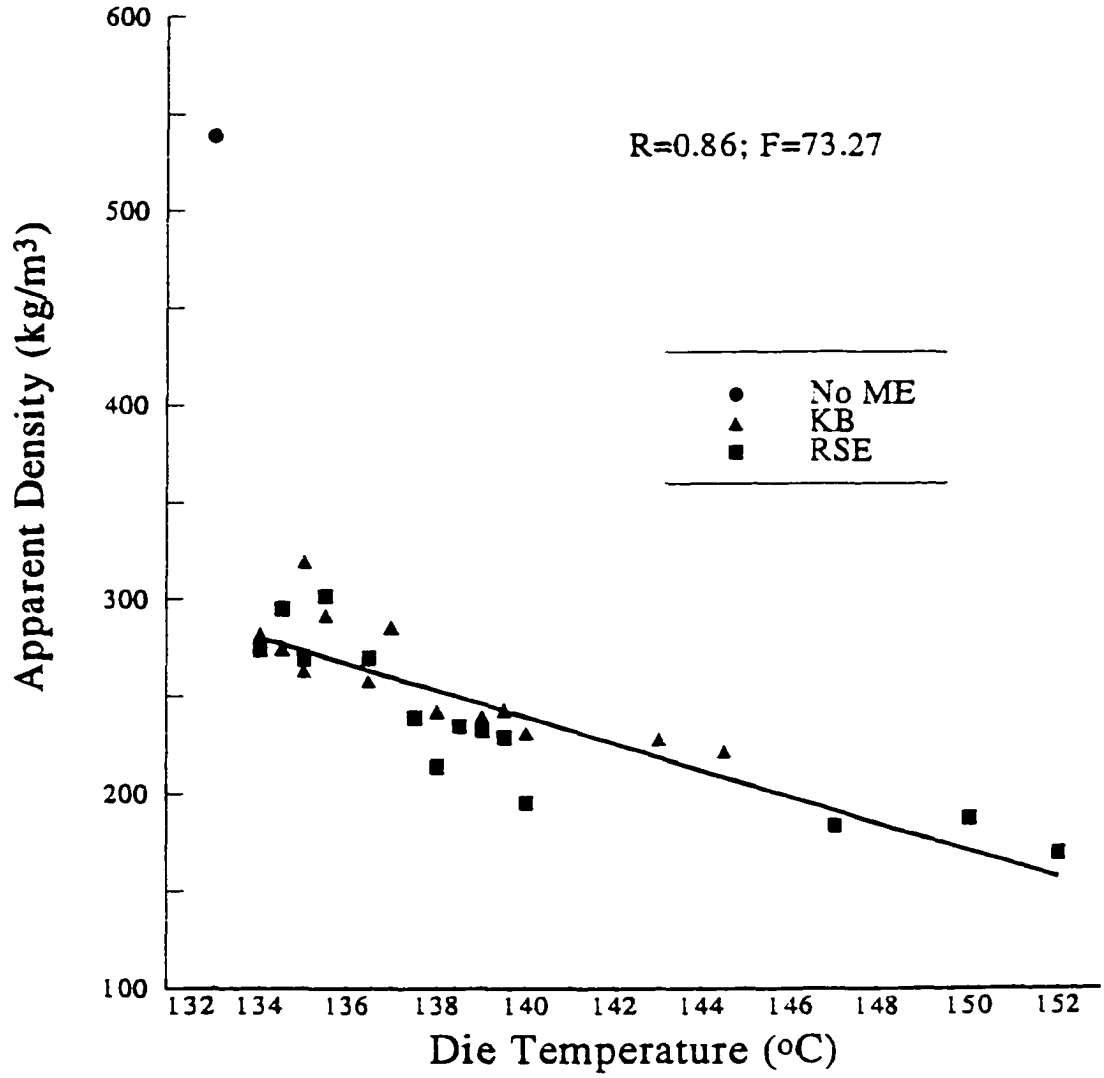

Figure 4.28 Relationship between apparent density and die temperature during twin-screw extrusion of rice flour. (No ME: no mixing element in the screw profile; KB: kneading element; RSE: reverse screw element).

Table 4.11 Effect of screw configuration with kneading block (KB) and reverse screw element (RSE) on true density (TD) of rice flour extrudates.

Location of KB(s) or RSE(s) from the Die (mm)	Parameters Evaluated	TD (kg/m^3) in Presence of	
		KB(s)	RSE(s)
None	-	1452.55±30.18	1552.21±30.18
0	Position	1479.26±34.31	1481.15±48.46
50		1450.00±47.38	1466.54±37.71
100		1445.60±52.33	1445.78±37.87
150		1479.26±16.41	1425.50±36.42
0 & 25	Length/ Spacing	1482.58±51.22	1450.92±27.89
50 & 75		1498.60±17.98	1439.25±17.58
100 & 125		1482.41±37.07	1444.00±23.76
150 & 175		1422.50±18.78	1412.50±31.54
0 & 50	Spacing	1497.29±37.61	1432.20±36.85
50 & 100		1442.56±27.70	1432.20±36.48
100 & 150		1412.56±42.76	1421.23±32.12
0 & 100		1475.10±36.20	1444.10±33.52
50 & 150		1423.45±31.91	1423.44±26.50
0 & 150		1430.90±45.11	1412.50±15.70

4.2.5.2 Expansion ratios

The extent of reactions during extrusion affects product expansion. The expanded matrix in the extrudate was provided by the starch component of rice flour. The expansion process can be described as nucleation in the die, extrudate swelling immediately beyond the die, followed by bubble growth and collapse (Kokini *et al.* 1991). When extrudate exits the die, it expands in both radial and axial direction.

Radial expansion: Extrudate from the conveying screw had a radial expansion ratio of 6.00 (Fig. 4.29). Incorporation of KB in the screw profile improved product expansion, irrespective of element length and position. However, this trend was not true with RSE (Fig. 4.29) Effects of type, length, and position of the mixing elements and their interaction on the radial expansion ratio were significant (Table 4.12). KB produced more expanded products than RSE, irrespective of position and length. Generally, longer mixing elements reduced extrudate expansion, except when placed at 0 mm from the die (Fig. 4.29). The trend of radial expansion ratio with the position of element from the die was different for type and length of the mixing element. When a KB (25 or 50 mm long) was moved farther away from the die the radial expansion increased. Maximum radial expansion (10.65) was obtained with a 25 mm long KB at 150 mm from the die. However, when RSE (25 mm long) was moved farther away from the die, the expansion first increased at 50 mm and than decreased continuously. A systematic decrease in the radial expansion was observed by moving 50 mm long RSE farther away from the die (Fig. 4.29 b).

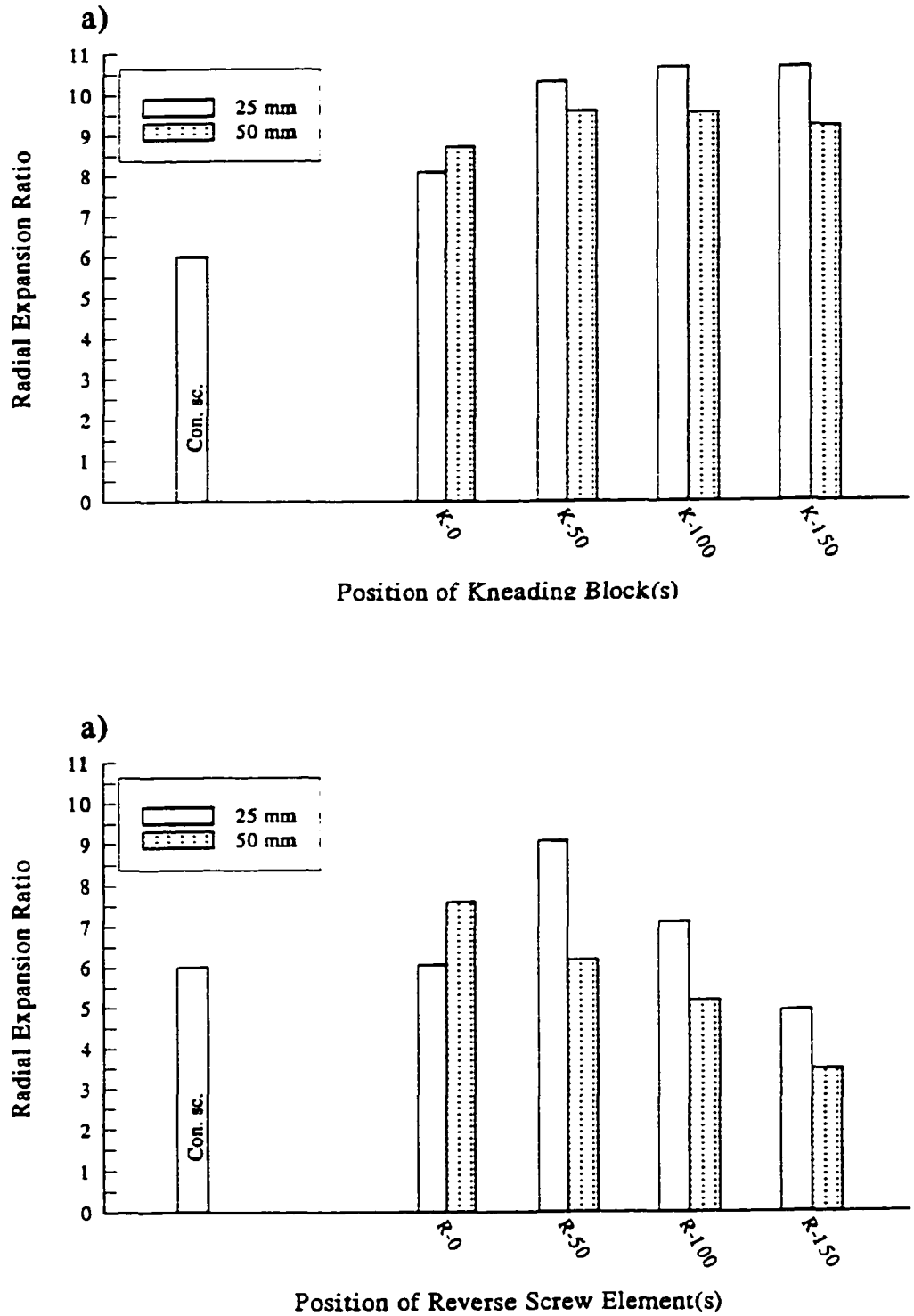

Figure 4.29 Position and length effects of (a) kneading block and (b) reverse screw element on radial expansion ratio during extrusion of rice flour.

Table 4.12 Analysis of variance data for expansion ratio of rice flour extrudates.

Source	DF	Mean Sum of Squares (MSS) and F-values for Expansion Ratios					
		Radial Expansion Ratio		Overall Expansion Ratio		Calculated Axial Expansion Ratio	
		MSS	F	MSS	F	MSS	F
Type (Typ)	1	93.06	1585.17**	5.61	41.14**	30.27	28.89**
Length (Len)	1	6.83	116.41**	8.63	63.33**	77.54	74.01**
Position (Pos)	3	4.29	73.04**	6.04	44.31**	39.35	37.56**
Typ x Len	3	0.56	9.53*	0.05	0.40	1.78	1.70
Typ x Pos	3	6.80	115.91**	1.32	9.66*	4.50	4.30
Pos x Len	3	3.64	62.00**	0.16	1.19	3.86	3.68
Typ x Len x Pos	1	0.86	14.64**	0.04	0.26	0.40	0.38
Error	16	0.06	-	0.14	-	1.05	-

**Highly significant at $p \leq 0.005$

*Significant at at $p \leq 0.05$

The radial expansion ratio decreased considerably when two RSEs with constant spacing were moved farther away from the die (Fig. 4.30 b). Also, by positioning the first RSE at 50 or 100 mm from the die, and moving the second RSE away from the die, caused a considerable decrease in expansion. However, with KBs the reduction in expansion was marginal for similar spacing (Fig. 4.30 a).

Extrudate expansion is influenced by degree of gelatinization (Mercier and Feillet 1975; Chinnaswamy and Bhattacharya 1983, 1984; Cai and Diosady, 1993), starch breakdown (Gomez and Aguilera, 1983, 1984; Kirby *et al.*, 1988; Cai and Diosady, 1993), and amylose content (Chinnaswamy and Hanna, 1990). Our DSC data proved that starch in extrudates obtained with all screw configurations was fully gelatinized (Fig. 4.25).

Effect of SME input on radial expansion ratio was less prominent in configuration with KBs than those with RSEs (Fig. 4.31). In general, the expansion ratio remained above 8.00 with all the position, length, and spacing of KBs, despite an increase in SME input (Fig. 4.31). Incorporation of KB might have provided optimum mechanical and thermal energy resulting in better expansion than with RSE. This may be due to an increase in amylose content as a result of starch breakdown during extrusion. Initial amylose content of the rice flour was 20-25%. This concentration might have increased to an optimum ($\approx$ 50%) by incorporation of KB. Chinnaswamy and Hanna (1990) observed maximum expansion during extrusion of corn starch with 50% amylose.

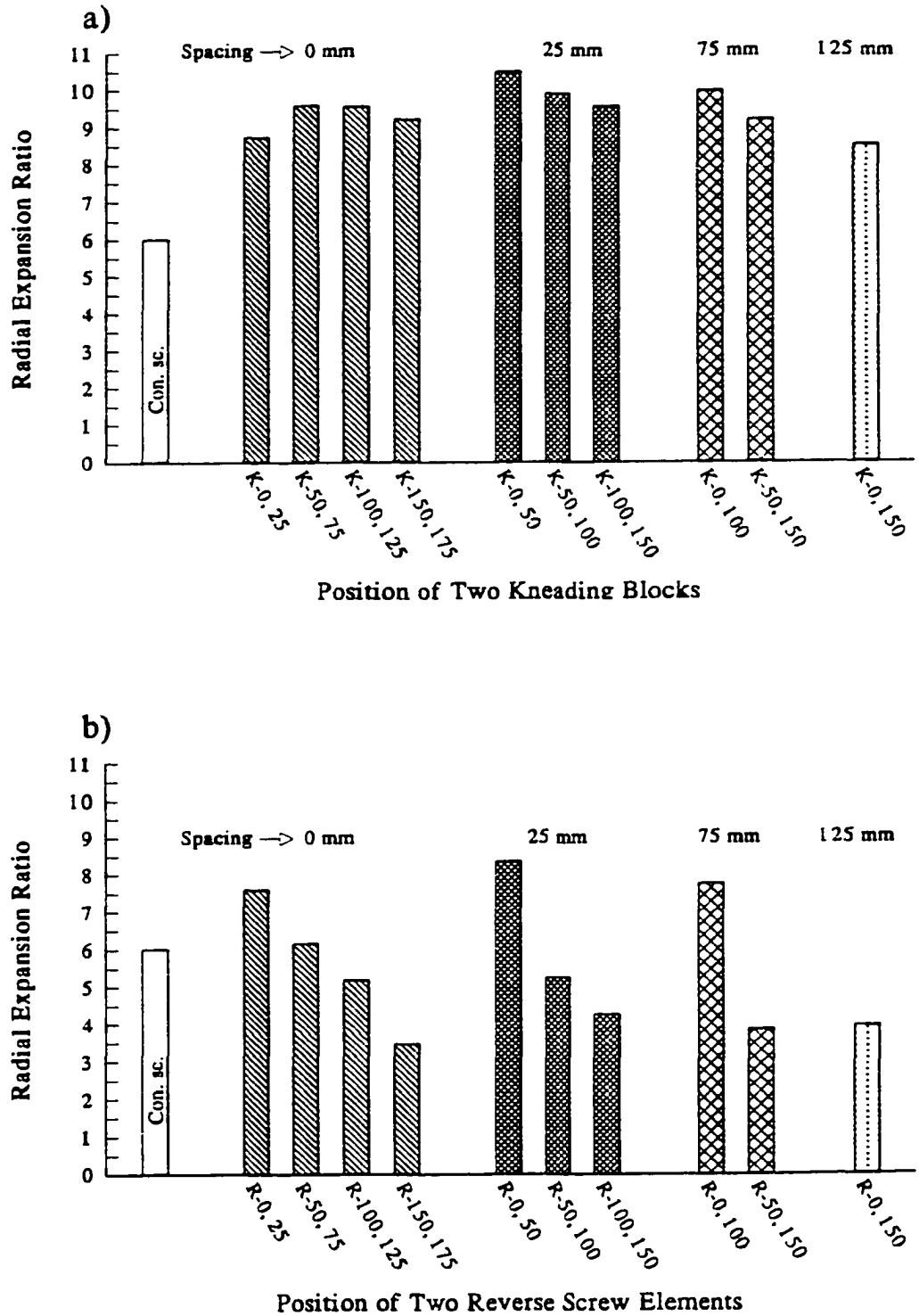

Figure 4.30 Position and spacing effects of (a) two kneading blocks and (b) two reverse screw elements on radial expansion during extrusion of rice flour.

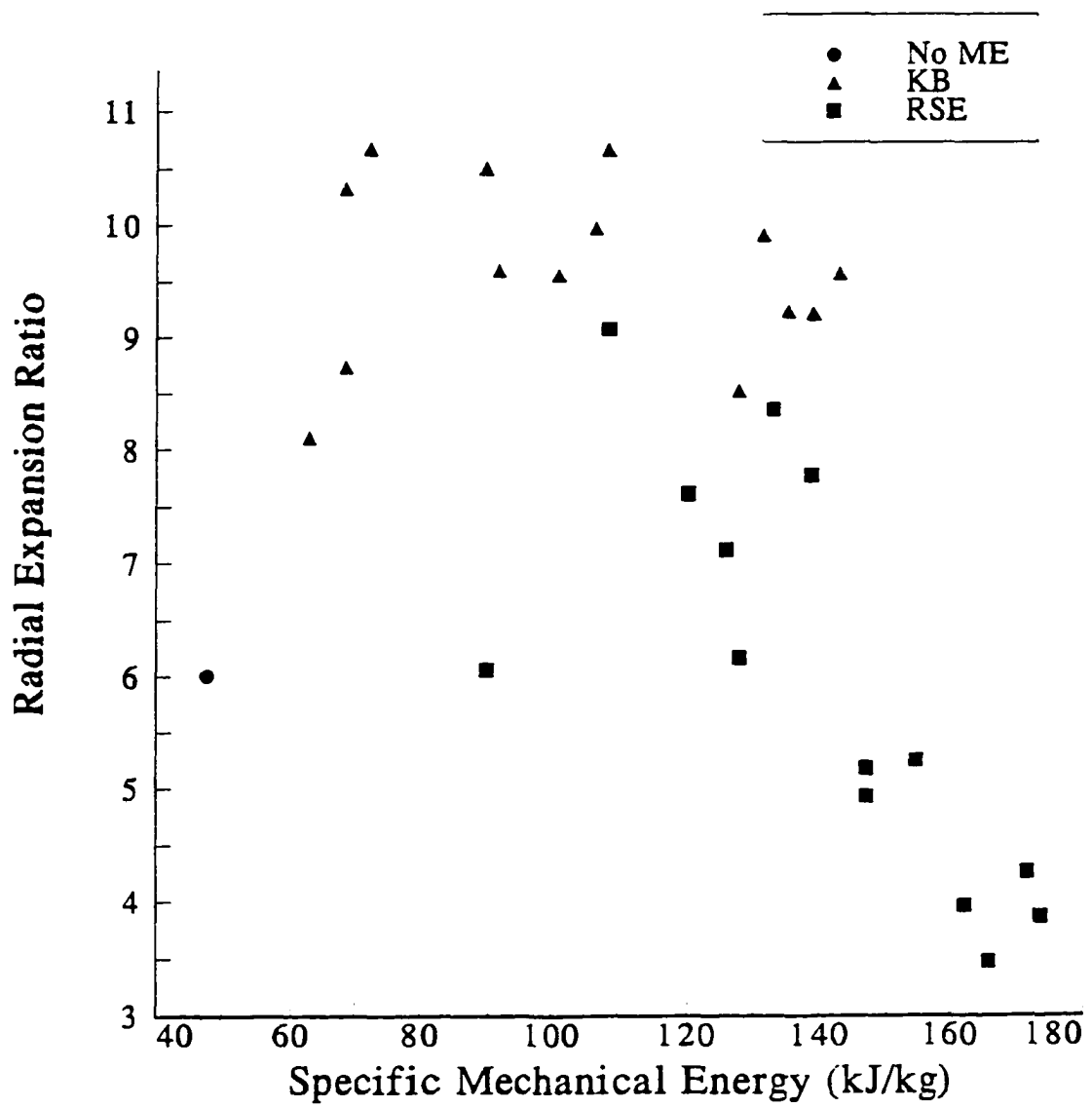

Figure 4.31 Influence of mixing elements on radial expansion ratio and specific mechanical energy for rice flour extrudates.

As shown from SME input and molecular breakdown data, RSE had a higher SME input and produced lower molecular weight fragments compared to that of KB. Increased distance from the die, longer element, and larger spacing between two elements also produced low molecular weight compounds. Very severe screw configuration (with SME input > 145 kJ/kg) resulted in radial expansion ratio less than 5.0 (Fig. 4.31). This reduction in expansion may be due to fragmentation of starch to dextrins. Similar reduced expansion due to dextrinization of starch have been observed by Gomez and Aguilera (1983, 1984), Colonna *et al.* (1984), and Davidson *et al.* (1984).

Axial expansion ratio: Effect of screw configuration on axial expansion is depicted in Figures 4.32 and 4.33. The trend is exactly opposite to that of radial expansion. The effects of position, length, type of elements and their interactions on axial expansion were significant (Table 4.12).

Overall expansion ratio: The trend of overall expansion ratio with screw configuration was exactly opposite to that of apparent density. Effects of type, length and position of screw elements affected the overall expansion ratio significantly (Table 4.12). But, the interaction effects were not significant. An overall expansion ratio of 2.88 was obtained with a conveying screw configuration. Incorporation of mixing elements increased the overall expansion ratio considerably (Fig. 4.34). RSE produced extrudates with higher overall expansion than KB at all positions and for both lengths. However, at the same position, larger overall expansion ratio was observed by longer element. For example, the values of overall expansion ratio obtained by a 25 mm KB

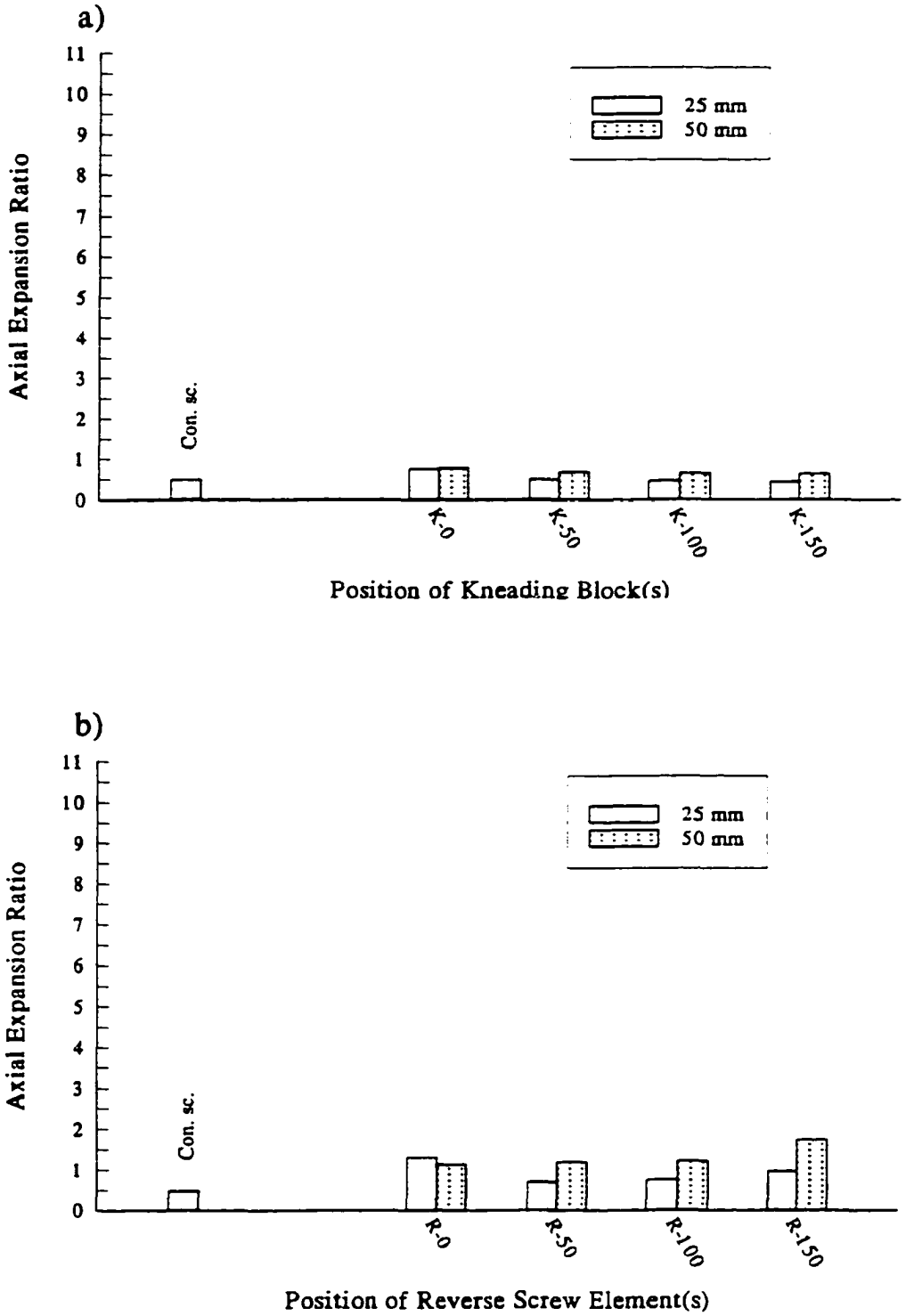

Figure 4.32 Position and length effects of (a) kneading block and (b) reverse screw element on axial expansion ratio during extrusion of rice flour.

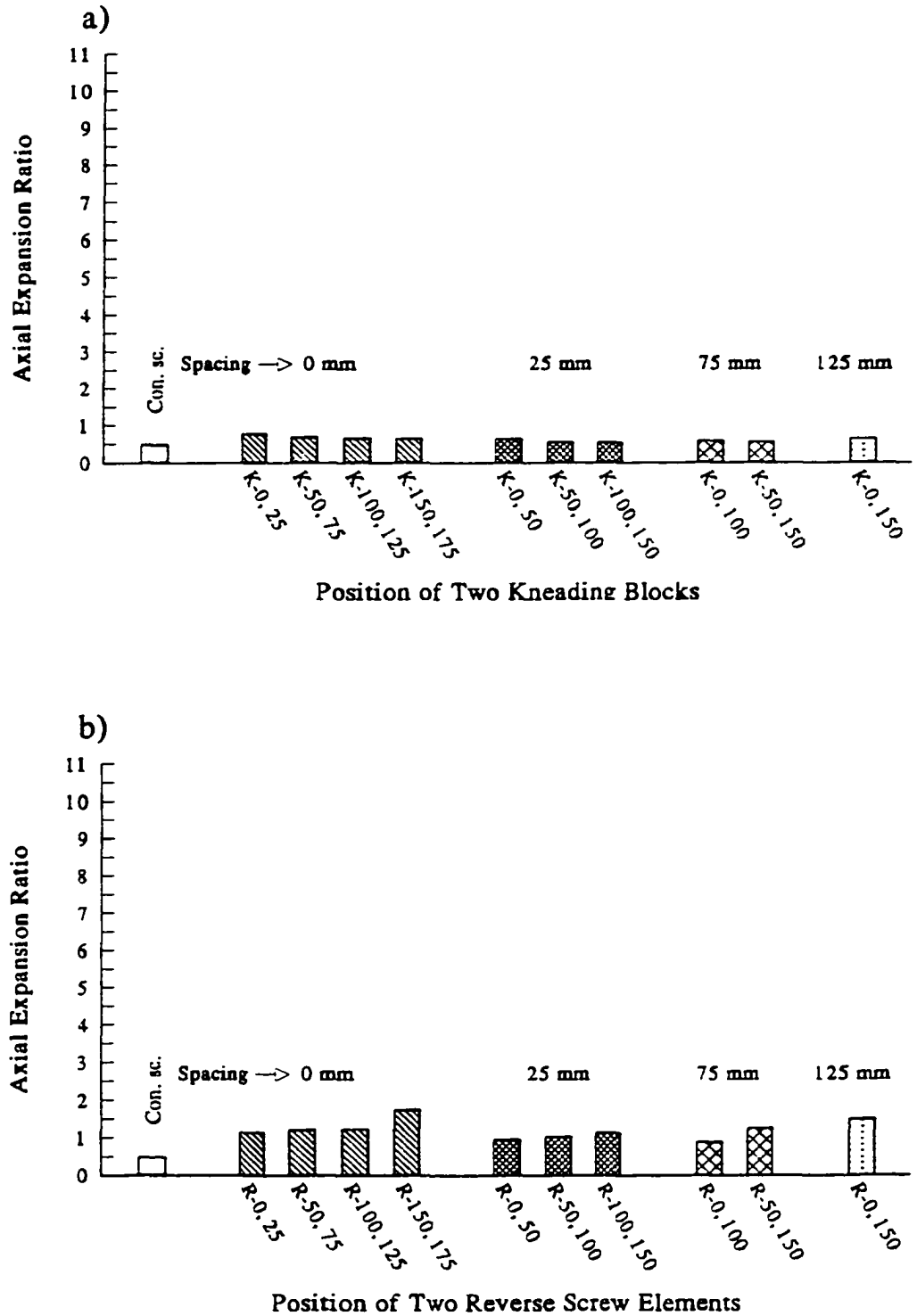

Figure 4.33 Position and spacing effects of (a) two kneading blocks and (b) two reverse screw elements on axial expansion ratio during extrusion of rice flour.

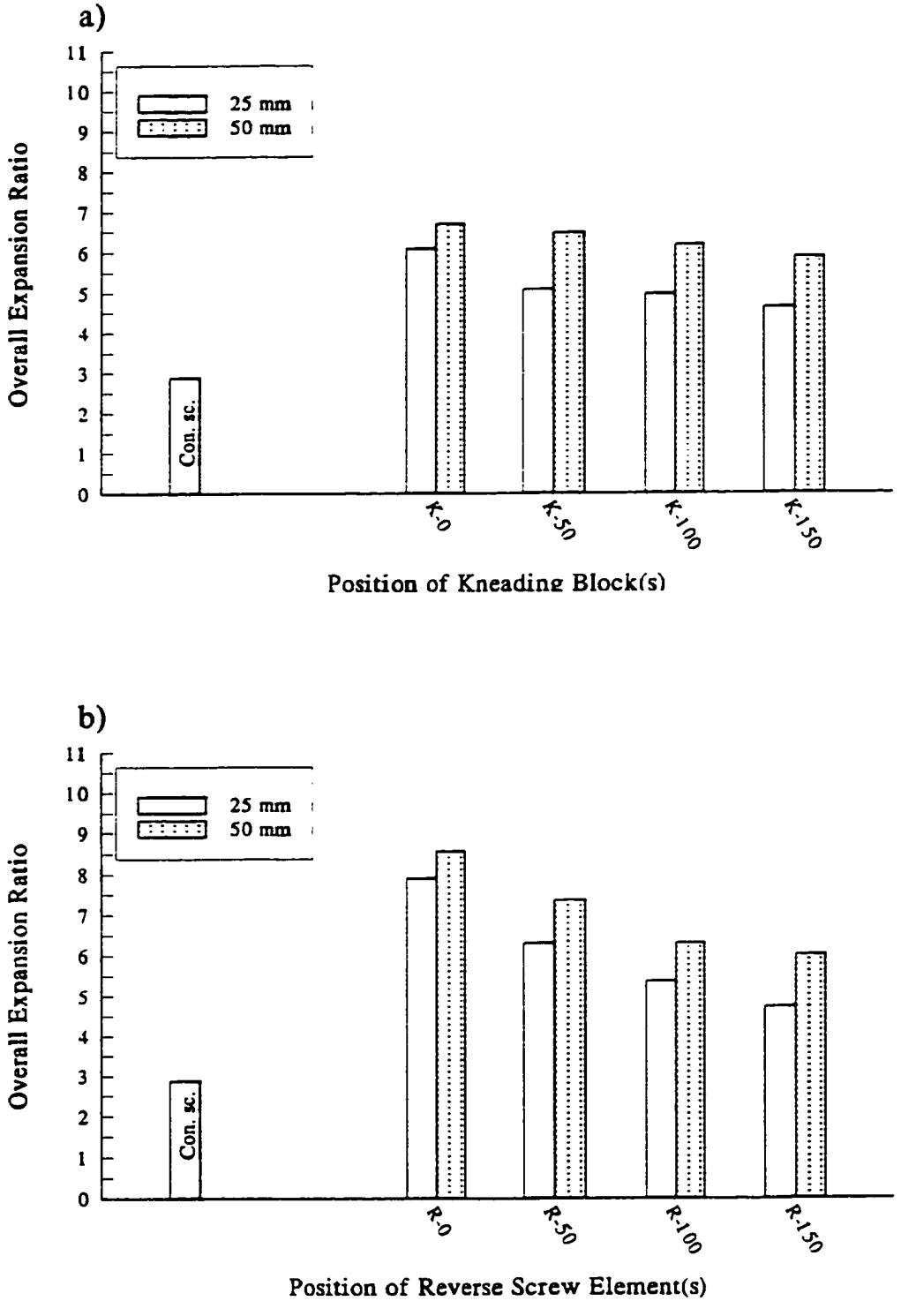

Figure 4.34 Position and length effects of (a) kneading block(s) and (b) reverse screw element(s) on overall expansion ratio during extrusion of rice flour.

and RSE positioned at the die were 6.09 and 7.90, respectively. But, 50 mm long KB and RSE at the same position produced extrudates with values of 6.69 and 8.56, respectively. Increased spacing between the two elements and moving the elements (with constant spacing) farther from the die, decreased the overall expansion ratio (Fig. 4.35).

Yacu (1995) have shown that overall expansion ratio and die temperature are directly related. In this study, a good correlation between die temperature and overall expansion ($R = 0.89$ and $F = 107.68$) was observed (Fig. 4.36 a). When die temperature was low, less flashing occurred at the die resulting in poor overall expansion. Both die temperature and overall expansion ratio decreased systematically as the mixing elements were moved farther away from the die, irrespective of element type and length (Table 4.5 and Fig. 4.34 a, b). A negative correlation between apparent density and overall expansion ($R = 0.97$ and $F = 522.78$) was observed (Fig. 4.36 b).

4.2.5.3 Porosity

The expanded extrudate is porous in nature, and the extent of voids created depends on independent process variables. Porosity of the extrudate obtained with a conveying screw element was about 65%. Inclusion of mixing elements in the screw profile increased the porosity considerably (Figs. 4.37 and 4.38). The trend is similar to that of overall expansion ratio. Table 4.13 shows that type, length, and position of the elements affected porosity significantly. Generally, incorporation of RSE produced more porous extrudates than with KB. Similarly, longer elements produced slightly more

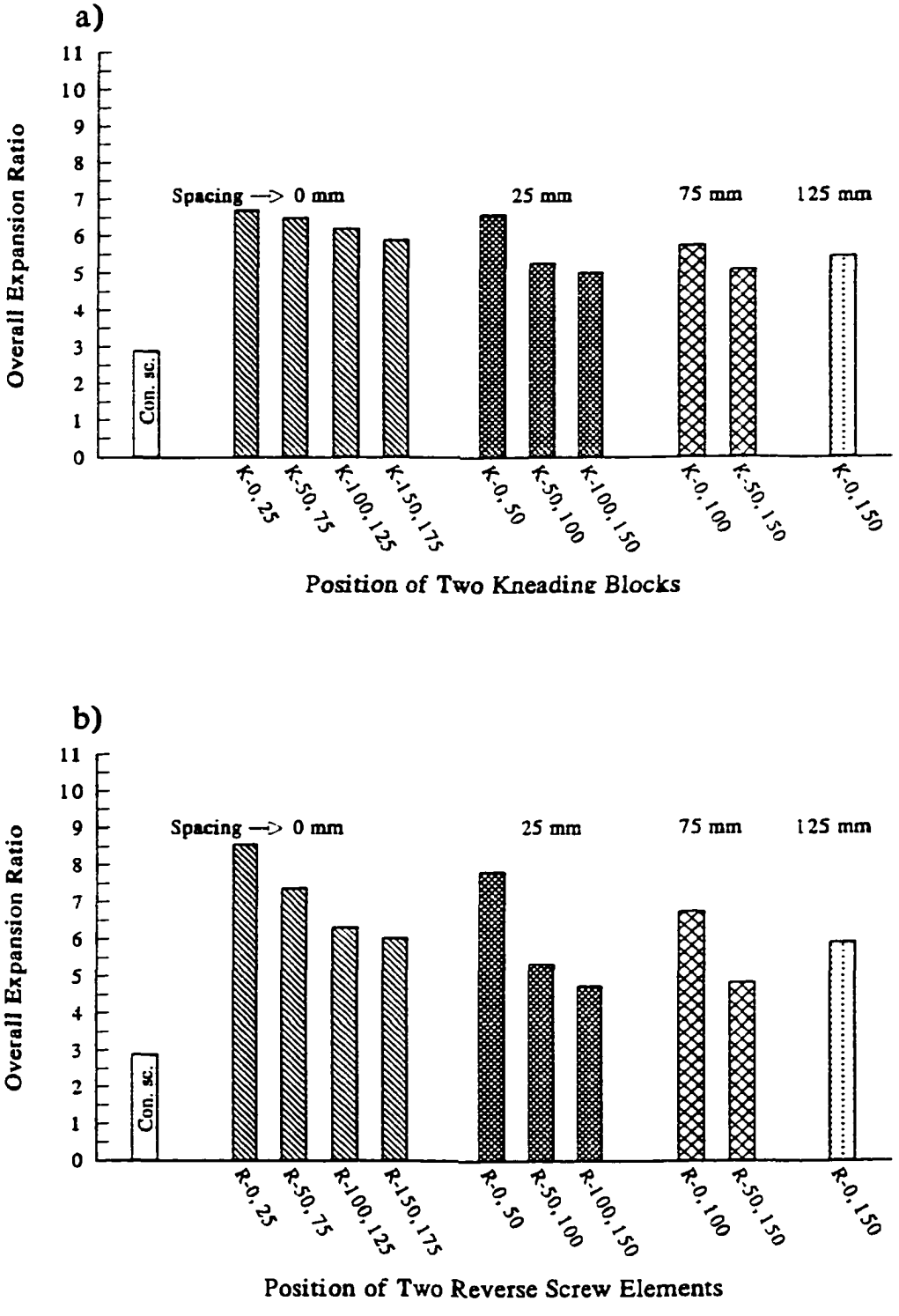

Figure 4.35 Position and spacing effects of (a) two kneading blocks and (b) two reverse screw elements on overall expansion ratio during extrusion of rice flour.

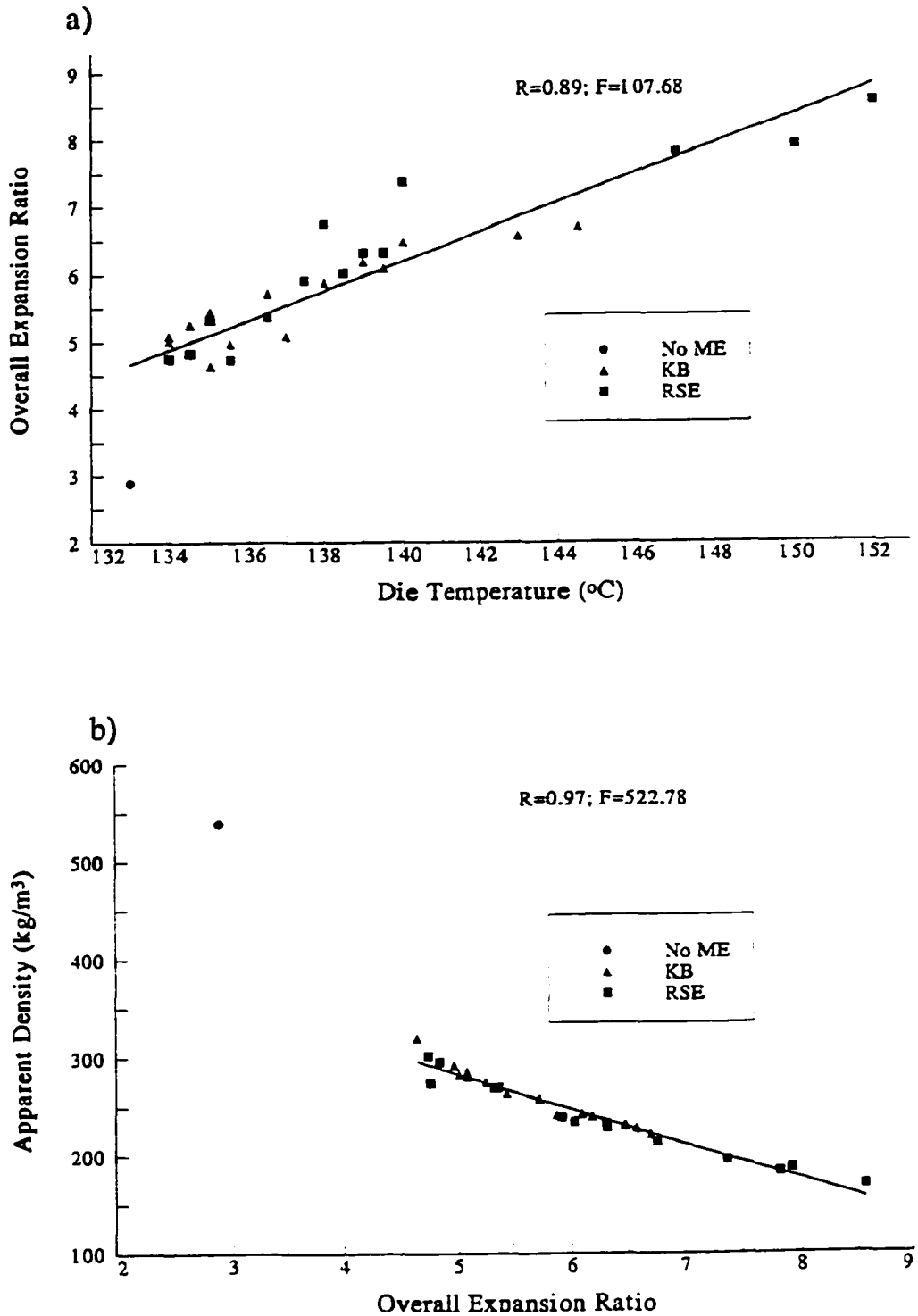

Figure 4.36 Relationships between overall expansion and die temperature (a) and between apparent density and overall expansion (b) of rice flour extrudates. (No ME: no mixing element in the screw configuration; KB: kneading block; RSE: reverse screw element).

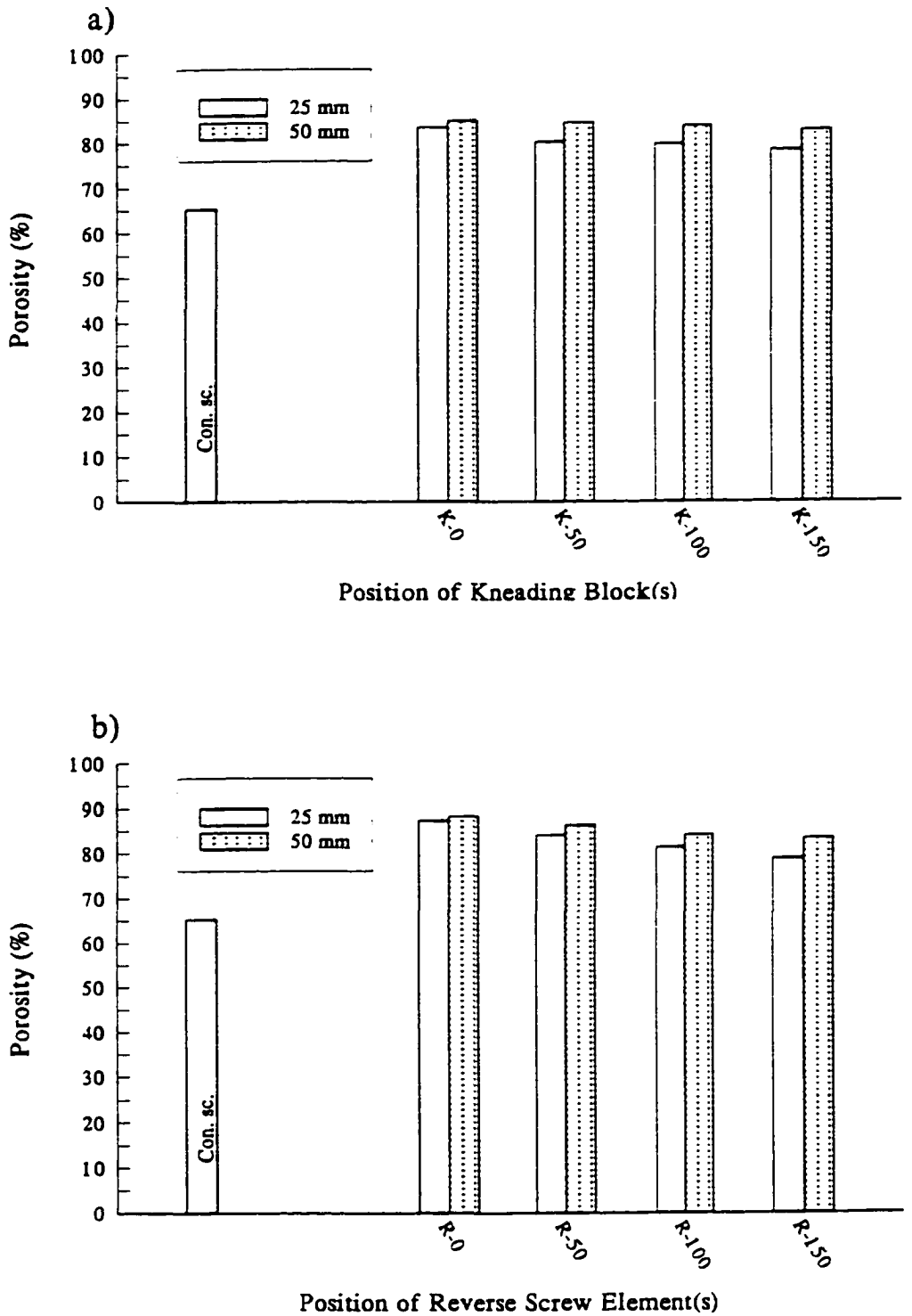

Figure 4.37 Position and length effects of (a) kneading block(s) and (b) reverse screw element(s) on porosity during extrusion of rice flour.

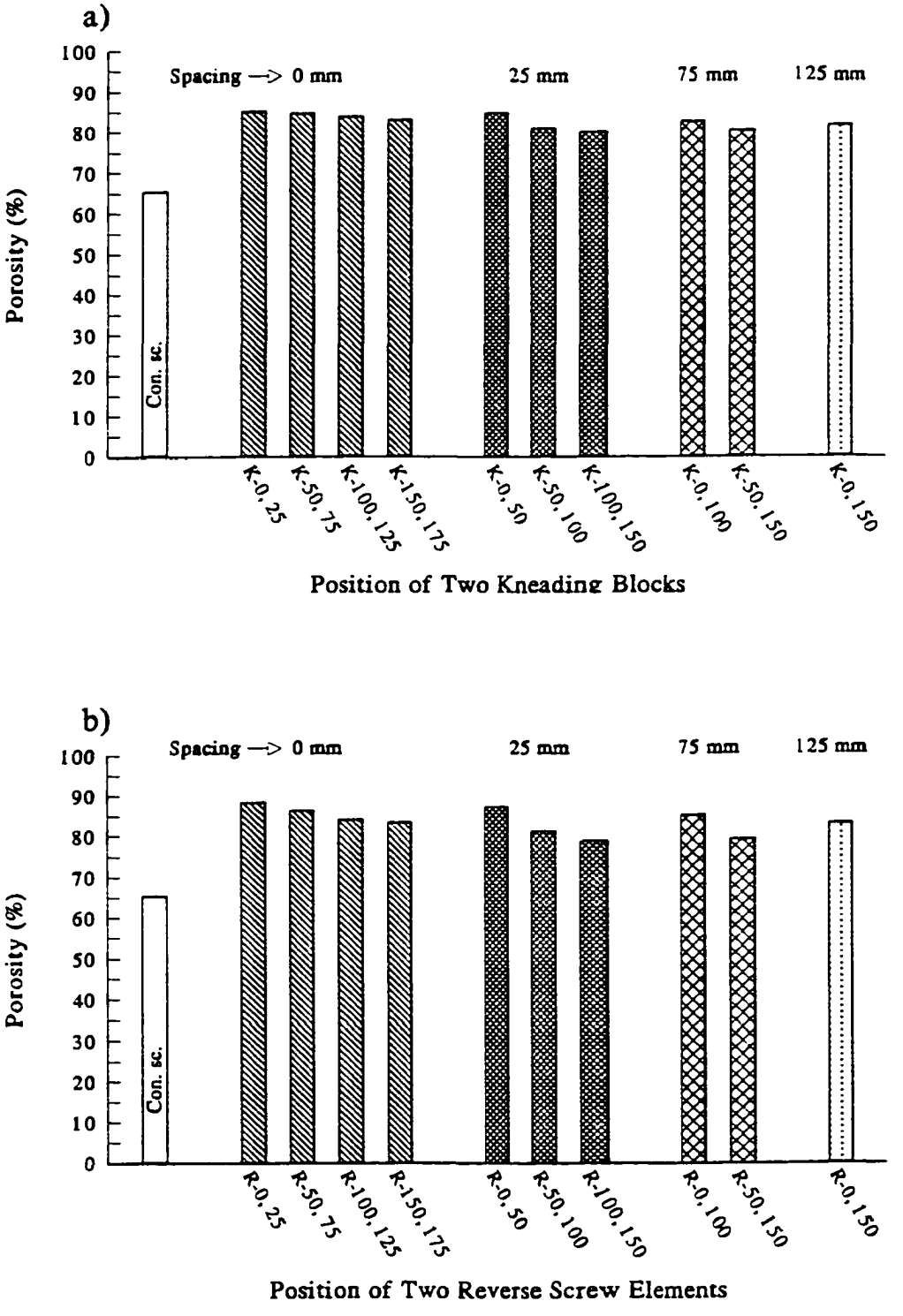

Figure 4.38 Position and spacing effects of (a) two kneading blocks and (b) two reverse screw elements on porosity during extrusion of rice flour.

Table 4.13 Analysis of variance data for porosity and breaking strength.

Source	DF	Mean Sum of Squares (MSS) and F-values for Porosity (%) and Breaking Strength (MPa)			
		Porosity		Breaking Strength	
		MSS	F	MSS	F
Type (Typ)	1	30.27	28.89**	0.43827735	468.01**
Length (Len)	1	77.54	74.01**	0.09343948	99.78**
Position (Pos)	3	39.52	37.56**	0.05342856	57.05**
Typ x Len	3	1.78	1.70	0.07560411	80.73**
Typ x Pos	3	4.50	4.30	0.07450636	79.56**
Pos x Len	3	3.86	3.68	0.03243571	34.64**
Typ x Len x Pos	1	0.40	0.38	0.02902760	31.00**
Error	16	1.05	-	0.00093647	-

Highly significant at $p \leq 0.005$
Significant at $p \leq 0.05$

porous extrudates than a shorter element (Fig. 4.37 a and b). For example, the values of porosity with 25 mm long KB and RSE at the die were 83.58% and 87.36%, respectively. The values increased to 85.05% and 88.32% with 50 mm long KB and RSE, respectively. The porosity of the extrudates decreased systematically, as the mixing elements were moved farther away from the die, irrespective of the element type and length (Fig 4.38 a and b). Again, the porosity decreased by increasing the spacing between the two elements, and by moving two elements (with same spacing) farther away from the die (Fig. 4.38 a and b). By definition, porosity and overall expansion ratio are related as:

$$P = (1 - \frac{1}{OER}) * 100 \qquad (30)$$

where, P = Porosity (%)

OER = Overall expansion ratio

Both overall expansion ratio and porosity therefore a followed similar trend. However, the relationship was not linear (Fig. 4.39).

Numerous investigators have qualitatively shown the effect of independent process variables such as barrel temperature, screw speed, and L/D ratio on the microstructure of the extrudates by scanning electron microscopy (Owusu-Ansah *et al.*, 1984; Bhattacharya *et al.*, 1986; Bhattacharya and Hanna, 1987; and Bhattacharya and Choudhury, 1994). These studies were limited in measuring the radial expansion of the product. Radially expanded products were very porous with a large number of air

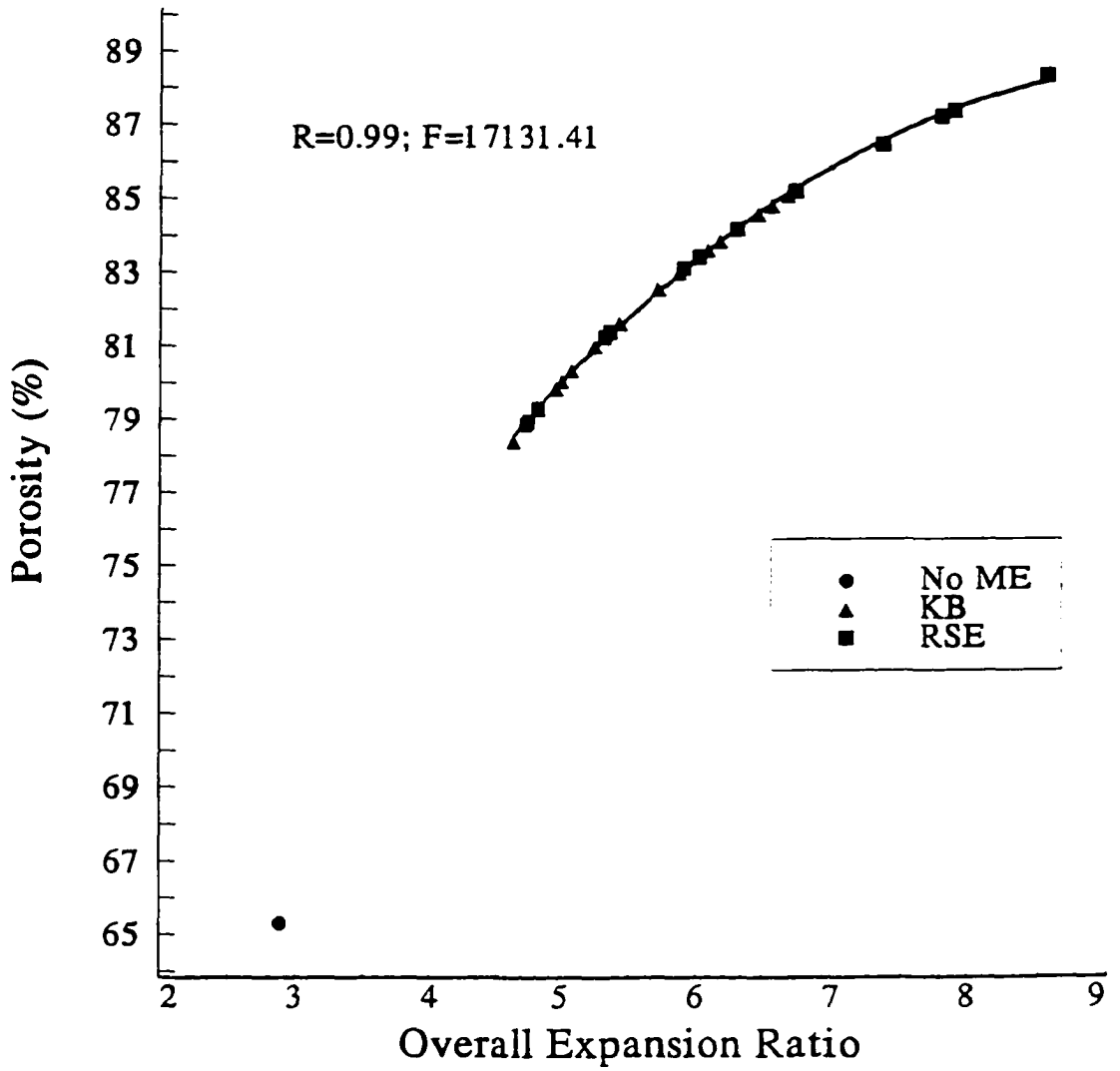

Figure 4.39 Relationship between porosity and overall expansion ratio of rice flour extrudate (No ME: no mixing element in the screw configuration; KB: kneading block; RSE: reverse screw element).

pockets distributed throughout the structure (Bhattacharya *et al.*, 1986; Bhattacharya and Hanna, 1987; Bhattacharya and Choudhury, 1994). Owusu-Ansah *et al.* (1984) stated that porosity increased with increasing expansion. However, they never measured porosity in their study. Porosity, by definition, is a three dimensional attribute of the extrudate and cannot be related with radial expansion.

4.2.5.4 Breaking strength

Textural properties of the extrudates are entirely different from the original raw material. Breaking strength is the most common textural attribute measured to determine hardness of extrudates (Owusu-Ansah *et al.*, 1984; Bhattacharya and Hanna, 1987; Chinnaswamy and Hanna, 1988).

Screw configuration affected the breaking strength in an exactly opposite fashion to that of radial expansion ratio (Figs. 4.40 and 4.41). Table 4.13 shows that the type, length, and position of mixing elements, and their interaction affected the breaking strength significantly. Conveying screw produced a product with a high breaking strength (0.42 MPa). In all cases, incorporation of kneading blocks lowered the breaking strength (Figs. 4.40 a and 4.41 a). Inclusion of RSEs of different lengths at various positions and spacings had a mixed effect on breaking strength (Figs. 4.40b and 4.41b). But, KB always produced extrudates with lower breaking strength than RSE. Longer mixing elements increased the breaking strength, except when placed at 0 mm from the die (Fig. 4.40). Longer RSE produced extrudates with very high breaking strength

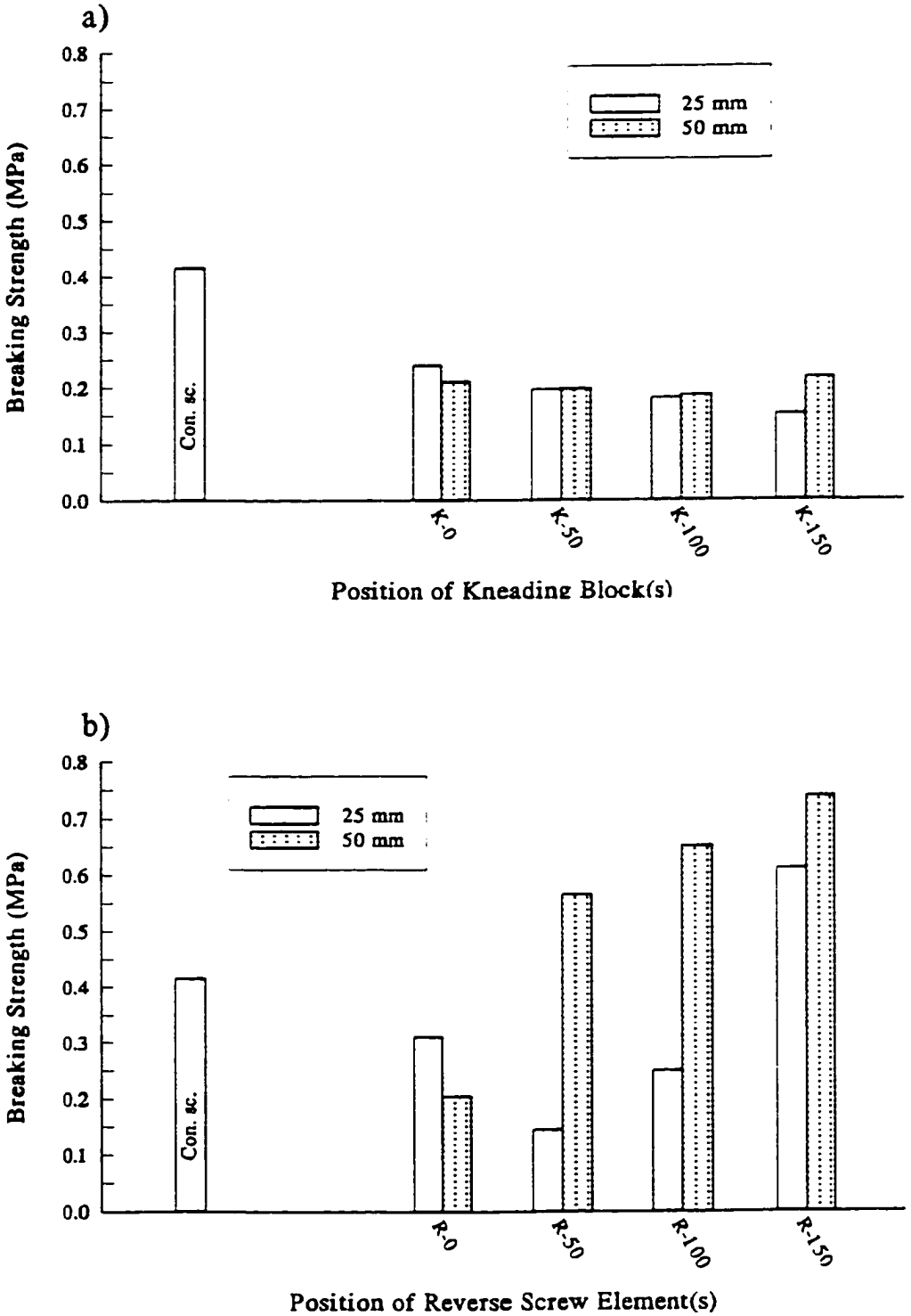

Figure 4.40 Position and length effects of (a) kneading block(s) and (b) reverse screw element(s) on breaking strength of rice flour extrudates.

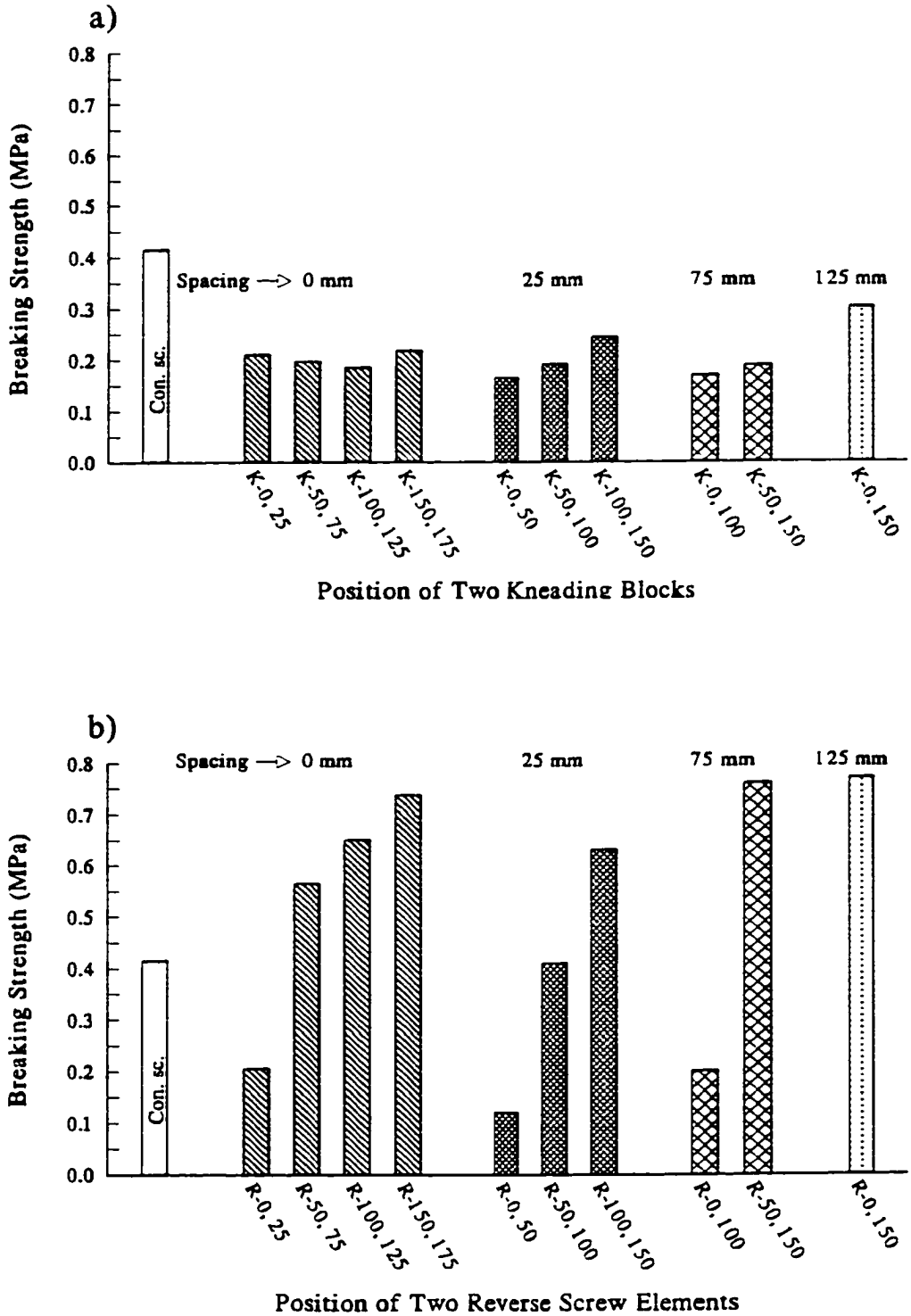

Figure 4.41 Position and spacing effects of (a) two kneading blocks and (b) two reverse screw elements on breaking strength of rice flour extrudates.

(> 0.5 MPa). Similarly, when the first RSE was positioned at 0 or 50 mm from die and the second RSE was moved farther away from the die, a considerable increase in breaking strength was observed.

The higher the radial expansion, the lower was the shear stress (Owusu-Ansah *et al.*, 1984; Bhattacharya and Hanna, 1987; Chinnaswamy and Hanna, 1988). The results of this study also confirmed the above finding. A negative correlation between the radial expansion ratio and breaking strength (R = 0.91 and F = 122.27) was observed (Fig. 4.42). Less peak force was required to cut a more expanded product into pieces by using a Warner Bratzler shear cell. For example, a peak force of about 50 N is required to break a product with the conveying screw (radial expansion ratio of about 6.0). However, a peak force of only 32 N is required to break a product with expansion ratio of 10.65 (obtained by incorporating a KB at 150 mm from the die).

Breaking strength cannot be correlated with either overall expansion ratios or porosity (three dimensional features) as shown in Figs. 4.43. Incorporation of KBs yielded extrudates with lower breaking strength, despite an increase in the SME input (Fig. 4.44). Extrudates obtained with KBs had higher radial expansion ratios (> 8.0), irrespective of type, length and position of extrudates. But, RSE in the screw profile and higher SME input increased the breaking strength considerably. RSEs, and increased spacing between the two RSEs produced extrudates with lower expansion ratios (< 5.0). Thus, textural attributes and other macroscopic characteristics of extrudates can be manipulated by screw configuration.

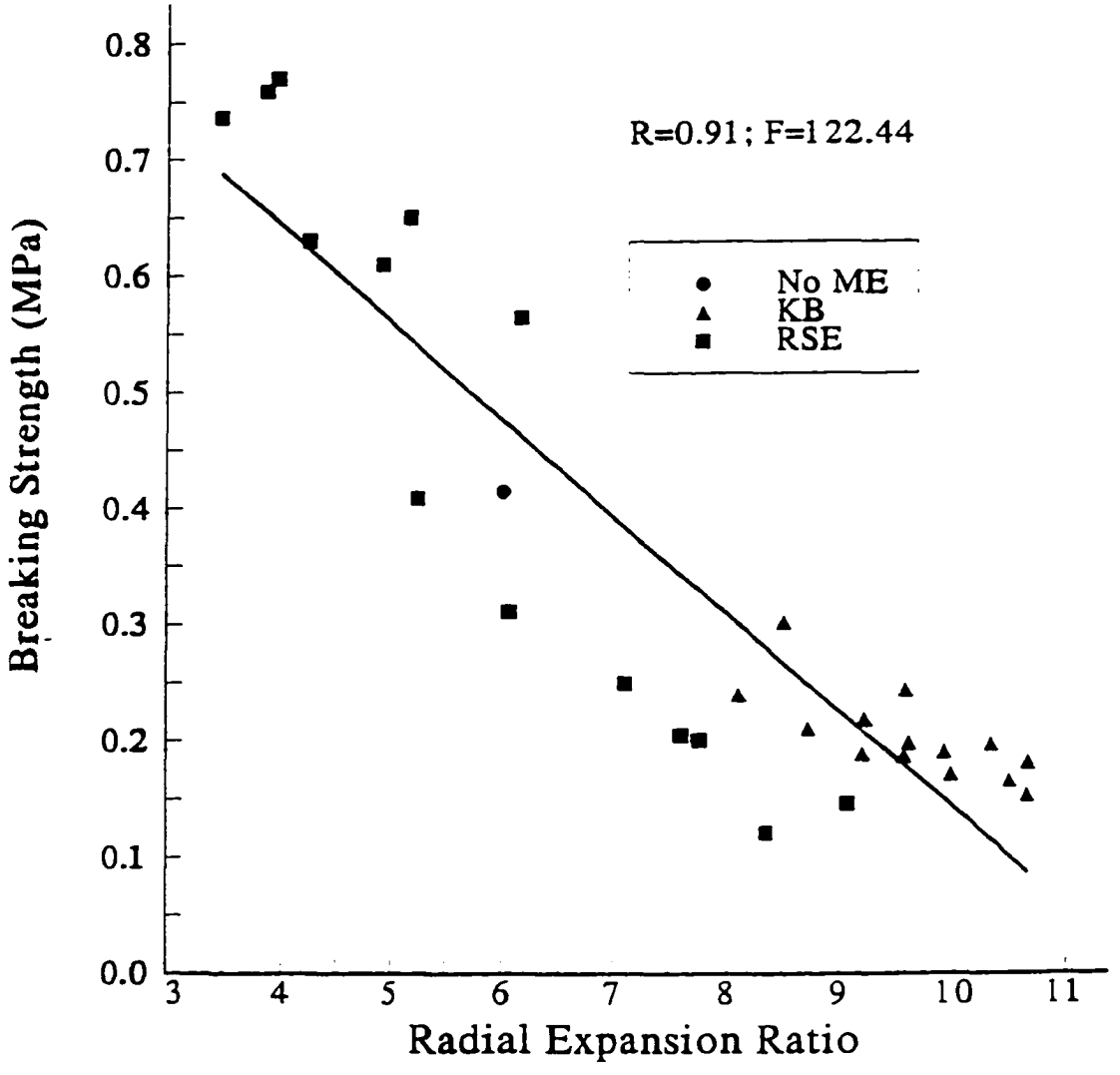

Figure 4.42 Relationship between breaking strength and radial expansion ratio of rice flour extrudates. (No ME: No mixing element in the screw profile; KB: Kneading block; RSE: reverse screw element).

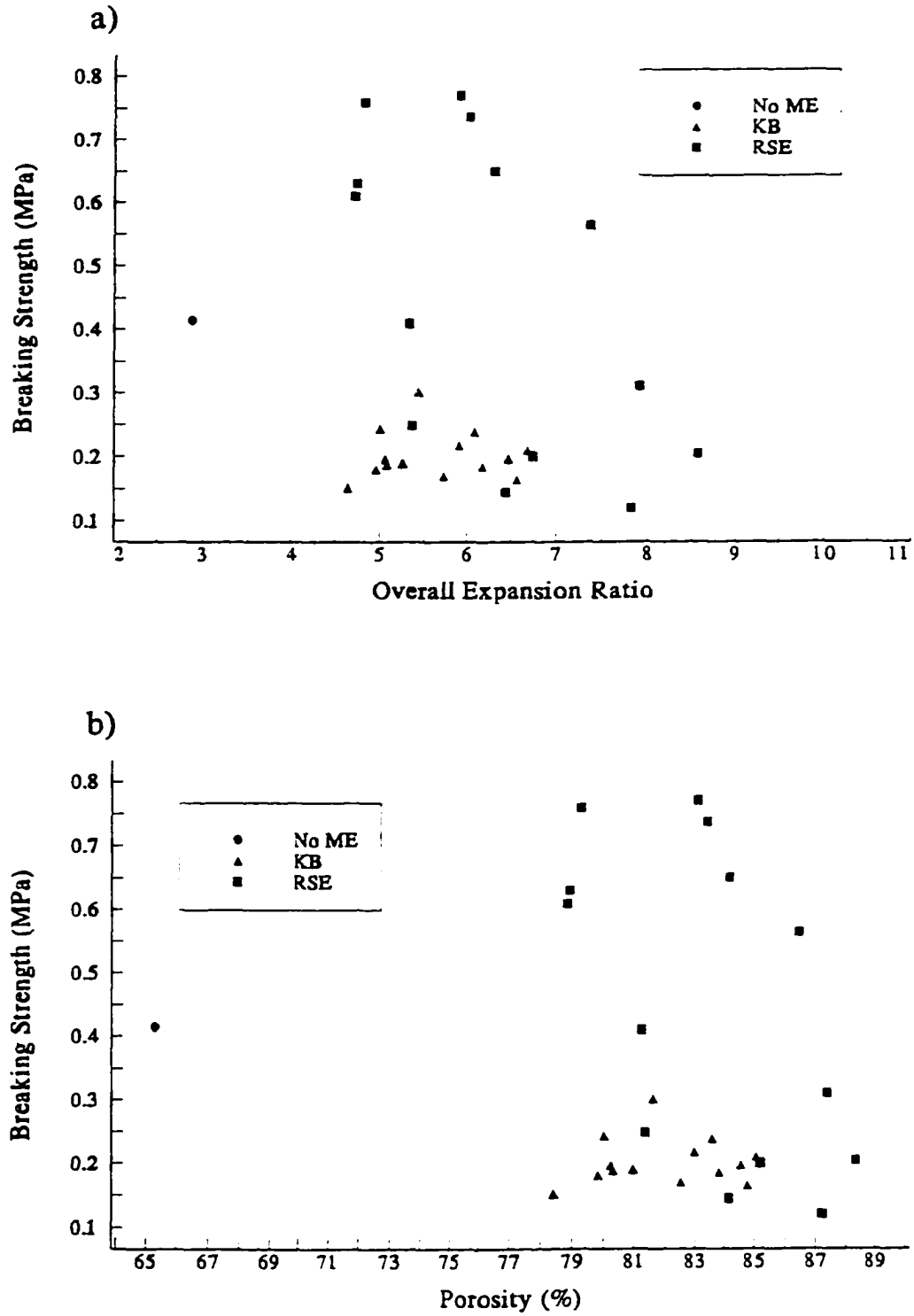

Figure 4.43 Influence of mixing elements on (a) breaking strength and overall expansion (b) breaking strength and porosity of rice flour extrudates.

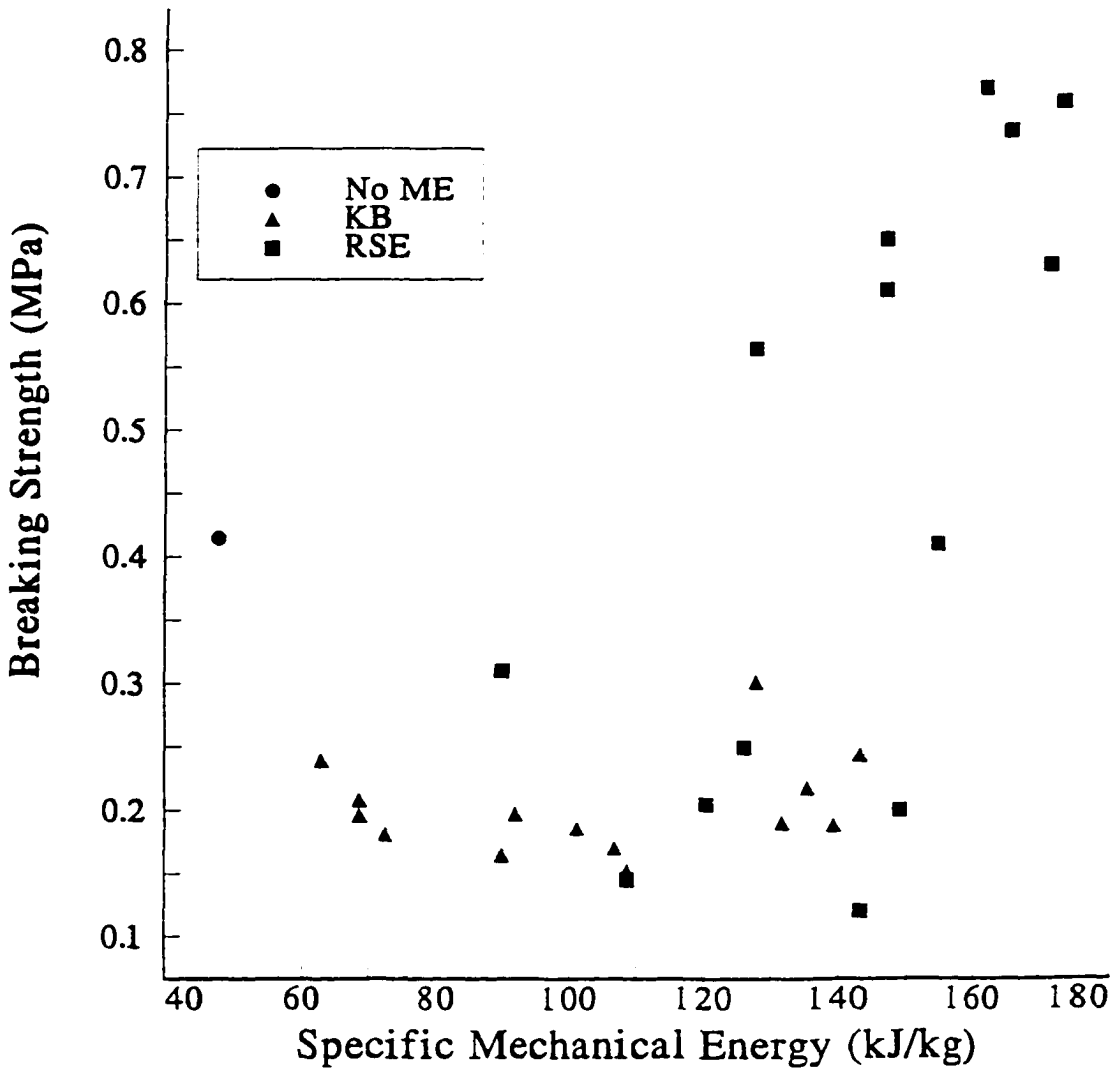

Figure 4.44 Influence of mixing elements on breaking strength and specific mechanical energy for rice flour extrudate.

4.3 EXTRUSION OF ARROWTOOTH FLOUNDER MUSCLE AND RICE FLOUR BLENDS

High molecular weight proteins in arrowtooth flounder mince were autolyzed for blending with rice flour. Autolysis led to an increase in low molecular weight peptides (Fig. 4.45). Actin appeared to be unaffected by hydrolysis. The gel electrophoresis showed that a 5 minute hydrolysis of arrowtooth flounder mince was sufficient to hydrolyse myosin. There was not a major difference between 5, 10, and 15 minutes of hydrolysis. Proteins with molecular weights less than 19,000 daltons were produced. Figure 4.45 also showed that the original mince and unhydrolysed mince were similar. The proximate and molecular composition of arrowtooth flounder mince (unhydrolysed and hydrolysed) and rice flour blends were different.

Starch and proteins behave remarkably different during extrusion processing. Starch undergoes molecular modification during extrusion and forms an expanded matrix (Choudhury and Gautam, 1998a). However, addition of proteins to starch-rich flours results in extrudates with poor expansion, low water solubility, and hard texture (Gogoi *et al.*, 1996 a and b; Gautam *et al.*, 1997; Choudhury *et al.*, 1998). It is generally believed that proteins behave as fillers in the expanded matrix provided by starch and do not transform into a melt phase during extrusion (Mohamed, 1990; Areas, 1992).

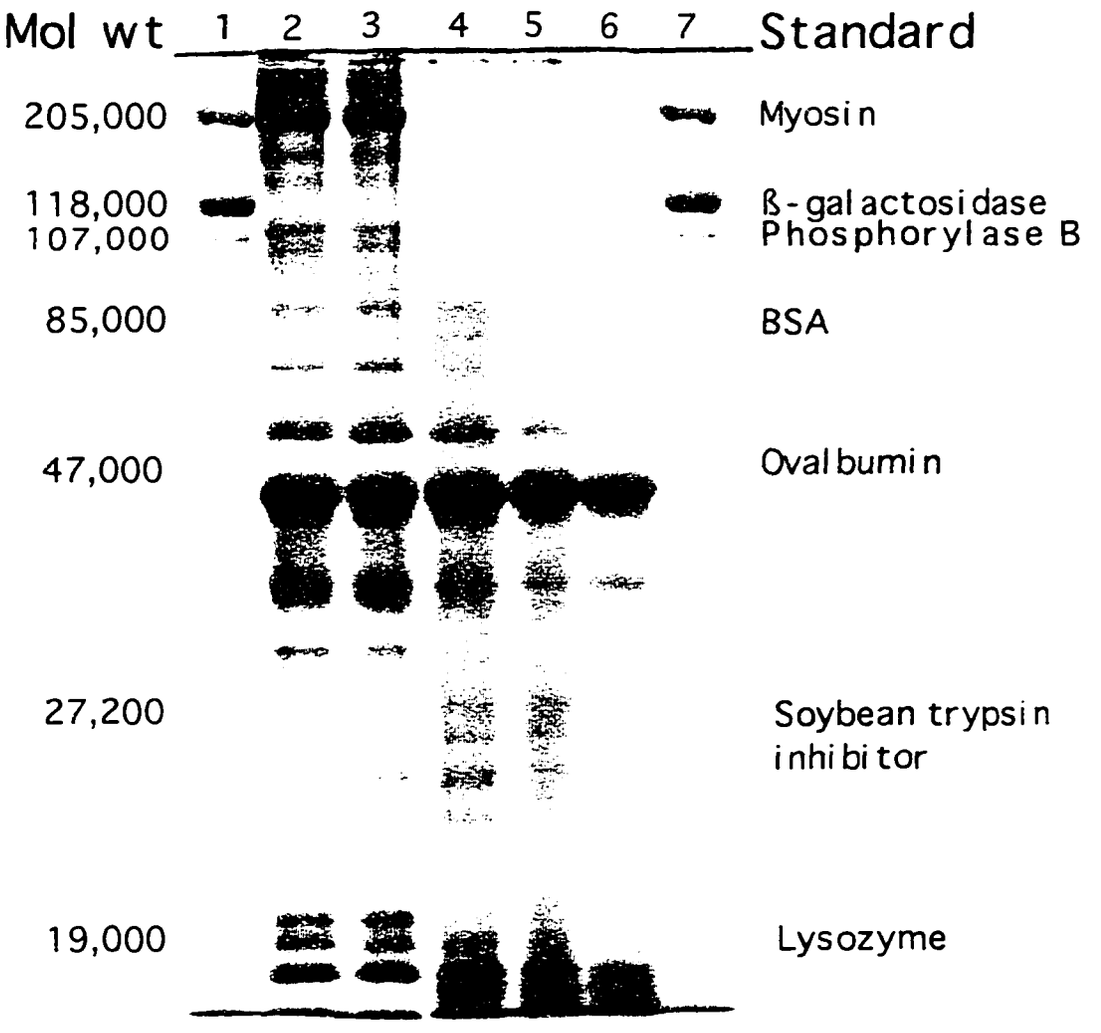

Figure 4.45 Time dependant autolysis of arrowtooth flounder muscle.
Lane 1 = broad m.w. standard; Lane 2 = arrowtooth mince;
Lane 3 = 0 minute hydrolysis; Lane 4 = 5 minute hydrolysis;
Lane 5 = 10 minute hydrolysis; Lane 6 = 15 minute hydrolysis;
Lane 7 = broad m.w. standard.

4.3.1 Effect of hydrolysis time and fish solids on energy consumption and system parameters

Feed composition, one of the independent process variables during extrusion, has a striking effect on extrudate characteristics (Fig. 1.1). It affects viscosity, thermal and other physical properties of the material thus influencing the energy input and system parameters.

4.3.1.1 Energy consumption

Both mechanical and thermal energies were affected by feed composition.

Specific mechanical energy: Hydrolysis time and fish solids content affected the SME input significantly (Table 4.14). However, comparison of means for 5, 10, and 15 minutes of hydrolysis at the same fish solids content showed that the means were not different. For example, the SME input with 10% fish solids in the blend was essentially the same (about 76 kJ/kg) for 5, 10, and 15 minutes hydrolysis. But, SME input with 10% unhydrolysed fish solid was a little less (66 kJ/kg). The value of SME input during extrusion of rice flour was 112.5 kJ/kg. Addition of both unhydrolysed and hydrolysed fish solids lowered the SME input systematically (Fig 4.46). The results are in complete agreement with the previous studies carried out in our laboratory (Gogoi *et al.*, 1996 a and b; Gautam *et al.*, 1997; Choudhury *et al.*, 1998). SME input was shown to decrease systematically upon addition of pink salmon fish solids to rice flour.

Table 4.14 Analysis of variance data for energy input during extrusion of rice flour and its blends with arrowtooth flounder muscle.

Source	DF	Mean Sum of Squares (MSS) and F-values for Energy Input (kJ/s)					
		Specific Mechanical Energy		Specific Thermal Energy		Total Energy	
		MSS	F	MSS	F	MSS	F
Hyd. time (HT)	3	125.23	20.81**	6738.43	76.41**	5069.19	50.53**
Fish solids (FS)	2	500.24	83.14**	9278.30	105.21**	5473.35	54.56**
HT X FS	6	14.43	2.40	885.46	10.04*	694.16	6.92*
Error	12	6.02	-	88.18	-	100.32	-

**Highly significant at $p \leq 0.005$

*Significant at $p \leq 0.05$

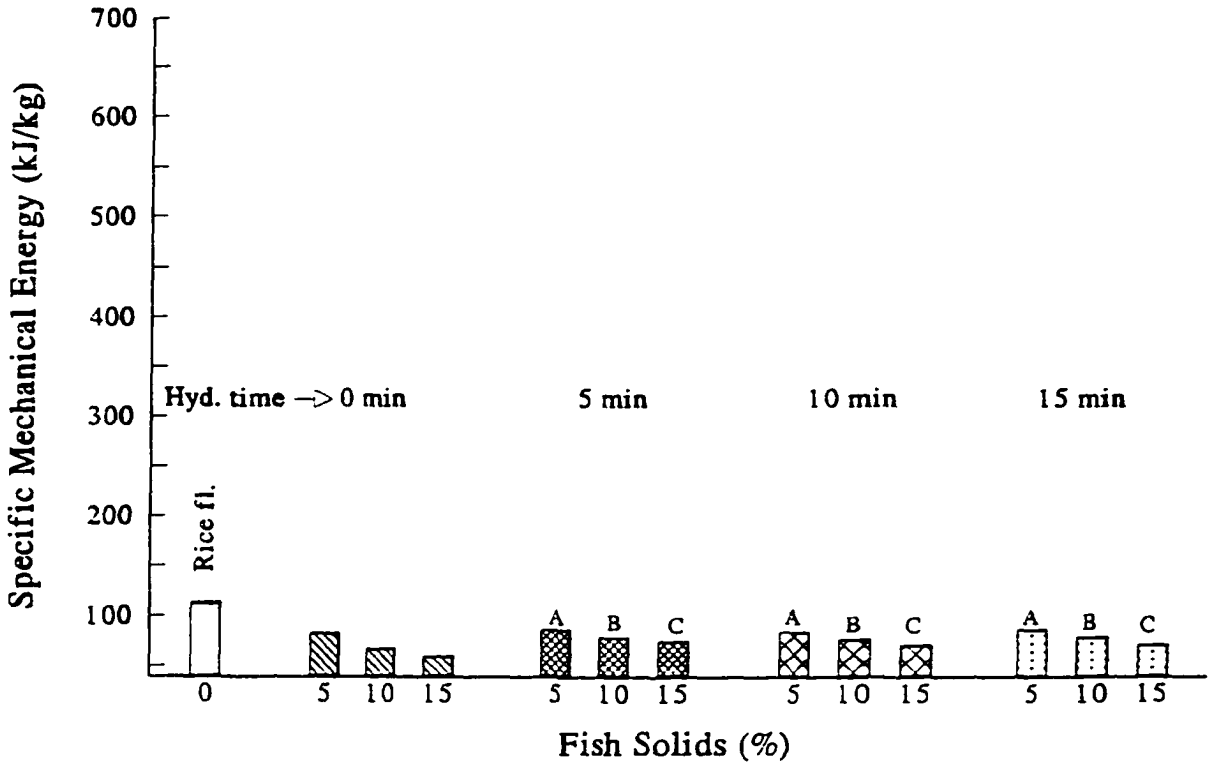

Figure 4.46 Effect of hydrolysis time and fish solids content on specific mechanical energy during extrusion of arrowtooth flounder muscle and rice flour blends. Means with same letters are not significantly different.

Both arrowtooth flounder muscle and rice flour contain lipids (Table 3.1). The amounts in arrowtooth flounder muscle and rice flour are approximately 17% (dry basis) and 0.066% (dry basis), respectively. Because of lubricating effects of oil in the fish solids and its effect on viscosity of blends, a decreasing trend in SME input with addition of fish solids to rice flour for each degree of hydrolysis was observed. Our results also agreed with the study of Grenus *et al.*, (1992) who observed decreasing SME values with addition of rice bran (fat content 20.9%) to rice flour.

Addition of hydrolysed fish solids produced slightly higher SME input compared to that of unhydrolysed solids. Hydrolysis of arrowtooth flounder muscle produced smaller peptides (Fig. 4.45). The low molecular weight proteins might have caused compaction during extrusion leading to higher SME input.

Specific thermal energy (STE): The effects of hydrolysis time and fish solids content on STE showed an opposite trend to that of SME input (Fig. 4.47). It increased systematically on addition of fish solids to rice flour. The STE value was about 400 kJ/kg during extrusion of rice flour alone. It increased to 600 kJ/kg on addition of 15% unhydrolysed fish solids. Table 4.14 shows that hydrolysis time and fish solid content affected the STE input significantly. However, 5, 10, and 15 minutes of hydrolysis had no effect on the STE input as shown by comparison of means (Fig. 4.47). For example, addition of 10% hydrolysed fish solids invariably produced about 470 kJ/kg of STE input for 5, 10, and 15 minutes of hydrolysis time.

Lower SME input causes a reduction in the material temperature. In this case

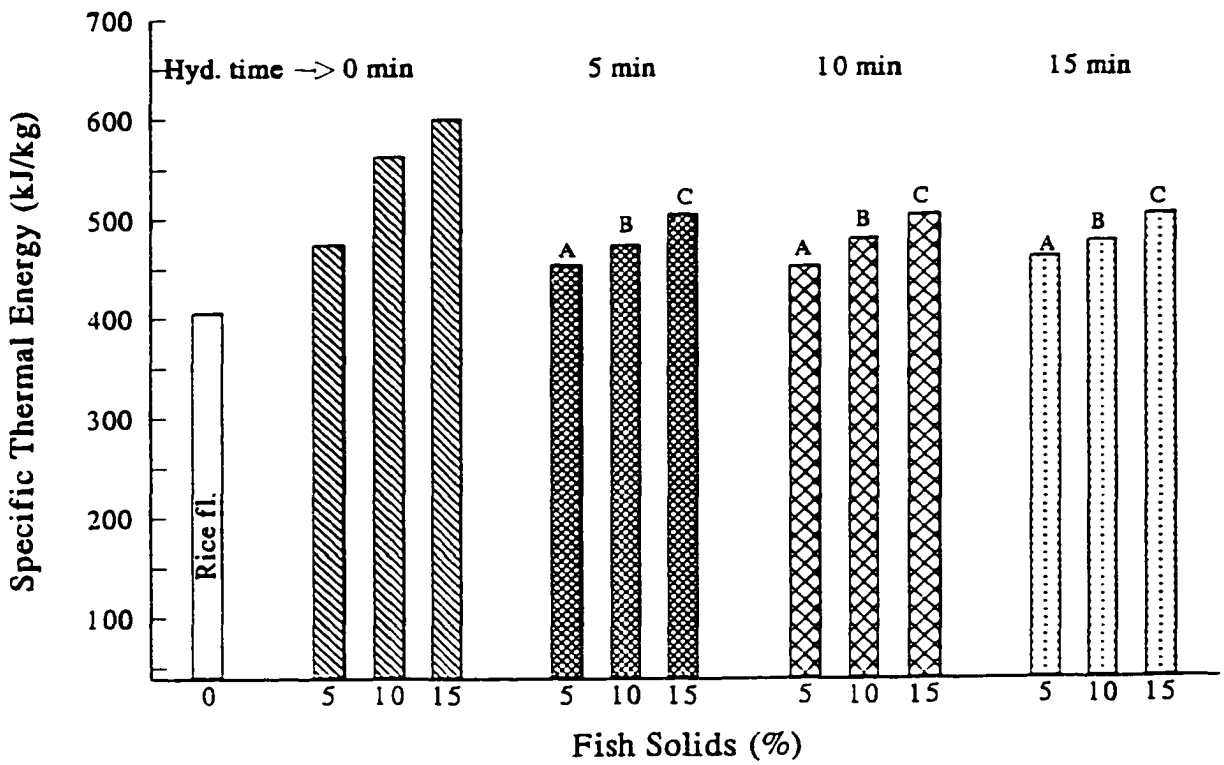

Figure 4.47 Effect of hydrolysis time and fish solids content on specific thermal energy during extrusion of arrowtooth flounder muscle and rice flour blends. Means with same letters are not significantly different.

there was higher demand for thermal energy to raise the temperature to the set barrel temperature values. Hence, the electrical heaters mounted on the extruder drew more current leading to higher thermal energy input.

Total specific energy: Total specific energy exhibited a similar trend to that of STE (Fig. 4.48). It increased upon addition of fish solids to the rice flour. Although the effects of hydrolysis time, fish solids, and their interactions on the total energy input was significant (Table 4.14), the total specific energies for 5, 10, and 15 minutes of hydrolysis at same fish solid content were essentially the same. Higher total energy input was observed by addition of unhydrolysed fish solids.

The magnitude of SME input was always less compared to STE input. When SME and STE input were added, the later dominated and thus total specific energy followed the trend of specific thermal energy.

4.3.1.2 System parameters

Die temperature, % torque and power meter readings were recorded from the control panel. The % torques and power meter readings were used to calculate the specific mechanical and thermal energies.

Table 4.15 indicates that the hydrolysis time (including 0 min), fish solids content and their interaction affected the die temperature significantly. However, comparison of means showed that the die temperatures obtained during extrusion of hydrolysed fish (5, 10, and 15 minutes) and rice flour blends were the same (for a

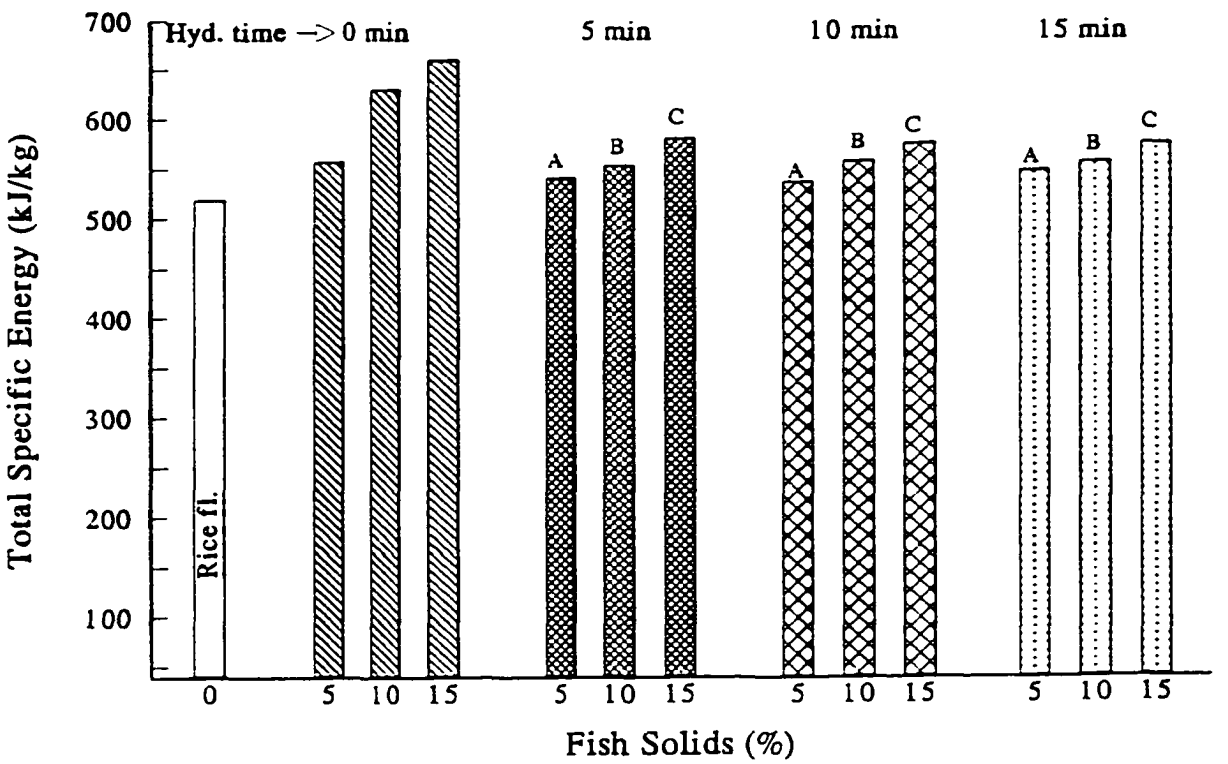

Figure 4.48 Effect of hydrolysis time and fish solids content on total specific energy during extrusion of arrowtooth flounder muscle and rice flour blends. Means with same letters are not significantly different.

Table 4.15 Analysis of variance data for die temperature during extrusion of rice flour and its blends with arrowtooth flounder muscle.

Source	DF	Mean Sum of Squares (MSS) and F-values for Die Temperature (°C)	
		MSS	F
Hyd. time (HT)	3	91.00	364.00**
Fish solids (FS)	2	6.50	26.00**
HT X FS	6	6.17	24.67**
Error	12	0.25	-

**Highly significant at $p \leq 0.005$

*Significant at $p \leq 0.05$

particular fish solids content). For example, 10% fish solids in the blends produced die temperature of about 138°C, irrespective of hydrolysis time (Table 4.16). This indicated that the difference in die temperature was a result of autolysis and not due to different levels of hydrolysis, i.e., the length of hydrolysis time. The effects were different for unhydrolysed (0 minute) and hydrolysed fish solids. The die temperature for rice flour extrudate was 134°C. It decreased systematically upon addition of unhydrolysed fish solids in the blends (Table 4.16).

Feed material in an extruder is heated by both viscous heat dissipation (friction) and thermal energy. Our results agree with the findings of Grenus *et al.* (1992) who studied the extrusion of rice flour and its blends with rice bran. Rice bran had a higher protein content (15.8%) compared to rice flour (7.8%). Decrease in die temperature with increasing % rice bran in the feed was reported. In the present study, increasing unhydrolysed fish protein content in feed, decreased the die temperature. It has been shown that decreasing the specific mechanical energy input lowers the die temperature (Della Valle *et al.*, 1987; Guy and Horne, 1988; Grenus *et al.*, 1992). In the present study also decreasing trend of SME input by increasing the unhydrolysed fish protein content was observed (section 4.3.1.1).

When hydrolysed fish solids were added to rice flour the die temperature increased. The value was maximum (140.5°C) for 15% hydrolysed fish solids. This increase in the product temperature due to addition of hydrolysed fish solids (Table 4.16) appeared to be due to changes in thermal properties.

Table 4.16 Effects of hydrolysis time and fish solids content on die temperature during extrusion of rice flour and its blends with arrowtooth flounder muscle.

Arrowtooth Flounder Solids Concentration (%)	Die temperature (°C) during extrusion of blends of rice flour and arrowtooth flounder solids hydrolysed for			
	0 min	5 min	10 min	15 min
5	132.5 ± 0.71	136.5 ± 1.41^{A}	137.0 ± 0.00^{A}	137.0 ± 0.00^{A}
10	130.5 ± 0.71	138.0 ± 0.00^{B}	138.5 ± 0.71^{B}	138.0 ± 0.00^{B}
15	129.0 ± 0.00	140.0 ± 0.00^{C}	140.5 ± 0.71^{C}	140.5 ± 0.71^{C}

Die temperature for rice flour = 134 ± 0.00 (°C)

Means with same letters are not significantly different

Upon hydrolysis, the proteins undergo molecular changes resulting in the production of smaller peptides. This might have changed the thermal properties of hydrolysed fish solids and thus, an increase in die temperature was noticed during extrusion of rice flour and hydrolysed fish muscle blends.

4.3.2 Effect of hydrolysis time and fish solids content on mean residence time and mixing index

Both hydrolysis time and fish solids content affected the mean residence time significantly (Table 4.17). However, the effect of hydrolysis (excluding 0 min) was insignificant as shown by the comparison of means. The mean residence time during extrusion of rice flour was 46.00 s. It increased when unhydrolysed and hydrolysed proteins were added (Table 4.18). As shown in Table 3.1, arrowtooth muscle has a significant amount of lipids (17%, dry basis). Addition of lipids produced a lubricating effect, lowering the viscosity of the feed material (section 4.3.1.1). Our findings agree with the results of Altomare and Ghossi (1986) and Lin and Armstrong (1990) who showed that decreased viscosity caused an increase in residence time of the material in the extruder. Increasing the moisture content from 10.0% to 28.4% have been shown to lower the viscosity of the material and thus longer mean residence time was observed (Altomare and Ghossi, 1986). Lin and Armstrong (1990) showed that decreasing the feed moisture from 30 to 20% in a Brabender DSE35 twin-screw extruder increased viscosity and therefore, decreased

Table 4.17 Analysis of variance data for mean residence time and Peclet number (mixing index) during extrusion of arrowtooth flounder muscle and rice flour blends.

Source	DF	Mean Sum of Squares (MSS) and F-values for			
		Mean Residence Time (s)		Peclet Number	
		MSS	F	MSS	F
Hyd. time (HT)	3	1.04	19.62**	0.02380	11.22*
Fish solids (FS)	2	8.57	162.16**	1.56605	738.41**
HT X FS	6	0.02	0.30	0.00318	1.50
Error	12	0.06	-	0.00212	-

**Highly significant at $p \leq 0.005$

*Significant at $p \leq 0.05$

Table 4.18 Effect of hydrolysis time and fish solids content on mean residence time during extrusion of arrowtooth flounder muscle and rice flour blends.

Arrowtooth Flounder Solids Concentration (%)	Mean residence time (s) during extrusion of blends of rice flour and arrowtooth flounder solids hydrolysed for			
	0 min	5 min	10 min	15 min
5	47.20 ± 0.10	47.69 ± 0.25^{A}	47.84 ± 0.25^{A}	47.64 ± 0.01^{A}
10	48.14 ± 0.14	48.49 ± 0.11^{B}	48.35 ± 0.28^{B}	48.55 ± 0.14^{B}
15	49.50 ± 0.69	50.30 ± 0.11^{C}	50.30 ± 0.18^{C}	50.35 ± 0.10^{C}

Mean residence time for rice flour = 45.99 ± 0.13 (s)

Means with same letters are not significantly different.

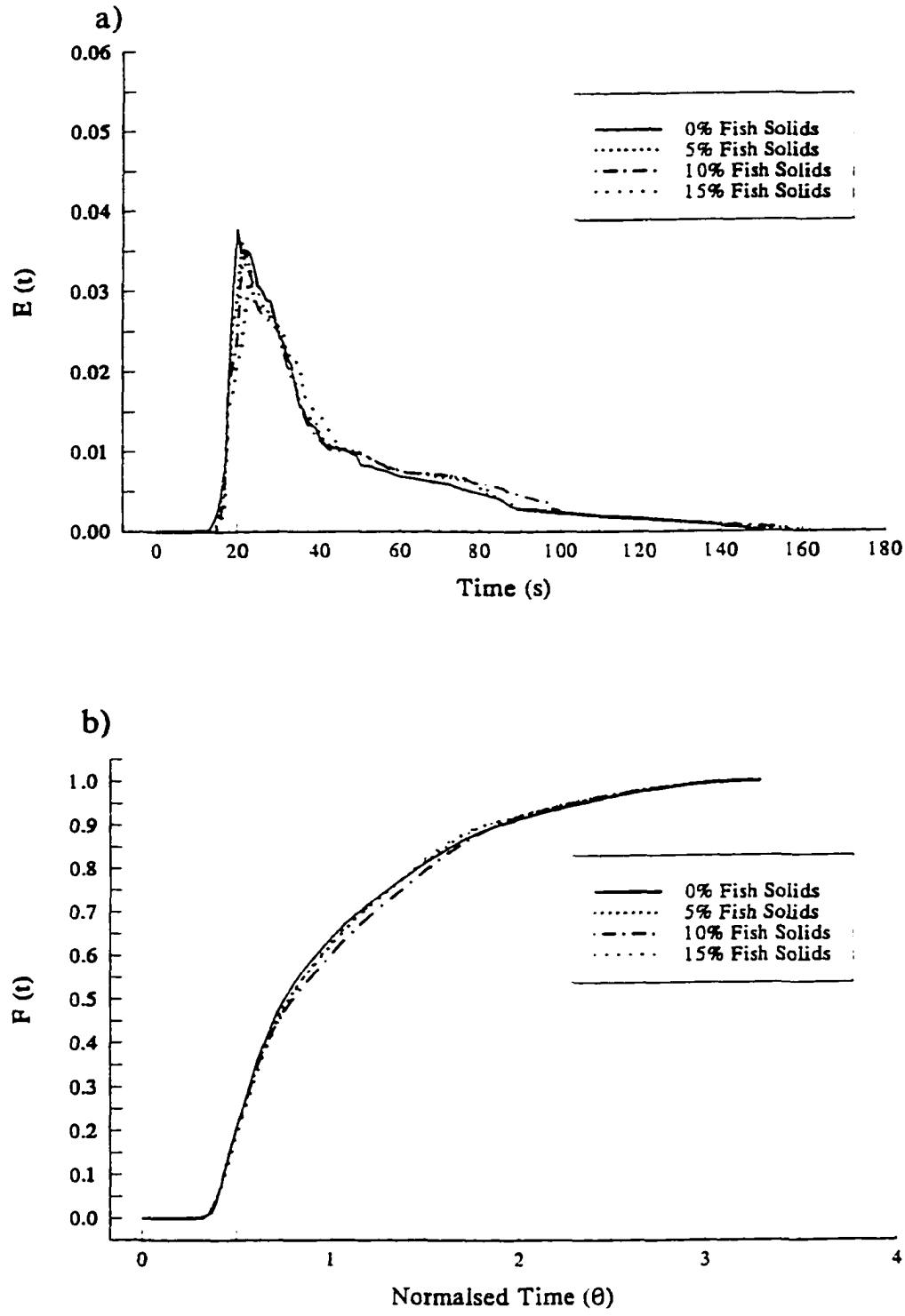

Figure 4.49 Effect of fish solids content on (a) age distribution and (b) cumulative age distribution curves.

the mean residence time from45.3 to 31.7 s.

Addition of fish solids to rice flour had a little affect on the shapes of residence time distribution or E(t) curves (Fig. 4.49a). In all cases, the long tail extended beyond 150 s. The peak of the E(t) curve decreased from 0.038 to 0.035 and shifted towards the right. Similarly, the cumulative function F(t) was almost the same for rice flour and its blends (Fig. 4.49b). As the specific mechanical energy input decreased upon addition of fish solids, the mean residence time increased (Fig. 4.50). Lower SME input and higher mean residence times were observed due to decreased viscosity upon addition of fish solids.

The Peclet number, an index of mixing, calculated from the spread of age distribution curves is given in Table 4.19. Addition of fish solids caused a lubricating effect thus leading to more slippage rather than positive conveyance of the material. This is reflected in higher Peclet number due to addition of fish solids, which is an indication of less mixing (Table 4.19).

4.3.3 Feed composition effects on macroscopic properties of extrudates obtained from blends of arrowtooth flounder and rice flour

Feed composition, an independent process variable affects the energy input and residence time distribution during extrusion of starchy and proteinaceous materials. The type and magnitude of energy input and residence time distribution of the material influences the macroscopic attributes of the extrudate.

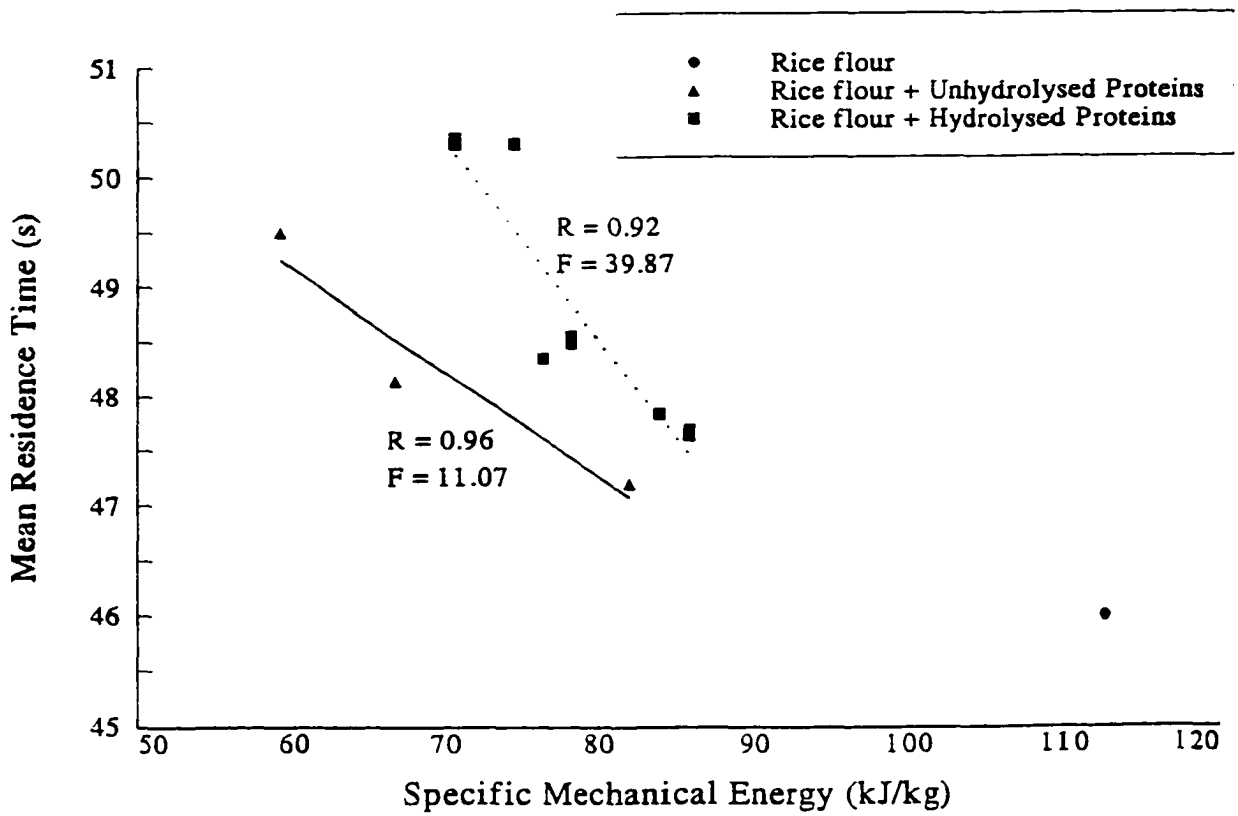

Figure 4.50 Relationship between mean residence time and specific mechanical energy during extrusion of arrowtooth flounder muscle and rice flour blends.

Table 4.19 Effect of hydrolysis time and fish solids content on Peclet number (mixing index) during extrusion of arrowtooth flounder muscle and rice flour blends.

Arrowtooth Flounder Solids Concentration (%)	Peclet Number (mixing index) during extrusion of blends of rice flour and arrowtooth flounder muscle hydrolysed for			
	0 min	5 min	10 min	15 min
5	4.53 ± 0.04^{A}	4.37 ± 0.02^{A}	4.38 ± 0.07^{A}	4.40 ± 0.05^{A}
10	4.87 ± 0.05^{B}	4.78 ± 0.01^{B}	4.76 ± 0.01^{B}	4.81 ± 0.06^{B}
15	5.37 ± 0.02^{C}	5.19 ± 0.01^{C}	5.28 ± 0.10^{C}	5.37 ± 0.02^{C}

Peclet Number for rice flour = 3.99 ± 0.01

Means with same letters are not significantly different.

4.3.3.1 Densities

Starch and proteins have different physical properties, and therefore the mixture affects the densities of the product.

Apparent density: Hydrolysis time, fish solids content, and their interactions affected the AD significantly (Table 4.20). But, AD for 5, 10, and 15 minutes hydrolysis at a particular protein concentration were essentially the same as shown by comparison of means. Unhydrolysed and hydrolysed fish solids affected the apparent density differently (Fig. 4.51). An apparent density of about 300 kg/m^3 was obtained with rice flour extrudate. Addition of unhydrolysed fish solids, increased the AD (Fig. 4.51) and decreased the die temperature (Table 4.16). These results are in agreement with the data of Bhattacharya and Hanna (1987); Grenus *et al.* (1992); Bhattacharya and Choudhury (1994), who showed that higher die temperature leads to a lower apparent density.

Raising the hydrolysed fish solids content, lowered the apparent density systematically (Fig. 4.51) and increased the die temperature (Table 4.16). A good correlation between apparent density and die temperature was observed (Fig. 4.52). Increasing the unhydrolysed fish solids from 0 to 15% decreased the die temperature from 134 to 129°C and increased the apparent density from 300 to 363 kg/m^3. Interestingly, addition of hydrolysed fish solids produced extrudates with AD lower than that of rice flour. Raising the hydrolysed fish solids content from 0 to 15% increased the die temperature to 140.5°C and thus decreased the AD from 300 to

Table 4.20 Analysis of variance data for densities of extrudates obtained from arrowtooth flounder muscle and rice flour blends.

Source	DF	Mean Sum of Squares (MSS) and F-values for Density (kg/m^3)			
		Apparent Density		True Density	
		MSS	F	MSS	F
Hyd. time (HT)	3	34429.88	612.75**	476.37	0.58
Fish Solids (FS)	2	653.58	11.63*	20714.58	25.31**
HT x FS	6	738.38	13.14**	146.85	0.18
Error	12	56.19	-	818.59	-

**Highly significant at $p \leq 0.005$

*Significant at $p \leq 0.05$

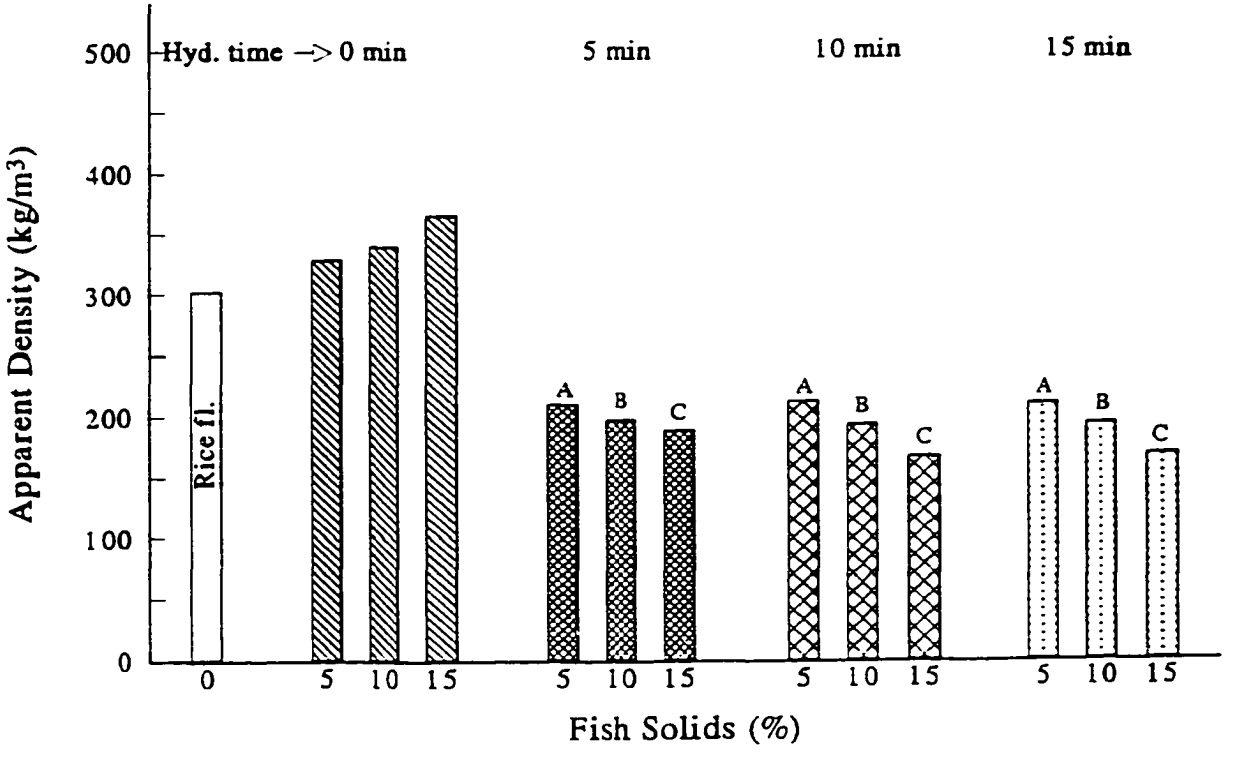

Figure 4.51 Effects of hydrolysis time and fish solids content on apparent density of extrudates obtained from arrowtooth flounder muscle and rice flour blends. Means with same letters are not significantly different.

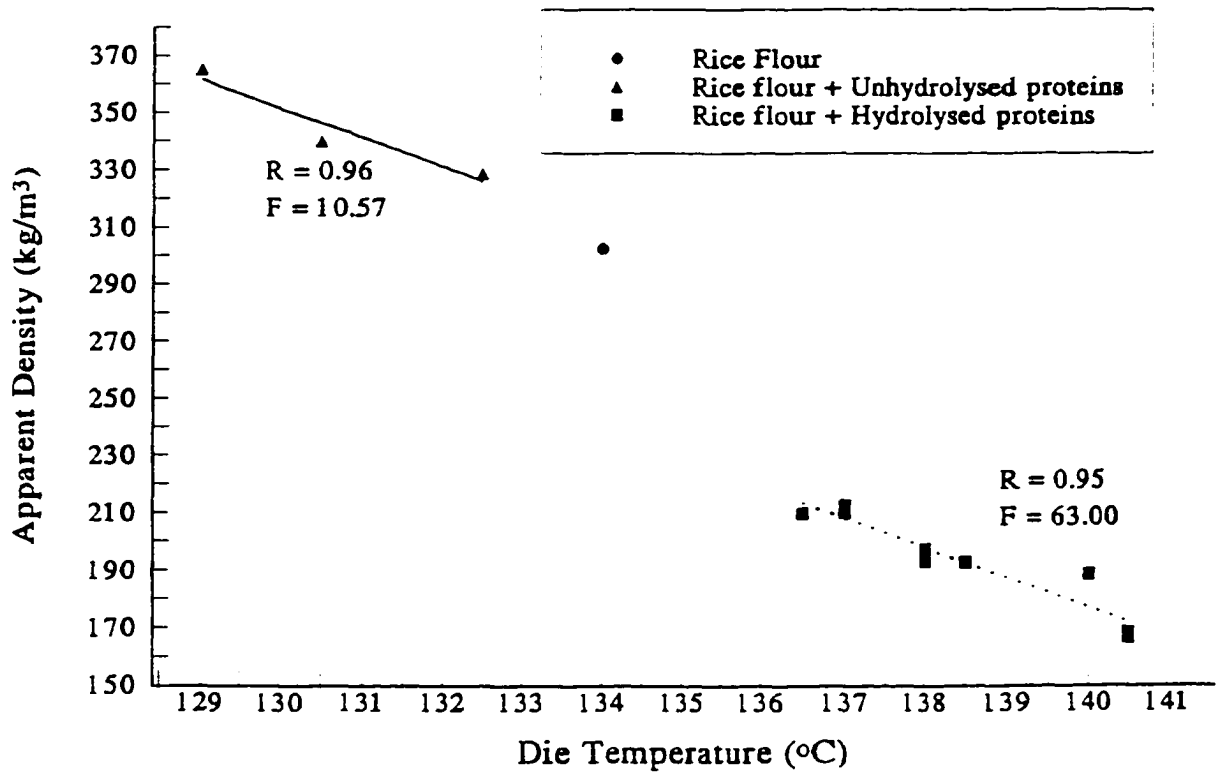

Figure 4.52 Relationship between apparent density and die temperature during extrusion of arrowtooth flounder muscle and rice flour blends.

170kg/m^3 (Fig. 4.52).

True density: Addition of fish solids to rice flour had a significant effect on true density (Table 4.20), which increased systematically with increasing fish solids concentration (Table 4.21). True densities at different hydrolysis times for same fish solids content were not significantly different as shown by comparison of means.

4.3.3.2 Expansion ratios

Feed composition plays an important role during extrusion of starchy and proteinaceous material. Generally, the expanded matrix is provided by starch, and proteins have a detrimental effect on extrudate expansion.

Radial expansion ratio: The statistical significance of feed composition effect on radial expansion was due to fish solids concentration and autolysis (Table 4.22). The hydrolysis time seemed to have no effect for a particular fish protein concentration, as shown by comparison of means. The rice flour extrudate had a radial expansion of 11.80. Upon addition of unhydrolysed fish solids, the expansion reduced systematically (Fig. 4.53). A blend of 15% fish solids (unhydrolysed) and 85% rice flour had a radial expansion ratio of about 9.00. The results agree with our previous findings with pink salmon muscle. Increasing the amount of pink salmon solids in blends with rice flour reduced the expansion considerably (Gogoi, *et al.* 1996 a and b; Gautam *et al.*, 1997; Choudhury *et al.*, 1998). Similar reduction in expansion was observed when the amount of soy protein and wheat gluten was increased during

Table 4.21 Effects of hydrolysis time and fish solids content on true density of extrudates obtained from blends of arrowtooth flounder muscle and rice flour.

Arrowtooth Flounder Solids Concentration (%)	True density (kg/m^3) during extrusion of blends of rice flour and arrowtooth flounder muscle hydrolysed for			
	0 min	5 min	10 min	15 min
5	1444.85 ± 32.22^{A}	1416.46 ± 20.41^{A}	1415.14 ± 25.60^{A}	1433.44 ± 10.16^{A}
10	1490.00 ± 28.28^{B}	1486.24 ± 24.49^{B}	1486.66 ± 59.44^{B}	1485.26 ± 29.61^{B}
15	1547.24 ± 12.09^{C}	1529.53 ± 24.14^{C}	1519.62 ± 15.90^{C}	1518.47 ± 28.61^{C}

True density for rice flour = 1454.70 ± 30.47

Means with same letters are not significantly different

Table 4.22 Analysis of variance data for expansion ratios of extrudates obtained from blends of arrowtooth flounder muscle and rice flour.

Source	DF	Mean Sum of Squares (MSS) and F-values for Expansion Ratios					
		Radial Expansion Ratio		Overall Expansion Ratio		Axial Expansion Ratio	
		MSS	F	MSS	F	MSS	F
Hyd. time (HT)	3	32.52	122.23**	17.37	400.56**	0.0178	15.49**
Fish Solids (FS)	2	4.37	16.42**	4.31	99.53**	0.0336	29.15**
HT x FS	6	0.54	2.00	0.72	16.57**	0.0061	5.30
Error	12	0.27	-	0.04	-	0.0012	-

**Highly significant at $p \leq 0.005$

*Significant at $p \leq 0.05$

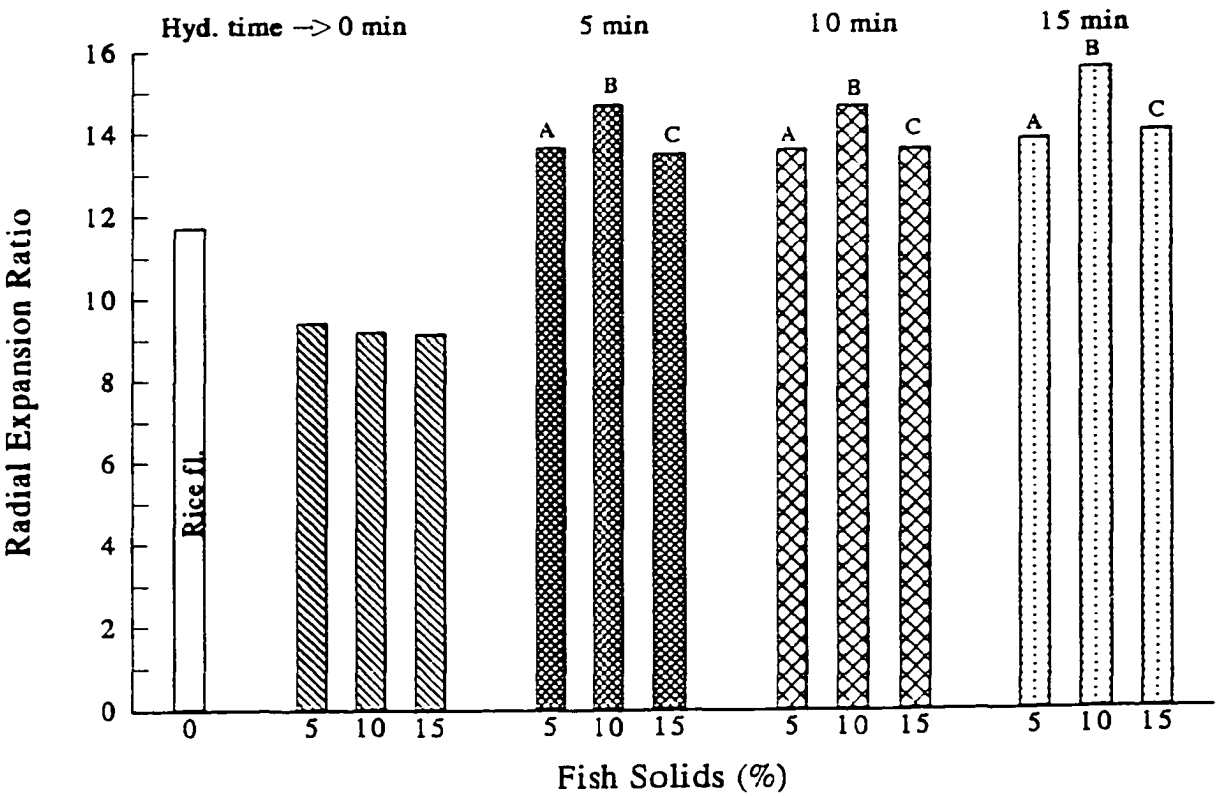

Figure 4.53 Effects of hydrolysis time and fish solids content on radial expansion of extrudates obtained from arrowtooth flounder muscle and rice flour blends. Means with same letters are not significantly different.

extrusion of corn starch (Mohamed, 1990) and wheat starch (Faubion and Hoseney, 1982), respectively. Reduced expansion was also observed with increasing lipid content (Faubion and Hoseney, 1982; Bhattacharya and Hanna, 1987). The lipid as well as protein content increased with the addition of arrowtooth muscle in the feed.

Hydrolysed arrowtooth flounder muscle was found to enhance the expansion characteristics of rice flour (Fig 4.53). The highest expansion (> 14.25) of the product was noticed at 10% fish solid level for the three hydrolysis times (5, 10, and 15 min) studied. This interesting result was postulated by Choudhury (1994). Further studies will be needed to explain this functional property of hydrolysed arrowtooth flounder muscle.

Axial expansion ratio: Effect of hydrolysis time and fish solids content on the axial expansion ratio is depicted in Fig. 4.54. The pattern was opposite to that of radial expansion. The effect of hydrolysis time and fish solids content was significant (Table 4.22).

Overall expansion ratio: The trend of overall expansion ratio with hydrolysis time and fish solids was exactly opposite to that of apparent density. Hydrolysis time (including 0 min), fish solids content, and their interactions affected the overall expansion ratio significantly (Table 4.22). An overall expansion ratio of 4.8 was obtained for rice flour extrudate. This ratio was different upon addition of unhydrolysed and hydrolysed fish solids (Fig. 4.55). It decreased systematically with

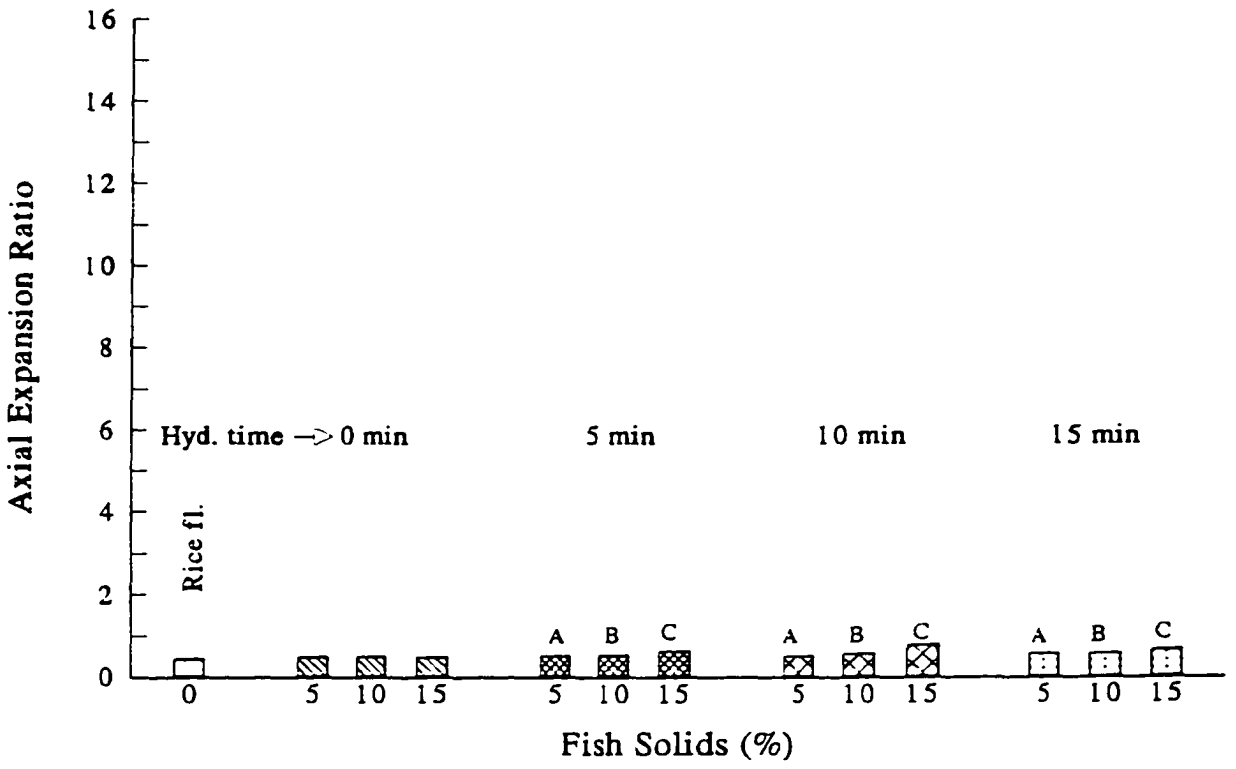

Figure 4.54 Effects of hydrolysis time and fish solids content on axial expansion of extrudates obtained from arrowtooth flounder muscle and rice flour blends. Means with same letters are not significantly different.

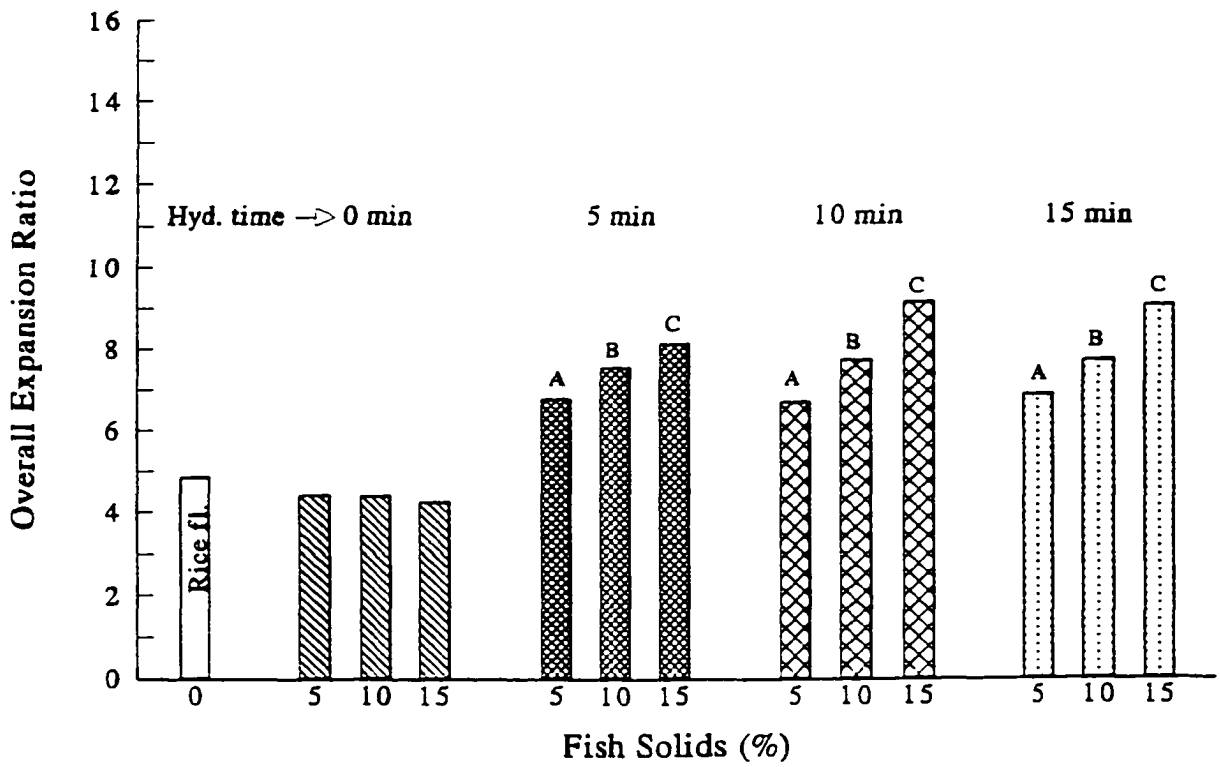

Figure 4.55 Effects of hydrolysis time and fish solids content on overall expansion of extrudates obtained from arrowtooth flounder muscle and rice flour blends. Means with same letters are not significantly different.

increasing concentration of unhydrolysed fish solids. According to Yacu (1995), overall expansion is a function of die temperature. Low die temperature results in less flashing and thus extrudates have poor overall expansion. Table 4.16 shows that increasing the unhydrolysed fish solids content in the feed resulted in a systematic decrease in die temperature. As a result, overall expansion decreased systematically.

However, as the hydrolysed fish solids content was raised in the blends, both overall expansion and die temperature increased (Fig. 4.55 and Table 4.16). Highest overall expansion (> 9.0) was obtained at 15 % fish solids for the three degree of hydrolysis.

The material temperature just before the die exit and overall expansion correlated well as shown in Fig. 4.56a. The die temperature and overall expansion decreased from 134 to 129°C and 4.8 to 4.2, respectively, upon increasing the unhydrolysed fish solids from 0 to 15%. On the other hand, raising the level of hydrolysed fish solids to 15% increased the die temperature to 140.5°C. Overall expansion also increased to 9.0. This desirable trend was a departure from the normal behavior of proteins during extrusion and needs further investigation. A negative correlation between apparent density and overall expansion was observed (Fig. 4.56b). Increasing the unhydrolysed fish solids (0-15%), increased the AD (300 to 365 kg/m^3), but decreased the overall expansion (4.8-4.2). Interestingly, an opposite trend was noticed with higher levels of hydrolysed fish solids. The AD decreased from 300 to 170 kg/m^3, and OER increased from 4.8 to 9.0.

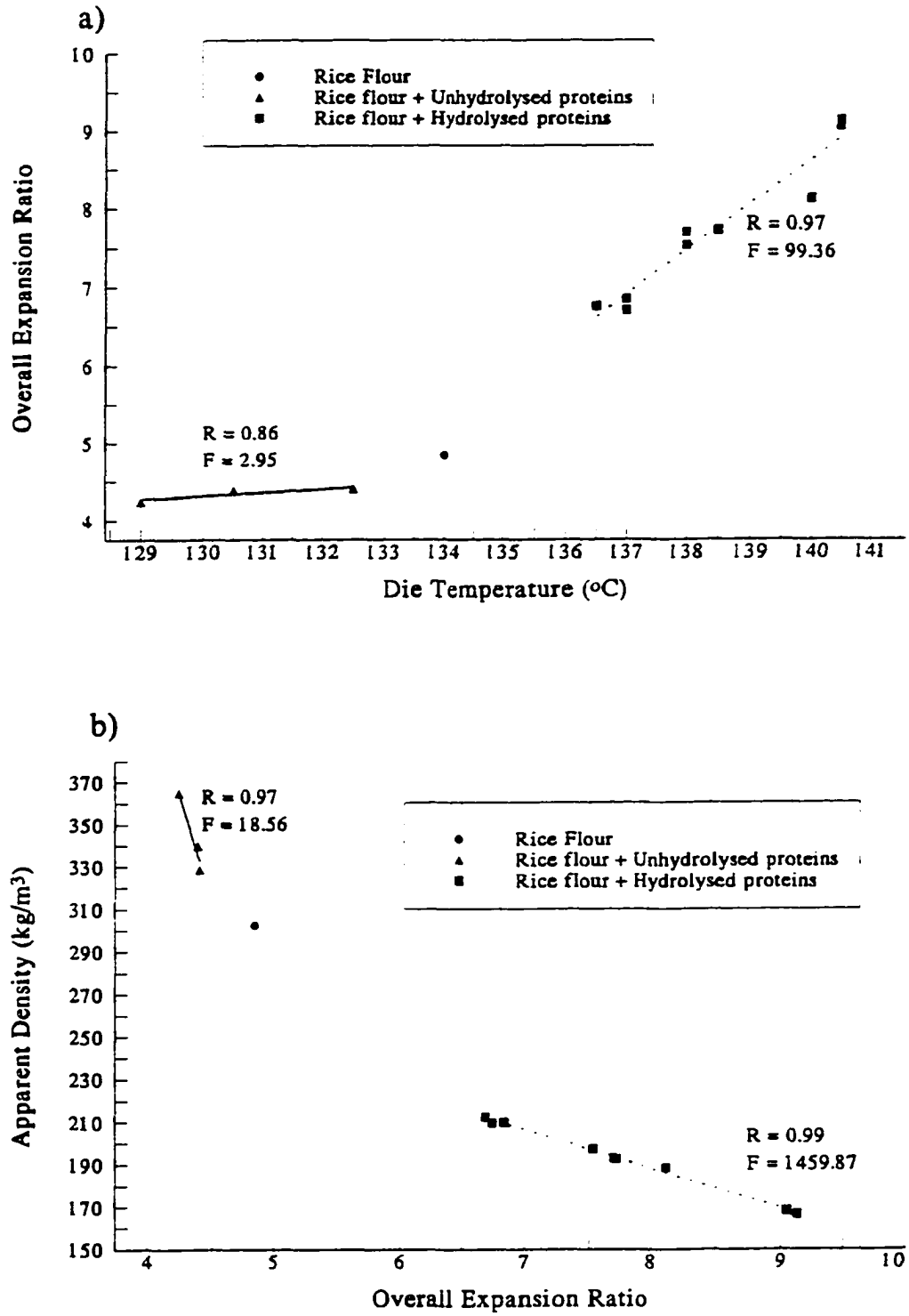

Figure 4.56 Relationship between (a) overall expansion and die temperature, (b) apparent density and overall expansion during extrusion of Arrowtooth flounder muscle and rice flour blends.

4.3.3.3 Porosity

Addition of proteins in feed affected the porosity of the extrudate. The pattern was similar to that of overall expansion ratio. Although comparison of means showed that degree of hydrolysis (5, 10, and 15 minutes) did not affect porosity, ANOVA elucidated that hydrolysis time, fish solids content, and their interactions affected the porosity significantly (Table 4.23). Porosity of rice flour extrudate was about 79%. Addition of unhydrolysed fish solids lowered the porosity systematically (Fig. 4.57).

Several studies have shown the effect of feed composition on the microstructure of the extrudates by scanning electron microscopy (Noguchi *et al.*, 1981; Bhattacharya *et al.*, 1986; Grenus *et al.*, 1992). Air cell localization was different for rice flour and its blends with soybean protein isolate (SPI). The former had more and larger air cells and addition of SPI made the extrudate more dense and rigid (Noguchi *et al.*, 1981). Similarly, Grenus *et al.* (1992) showed that the air cell size of the extrudate decreased with higher levels of rice bran in the feed. Our porosity data of unhydrolysed fish agreed with these findings.

Interestingly, increasing the hydrolysed fish solids content improved the porosity of the extrudate (Fig. 4.57). The relationship between porosity and overall expansion was not linear (Fig. 4.58). Increasing unhydrolysed fish solids decreased both porosity and overall expansion. On the other hand, these properties increased upon addition of hydrolysed fish solids.

Table 4.23 Analysis of variance data for porosity and breaking strength of extrudates obtained from blends of rice flour and hydrolysed arrowtooth flounder muscle.

Source	DF	Mean Sum of Squares (MSS) and F-values for Porosity (%) and Breaking Strength (MPa)			
		Porosity		Breaking Strength	
		MSS	F	MSS	F
Hyd. time (HT)	3	148.28	1079.69**	0.03452835	497.84**
Fish Solids (FS)	2	10.72	78.08**	0.00011350	1.64
HT x FS	6	2.48	18.08**	0.00052143	7.52
Error	12	0.14	-	0.00006936	-

**Highly significant at $p \leq 0.005$

*Significant at $p \leq 0.05$

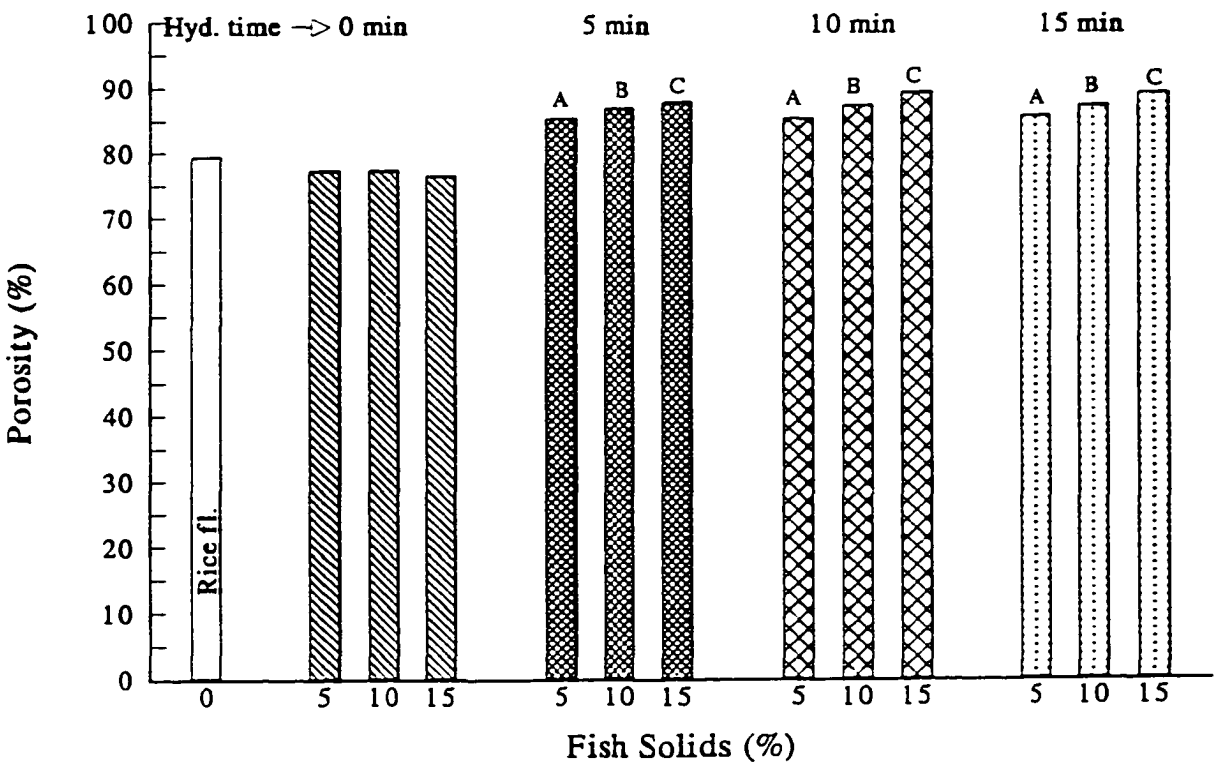

Figure 4.57 Effects of hydrolysis time and fish solids content on porosity of extrudates obtained from arrowtooth flounder muscle and rice flour blends. Means with same letters are not significantly different.

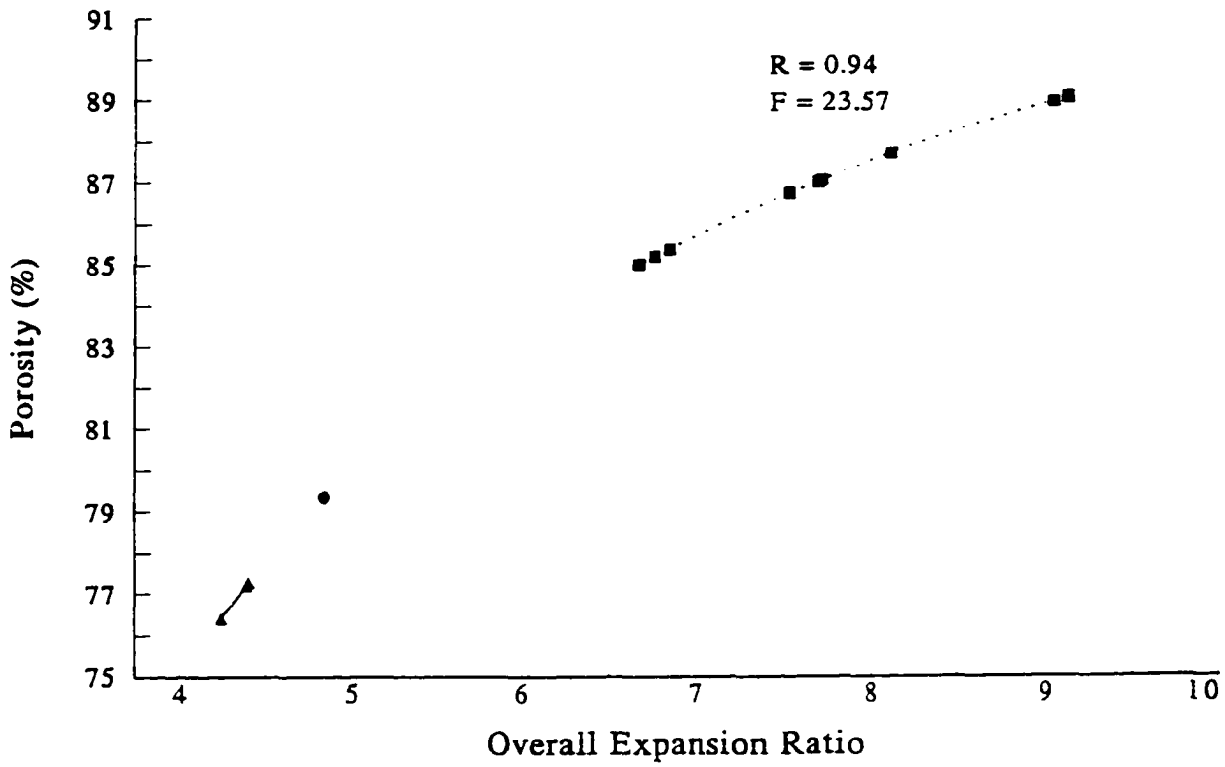

Figure 4.58 Relationship between porosity and overall expansion of extrudates obtained from arrowtooth flounder muscle and rice flour.

4.3.3.4 Breaking strength

Among all the macroscopic properties studied, breaking strength was considerably affected by feed composition (Table 4.23). Hydrolysis of arrowtooth flounder produced dramatic effects on textural attributes of extrudates. The breaking strength for the rice flour extrudate was about 0.12 MPa (Fig. 4.59). Addition of unhydrolysed arrowtooth flounder muscle produced the usual "protein-type" of extrudates (Areas, 1992). The breaking strength increased considerably upon addition of unhydrolysed fish solids. Blend with 15% unhydrolysed fish solid had a breaking strength of 0.23 MPa (Fig. 4.59). Autolysis of arrowtooth flounder changed the properties of proteins so much that the breaking strength values of the blends were below the value of rice flour extrudates. The lowest breaking strength (0.06 MPa) was achieved with 10% blends of hydrolysed fish (Fig. 4.59).

Hydrolysis time and fish solids content affected the breaking strength in an exactly opposite fashion to that of radial expansion ratio. During the screw configuration study a negative correlation between breaking strength and radial expansion was established. The feed composition had a similar effect (Fig. 4.60). Addition of unhydrolysed fish solids increased the breaking strength and lowered the radial expansion. On the other hand, hydrolysed fish solids decreased the breaking strength and increased the radial expansion. Thus, enzymatically modified proteins can be used to enhance the macroscopic properties and nutritional value of snack food.

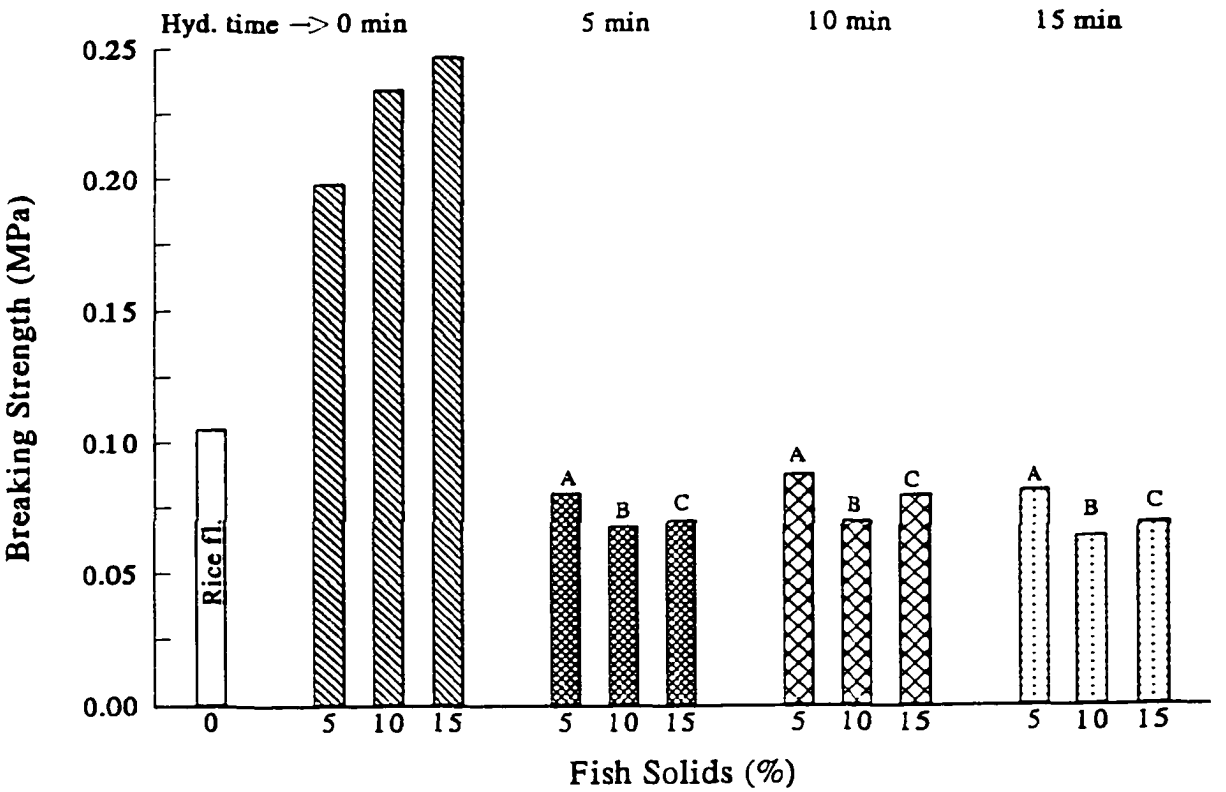

Figure 4.59 Effects of hydrolysis time and fish solids content on breaking strength of extrudates obtained from arrowtooth flounder muscle and rice flour blends. Means with same letters are not significantly different.

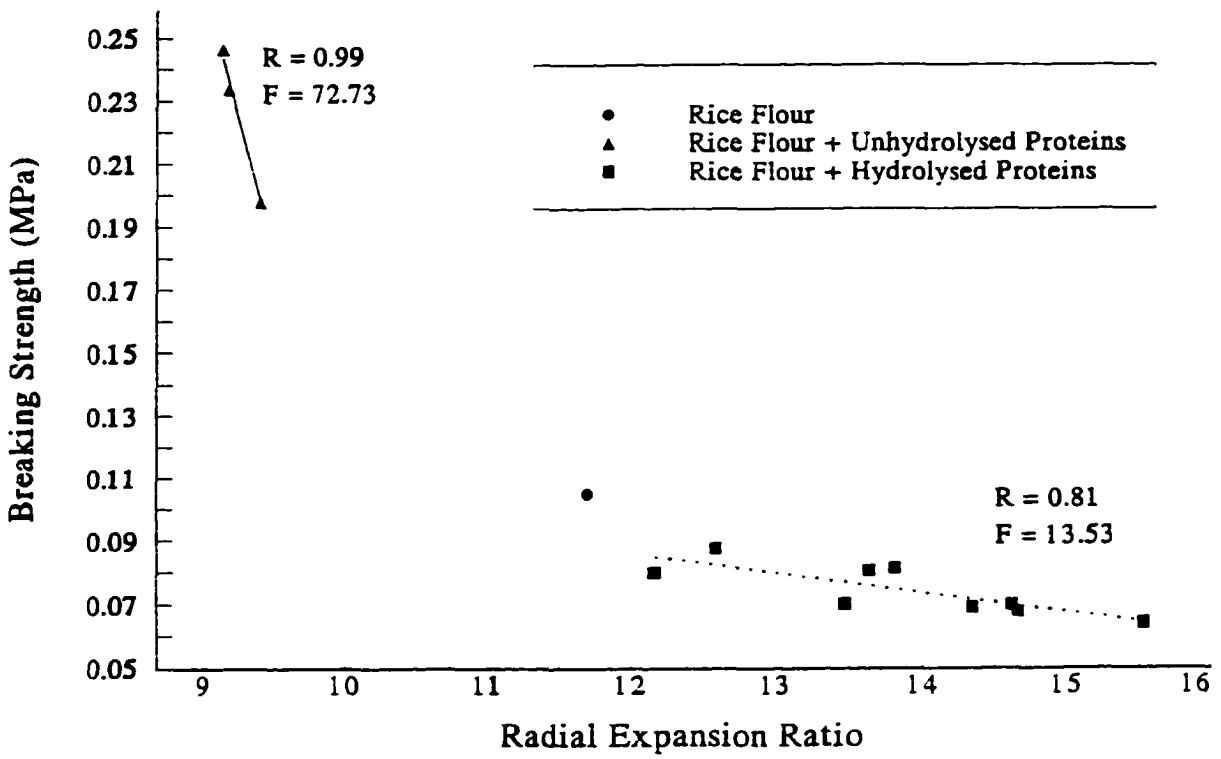

Figure 4.60 Relationship between breaking strength and radial expansion of extrudates obtained from arrowtooth flounder muscle and rice flour blends.

CHAPTER 5

CONCLUSIONS

This study investigated the effects of two independent process variables, viz., screw configuration and feed composition on various system parameters and extrudate characteristics. The results provided a systematic and deeper understanding of the screw configuration and feed composition effects. In addition, the study contributed basic data on design considerations for development of an extrusion process for utilization of fish containing proteolytic enzymes.

In the course of this study, an on-line method to measure the residence time distribution in a food extruder was developed. The new on-line method for RTD measurement, based on material electrical conductivity, accurately measured the tracer movement through the die. The on-line method correlated well with the established erythrosine dye method. The RTDs obtained by both methods superimposed on each other. The mean and total residence times measured by the two methods were essentially the same. The on-line method accurately determined the effects of screw configuration, screw speed and feed flow rate on RTD. The new method was simple, fast, and can be adapted for on-line measurement of RTD in other reaction vessels. This technique will find extensive application in academic and industrial research.

The type, length, position of mixing elements and spacing between two elements significantly affected energy inputs, residence time distribution, molecular changes of

starch, and macroscopic extrudate characteristics during twin-screw extrusion of rice flour. Specific mechanical energy (SME) input, mean residence time (t_{mean}), extent of mixing and starch breakdown were lower for screw profiles with KB than with RSE. A systematic increase in SME input, t_{mean}, and extent of starch breakdown was observed as the mixing elements were moved farther away from the die, with longer elements, and with increased spacing between two elements. Radial expansion was higher with KB in the screw profile than with RSE, irrespective of element length, position, and spacing. For KB and RSE, maximum expansion was observed when the element was placed at 150 and 50 mm from the die end, respectively. KB seemed to be the element of choice for maximizing extrudate radial expansion. Apparent density and overall expansion were a function of die temperature. Maximum material temperature in the die was observed when a mixing element was positioned at the die, which resulted in highest overall expansion and lowest apparent density. Textural attributes of extrudates were significantly affected by screw configuration. Hardness of the product, as measured by breaking strength, decreased with increasing radial expansion.

Screw configuration was found to be a dominant process variable affecting intermediate process parameters and extrudate characteristics. The findings can be used for process scale up and to manipulate the extent of physicochemical changes during extrusion. Mild to very severe processing can be induced by manipulation of screw configuration with mixing elements. Such maneuvering can be used to alter residence time distribution, mixing, degree of fill, and extent of starch degradation during

extrusion, all of which affects extrudate characteristics. Desired product expansion and textural attributes can be achieved by appropriate selection of type, location, and length of mixing elements.

The feed composition study evaluated the effects of hydrolysis time and levels of arrowtooth flounder muscle in feed mixtures. Hydrolysis for different times (5, 10, & 15 min) produced low-molecular weight peptides with similar bands in SDS gels. Extrusion with increasing amount of fish solids (protein concentration) played a key role in effecting the viscosity of the material and thus lowering the SME input and raising the mean residence time of the material in the extruder. The behavior of two types of blends were also different during extrusion. The material temperature in the die was strikingly higher for blends with hydrolysed fish solids than that with unhydrolysed fish. This led to a very high overall expansion and low apparent density of extrudates produced from blends of hydrolysed arrowtooth flounder and rice flour. Interestingly, hydrolysis changed the properties of arrowtooth flounder proteins so much that the extrudates obtained form blends of hydrolysed fish solids and rice flour had higher expansion than those produced from rice flour alone.

The data from the feed composition study indicated that the detrimental effects of proteins on extrudate characteristics can be minimized or eliminated by enzymatic modification of fish proteins. Nutritional snacks can be produced without compromising the sensory attributes of the product.

It is reasonable to conclude that both screw configuration and feed composition

are important process variables influencing the physicochemical changes in the material during extrusion, which in turn controls the extrudate characteristics. It is hoped that the data will find extensive application in altering material properties as a function of machine parameters, and in designing improved extrusion processes. This study may lead to increased use of proteins in extruded products. Further research will be necessary to investigate the interesting functional property of hydrolysed arrowtooth flounder muscle that enhanced the expansion capacity of starch in rice flour.

BIBLIOGRAPHY

Aguilera, J.M. and Stanley, D.W. 1986. Extrusion processing as applied to proteinaceous materials. In: *Food Engineering and Process Application. Unit Operation*, Vol. 2, M. LeMaguer and P. Jelen (Eds.), Elsevier Applied Science Publishers, New York. pp. 131-141.

Altomare, R.E. and Ghossi, P. 1986. An analysis of residence time distribution patterns in a twin screw cooking extruder. Biotech. Prog. 2(3): 157-163.

AOAC. 1984. *Official Methods of Analysis*. 14th edition. Association of Official Analytical Chemists, Arlington, VA.

Aoki, K., Hara, F. and Ohimichi, M. 1989. Texturization of surimi using twin screw extruder. Nippon Shokuhin Kogyo Gakkaishi, 36(9): 748-753.

Areas, J.A.G. 1992. Extrusion of Food Proteins. Crit. Rev. Food Sci. Nutri. 32(4): 365-392.

Barres, C., Vergnes, B., Tayeb, J. and Della Valle G. 1990. Transformation of wheat flour by extrusion cooking: Influence of screw configuration and operating conditions. Cereal Chem. 67(5): 427-433.

Bhattacharya, S., Das, H. and Bose, A.N. 1988. Effect of extrusion process variables on in-vitro protein digestibility of fish-wheat flour blends. Food Chem. 28: 225-231.

Bhattacharya, S., Das, H. and Bose, A.N. 1990. Effect of extrusion process variables on microstructure of blends of minced fish and wheat flour. J. Food Sci. Technol. 27(1): 22-28.

Bhattacharya, S. and Choudhury, G. S. 1994. Twin-screw extrusion of rice flour: effect of extruder length-to-diameter ratio and barrel temperature on extrusion parameters and product characteristics. J. Food Proc. Preserv. 18: 389-406.

Bhattacharya, M. Hanna, M.A. and Kaufman, R.E. 1986. Textural properties of extruded plant protein blends. J. Food Sci., 51(4): 988-993.

Bhattacharya, M. and Hanna, M.A., 1987. Kinetics of starch gelatinization during extrusion cooking. J. Food Sci. 52(3):764-766.

Biliaderis, C.G., Page, C.M., Maurice, T.J. and Juliano B.O. 1986a. Thermal characterization of rice starches: A polymeric approach to phase transitions of granular starch. J. Agric. Food Chem, 34:6-14.

Biliaderis, C.G., Page, C.M. and Maurice, T.J. 1986b. On the multiple melting transitions of starch/monoglyceride systems. Food Chem. 22:279-295.

Bounie, D. 1988. Modelling of the flow pattern in a twin-screw extruder through residence time distribution experiments. J. Food Eng. 7: 223-246.

Brenner, P.E., Richmond, P. and Smith, A.C. 1986. Aqueous dispersion rheology of extrusion cooked maize. J. Texture Studies, 17: 51-60.

Burgess, L.D. and Stanley, D.W. 1976. A possible mechanism for thermal texturization of soybean protein. J. Inst. Can. Sci. Technol. Aliment. 9(4): 228-231.

Cai, W. and Diosady, L.L. 1993. Modeling of expansion and water solubility index of wheat starch during extrusion cooking. Acta Alimentaria, 22(3): 181-192.

Chang, C.S., 1988. Measuring density and porosity of grain kernels using a gas pycnometer. Cereal chem. 65(1):13-15.

Chang, K.L.B. and Halek, G.W. 1991. Analysis of shear and thermal history during co-rotating twin-screw extrusion. J. Food Sci. 56(2): 518-531.

Chen, T., Patterson, W.I. and Dealy, J.M. 1995. On-line measurement of residence time distribution in a twin-screw extruder. Intern. Polymer Processing, X: 3-9.

Chinnaswamy, R. and Bhattacharya, K.R. 1983. Studies on expanded rice. Physicochemical basis of varietal differences. J. Food Sci. 48: 1600-1603.

Chinnaswamy, R. and Bhattacharya, K.R. 1984. Relationship between amylose content and expansion characteristics of parboiled rice. J. Cereal Sci. 2: 273-279.

Chinnaswamy, R. and Hanna, M.A. 1988. Optimum extrusion-cooking conditions for maximum expansion of corn starch. J. Food Sci. 53(3):834-840.

Chinnaswamy, R. and Hanna, M.A. 1990. Macromolecular and functional properties of native and extrusion-cooked corn starch. Cereal Chem. 67(5):490-499.

Choudhury, G.S. 1994. In enzyme biotechnology for utilization of arrowtooth flounder. A proposal submitted to Sea Grant, National Oceanic and Atmospheric Administration, Washington, D.C.

Choudhury, G.S. and Bhattacharya, S. 1994. Twin-screw extrusion of fish mince: effect of extrusion temperature and level of additives on extrudate characteristics. Paper No. 34-6, presented at the Annual Meeting of Institute of Food Technologists, Atlanta, June 25-29.

Choudhury, G.S. and Gogoi, B.K. 1994. Enzyme inhibition by high-moisture twin-screw extrusion. Paper No. 71E-11, presented at the Annual Meeting of Institute of Food Technologists, Atlanta, June 25-2

Choudhury, G.S. and Gogoi, B. K. 1995. Extrusion processing of fish muscle: a review. J. Aq. Food Prod. Technol. 4(4): 37-67.

Choudhury, G.S. and Gogoi, B.K. 1996. Protease inactivation in fish muscle during high moisture twin-screw extrusion. J. Food Sci. 61(6): 1219-1222.

Choudhury, G.S., Moir, M.A. and Gogoi, B.K. 1997. High Moisture Extrusion: Possibilities and Prospects. In *Advances in Food Engineering (Proceed. 4th Conf. Food Eng.)*, G. Narsimhan, M.R. Okos, and S. Lombardo (Eds.), pp. 117-124. American Institute of Chemical Engineers, New York, NY.

Choudhury, G.S. and Gautam A. 1998a. Comparative study of mixing elements during twin-screw extrusion of rice flour. Food Research International. (In press).

Choudhury, G.S. and Gautam A. 1998b. On-line measurement of residence distribution in a food extruder. J. Food Sci. (In press).

Choudhury, G.S., Gogoi, B.K. and Oswalt, A.J. 1998. Twin-screw extrusion of pink salmon muscle and rice flour blends: effects of kneading elements. J. Aqua. Food Prod. Technol. (In press).

Colonna, P., Melcion, J.P., Vergnes, B. and Mercier, C. 1983. Flow, mixing and residence time distribution of maize starch within a twin-screw extruder with a longitudinally - split barrel. J. Cereal Sci. 1: 115-125.

Colonna, P., Doublier, J.L., Melcion, J.P., de Monredon, F. and Mercier, C. 1984. Extrusion cooking and drum drying of wheat starch. I. Physical and macromolecular modifications. Cereal Chem. 61(6): 538-543.

Clayton, J.T. and Miscourides, D.N. 1992. Extruder texturized foods from underutilized fish tissue. J. Aq. Food prod. Technol. 1(3/4): 65-89.

Cullenberg, P. 1995. Commercialization of arrowtooth flounder: the next step. In *Proceedings of the International Symposium on North Pacific Flatfish, P. 623-630.* Alaska Sea Grant College Program Report No. 95-04, Fairbanks, AK.

Davidson, V.J., Paton, D., Diosady, L.L. and Larocque, G. 1984a. Degradation of wheat starch in a single screw extruder: Characteristics of extruded starch polymers. J. Food Sci. 49: 453-458.

Della Valle, G., Tayeb, J. and Melcion, J. P., 1987. Relationship of extrusion variables with pressure and temperature during twin screw extrusion cooking of starch. J. Food Eng., 6: 423-444.

Diosady, L.L., Paton, D., Rosen, N., Rubin, L.J., and Athanassoulias, C. 1985. Degradation of wheat starch in a single-screw extruder: mechano-kinetic breakdown of cooked starch. J. Food Sci. 50:1697-1699.

Dubois, M., Gilles, K.A., Hamilton, J.K., Rebers, P.A. and Smith, F. 1956. Colorimetric method for determination of sugars and related substances. Analytical Chemistry, 28(3):350-356.

Dziezak, J.D. 1989. Single- and twin-screw extruders in food processing. Food Technol. 43(4): 163-174.

Erdemir, M.M., Edwards, R.H. and McCarthy, K.L. 1992. Effect of screw configuration on mechanical energy transfer during twin-screw extrusion of rice flour. Lebensm-Wiss.u.-Technol. 25: 502-508.

Faubion, J.M. and Hoseney, RC. 1982. High-temperature short-time extrusion cooking of wheat starch and flour. I. Effect of moisture and flour type on extrudate properties. Cereal Chem., 59(6):529-533.

Fretzdorff, B. and Seiler, K. 1987. The effects of twin-screw extrusion cooking on cereal enzymes. J. Cereal Sci. 5: 73-82.

Gautam, A., Choudhury, G.S. and Gogoi, B.K. 1997. Twin-screw extrusion of pink salmon muscle: effect of mixing elements and feed composition. J. Muscle Foods, 8: 265-285.

Geankoplis, C. 1983. Transport Process and Unit Operations, 2nd ed. Allyn and Bacon, Inc., Boston.

Gogoi, B.K. and Yam, K.L. 1994. Relationships between residence time and process variables in a corotating twin-screw extruder. J. Food Eng. 21: 177-196.

Gogoi, B.K., Choudhury, G.S. and Oswalt, A.J. 1996a. Effects of location and spacing of reverse screw and kneading element combination during twin-screw extrusion of starchy and proteinaceous blends. Food Research Int., 29(5/6): 505-512.

Gogoi, B.K., Oswalt, A.J. and Choudhury, G.S. 1996b. Reverse screw element(s) and feed composition effects during twin-screw extrusion of rice flour and fish muscle blends. J. Food Sci. 61(3): 590-595.

Golba, J.C. 1980. A new method for the on-line determination of residence time distributions in extruders. Society of Plastics Engineers. Antec 26: 83-85.

Gomez, M.H. and Aguilera, J.M. 1983. Changes in the starch fraction during extrusion-cooking of corn. J. Food Sci. 48: 378-381.

Gomez, M.H. and Aguilera, J.M. 1984. A physicochemical model for extrusion of corn starch. J. Food Sci. 49: 40-49.

Gopalakrishna, S. and Jaluria, Y. 1991. Modeling of starch gelatinization in a single-screw extruder. In *Food Extrusion Science and Technology*, J.L. Kokini, C-T Ho, and M.V. Karwe (Eds.). pp. 345-360. Marcel Dekker, New York, NY.

Green, D. and Babbitt, J. 1990. Control of muscle softening and protease parasite interactions in arrowtooth flounder *(Atheresthes stomias)*. J. Food Sci. 55:579-580.

Greghaigne, B., Chouvel, H., Pina, M., Graille, J. and Cheftel, J.C. 1983. Extrusion-cooking of aflatoxin-containing peanut meal with and without addition of ammonium hydroxide. Lebensm.-Wiss. u.-Technol. 16(6): 317-322.

Grenus, K.M., Hsieh, F. and Huff, H.E. 1992. Extrusion and extrudate properties of rice flour. J. Food Eng. 18:229-245.

Guy, R.C.E. and Horne, A.W. 1988. Extrusion and co-extrusion of cereals. In Food structure-its Creation and Evaluation (Eds.) J.M.V. Blanshard and J.R. Marshal. Buttersworth, London. 331-349.

Hakulin, S., Linko, Y.Y., Linko, P., Seiler, K. and Seibel, W. 1983. Enzymatic conversion of starch in twin-screw HTST-extruder. Starch/Starke 35: 411-414.

Hager, D.F. 1984. Effects of extrusion upon soy concentrate solubility. J. Agri. Food Chem. 32: 293-296.

Harper, J.M. 1981. *Extrusion of Foods*. Vol. 1, pp. 7-19, CRC Press, Inc., Boca Raton, FL.

Hauck, B.W. 1980. Marketing opportunities for extrusion cooked products. Cereal Foods World. 25(90): 594-595.

Heldman, D.R. and Singh, R.P. 1981. Heating and cooling processes. In Food Process Engineering, AVI Publishing Co. Inc., Westport Connecticut.

Hilmarsdottir, E., and Karmas, E. 1984. Microbial stability of a fermented intermediate moisture fish product. Lebensm. Wiss. u. Technol. 17(6): 328-330.

Huang, R-M., Chang, W-H., Chang, Y-H. and Lii, C-Y., 1994. Phase transitions of rice starch and flour gels. Cereal Chem. 70(2):202-207.

Isobe, S., Uemura, K. and Noguchi, A. 1990. Texturization of chum salmon muscle harvested during spawning migration (Bunazake). Nippon Shokuhin Kogyo Gakkaishi, 37(12): 965-970.

Jeunink, J. and Cheftel, J.C. 1979. Chemical and physicochemical changes in field bean and soybean texturized by extrusion. J. Food Sci. 44: 1322-1325.

Juliano, B.O. 1994. Polysaccharides, proteins, and lipids of rice. *In Rice Chemistry and Technology,* B.O. Juliano (Ed.). pp. 59-160. The American Association of Cereal Chemists, Inc., St. Paul, MN.

Kainuma, K. 1982. Starch oligosaccharides: linear, branched, and cyclic In *Starch: Chemistry and Technology*, R.L. Whistler, J.N. Bemiller, E.F. Paschall (Eds.). pp. 125-150. Academic Press, Inc., NY

Kao, S.V. and Allison, G.R. 1984. Residence time distribution in a twin-screw extruder. Polymer Eng. Sci. 24(9): 645-651.

Karmas, E. and Lauber, E. 1987. Novel products from underutilized fish using combined processing technology. J. Food Sci. 52(1): 7-9.

Kiani, A., Burkhardt, U., Heidemeyer, P., Franzheim, O., Rische, T., Stephan, M., Baetz, H., Pallas, R., Sahoub, M. and Zeuner, A. 1996. A new online technique for morphology analysis and residence time measurement in a twin screw extruder. Society of Plastics Engineers. Antec 54: 427-434.

Kirby, A.R., Ollett, A-L., Parker, R. and Smith, A.C. 1988. An experimental study of screw configuration effects in the twin-screw extrusion-cooking of maize grits. J. Food Eng. 8: 247-272.

Kitabatake, N., Shimizu, Y. and Doi, E. 1988. Continuous production of fish meat sol using a twin-screw extruder. J. Food Sci. 53(2): 344-348.

Kitagawa, M. and Nishi, K. 1987. Studies on the extrusion cooking of marine products. I. Utilization of sardine (*Sardinops melanostica*) with extrusion cooking. Hokkaido Fish Res. Stn. Rep. 44: 151-168.

Kitagawa, M., and Nishi, K. 1989. Studies on extrusion cooking of marine products III. Effect of various extrusion conditions on freeze-pulverized-Bunasake (fall chum salmon). Sci. Rep. Hokkaido Fish. Exp. Stn. 32: 19-32.

Kramer, D., Barss, W., Paust, B. and Bracken, B. 1995. Guide to Northeast Pacific flatfishes. 36-37. Alaska Sea Grant College Program. University of Alaska Fairbanks, AK.

Kristensen, K.H., Gray, P. and Holm, F. 1984. Extruded protein-rich animal by-products with improved texture. In: *Thermal Processing and Quality of Foods*, P. Zeuthen, J.C. Cheftel, C. Ericksson, M. Jul, H. Leninger, P. Linko, G. Varella and G. Vos (Eds.), Elsevier Applied Science Publishers, New York. pp. 113-121.

Kokini, J.L., Chang, C.N. and Lai, L.S. 1991. The role of rheological properties on extrudate expansion. In *Food Extrusion Science and Technology*, J.L. Kokini, C-T Ho, and M.V. Karwe (Eds.). pp. 345-360. Marcel Dekker, New York, NY.

Levenspiel, O. 1972. Chemical Reaction Engineering, 2nd Ed., Wiley, N.Y.

Lee, C.M. 1986. Fabricated seafood products: Surimi manufacture and fabrication of surimi-based products. Food Technol. 40(3): 115-124.

Lin, J.K. and Armstrong, D.J. 1990. Process variables affecting residence time distributions of cereals in an intermeshing, counter rotating twin-screw extruder. Trans. ASAE. 33(6): 1971-1978.

Maga, J.A. and Reddy, T. 1985. Co-extrusion of carp (*Cyprinus carpio*) and rice flour. J. Food Proc. Pres. 9: 121-128.

Martelli, F.G. 1983. *Twin-screw extruders: A basic understanding.* Van Nostrand Rheinhold Company, New York, NY.

Mercier, C., and Feillet, P. 1975. Modification of carbohydrate components by extrusion-cooking of cereal products. Cereal Chem. 52(3): 283-297.

Meuser, F., Pfaller, W. and van Lengerich, B. 1987. Technological aspects regarding specific changes to the characteristic properties of extrudates by HTST extrusion cooking. In: *Extrusion Technology for the Food Industry*, C. O'Connor (Ed.), pp. 35-53, Elsevier Applied Science Publishers, New York, NY.

Meuser, F., Gimmler, N., and Van Lengrich, B. 1991. A system analytical approach to extrusion. In *Food Extrusion Science and Technology*, J.L. Kokini, C-T Ho, and M.V. Karwe (Eds.). pp. 619-630. Marcel Dekker, New York, NY.

Mohamed, S. 1990. Factors affecting extrusion characteristics of expanded starch-based products. J. Food Proc & Pres. 14:437-452.

Murray, B.P. and Stanley, D.W. 1980. Improved utilization of fish protein - co-extrusion of mechanically deboned salted minced fish. Can. Inst. Food Sci. Technol. J. 13(3): 125-130.

Normand, F.L. and Marshall, W.E. 1989. Differential scanning calorimetry of whole grain milled rice and milled rice flour. Cereal Chem. 66(4):317-320.

Noguchi, A., Kugimiya, W., Haque, Z. and Saio, K. 1981. Physical and chemical characteristics of extruded rice flour and rice flour fortified with soybean protein isolate. J. Food Sci. 47:240-245.

Olkku, J., Antila, J., Heikkinen, J. and Linko, P. 1980. Residence time distribution in a twin-screw extruder. In *Food Process Engineering*, Vol. 1, P. Linko, Y. Malkki, J. Olkku and J. Larinkari (eds.). pp. 791-794. Elsevier Applied Science Publishers, London.

Olkku, J. 1981. Extrusion processing-a study in basic phenomena and application of system analysis. In *Developments in Food Preservation*, S. Thorne (Ed.), pp. 177-214, Elsevier Applied Science Publisher, London.

Olkku, J, Hagqvist, A. and Linko, P. 1983. Steady state modelling of extrusion cooking employing response surface methodology. In: Jowitt, R. (Ed.) *Extrusion-cooking technology*. Elseiver Applied Science Publisher, NY.

Otto, B. 1996. Stock assessment and fishery evaluation report for the groundfish resources of the Gulf of Alaska as projected for 1997. North Pacific Fisheries Management Council, Anchorage, AK.

Owusu-Ansah, J., van de Voort, F.R. and Stanley, D.W. 1983. Physicochemical changes in cornstarch as a function of extrusion variables. Cereal Chem. 60(4): 319-324.

Owusu-Ansah, J., van de Voort, F.R. and Stanley, D.W. 1984. Textural and microstructural changes in corn starch as a function of extrusion variables. Can. Inst. Food Sci. Technol. J. 17(2): 65-70.

Park, K.H. and Hyun, C.K. 1989. Differential scanning calorimetry (DSC) of rice starch. Singapore. Institute of Food Sci. & Technol. pp. 144-147.

Pedersen, L.D., Rose, W.W., Deniston, M.F., and Merlo, C.A. 1989. Hyperfiltration Technology for the Recovery and Utilization of Protein Materials in Surimi Process Wash waters. Final Report of Project # NA 86AA-H-SK140. Prepared for National Marine Fisheries Service, U.S. Dept. of Commerce, NOAA.

Quantachrome Corporation. 1995. Instruction manual. Boyton Beach, FL.

Reppond, K.D. and Babbitt, J.K. 1993. Protease inhibitors affect physical properties of arrowtooth flounder and pollock surimi. J. Food Sci. 58:96-98.

Rossi, M. and Peri, C. 1986. Effect of extrusion cooking on the structural and functional characteristics of sunflower protein. In: *Food Engineering and Process Application. Unit Operation*, Vol. 2, M. LeMaguer and P. Jelen (Eds.), Elsevier Applied Science Publishers, New York. pp. 197-209.

SAS Institute, Inc. 1996. Statistical Analysis System, SAS Version 6.12. SAS Analytical Institute, Gary, NC.

Scopes, R.K. 1994. *Protein purification principles and practice*, Springer-Verlag, NY.

Sheard, P.R., Ledward, D.A. and Mitchell, J.R. 1984. Role of carbohydrates in soya extrusion. J. Food Technol. 19: 475-483.

Tayeb, J., Vergnes, B. and Della Valle, G. 1988. A basic model for a twin-screw extruder. J. Food Sci. 53(4): 1047-1056.

Todd, D.B. and Irving, H.F. 1969. Axial mixing in a self-wiping reactor. Chem. Eng. Prog. 65(9): 84-89.

Todd, D.B. 1975. Residence time distribution in twin-screw extruders. Polymer Eng. Sci. 15(6): 437-443.

Trimetrix, 1992. Axum Technical Graphics and Data Analysis. 444 NE Ravenna Boulevard, Suit 10, Seattle, WA.

Van Zuilichem, D.J., Jager, T. and Stolp, W. 1988. Residence time distribution in extrusion cooking. Part III: Mathematical modelling of axial mixing in a conical, counter rotating, twin-screw extruder processing maize grits. J. Food Eng. 8: 109-127.

Venugopal, V. 1987. Feasibility of incorporation of partially deodourized fish meat in extrusion cooked products. J. Food Sci. Technol. 24: 147-148.

Vergnes, B., Barres, C. and Tayeb, J. 1992. Computation of residence time and energy distribution in a reverse screw element of a twin-screw extrusion-cooker. J. Food Eng. 16: 215-237.

Wasson, D.H., Babbit, J.K. and French, J.S. 1992a. Characterization of heat stable protease from arrowtooth flounder. J. Aq. Food Prod. Technol. 1(3/4):167-168.

Wasson, D.H., Reppond, K.D., Babbit, J.K. and French, J.S. 1992b. Effects of additiveson proteolytic and functional properties of arrowtooth flounder surimi. J. Aq. Food Prod. Technol. 1(3/4):147-165.

Wen, L-F., Rodis, P. and Wasserman, B.P. 1990. Starch fragmentation and protein insolubilization during twin-screw extrusion of corn meal. Cereal Chem. 67(3):268-275.

Wilderbuer, T. and Brown, E. 1994. Flatfish. In Stock assessment and fishery evaluation report for the groundfish resources of the Gulf of Alaska as projected for 1995. North Pacific Fishery Management Council, Anchorage, AK.

Wilson, D. and Choudhury, G.S. 1998. A rapid method for studying the modori protease in arrowtooth flounder in-situ. To be submitted to J. Food Sci.

Witherell, D. 1995. Commercialization of arrowtooth flounder: the next step. In *Proceedings of the International Symposium on North Pacific Flatfish, P. 573-589.* Alaska Sea Grant College Program Report No. 95-04, Fairbanks, AK.

Wolf, D., Holin, N. and White, D.H. 1986. Residence time distribution in a commercial twin-screw extruder. Polymer Eng. Sci. 26:640-646.

Wolf, D. and White, D.H. 1976. Experimental study of residence time distribution in plasticating screw extruders. AIChE J. 22(1): 122-130.

Yacu, W.A. 1995. Thermoplastic and food extrusion general introduction. Short course: Food Extrusion Technology.

Yam, K.L, Gogoi, B.K. Karwe, M.V. and Wang, S.S. 1994. Shear conversion of corn meal by reverse screw elements during twin-screw extrusion at low temperatures. J. Food Sci. 59(1): 113-114.

Yates, L.D. and Greaser, M.L. 1983. Quantitative determination of myosin and actin in rabbit skeletal muscle. J. Mol. Biol. 168:123-141.

Yeh, A.I., Hwang, S.J. and Guo, J.J. 1992. Effects of screw speed and feed rate on residence time distribution and axial mixing of wheat flour in a twin-screw extruder. J. Food Eng. 17:1-13.

Yu, S.Y., Mitchell, J.R. and Abdullah, A. 1981. Production and acceptability testing of fish crackers ('keropok') prepared by the extrusion method. J. Food Technol. 16: 51-58.

APPENDIX 1

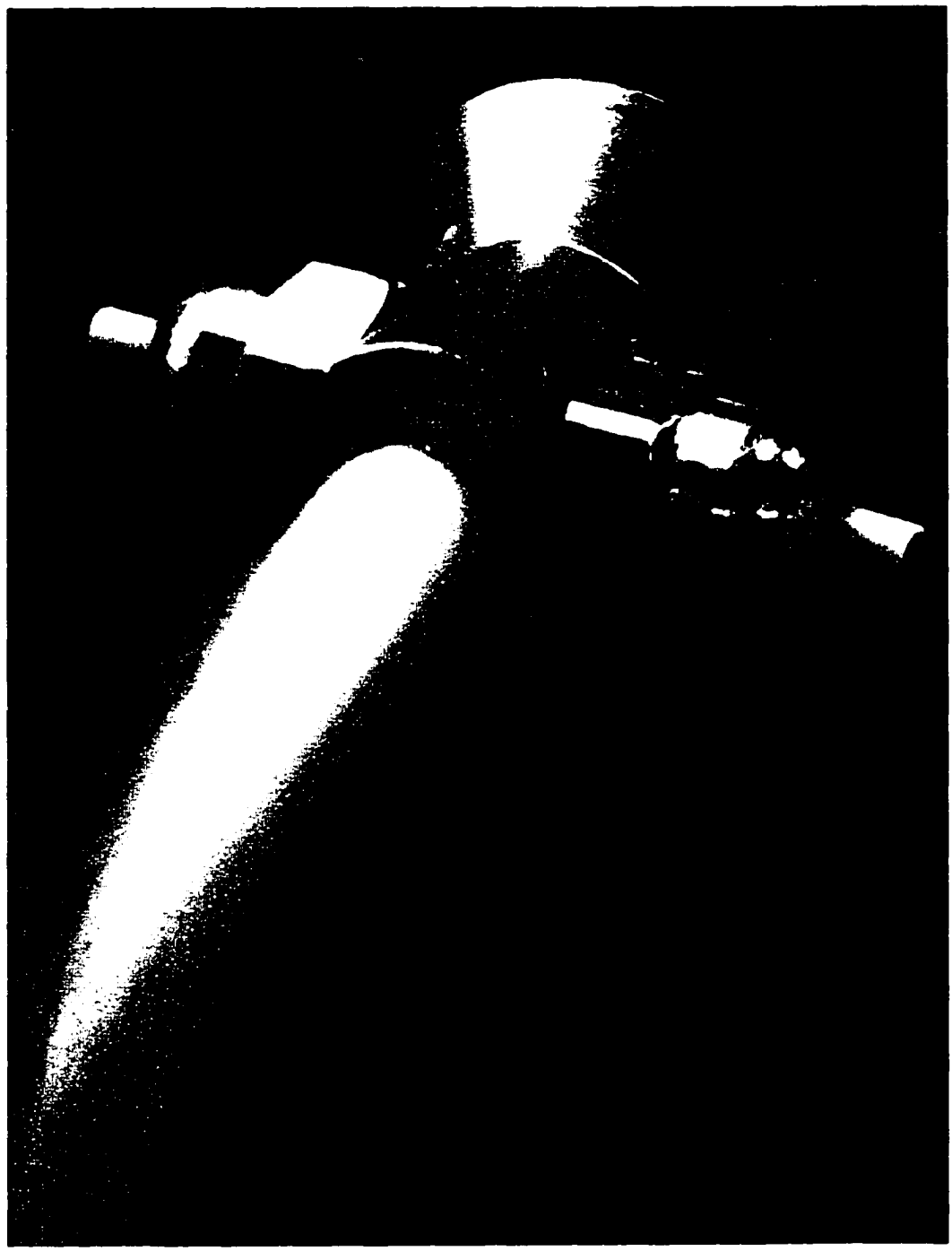

Extrudate expands as it leaves the die

APPENDIX 2

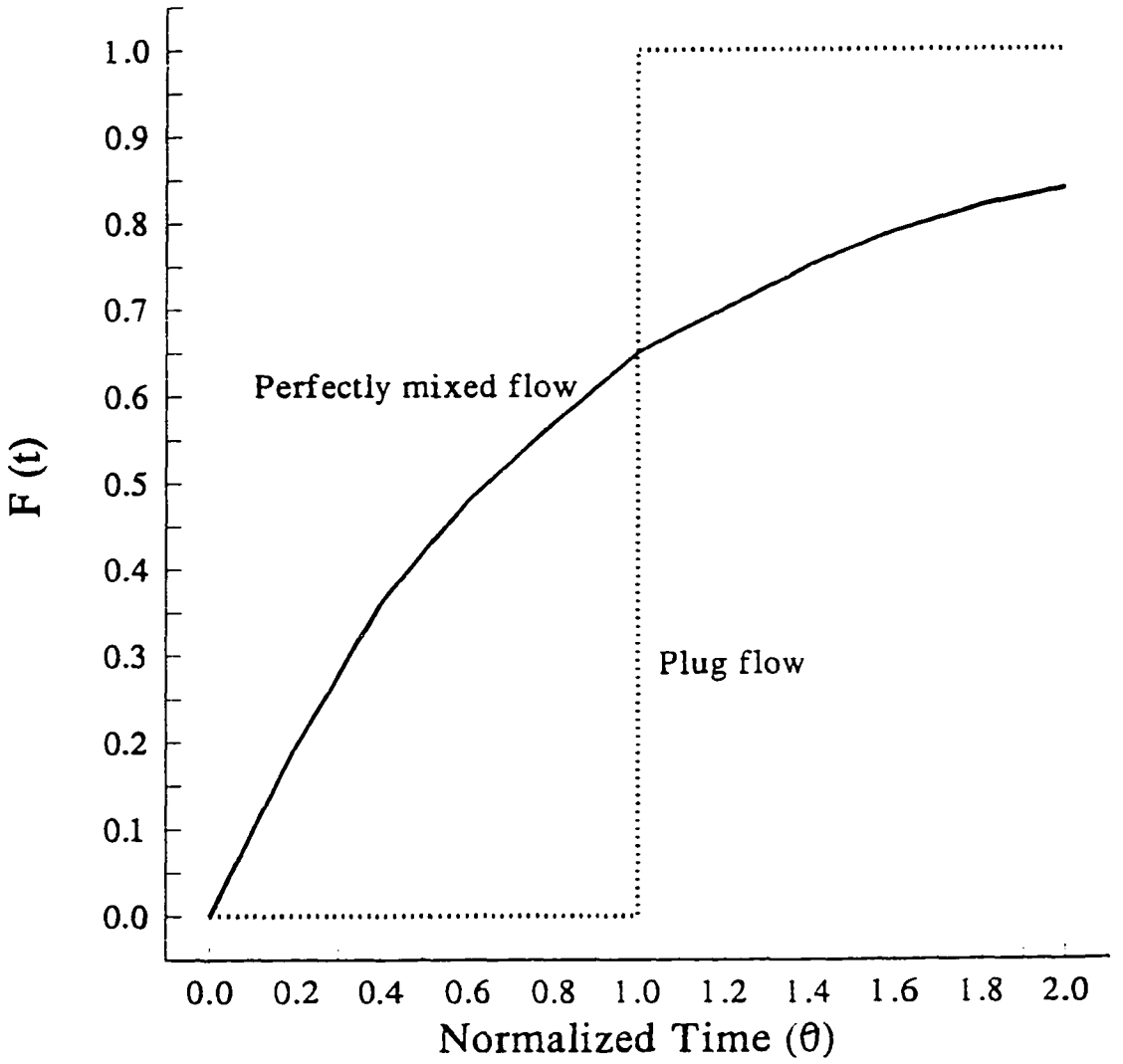

Perfectly mixed and plug flow (Adapted from Altomare and Ghossi, 1986)

IMAGE EVALUATION
TEST TARGET (QA-3)

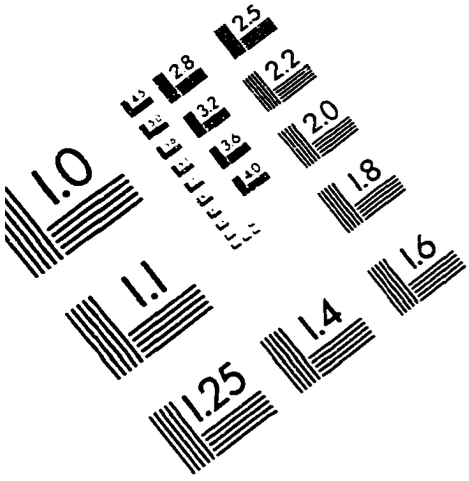

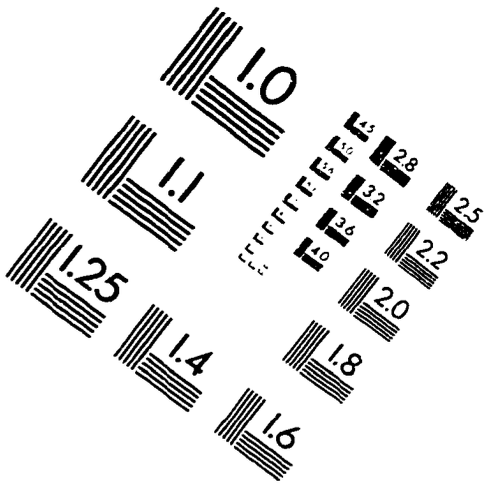

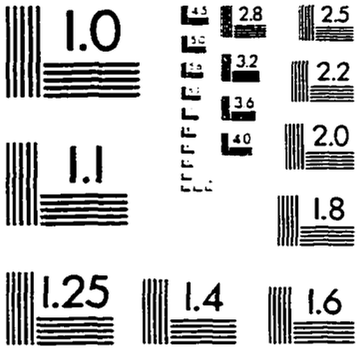

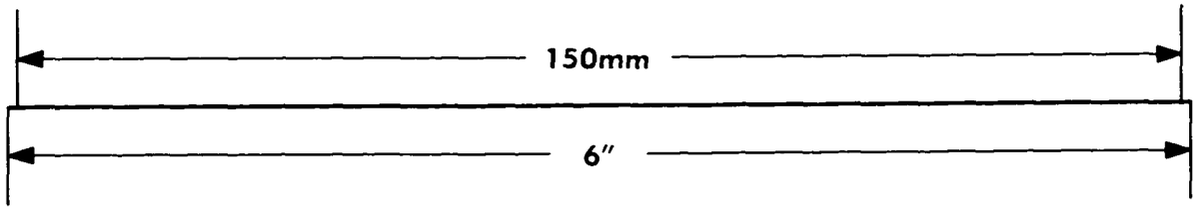

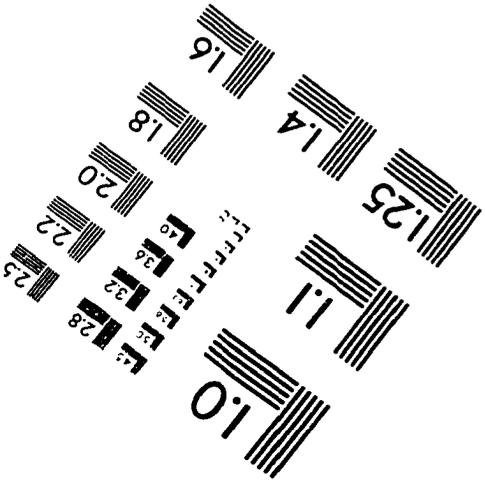

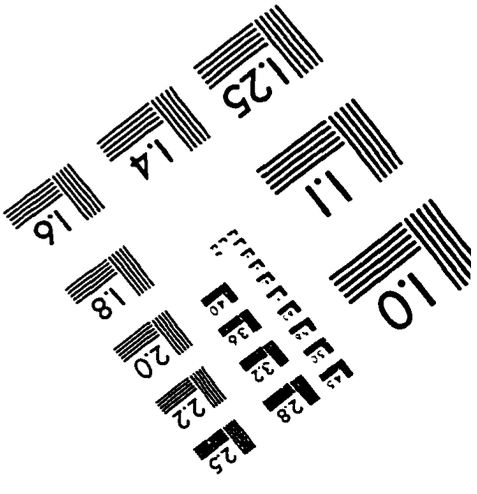

APPLIED IMAGE . Inc
1653 East Main Street
Rochester, NY 14609 USA
Phone: 716/482-0300
Fax: 716/288-5989